Water storage and release dynamics in nested prairie watersheds

by

Samuel Bansah

A thesis submitted to the Faculty of Graduate Studies of

The University of Manitoba

in partial fulfillment of the requirements for the degree of

DOCTOR OF PHILOSOPHY

Department of Geological Sciences

University of Manitoba

Winnipeg, Manitoba, Canada

ABSTRACT

Examining the dynamics pertaining to the storage of water in different watershed zones, and its release from these zones, is essential, not only for better hydrological process understanding, but also for biogeochemical reasons. When it comes to the release of water from storage zones, two main types of dynamics are generally considered; (1) active storage release dynamics, which relate to the fast release and transfer of water from surface and near surface sources, and (2) passive storage release dynamics, which rather refer to the slow release and transfer of water from the saturated zone to streams. While the literature is rich in theoretical, field and modelling studies targeting the assessment of water storage and release dynamics, few have attempted to compare several different storage assessment approaches at the same site, i.e., approaches that involve the use of hydrometric data only, approaches that involve the use of isotopic data only, and approaches that combine both. The extent to which those different approaches provide consistent information about the hydrological behavior of a given watershed is not routinely examined. Undertaking a study of this nature in the Canadian prairie region is especially important in view of the numerous surface storage depressions that are naturally present, the man-made ponds built for stormwater control purposes, and the many bridges and ditches that all together modify the release and transport of water to streams in ways that are not yet fully understood. In this PhD work, a study was undertaken to assess water storage and release dynamics within a nested system of eight prairie watersheds located in Manitoba, Canada. The physiographic diversity of the nested watersheds is such that six of the watershed outlets are located above a fractured escarpment, one is located right at the edge of the escarpment while the last one is located below the escarpment. Hydrometric data analysis was first used to define the storage release dynamics in a qualitative manner. Results from the hydrometric approach, though quite inconclusive at many of the studied outlets, was essential in putting forward a

hypothesis about the possible piston flow transport of water at the edge of the escarpment. Notably, flow duration curves and aridity index approaches failed to provide much relevant information about the storage and release dynamics in the watersheds. Furthermore, high runoff ratios were at odds with high baseflow index values observed at the edge of the escarpment. The piston-flow hypothesis was further validated with an isotope-based assessment of water storage and release dynamics across the study watershed outlets. Very high fractions of old water, coupled with very short mean transit times at the edge of the escarpment, suggested a quick transmission of passive stores of old water in response to input precipitation. This behavior observed at the edge of the escarpment is consistent with response mechanisms akin to water pressure propagation. Through the synthesis of hydrometric data analysis results and isotopic data analysis results, a conceptual framework detailing the dominant flow processes prevailing in each of the studied watersheds has been suggested – with watersheds located above the escarpment experiencing dominant flow processes consistent with Hortonian overland flow while those located at the edge and below the escarpment experience vertical percolation of water and deep groundwater upwelling, respectively. This study showed value in combining many different assessment approaches when characterizing water storage and release dynamics, as the plausibility of different hypotheses could be evaluated on the basis of convergent and divergent conclusions reached via different assessment approaches.

ACKNOWLEDGMENTS

This thesis was made possible with the support and funding from the University of Manitoba Faculty of Graduate Studies; the Clayton H. Riddell Faculty of Environment, Earth, and Resources; the Department of Geological Sciences, the Department of Soil Science, and the Center for Earth Observation Science at the University of Manitoba; the Natural Sciences and Engineering Research Council of Canada (NSERC); Environment and Climate Change Canada; and Agriculture and Agri Food Canada (AAFC). I warmly thank my graduate-student colleagues, notably, Aminul Haque, Maliheh Rabie and Cody Ross, who helped me with site set-up, water sampling, and laboratory analyses. Special heartfelt gratitude goes to my advisor, Dr. Genevieve Ali, who meticulously guided me throughout my research. A big thank you to my advisory committee members, Drs. Chris Spence, Tricia Stadnyk, and Zou Zou Kuzyk for their immense support and advice during the course of this work. I also want to thank all the farmers, landowners and support staff at the Steppler Watershed of the South Tobacco Creek Watershed for allowing access to the research site. A huge thank you to my supportive wife, Gloria, my children Marvin, Medwin, and Michael for every sacrifice, their understanding and encouragements over the years. I am forever grateful to my late Dad, Solomon, my mom Mabel, my siblings Alexander, Maxwell, and Benedicta for their prayers and support throughout my life. To my uncle Lawrence Bribinti and Francis Bansah, I say a big thank you to you. My gratitude goes to all my great “lab mates” who worked with my advisor at different times during the course of my PhD work: Nicole Pogorzelec, Adrienne Schmall, Janelle Laing, Mathew Walker, Halya Petzold, Amber Penner, Jonathon Belanger - all these guys were helpful in my research work as well. I finally want to thank Erin Zoski, Don Cruikshank, Kelvin Hildebrandt, Larry Braul, Drs. Henry Wilson, Marcos Lemes, and David Lobb for all their support in making this work possible.

DEDICATION

This thesis is dedicated to my lovely and supportive wife Gloria Bansah

TABLE OF CONTENTS

LIST OF TABLES

LIST OF FIGURES

LIST OF APPENDICES

CHAPTER 1: BACKGROUND AND MOTIVATION

1.1 Introduction to water storage and release dynamics in watersheds

Understanding the transformation of precipitation into runoff is one of the primary goals of hydrology. Runoff is produced in response to a precipitation event and will typically be composed of not only water that already existed in the watershed before the onset of the current precipitation event, but also newly introduced water; the latter either infiltrates the soil and flows in the subsurface to join streams, or it flows overland into streams due to saturation-excess or infiltration-excess processes (e.g., Brooks et al., 2012; McDonnell, 2013). Water entering a watershed at one point is composed of water molecules that move with varying velocities, taking different flowpaths and hence spending different amounts of time in the watershed before reaching the outlet (McGuire and McDonnell, 2006). Subsequent pulses of introduced water can exhibit totally different flow characteristics and pathway behaviours. Thus, for similar precipitation events occurring at different times, the amount of water discharged to the outlet and associated flow characteristics are expected to vary.

Watershed hydrologic response to incoming water and energy fluxes is complex and highly nonlinear. This nonlinearity stems from, among other things, the fact that different flowpaths are active depending on water storage conditions (Heidbuchel et al., 2012). When water storage is low (compared to storage capacity), most incoming precipitation will go into satisfying the storage deficit after losses to evapotranspiration, and thus runoff response is minimal. When storage is high, infiltrating water can move quickly to saturated storage where it increases hydraulic head, inducing rapid evacuation of previously stored water (Sklash and Farvolden, 1979; McDonnell, 1990). At the same time, areas with near-saturated surface soils close to the channel network can cause saturation-excess overland flow and return flow during storm runoff (Dunne and Black, 1970). Under these conditions, the runoff response will be high. The occurrence of infiltration-excess overland flow during precipitation events of high intensity adds to the nonlinear nature of watershed response (Heidbuchel et al., 2012). In a nutshell, the

response of a watershed to introduced precipitation is dependent on, but not limited to, a combination and/or interplay of the following: 1) the amount of water already in storage in the vadose and saturated zones of the watershed, 2) the nature (whether snow or rain) and characteristics (such as intensity and duration) of introduced precipitation, 3) the type and amount of vegetation as well as the climatic conditions (these determine evapotranspiration), 4) the nature and characteristic of geologic formations in the watershed, 5) other landscape characteristics such as topography, and 6) the time of the year (i.e., season).

It is essential to examine the water storage and release characteristics of a watershed and, whenever possible, devise ways of estimating how much storage there is. This is important in understanding environmental water management issues related to diffuse pollution and nutrient transport to streams, clean-up times from pollution events, and flood prediction. Birkel et al. (2011) and Heidbuchel et al. (2012) have categorised watershed storage into two forms: 1) active or dynamic storage, that corresponds to the near-surface, short duration storage of rainwater or meltwater that can be released quickly as surface or near-surface runoff during events; and 2) passive storage, that corresponds to the long-duration and persistent storage of water in the saturated zone and is mainly associated with baseflow. Prior to that, Black (1997) and others had described the different types of water storage zones that coexist in a given landscape: storage on vegetation (canopy storage), in snowpacks, in small topographic depressions and wetlands, as well as in soils and bedrocks. It should be noted that even though many classification schemes refer to water storage zones as discrete entities, in reality these zones exist along a continuum, making it difficult to distinguish them. This is also true for water storage and release dynamics where “old” and “new” water may not have a clearly distinguishable age threshold above and below which they qualify as old or new.

Attempts have been made, with the use of large satellite-derived measurements (e.g., GRACE, see Rodell et al., 2009), to estimate storage and storage changes in watersheds. The use of other

conventional methods, in comparison to estimating water fluxes, can be challenging, thus making the study of watershed storage a difficult task until it recently started gaining grounds in watershed science (McNamara et al., 2011). This is mainly due to the fact that storage is characterised by marked spatial heterogeneity, thus making it difficult to perform point-scale measurements and then extrapolate them to the watershed scale (Spence, 2007; Soulsby et al., 2008; Seyfried et al., 2009). Inasmuch as it is becoming obsolete to effectively characterize a watershed by a fixed unit hydrograph (Brutsaert, 2005), it is often thought that watershed storage is greater than that which can be inferred solely by traditional hydrometric data analyses (Barnes and Bonell, 1996). For example, calculation of the annual water balance using hydrometric data alone may only illustrate changes in dynamic storage, which may be far less than the conservative tracer-inferred total storage (Soulsby et al., 2010). This brings to the fore the importance of the use of environmental tracers in watershed hydrology. Stable isotopes of oxygen and hydrogen (^{18}O, ^{16}O, ^{2}H and ^{1}H), which are part of the water molecule, have served as excellent tracers for several decades (Sklash and Farvolden, 1979; McDonnell, 1990; McGuire and McDonnell, 2006). Their use in hydrology has been effective in identifying source areas of water and water flowpaths from various storage zones (e.g., Ogunkoya and Jenkins, 1994; McDonnell, 2003; McDonnell et al., 2010; Klaus and McDonnell, 2013).

In recent years, several studies have aimed at presenting a better understanding of watershed scale storage dynamics in hilly to steep and/or quasi-pristine watersheds (Birkel et al., 2011; Tetzlaff et al.,2011; Heidbuchel et al., 2012) but not much has been investigated in Canadian prairie watersheds. The Canadian prairies, which stretch across the provinces of Alberta, Saskatchewan and Manitoba do not function the same way as high-relief, pristine watersheds. According to Fang et al. (2007), the Canadian prairies are characterised by a long cold winter period (greater than five months) as well as heterogeneous snowpacks that cover most of the land surface and flow channels over most of that period. The snowmelt period lasts for a relatively short period of time. After rainfall, flow is driven not by slope

gradient but often by a fill-and-spill runoff mechanism, especially in the Prairie Pothole Region that spans Saskatchewan as well as Western Manitoba. Coming towards Central Manitoba and to the east of it, however, potholes are essentially nonexistent over the flat terrain, thus making the dynamics of flow even more complex. The central and eastern portions of the Canadian prairies are characterized by rolling to flat topography, many forested riparian areas, and a sub-humid to semi-arid climatic regime with alternating years of floods and droughts. The region is further impacted by many man-made stormwater control structures such as drainage ditches, farm dams, and drained wetlands. These peculiar features of the prairie landscape strengthen the argument towards conducting research that will enhance our understanding of surface and subsurface flow characteristics emanating from water storage and release dynamics in the region.

1.2 Thesis research objectives

This Ph.D. thesis focuses on water storage and release dynamics in a prairie watershed. It is guided by the following three major research objectives that have yet to be addressed in cold prairie regions, namely to:

1) formulate a qualitative baseline contextualisation of water storage and release dynamics using hydrometric data;

2) determine the fractions of "new" and "old" water in event hydrographs in order to infer dominant runoff pathways (i.e., surface versus shallow and deep subsurface flowpaths) and their spatiotemporal variability; and

3) determine the mean transit time (MTT) of water and assess if the water age and transit time estimation methods that are widely used in high-relief watersheds are also applicable in a prairie context.

Detailed justifications for those three thesis objectives are provided in the next section.

1.3 Rationale behind the thesis research objectives

Thesis objective #1: *formulate a qualitative baseline contextualisation of water storage and release dynamics using hydrometric data*

Hydrometric approaches, mainly involving the use of precipitation and streamflow time series data, have been key to our understanding of watershed functioning and processes over the past decades (Stahl et al., 2010; Wilson et al., 2010; Karlsson et al., 2014). Various analyses have been conducted with the aid of hydrometric data to help understand hydrologic systems but their use for quantifying watershed water storage and release dynamics is relatively limited. Recent attempts at using hydrometric data to help contextualise watershed water storage and release dynamics have involved analyses targeted at baseflow separation and computations of baseflow indices on mainly seasonal and annual timescales (Yaeger et al., 2012; Buttle, 2016; Miller et al., 2016). Other approaches included analyses of seasonal and annual runoff ratios, flow duration curves, and the superimposition of these results on climate indices such as the aridity index, the seasonality index, etc. (e.g., Yuan et al., 2001; Baltas et al., 2007; McNamara et al., 2011; Cheng et al., 2012; Coopersmith et al., 2012; Yaeger et al., 2012; Buttle, 2016; Buttle, 2018). While many individual hydrometric data analysis techniques (e.g., hydrograph analysis, flow frequency analysis, dryness index analysis, etc.) can only partially inform us about water storage and release dynamics (Yuan et al., 2001; McNamara et al., 2011), the literature does not report on attempts at combining these individual techniques to gain more insights into those dynamics. Using a multi-technique approach based on hydrometric data may, indeed, provide a first-order approximation of passive and active storage release dynamics, which would be especially valuable in a prairie watershed context. The present Ph.D. thesis therefore tests such a multi-technique approach as a way to confront different lines of evidence and put forward qualitative hypotheses related to watershed water storage and release dynamics.

Thesis objective #2: *determine the fractions of "new" and "old" water in event hydrographs in order to infer dominant runoff travel pathways (i.e., surface versus shallow and deep subsurface flowpaths) and their spatiotemporal variability*

The recharge, storage and discharge characteristics of a watershed are reflected by the watershed's behaviour both during and between precipitation events. Surface runoff resulting from storm events is of major concern to engineers responsible for routing of water through channels, drainage systems and natural waterways (Clark and Fritz, 1997). The interaction between surface water, soil water and deep groundwater during a storm event is also an important aspect of contaminant transport in soils (Iqbal, 1998). The total volume of precipitation water that infiltrates into the subsurface and the volume that makes overland flow play a key role in vertical leaching of contaminants from surface to the water table (Iqbal, 1998). It is thus very important to consider proportions of precipitation that recharge groundwater (i.e., passive storage) and those that are temporarily stored in the vadose zone to be released later as surface and shallow subsurface runoff (i.e., active storage). Water that flows to streams during or after a precipitation event can, therefore, be made of "old water" (i.e., water that is stored in the watershed prior to the event) and "new water" (i.e., water brought in by the current precipitation event) Sklash and Farvolden, 1979; McDonnell, 1990). While passive storage is solely made of "old' water from deep soil layers or rock, active storage can be a mixture of both "old" water (from shallower, saturated soil layers) and "new" water.

Hydrograph separation (HS) is a technique designed to differentiate, in relative terms, the contributions of "old" and "new" water to storm hydrographs (Sklash and Farvolden, 1979; Buttle, 1994, 2005). The importance of performing HS for any given watershed is two-fold: 1) it provides information about the dominant pathways via which water flows to the outlet during a precipitation event, which is crucial in assessing how connected a watershed is to storage sources, and 2) it may help infer the major sources of contaminants/nutrients that flow into the outlet during storm events. The idea of runoff source

apportionment was notably suggested by Hewlett and Hibbert (1967), who proposed a variable source area concept which sought to answer questions regarding the path and destination of water during a storm event. However, it is only later that HS was suggested as a tangible method to infer the sources and destination of water during an event. Sklash and Farvolden (1979) proposed that pre-event (i.e., old) water forms a significant proportion of peak flow in an event hydrograph, based on information provided by environmental tracers. Earlier attempts to quantify the fraction of this pre-event water relied on the use of ionic tracers such as chloride, silica and calcium (Pinder and Jones, 1969; Kennedy, 1971), with the assumption that those tracers behaved in a conservative manner. The chemical characteristics of conservative tracers, as they move through watersheds, are supposed to remain unaffected by water transport processes but that is rarely the case with ions. Indeed, the majority of chemicals either undergo reactions with other salts, change state by precipitation and thus don't leave the watershed at all, or are taken up by biota (Kirchner et al., 2010; Svensson et al., 2012). Notably, chloride is known to be chemically inert but it is still used up by biota to some degree (Svensson et al., 2012). In contrast, the use of stable isotopes (i.e., $\delta^{18}O$ and $\delta^{2}H$) as conservative tracers has proved to be an effective tool in differentiating the event water (new water) component from the pre-event water (old water) (Jenkins et al., 1994; Iqbal, 1998; Brown et al., 1999). Isotope-based HS has the advantage of separating stream hydrographs into components according to a qualitative assessment of water age (i.e., "old" water and "new"), as opposed to graphical hydrograph separation that rather partitions stream hydrographs into baseflow and stormflow components (Sklash and Farvolden, 1979). However, while isotope-based HS has been carried out in various landscapes and climatic regions across the world (Jenkins et al., 1994; Ogunkoya and Jenkins, 1994; Uhlenbrook et al., 2002; McDonnell, 2003; McDonnell et al., 2010; Klaus and McDonnell, 2013), its use has been very limited to nonexistent in cold prairie watersheds. By making isotope-based HS a key research objective, the present Ph.D. thesis therefore aims to enhance our

understanding of the relative importance of active versus passive storage in prairie landscapes, this by quantifying the relative proportions of old and new water in event hydrographs.

Thesis objective #3: *determine the mean transit time (MTT) of water and assess if the water age and transit time estimation methods that are widely used in high-relief watersheds are also applicable in a Prairie context*

Watershed hydrologists, over the past few decades, have concerned themselves with questions such as: where water goes after a precipitation event, what flowpaths does water take to the stream, and how long does water reside in a watershed (Stewart et al., 2010). Answers to these questions are critical to our understanding of how a watershed retains and releases water and solutes that, in turn, control geochemical and biogeochemical cycling and contaminant persistence (McGuire and McDonnell, 2006; McDonnell et al., 2010). Evaluations of streamflow generation processes (Wolock et al., 1997; Kendall and McDonnell, 1998; McGuire and McDonnell, 2006), weathering rates in watersheds (Pacheco and Van der Weijden, 2012; Frisbee et al., 2013), timescales of ecological processes (Brunke and Gonser, 1997; Hancock et al., 2005) and watershed response to climate change (Rademacher et al., 2005; Singleton and Moran, 2010; Manning et al., 2012) have all been aided by the estimation of transit times of water in a watershed. The transit time is defined as the time water spends travelling from an input point (e.g., surface of the watershed after a precipitation event) to an output point (e.g., stream at the watershed outlet) via flowpaths in a watershed (McGuire and McDonnell, 2006; McDonnell and Beven, 2014). The interest in watershed transit time distributions stems from the fact that streamflow measured at a particular gauging point along a stream channel is an integrated response to: (1) spatially and temporally varying water input rates; (2) the time it takes for a given "drop" of water to travel from where it enters a watershed to where it first enters a stream network; (3) the time it takes for the water to travel from where it first enters a stream channel to the point of measurement (Figure 1-1).

The determination of the mean transit time (MTT), which is the average time spent by water molecules in a watershed, is via analysis of transit time distributions (TTDs). Because water molecules that enter a watershed at a point will spend different amounts of time in the watershed before exiting it, they are governed by different transit times which, when combined at the watershed scale, result in TTDs. These TTDs are, therefore, akin to probability density functions. Since tracers are widely used to characterize flowpaths and estimate groundwater velocities (Divine and McDonnell, 2005), they are natural tools to support the modelling of TTDs.

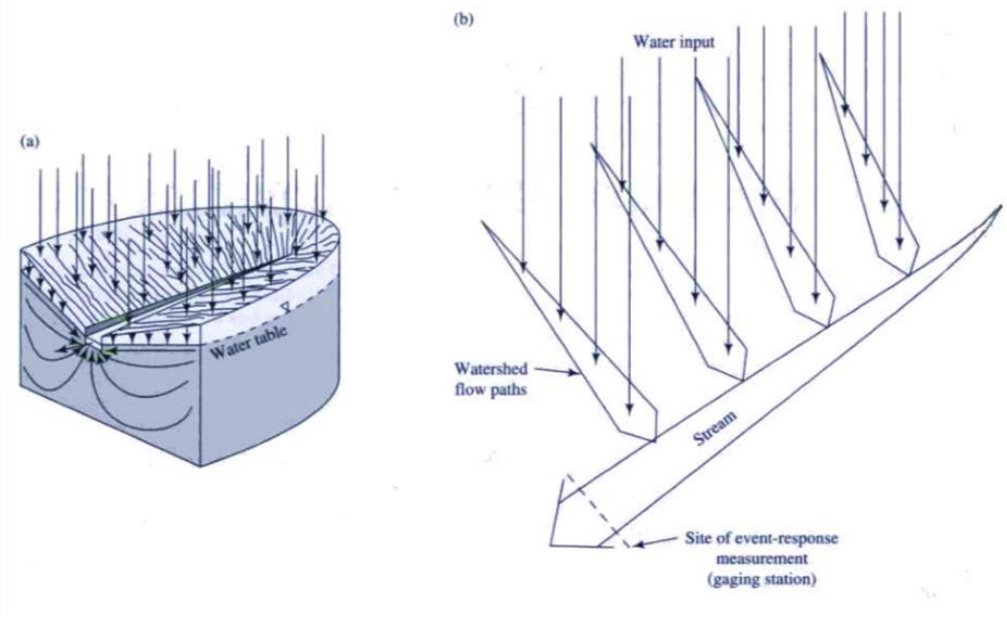

Figure 1-1. Schematic representation of watershed response to precipitation. (a) precipitation input onto a watershed, (b) flowpaths of various parcels of water traveling to the sampling point (from Dingman, 2002).

Stable isotopic ratios ($^{18}O/^{16}O$, $^{2}H/^{1}H$) as well as radioactive isotopes, such as ^{3}H, have been used extensively in many MTT modeling exercises in various watersheds of different sizes and physiographic characteristics across the globe (Jenkins et al., 1994; Ogunkoya and Jenkins, 1994; Uhlenbrook et al., 2002; McDonnell, 2003; McDonnell et al., 2010; Klaus and McDonnell, 2013; Frisbee et al., 2013). However, limited studies have been carried out to compute MTTs in the Canadian prairies. The present Ph.D. thesis, therefore, uses the unique opportunity offered by prairie landscapes to examine watershed transit time estimation methods and their underlying assumptions in a challenging environment that has, to date, been largely omitted from the transit time modelling literature.

1.4 Study Area

1.4.1 Location

The area chosen for this Ph.D. study is the South Tobacco Creek Watershed (STCW), located in south central Manitoba, about 150 km southwest of Winnipeg. It is situated on the eastern edge of the Manitoba Escarpment (also referred to as the Pembina Escarpment), which originated approximately 50 to 84 million years ago as a result of the Laramide Orogeny and is composed mainly of Cretaceous sedimentary beds. The STCW has a drainage area of about 74.6 km^2 with its headwaters originating from the Pembina Hills and its outlet near the town of Miami, Manitoba. From the outlet, the South Tobacco Creek flows east into the Tobacco Creek, which continues east to drain into the Morris River. The Morris River drains into the Red River near Morris before draining north into Lake Winnipeg. Within the STCW is the Steppler watershed which constitutes some of the STCW headwaters (Figure 1-2). It is described separately here because it houses hydrometric research equipment from Environment Canada (EC) and Agriculture and Agri-Food Canada (AAFC) as part of the Watershed Evaluation of Beneficial Management Practices (WEBs) project. The WEBs project was initiated in 1991 to examine the

environmental and economic impacts of beneficial management practices (BMPs) at a small watershed scale. The Steppler watershed is also located within a single farm operation, with each individual field boundary being aligned with the boundaries of 9 sub-watersheds within it. Six of the outlets chosen for this study (referred to as “MS” sites) are located within the Steppler watershed. Water quality is used as the primary indicator of the environmental impact of the BMPs in each of those fields (or sub-watersheds).

1.4.2 Geology, soils, and climate

The STCW is dominated by an undulating and hummocky topography and a well-developed drainage system consisting of various channels, gullies and moderately steep slopes. The STCW provides a mix of different landscapes namely: 1) an undulating terrain above the escarpment; 2) the escarpment itself; and 3) flatter plains below the escarpment. The Pembina escarpment had its origin approximately 50 to 84 million years ago because of the Laramide Orogeny (Matile and Keller, 2004; Tiessen et al., 2010). The escarpment causes an elevation drop of approximately 200 m between the STCW headwaters and its outlet near the town of Miami (Figure 1-2). This site therefore offers the opportunity to compare hydrological dynamics in landscapes with rolling topography as well as in flatter landscapes that are typical of the Eastern Canadian prairies. The STCW is predominantly underlain by shale, sandstone, limestone, carbonates and evaporates. The surficial geology is predominantly calcareous silt diamicton with minor eolian deposits, alluvial sediments, colluvium, distal glaciofluvial sediments and marginal glaciolucustrine sediments (Matile and Keller, 2004). Glacial debris deposited as moraines during successive glaciations also form the escarpment, marking the boundary of Glacial Lake Agassiz (Bamburak and Christopher, 2004).

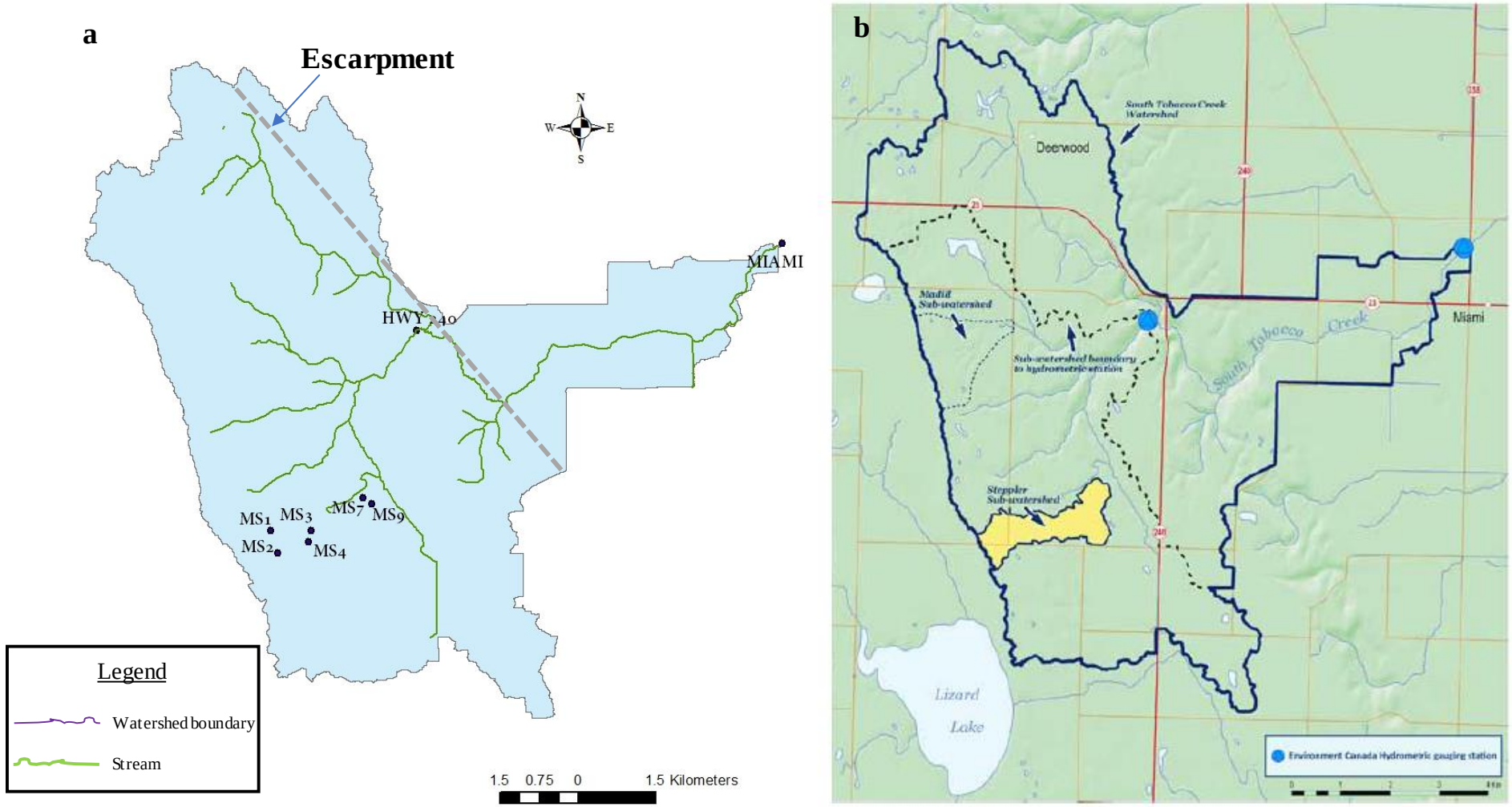

Figure 1-2. (a) The South Tobacco Creek Watershed with the eight outlets considered in the present Ph.D. study and the escarpment. (b) The Steppler watershed (in yellow) houses the "MS" sites (from AAFC WEBs, 2010).

Cold lengthy winters and short cool summers are common in southern Manitoba; the climate in the STCW is classified as sub-humid continental (Tiessen et al., 2010). Long-term mean annual temperature is ~ 3^{o}C and the annual precipitation is ~ 550 mm, 25 to 30% of which is snowfall (Li et al., 2011). Areas above the escarpment are considered slightly cooler (1.9^{o}C versus 3.3^{o}C since 1982) and receive slightly more precipitation (596 mm versus 530 mm since 1982) than areas below the escarpment (Environment Canada, 1982). Crops cultivated in the watershed include wheat, canola, oat, barley, corn and flax, with wheat, corn, and canola being the dominant crops. There are small dams within the watershed designed as part of the EC/AAFC BMPs projects and are built as holding ponds to primarily prevent nutrient loading and flooding downstream.

1.4.3 Field equipment and installations

For the present Ph.D. study, eight outlets (Figure 1-2) were chosen within the STCW so that the three thesis objectives previously described could be examined across eight nested sub-watersheds. The outlets were chosen to coincide with WEBs monitoring stations in order to benefit from already deployed hydrometric and water sampling instrumentation. Specifically, the sub-watersheds referred to as MS1, MS2, MS3, MS4, MS7 and MS9 are located within the Steppler watershed, in the southwestern corner of the STCW above the escarpment and near the headwaters of the South Tobacco Creek. The sub-watershed referred to as HWY240 occupies the western half of the larger STCW and spans across the escarpment, while Miami is the outlet for the entire STCW (Figure 1-2). The weather station used for this project was located about 800 m northwest of the MS9 outlet.

Flow is measured at HWY240 and Miami via a rectangular weir installed by EC as those are standard Water Survey of Canada gauging stations. The frequency of measurement is every 30 minutes. Within the Steppler watershed, a combination of V-notched weirs and water level loggers is used to

determine flow at the outlet of each subwatershed. Autosamplers placed at the outlets of each sub-watershed collect surface water on an event basis: these samplers are automatically triggered to collect water into sampling bottles whenever there is flow in the channel. A logger registers the date, time, and the portion of hydrograph each collected sample is coming from. In addition to the existing WEBs research equipment, field installations also took place in spring 2014. Nested pairs of shallow (screened from the surface down to 60 cm) and deep (screened at a depth of 1.5 m) piezometers were installed in the riparian areas adjacent to selected WEBs monitoring stations, namely Miami, HWY240, MS7 and MS9. Sites MS1, MS2, MS3 and MS4 were each equipped with a shallow piezometer; however only one deep piezometer was installed in the area and assumed to be representative of all four sub-watersheds due to their spatial proximity to each other. Throughfall collectors were also deployed in all eight sub-watersheds in early June 2014 for the purposes of collecting rainwater samples. Snow and snowmelt samples were collected from installed lysimeters throughout the STCW.

1.4.4 Data acquisition and laboratory analyses

During the 2014 and 2015 sampling years, the automatic water samplers located at the outlet of each of the eight watershed/sub-watersheds collected several dozens of storm-based stream water samples. This was especially important to capture major events in 2014, which was a flood year (June-July floods) in Manitoba. In addition, rainwater samples, depth-specific soil water samples (from the shallow and deep piezometers), and grab streamwater samples were collected once a week until the end of each field season. Since the automatic water samplers associated with the WEBs project mostly collect water samples during major hydrological events, the weekly collection of grab streamwater samples ensured that periods between events would also be represented in the dataset. Over the two years, the different types of samples, including baseflow samples, totalled 1114 and covered a total of 47 and 53 hydrological events respectively for the 2014 and 2015 sampling years. All snow and water samples were

analysed for $\delta^{18}O$ and $\delta^{2}H$ using a Picarro Liquid Water Isotope Analyzer (LWIA) based on Cavity Ring-Down Spectroscopy (CRDS) technology. δ values were recorded in permil (‰) deviations from the Vienna Standard Mean Ocean Water (VSMOW) (Craig, 1961).

With regards to streamflow information at each of the eight selected outlets, data was obtained from the AAFC staff working on the WEBs project and managing the hydrometric equipment in the field. Real-time (i.e., updated every 30 minutes), provisional flow and water level data is also provided online by Environment Canada for stations G05OF017 and G05OF023 that correspond to the Miami and HWY240 sites since 1961; those provisional data were, however, not used for analyses. Instead, operational flow data provided at the end of each year were used. Rainfall and snow survey data were also obtained from the AAFC WEB's project. The WEBs weather station houses the rainguage and records daily rainfall throughout the year.

1.5 Significance of the Ph.D. study

Our understanding of watershed water storage and release mechanisms has been limited to quasi-pristine hillslopes and small watersheds where flow is primarily driven by topography. Considering the unique nature of the Canadian prairies where human impacts (e.g., agricultural activities) are present across a range of topographies (e.g., steep, hummocky, flat), it is obvious there are knowledge gaps when it comes to our understanding of storage and release mechanisms in such watersheds. The presence of roads, surface drains, small dams, and numerous agricultural activities that are characteristic of the prairies provide a unique opportunity for exploring storage concepts in a region where both natural water storage and infrastructure-driven water storage are present at the watershed scale. Knowing the partitioning of "new" and "old" water at the watershed outlet as well as the transit times will be vital in evaluating water management strategies. Our understanding of how watersheds in the prairies are responding to climate change, contaminant persistence, as well as strategies of remediation could be

informed by the outcomes of this study. This Ph.D. study is novel in the context of prairie watersheds and will serve as a useful tool in the assessment of water supply, flood prediction/forecasting, land management planning, and water quality issues.

1.6 Structure of Ph.D. thesis

This thesis has been prepared in the manuscript format, according to guidelines established by the Department of Geological Sciences at the University of Manitoba. The first chapter introduces the topic, the major research themes to be considered, and the general outline of the thesis. Chapters 2, 3, and 4 form the major data chapters of the thesis and have been structured as three separate manuscripts, each geared towards meeting the objectives stated in Chapter 1. Chapter 2 is a manuscript to be reorganised and submitted to a journal for publication at a later date. Chapters 3 and 4 have been published in the journals *Water Resources Research* and *Hydrological Processes*, respectively:

> Bansah, S. and Ali, G. (2017) Evaluating the effects of tracer choice and end-member definitions on hydrograph separation results across nested, seasonally cold watersheds. *Water Resources Research,53.* https://doi.org/10.1002/2016WR020252.

> Bansah, S. and Ali, G. (2019) Streamwater Ages in Nested, Seasonally Cold Canadian Watersheds. *Hydrological Processes*. 2019;1–17. https://doi.org/10.1002/hyp.13373

The two published chapters have been reformatted from the published versions for inclusion in this thesis. Chapter 5 provides a synthesis of the major findings of Chapters 2, 3, and 4, as well as discussions of the links between the findings detailed in each manuscript. Discussions of the limitations of this work and recommendations for future work are also included in Chapter 5. Chapter 1 was written by me with

suggested revisions from my advisor. The hydrometric data was obtained from Agriculture and Agri-Food Canada and the event delineation in Chapter 2 was performed by Weigang Tang, while the remainder of the analysis was done by me. Chapters 2, 3 and 4 were written by me with suggested revisions from my advisor. All the field set up and instrumentations, sample collection and laboratory analysis, and the data processing detailed in Chapters 3 and 4 were undertaken by me. The data analysis and discussion that make up Chapter 5 were undertaken by me with guidance from my advisor.

1.7 References

Agriculture and Agri-Food Canada (2010) Watershed Evaluation of Beneficial Management Practices. Technical summary #1: Biophysical Component. pp.18-19.

Alexander, R. B., Boyer, E. W., Smith, R. A., Schwarz, G. E., & Moore, R. B. (2007). The role of headwater streams in downstream water quality. *Journal of the American Water Resources Association, 43*(1), 41-59. doi:10.1111/j.1752-1688.2007.00005.

Baltas, E.A., Dervos, N.A., & Mimikou, M.A. (2007). Technical Note: Determination of the SCS initial abstraction ratio in an experimental watershed in Greece, *Hydrology and Earth System Sciences, 11*(6), 1825-1829.

Bamburak, J.D. & Christopher, J.E. (2004). Mesozoic stratigraphy of the Manitoba Escarpment; WCSB/TGI II, Fieldtrip Guidebook, September 7-10, 2004, 87pp.

Barnes, C. J., & Bonell, M. (1996). Application of unit hydrograph techniques to solute transport in catchments. *Hydrological Processes, 10*(6), 793-802.

Birkel, C., Soulsby, C., & Tetzlaff, D. (2011). Modelling catchment-scale water storage dynamics: reconciling dynamic storage with tracer-inferred passive storage. *Hydrological Processes, 25*(25), 3924-3936. doi:10.1002/hyp.8201.

Birkel, C., Soulsby, C., Tetzlaff, D., Dunn, S., & Spezia, L. (2012). High-frequency storm event isotope sampling reveals time-variant transit time distributions and influence of diurnal cycles. *Hydrological Processes, 26*(2), 308-316. doi:10.1002/hyp.8210.

Black, P.E. (1997). Watershed functions, *Journal of the American Water Resources Association, 33*(1), 1-11.

Brooks, K.N., Ffolliott, P.F., & Magner, J.A. (2012). Infiltration, pathways of water flow, and recharge. In: *Hydrology and the management of watersheds*, 4th ed., pp113-140. doi: 10.1002/9781118459751.ch5.

Brown, V. A., McDonnell, J. J., Burns, D. A., & Kendall, C. (1999). The role of event water, a rapid shallow flow component, and catchment size in summer stormflow. *Journal of Hydrology, 217*(3-4), 171-190. doi:10.1016/s0022-1694(98)00247-9.

Brunke, M., & Gonser, T. (1997). The ecological significance of exchange processes between rivers and groundwater. *Freshwater Biology, 37*(1), 1-33. doi:10.1046/j.1365-2427.1997.00143.

Brutsaert, W. (2005). Hydrology: An introduction. Cambridge University Press, Cambridge, U.K. 435pp.

Buttle, J.M. (1994). Isotope hydrograph separations and rapid delivery of pre-event water from drainage basins. Progress in Physical Geography, 18(1), 16–41.

Buttle, J.M. (2005). Isotope hydrograph separation of runoff sources. In M. G. Anderson (Ed.), Encyclopedia of hydrological sciences (pp. 1763–1744). New York, NY: John Wiley.

Buttle, J.M. (2016). Dynamic storage: a potential metric of inter-basin differences in storage properties, *Hydrological Processes*, *30*(24), 4644-4653.

Buttle, J.M. (2018). Mediating stream baseflow response to climate change: The role of basin storage, *Hydrological Processes*, *32*(2018), 363-378.

Cheng, L., Yaeger, M., Viglione, A., Coopersmith, E., Ye, S. & Sivapalan M. (2012). Exploring the physical controls of regional patterns of flow duration curves - Part 1: Insights from statistical analyses, *Hydrology and Earth System Sciences*, *16*(11), 4435-4446.

Clark, I. & Fritz, P. (1997). Environmental isotopes in hydrogeology. Lewis publishers, NY. 328pp.

Clearwater, L. (2010). Watershed evaluation of beneficial management practices (WEBs). Four year review (2004/5 – 2007/8); Agriculture and Agri-Food Canada, 50pp.

Coopersmith, E., Yaeger, M.A., Ye, S., Cheng, L. & Sivapalan, M. (2012). Exploring the physical controls of regional patterns of flow duration curves - Part 3: A catchment classification system based on regime curve indicators, *Hydrology and Earth System Sciences*, *16*(11), 4467-4482.

Craig, H. (1961). Standard for reporting concentrations of deuterium and oxygen-18 in natural waters. *Science*, 133: (1833). doi: 10.1126/science.133.3467.1833.

Divine, C. E., & McDonnell, J. J. (2005). The future of applied tracers in hydrogeology. *Hydrogeology Journal, 13*(1), 255-258. doi:10.1007/s10040-004-0416-3.

Dingman, S.L. (2002). Physical Hydrology. Volume 1. Princeton Hall, NJ. 646pp.

Dunne, T., & Black, R. D. (1970). Partial area contributions to storm runoff in a small New-England watershed. *Water Resources Research, 6*(5), 1296-&. doi:10.1029/WR006i005p01296.

Efron, B., & Gong, G. (1983). A leisurely look at the bootstrap, the jackknife, and cross-validation. *American Statistician, 37*(1), 36-48. doi:10.2307/2685844.

Fang, X., Minke, A., Pomeroy, J., Brown, T., Westbrook, C., Guo, X., & Guangul, S. (2007). A review of Canadian Priaire Hydrology: Principles, Modelling and response to Land Use and Drainage Change. Center for Hydrology Report #2, Version2. University of Saskatchewan.

Frisbee, M. D., Phillips, F. M., White, A. F., Campbell, A. R., & Liu, F. (2013). Effect of source integration on the geochemical fluxes from springs. *Applied Geochemistry, 28*, 32-54. doi:10.1016/j.apgeochem.2012.08.028.

Hancock, P. J., Boulton, A. J., & Humphreys, W. F. (2005). Aquifers and hyporheic zones: Towards an ecological understanding of groundwater. *Hydrogeology Journal, 13*(1), 98-111. doi:10.1007/s10040-004-0421-6.

Heidbuechel, I., Troch, P. A., Lyon, S. W., & Weiler, M. (2012). The master transit time distribution of variable flow systems. *Water Resources Research, 48*. doi:10.1029/2011wr011293.

Hewlett, J. D. & Hibbert, A. R. (1967). Factors affecting the response of small watersheds to precipitation in humid areas, in: Proceedings of the International Symposium on Forest Hydrology, Pergamon, New York, p. 275-290.

Hrachowitz, M., Soulsby, C., Tetzlaff, D., Dawson, J. J. C., & Malcolm, I. A. (2009). Regionalization of transit time estimates in montane catchments by integrating landscape controls. *Water Resources Research, 45*. doi:10.1029/2008wr007496.

Hrachowitz, M., Soulsby, C., Tetzlaff, D., Malcolm, I. A., & Schoups, G. (2010). Gamma distribution models for transit time estimation in catchments: Physical interpretation of parameters and implications for time-variant transit time assessment. *Water Resources Research, 46*. doi:10.1029/2010wr009148.

Iqbal, M. Z. (1998). Application of environmental isotopes in storm-discharge analysis of two contrasting stream channels in a watershed. *Water Research, 32*(10), 2959-2968. doi:10.1016/s0043-1354(98)00070-0.

Jenkins, A., Ferrier, R. C., Harriman, R., & Ogunkoya, Y. O. (1994). A case-study in catchment hydrochemistry-conflicting interpretations from hydrological and chemical observations. *Hydrological Processes, 8*(4), 335-349. doi:10.1002/hyp.3360080406.

Karlsson, I. B., Sonnenborg, T. O., Jensen, K. H., & Refsgaard, J.C. (2014). Historical trends in precipitation and stream discharge at the Skjern River catchment, Denmark. *Hydrology and Earth System Sciences*, 18, 595–610. doi:10.5194/hess-18-595-2014.

Kendall, C. & McDonnell, J. J. (1998). Isotope tracers in watershed hydrology. Elsevier Science B.V., Amsterdam Netherlands, 870 pp.

Kennedy, V. C. (1971). Silica variation in stream water with time and discharge. *Advances in Chemistry Series*(106), 94-106.

Khakbazan, M., Hamilton, C., Elliott, J., & Yarotski, J. (2013). Economic analysis of agricultural nutrient management practices in the South Tobacco Creek Watershed in Manitoba, Canada. *Journal of Soil and Water Conservation, 68*(4), 257-269. doi:10.2489/jswc.68.4.257.

Kirchner, J. W. (2009). Catchments as simple dynamical systems: Catchment characterization, rainfall-runoff modeling, and doing hydrology backward. *Water Resources Research, 45*. doi:10.1029/2008wr006912.

Kirchner, J. W., Tetzlaff, D. & Soulsby, C. (2010). Comparing chloride and water isotopes as hydrological tracers in two Scottish catchments. *Hydrological Processes*, 24, 1631–1645 (2010). doi: 10.1002/hyp.7676.

Klaus, J. & McDonnell, J. J. (2013). Hydrograph separation using stable isotopes: Review and evaluation. *Journal of Hydrology*, 505 (2013), 47-64. http://dx.doi.org/10.1016/j.jhydrol.2013.09.006.

Li, S., Elliott, J. A., Tiessen, K. H. D., Yarotski, J., Lobb, D. A., & Flaten, D. N. (2011). The Effects of Multiple Beneficial Management Practices on Hydrology and Nutrient Losses in a Small Watershed in the Canadian Prairies. *Journal of Environmental Quality, 40*(5), 1627-1642. doi:10.2134/jeq2011.0054.

Liu, K., Elliott, J. A., Lobb, D. A., Flaten, D. N., & Yarotski, J. (2013). Critical Factors Affecting Field-Scale Losses of Nitrogen and Phosphorus in Spring Snowmelt Runoff in the Canadian Prairies. *Journal of Environmental Quality, 42*(2), 484-496. doi:10.2134/jeq2012.0385.

Lyon, S. W., Desilets, S. L. E., & Troch, P. A. (2008). Characterizing the response of a catchment to an extreme rainfall event using hydrometric and isotopic data. *Water Resources Research, 44*(6). doi:10.1029/2007wr006259.

Maloszewski, P., & Zuber, A. (1982). Determining the turnover time of groundwater systems with the aid of environmental tracers .1. models and their applicability. *Journal of Hydrology, 57*(3-4), 207-231.

Manning, A. H., Clark, J. F., Diaz, S. H., Rademacher, L. K., Earman, S., & Plummer, L. N. (2012). Evolution of groundwater age in a mountain watershed over a period of thirteen years. *Journal of Hydrology, 460,* 13-28. doi:10.1016/j.jhydrol.2012.06.030.

Martinec, J. (1975). Subsurface flow from snowmelt traced by tritium. *Water Resources Research, 11*(3), 496-498. doi:10.1029/WR011i003p00496.

Matile, G. L. D., & Keller, G.R. (2004). Surficial geology of the Brandon map sheet (NTS 62G), Manitoba Geological Survey, Surficial Geology Compilation Map Series, SG-62G, scale 1:250,000.

McDonnell, J. J. (1990). A rationale for old water discharge through macropores in a steep, humid catchment. *Water Resources Research, 26*(11), 2821-2832. doi:10.1029/WR026i011p02821.

McDonnell, J. J., & Beven, K. (2014). Debates-The future of hydrological sciences: A (common) path forward? A call to action aimed at understanding velocities, celerities and residence time distributions of the headwater hydrograph. *Water Resources Research, 50*(6), 5342-5350. doi:10.1002/2013wr015141.

McDonnell, J. J., McGuire, K., Aggarwal, P., Beven, K. J., Biondi, D., Destouni, G., Wrede, S. (2010). How old is streamwater? Open questions in catchment transit time conceptualization, modelling and analysis. *Hydrological Processes, 24*(12), 1745-1754. doi:10.1002/hyp.7796.

McDonnell, J. J. (2013). Are all runoff processes the same? *Hydrological processes*, 27 (4103-4111), https://doi.org/10.1002/hyp.10076.

McDonnell, J. J. (2003). Where does water go when it rains? Moving beyond the variable source area concept of rainfall-runoff response. *Hydrological processes*, 17 (1869-1875), https://doi.org/10.1002/hyp.5132.

McGlynn, B. L., McDonnel, J. J., & Brammer, D. D. (2002). A review of the evolving perceptual model of hillslope flowpaths at the Maimai catchments, New Zealand. *Journal of Hydrology, 257*(1-4), 1-26. doi:10.1016/s0022-1694(01)00559-5.

McGuire, K. J., & McDonnell, J. J. (2006). A review and evaluation of catchment transit time modeling. *Journal of Hydrology, 330*(3-4), 543-563. doi:10.1016/j.jhydrol.2006.04.020.

McGuire, K. J., McDonnell, J. J., Weiler, M., Kendall, C., McGlynn, B. L., Welker, J. M., & Seibert, J. (2005). The role of topography on catchment-scale water residence time. *Water Resources Research, 41*(5). doi:10.1029/2004wr003657.

McNamara, J. P., Tetzlaff, D., Bishop, K., Soulsby, C., Seyfried, M., Peters, N. E., Hooper, R. (2011). Storage as a Metric of Catchment Comparison. *Hydrological Processes, 25*(21), 3364-3371. doi:10.1002/hyp.8113.

Miller, P.M., Buto, S. G., Susong, D.D. & Rumsey, C. A. (2016). The importance of base flow in sustaining surface water flow in the Upper Colorado River Basin, *Water Resources Research, 52,* doi:10.1002/2015WR017963.

Mohamoud, Y. M. (2008). Prediction of daily flow duration curves and streamflow for ungauged catchments using regional flow duration curves, *Hydrological Sciences Journal-Journal Des Sciences Hydrologiques, 53*(4), 706-724.

Mosley, M. P. (1979). Streamflow generation in a forested watershed, New-Zealand. *Water Resources Research, 15*(4), 795-806. doi:10.1029/WR015i004p00795.

Mosley, M. P. (1982). Subsurface flow velocities through selected forest soils, South Island, New-Zealand. *Journal of Hydrology, 55*(1-4), 65-92. doi:10.1016/0022-1694(82)90121-4.

Nippgen, F., McGlynn, B. L., Marshall, L. A., & Emanuel, R. E. (2011). Landscape structure and climate influences on hydrologic response. *Water Resources Research, 47*. doi:10.1029/2011wr011161.

Ogunkoya, O. O. & Jenkins, A. (1993). Analysis of storm hydrograph and flow pathways using a three-component hydrograph separation model. *Journal of hydrology* 142, 1-4, 71-88.

Pacheco, F. A. L., & Van der Weijden, C. H. (2012). Integrating topography, hydrology and rock structure in weathering rate models of spring watersheds. *Journal of Hydrology, 428*, 32-50. doi:10.1016/j.jhydrol.2012.01.019.

Pinder, G. F., & Jones, J. F. (1969). Determination of the groundwater component of peak discharge from the chemistry of total runoff. Journal of water resources research, volume 5, No 2, pp.438-445.

Rademacher, L. K., Clark, J. F., Clow, D. W., & Hudson, G. B. (2005). Old groundwater influence on stream hydrochemistry and catchment response times in a small Sierra Nevada catchment: Sagehen Creek, California. *Water Resources Research, 41*(2). doi:10.1029/2003wr002805.

Roa-Garcia, M. C., & Weiler, M. (2010). Integrated response and transit time distributions of watersheds by combining hydrograph separation and long-term transit time modeling. *Hydrology and Earth System Sciences, 14*(8), 1537-1549. doi:10.5194/hess-14-1537-2010.

Rodell, M., Velicogna, I., & Famiglietti, J. S. (2009). Satellite-based estimates of groundwater depletion in India. *Nature, 460*(7258), 999-U980. doi:10.1038/nature08238.

Seyfried, M. S., Grant, L. E., Marks, D., Winstral, A., & McNamara, J. (2009). Simulated soil water storage effects on streamflow generation in a mountainous snowmelt environment, Idaho, USA. *Hydrological Processes, 23*(6), 858-873. doi:10.1002/hyp.7211.

Shaman, J., Stieglitz, M., & Burns, D. (2004). Are big basins just the sum of small catchments? *Hydrological Processes, 18*(16), 3195-3206. doi:10.1002/hyp.5739.

Singleton, M. J., & Moran, J. E. (2010). Dissolved noble gas and isotopic tracers reveal vulnerability of groundwater in a small, high-elevation catchment to predicted climate changes. *Water Resources Research, 46*. doi:10.1029/2009wr008718.

Sivapalan, M. (2003). Process complexity at hillslope scale, process simplicity at the watershed scale: is there a connection? *Hydrological Processes, 17*(5), 1037-1041. doi:10.1002/hyp.5109.

Sklash, M. G., & Farvolden, R. N. (1979). The Role of groundwater in storm runoff. *Journal of Hydrology*, volume 43, pp. 45-65.

Stahl, K., Hisdal, H., Hannaford, J., Tallaksen, L. M., Lanen, H. A. J. V., Sauquet, E., Demuth, S., Fendekova, M., & J'odar, J. (2010). Streamflow trends in Europe: evidence from a dataset of near natural catchments, *Hydrology and Earth System Sciences*, 14, 2367–2382, doi:10.5194/hess-14-2367-2010.

Smith, R. E., Veldhuis, H., Mills, G.F., Eilers, R. G., Fraser, W. R., & Lelyk, G.W. (1998). Terrestrial ecozones; Agriculture and Agri-food Canada, Manitoba, Brandon Research Center, Research Branch, Land Resource Unit, Technical Bulletin 98pp.

Soulsby, C., Tetzlaff, D., Hrachowitz, M., & Birkel, C. (2010). What is the total water storage in watersheds and can tracer help? *American Geophysical Union*, Fall meeting 2010. 2010AGUFM.H13I.06S.

Soulsby, C., Neal, C., Laudon, H., Burns, D. A., Merot, P., Bonell, M., Dunn, S.M., & Tetzlaff, D. (2008) Watershed data for process conceptualisation: simply not enough. Journal of *Hydrological Processes*, volume 2, pp. 2057-2061.

Spence, C. (2007). On the relation between dynamic storage and runoff: A discussion on thresholds, efficiency, and function. *Water Resources Research, 43*(12). doi:10.1029/2006wr005645.

Stewart, M. K., Morgenstern, U., & McDonnell, J. J. (2010). Truncation of stream residence time: how the use of stable isotopes has skewed our concept of streamwater age and origin. *Hydrological Processes*, *24*(12), 1646-1659. doi:10.1002/hyp.7576.

Svensson, T., Lovett, G. M., and Likens, G. E. (2012). Is chloride a conservative ion in forest ecosystems? *Biogeochemistry*, *107*(1-3), 125–134. doi:10.1007/s10533-010-9538-y.

Tetzlaff, D., Soulsby, C., Hrachowitz, M., & Speed, M. (2011). Relative influence of upland and lowland headwaters on the isotope hydrology and transit times of larger catchments. *Journal of Hydrology, 400*(3-4), 438-447. doi:10.1016/j.jhydrol.2011.01.053.

Tiessen, K. H. D., Elliott, J. A., Yarotski, J., Lobb, D. A., Flaten, D. N., & Glozier, N. E. (2010). Conventional and Conservation Tillage: Influence on Seasonal Runoff, Sediment, and Nutrient Losses in the Canadian Prairies. *Journal of Environmental Quality, 39*(3), 964-980. doi:10.2134/jeq2009.0219.

Turner, J. V., Macpherson, D. K., & Stokes, R. A. (1987). The mechanisms of watershed flow processes using natural variations in deterium and oxygen-18. *Journal of Hydrology*, volume 94, pp. 143-162.

Uchida, T., Asano, Y., Onda, Y., & Miyata, S. (2005). Are headwaters just the sum of hillslopes? *Hydrological Processes, 19*(16), 3251-3261. doi:10.1002/hyp.6004.

Uhlenbrook, S., Frey, M., Leibundgut, C., & Maloszewski, P. (2002). Hydrograph separations in a mesoscale mountainous basin at event and seasonal timescales. *Water Resources Research*, 38(6), 1096. https://doi.org/10.1029/2001WR000938.

Vogel, R. M., & Fennessey, N. M. (1994). Flow-duration curves: New interpretation and confidence-intervals, *Journal of Water Resources Planning and Management-Asce*, *120*(4), 485-504.

Weiler, M., McGlynn, B. L., McGuire, K. J., & McDonnell, J. J. (2003). How does rainfall become runoff? A combined tracer and runoff transfer function approach. *Water Resources Research, 39*(11). doi:10.1029/2003wr002331.

Wilson, D., Hisdal, H., & Lawrence, D. (2010). Has streamflow changed in the Nordic countries? – Recent trends and comparisons to hydrological projections, *Journal of Hydrology*, 394, 334–346, doi:10.1016/j.jhydrol.2010.09.010, 2010.

Wolock, D. M., Fan, J., & Lawrence, G. B. (1997). Effects of basin size on low-flow stream chemistry and subsurface contact time in the Neversink River Watershed, New York. *Hydrological Processes*, *11*(9), 1273-1286.

Yaeger, M., Coopersmith, E., Ye, S., Cheng, L., Viglione, A., & Sivapalan, M. (2012). Exploring the physical controls of regional patterns of flow duration curves - Part 4: A synthesis of empirical analysis, process modeling and catchment classification, *Hydrology and Earth System Sciences*, *16*(11), 4483-4498.

Yuan, Y., Mitchell, J. K., Hirschi, M. C., & Cooke, R. A. C. (2001). Modified SCS curve number method for predicting subsurface drainage flow, *Transactions of the Asae*, *44*(6), 1673-1682.

CHAPTER 2: MULTISCALE ANALYSIS OF STREAM HYDROGRAPHS TO INFER STORAGE RELEASE DYNAMICS IN NESTED CANADIAN PRAIRIE WATERSHEDS

Abstract

Understanding of a watershed's water storage and release (WSR) dynamics is essential in evaluating contaminant and nutrient storage and their subsequent movements through watersheds. In making an assessment of WSR mechanisms, several methodological choices exist. Some of the methods relate to the use of hydrometric data, some use isotopic data, whiles others use a combination of both. In the current study, we relied on hydrometric data and computed several metrics to help obtain a qualitative assessment of WSR dynamics in a 74.4 km^2 nested system of prairie watersheds located in Manitoba, Canada. Eight outlets were chosen for the study, six of which (referred to as "MS" sites) were located above a fractured escarpment, one on the edge of the escarpment, and the last outlet – which forms the overall exit of the whole nested system – was located below the escarpment. Baseflow separation, baseflow duration curves, and the baseflow index (BFI) were used to characterise passive storage release dynamics while fastflow duration curves and event-specific values of the initial abstraction and the runoff ratio (RR) were used to assess active storage release dynamics. Results show that the use of the duration curves sometimes led to counter-intuitive conclusions about storage release dynamics. BFI values were about 0.2 at the "MS" sites but increased for the bigger watersheds located at the edge and below the escarpment. RR was close to 1 at the site located at the edge of the escarpment, suggesting a passive release of old water in view of the relatively high BFI at that site. Future work will focus on aligning these results with isotope-based analysis such as hydrograph separation and water age assessments to help better define WSR dynamics.

Keywords: hydrographs, passive storage, dynamic storage, flow duration curve (FDC), baseflow index, initial abstraction, runoff ratio

2.1 Introduction

Over the years, many researchers in the hydrology community have resorted to the use of various techniques to analyze hydrographs and thus describe a watershed's response to introduced precipitation. On the one hand, some techniques are purely statistical in nature and are typically applied to long-term hydrographs so that historical flow dynamics can be inferred and used to contextualize future dynamics. Such techniques notably include flood frequency curves (e.g., Basso et al., 2016) to establish recurrence intervals (Ahilan et al., 2013), but also low flow duration and severity (Cancelliere et al., 2004). On the other hand, some techniques are physically-based, in that they target the quantification of metrics or parameters that inform on the actual hydrological processes driving a watershed's response to precipitation. Indeed, precipitation input is known to be a major forcing factor that can trigger runoff generation and influence other hydrological processes in a watershed. As a result, the analysis of hyetographs and hydrographs has been relied upon for decades to understand how rainfall or snowmelt is transformed into runoff (Dingman, 2002; Tang and Carey, 2017). Several studies have notably inferred watershed response by separating streamflow hydrographs into key components, namely baseflow – the delayed subsurface flow that can feed streams during dry and recession periods – and fastflow, the short-term response to a rainfall or snowmelt event (Narayanan and Jaehak, 2011).

The two key components of flow hydrographs (i.e., baseflow and fastflow) that have been of interest to process hydrologists depend on water originating from different storage zones in a watershed. Understanding the mechanisms of release of water from these storage zones is fundamental to understanding runoff and streamflow generation processes. The literature is rich of conceptual, data-driven and modeling studies that have described the different types of water storage that coexist in a given landscape (e.g., Black, 1997; Biswas et al., 2012; Szeftel et al., 2012; Li and Shao, 2015; Geris et al., 2015). Those descriptions of storage types, however, fall in at least two different classifications: a

classification based on the physical location of storage zones in the landscape, and a classification rather based on the timescales of water release from storage zones. Regarding the physical location of water storage zones in the landscape, the literature refers to storage on vegetation (canopy storage), in snowpacks, in small topographic depressions and wetlands, as well as in soils and bedrock (Black, 1997). Water in any of the storage zones can be further categorized into retention and detention storage. Retention storage water, either in managed surface ponds or held at high tensions in the soil capillary pores, for instance, is not available to contribute to streamflow but can be removed by evaporative processes. As for water held in detention storage, for example in small surface topographic depressions or in the vadose zone of soils, it can be released into streams when conditions are ideal, often within 24 hours after a precipitation event (Chow, 1964). The balance between detention and retention storage plays a critical role in determining how much water is stored and released to feed streamflow (Black, 1997). Regarding the time-dependent classification of storage types, the recent literature has notably referred to the concepts of passive versus dynamic (active) storage (Birkel et al., 2011; Heidbuchel et al., 2012). Passive storage corresponds to the long-duration and persistent storage of water in the saturated zone and it is mainly associated with baseflow in streams (Birkel et al., 2011). Contrary to passive storage, active or dynamic storage corresponds to the surface or near-surface, short-duration storage of water that can be released quickly as surface or near-surface runoff during events, thus making up the fastflow component of storm hydrographs (Heidbuchel et al., 2012). Total storage is then defined as the sum of all passive and dynamic storage within a watershed. Regardless of the classification system used, the direct quantification of storage is extremely difficult and can involve a range of different methods, hydrograph-based or otherwise (Kirchner, 2009; McNamara et al., 2011). One question that has yet to be addressed is whether metrics based on both long-term hydrographs and event-based hydrograph

analysis can be combined to infer streamflow generation triggered by the release of water from different storage types.

The flow duration curve (FDC), as a metric, is traditionally developed from medium- or long-term hydrographs (i.e., seasonal, annual and multi-annual data) and it may serve as a useful metric for inferring the amount of total storage released and contributing to streamflow (Verma et al., 2017; Vogel and Fennessey 1994; Mueller et al., 2014). Indeed, the FDC is a graphical representation of the percentage of time that streamflow exceeds a given magnitude over a given period (Ward and Robinson, 1990), thus making it useful to assess streamflow – or storage release dynamics – across the whole flow regime. The FDC has been applied not only in studies to assess the hydrological impacts of land use changes (Zhao et al., 2012) and water resource allocations (Vogel and Fennessey, 1995; Vogel and Fennessey, 1994), but also in studies focusing on flood and low-flow conditions (Smakhtin, 2001), water quality management (Searcy, 1959), and temporal trends in baseflow (Buttle, 2018). In recent studies, the focus has been placed on the slopes of different segments of the FDC and their usefulness for hydrologic process conceptualizations. For example, Yaeger et al. (2012), Coopersmith et al. (2012), and Cheng et al. (2012) used the slopes of the middle segment of the FDC to assess the average flow regime, i.e., to assess whether flow is perennial, intermittent, or ephemeral for streams across the continental USA. Chouaib et al. (2018) and Sawicz et al. (2011) also used the slope of the middle segment of the FDC in watersheds spanning the Eastern USA, this time to assess flow variability in streams and to help contextualize the watersheds' retention capacities in response to precipitation. One consensus emerging from those studies is, notably, that low slopes of the middle segment of the FDC can be linked to predominant baseflow conditions and, thus, the predominance of passive storage release dynamics.

Baseflow separation is another important hydrograph analysis technique routinely used in hydrology, and it is particularly useful for inferring passive storage release dynamics over long timescales. Indeed, baseflow is defined as the portion (or component) of streamflow that originates from

groundwater storage and/or other delayed sources such as channel bank storage, lakes, wetlands, and natural topographic depressions (Hall, 1968; Griffiths and Clausen, 1997; Smakhtin, 2001). This component of stream hydrographs is important for many reasons, including for better understanding surface water-groundwater interactions and for water resource management (e.g., Campolo et al., 1999; Brauman et al., 2007; Cyr et al., 2011). Baseflow separation has been employed in many studies to evaluate the low-flow characteristics of rivers (Mohamoud, 2008), identify climatic and physiographic controls on river low-flow conditions (Chouaib, 2018), and estimate a watershed's passive storage potential during low flow regimes (McNamara et al., 2011), among others. In this regard, the baseflow index (BFI), defined as the ratio of the total baseflow to the total streamflow over a study period, has been used as a long-term surrogate measure of the collective impact of climate, geology, and vegetation on a catchment's response to precipitation input (Cheng et al., 2012; Bloomfield et al., 2009). The BFI has also been used as a predictor of low-flow regimes in a stream (Mohamoud, 2008), and thus as a potential indicator of a stream's ability to sustain flow. Buttle (2017) used the BFI to infer the response of a watershed to climate change, thereby pointing to BFI as a measure of passive storage-release mechanisms in watersheds. A baseflow duration curve (i.e., a duration curve solely for the baseflow component of a hydrograph) is a visualization tool that can also be used to assess exceedance probabilities for the release of different amounts of passive storage.

While FDCs and metrics such as the BFI mainly apply to long-term hydrographs, interesting storage-related information can also be extracted from event-specific hydrograph analysis. The initial abstraction (Ia), for instance, is a metric that controls water storage release over short (i.e., hours to days) timescales. Indeed, the Ia, which is estimated as the amount of event rainfall accumulated in a watershed before the initial rise of the event hydrograph (Carey and DeBeer, 2008), reflects a catchment's ability to retain input precipitation before the initiation of event runoff. Ia has been known to depend on soil types, topographic characteristics (e.g., slope) and geology (Yuan et al., 2001), and it has mainly been

computed to estimate direct runoff in response to known precipitation inputs in ungauged catchments (Yuan et al., 2001). The Ia represents the watershed storage deficit to be satisfied prior to stormflow initiation and as such, it has been used as a surrogate for evaluating variations in dynamic storage and release patterns in response to individual precipitation events (Buttle, 2016; Baltas et al., 2007). Another interesting metric that can be derived from event-specific hydrograph analysis is the runoff ratio (RR), which can also be used to infer dynamic storage release over shorter timescales. The RR, which quantifies the proportion of event precipitation that becomes streamflow, has been employed in many basin-scale runoff studies, including studies focusing on the influence of geology and topography (e.g., Jencso and McGlynn, 2011; Huang et al., 2008; Freer, 2002), vegetation cover (e.g., Nosetto et al., 2012), and atmospheric trends (Kneis et al., 2012; Day, 2009) on streamflow. While there are different formulas published in the literature for the runoff ratio (e.g., Hewlett and Hibbert, 1967), one common practice at the event scale is to first perform baseflow separation and then compute the ratio of the event fastflow component, only, divided by the total event precipitation – as opposed to taking the total event flow divided by total event precipitation. Such a method ensures that the RR explicitly quantifies the amount of dynamic storage contributing to streamflow during a given event (Muller-Wohlfeil et al, 2002; Kirchner, 2009; Kronholm and Capel, 2016).

As alluded to earlier, it is rare for studies to combine the analysis of longer-term hydrographs and event-specific hydrographs, regardless of whether the aim is to infer watershed storage dynamics or not. Undertaking a study of this nature is particularly important in the context of the prairie environment that is subject to detention and retention storage in hummocks, man-made reservoirs in agricultural areas, and natural depressions such as ponds and lakes; snow storage on land and in stream channels; and groundwater storage in deep aquifers. The extent to which water is released from those different storage types to influence streamflow across various timescales is not fully understood in the prairies. The observed strong seasonality in precipitation input, air temperature, and streamflow regimes (i.e., with a

combination of perennial, intermittent, and ephemeral flow behaviors) is a complexifying factor. The sub-humid to semi-arid climatic regime resulting in alternating years of floods and droughts, and the lengthy winter season during which the ground is frozen, are some of the additional peculiarities of the prairie environment. Man-made stormwater control structures such as drainage ditches, farm dams, and drained wetlands altogether impact storage dynamics and, consequently, streamflow generation processes in the prairies, prompting the regional research community to evaluate the usefulness of simple tools – hydrograph-based and otherwise – in differentiating storage-release mechanisms across contrasted watersheds. In the current study, the focus was on a nested system of prairie watersheds that exhibit markedly different characteristics, in terms of macro-topography, surficial geology and bedrock geology. Various analyses were performed to answer the following research questions:

(i) To what extent do flow duration curves reflect the different physiographic characteristics influencing storage-release dynamics across contrasted prairie watersheds?

(ii) Can surrogate measures of passive storage release derived from the analysis of annual-scale hydrographs help differentiate streamflow regimes across contrasted watersheds?

(iii) How do surrogate measures of dynamic storage release mechanisms at short timescales capture streamflow generation processes across contrasted watersheds?

2.2 Methods

2.2.1 Study site

The chosen study site is the 74.41 km^2 South Tobacco Creek Watershed (STCW), within which the focus was on a nested system of sub-catchments ranging in size from 0.19 km^2 to 34.65 km^2, in addition to the overall watershed (i.e., 8 outlet locations in total). The STCW is located within the semi-arid to sub-humid prairie ecozone in Central Manitoba, Canada (Figure 2-1). The prairie ecozone is

characterized by cold lengthy winters and short cool summers (Tiessen et al., 2010). Long-term average (1996-2015) total annual precipitation (including snowfall) and mean daily temperature in the region are 595.2 mm and 4.4°C, respectively (Environment Canada, 2015). In 2014, 529.5 mm of total annual precipitation was recorded and included 257.5 mm of rainfall. In 2015, it was rather 607.5 mm of total annual precipitation that was recorded, including 243.7 mm of rainfall (Environment Canada, 2014, 2015). The mean daily air temperature was 2.9°C and 5.8°C in 2014 and 2015, respectively (Environment Canada, 2014, 2015). The mean annual daily precipitation and the fraction of "zero rain" days recorded in 2014 were, respectively, 0.75 mm and 0.39, while in 2015 those values were 2.29 mm and 0.51. Due to limited weather variables being available at the site, potential evapotranspiration was estimated using the Blaney-Criddle formula (Blaney and Criddle, 1962). The mean annual aridity index (AI)[1] used in this study was defined as the ratio of the total potential evapotranspiration to total precipitation (as done in Brooks et al., 2011; Cheng et al., 2012; and Li, 2014), and estimated to be 1.19 and 1.49 in 2014 and 2015, respectively. The stated temporal variability (i.e., inter-annual) in climatic characteristics across the watersheds was reflected in the inter-annual variability in streamflow (Figure 2-2).

[1] Aridity Index (also called dryness index) is traditionally defined (as done by the Food and Agriculture Organization) as the ratio of precipitation to potential evapotranspiration. Here the different definition that was adopted was in line with the papers cited in this Chapter.

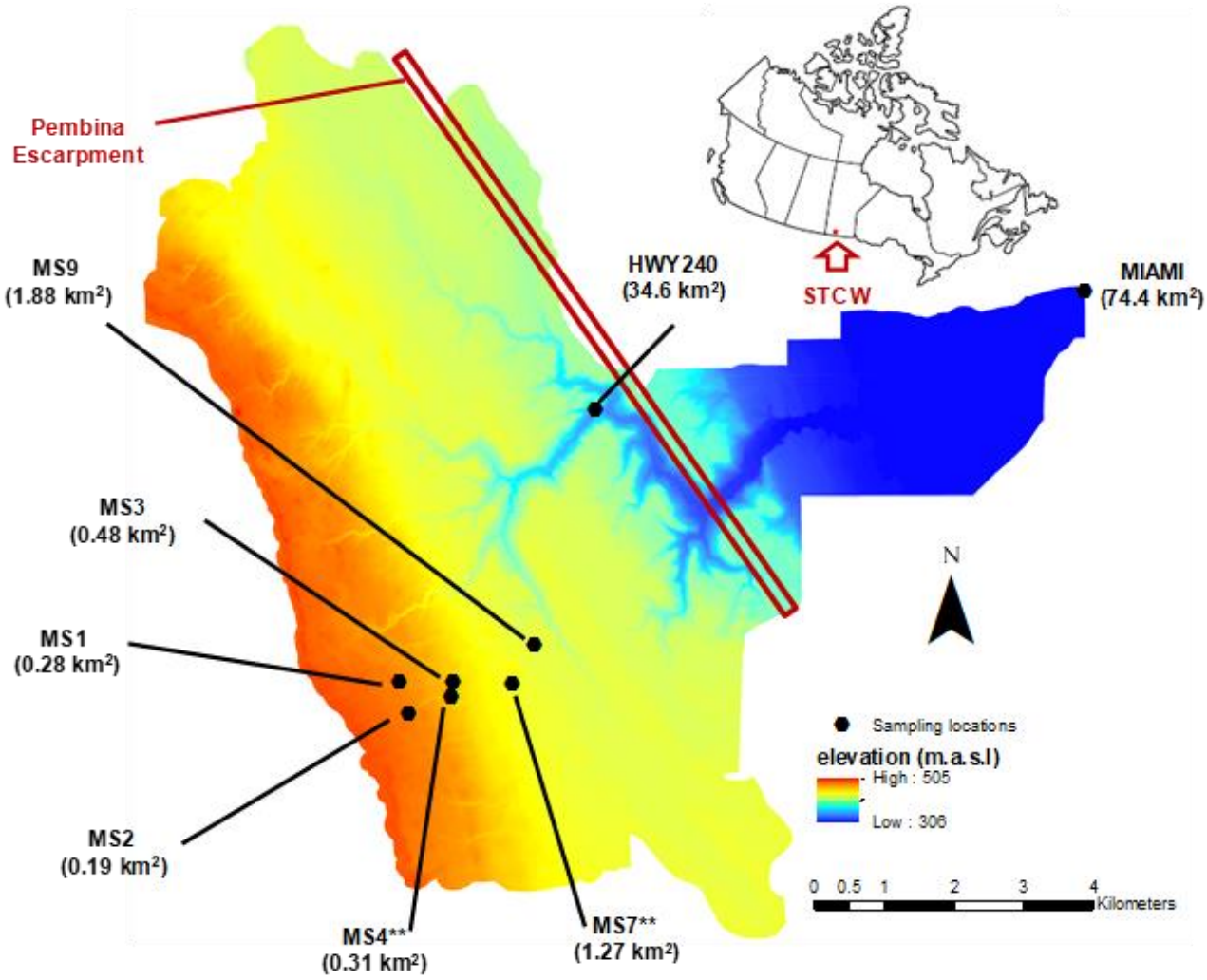

Figure 2-1. Digital elevation model (horizontal resolution: 1 m) with sub-catchment outlets and drainage areas (in brackets) of the South Tobacco Creek Watershed (STCW) in Canada. Elevation is in meters above sea level. '**' indicates MS outlets with holding dams.

The parent material in the STCW is a shale bedrock overlain by moderately to strongly calcareous glacial till and clay-loam soils (Matile and Keller, 2004; Tiessen et al., 2010). The Pembina escarpment, which trends NW-SE (Figure 2-1) within the watershed, originated approximately 50 to 84 million years ago because of the Laramide Orogeny (Matile and Keller, 2004; Tiessen et al., 2010); it causes an elevation drop of approximately 200 m between the STCW headwaters and its outlet near the town of

Miami (Figure 2-1). The escarpment is made of largely interconnected joints and fractures which provide seepage of groundwater as a main source of recharge to the nearby streams (Hutchinson, 1977). Glacial tills (ranging in thickness from a few centimeters up to 20 m) comprising of mixed deposits of shale, limestone and granite make up the surficial materials atop the escarpment.

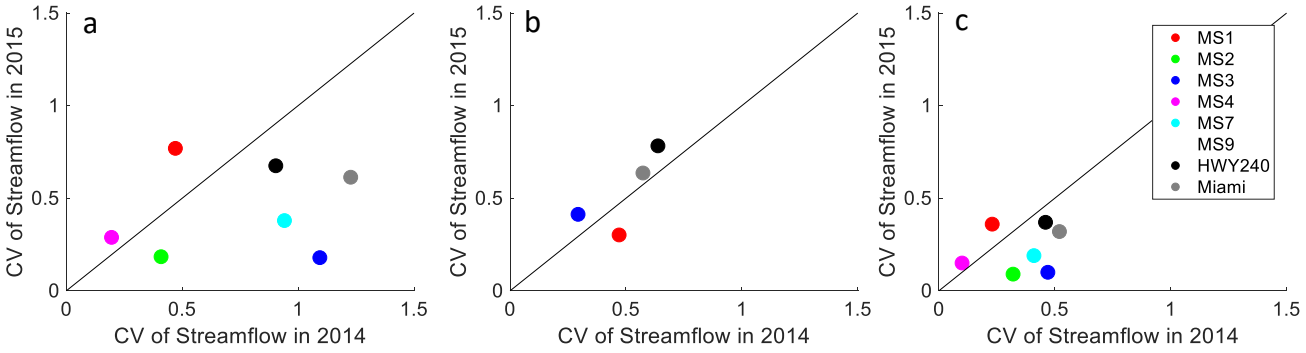

Figure 2-2. Scatter plots of the coefficients of variation (CV) of streamflow in 2014, plotted against the CV of streamflow in 2015. Panels (a), (b), and (c) show dynamics for the spring season only, the summer season only, and the whole year, respectively. Symbols are color-coded by outlet location, while the solid black diagonal line is the 1:1 line. Note that instrumental failure occurred at site MS9 in 2015; hence there were no flow readings recorded. Fall data are not plotted because most of the flow readings in that season were zero.

The outlets of the watershed and sub-catchments chosen for the current study reflect the landscape diversity encountered in the region. The 'MS' sites are located above the escarpment (Figure 2-1) where low-relief to undulating landscapes with slopes of up to 10 % are present (Tiessen et al., 2010). Dominant soil types are from the Dezwood soil series (Orthic Dark Gray Chernozems) with primarily clay-loam texture, and the Zaplin soil series (Gleyed Dark Gray Chernozem) (Manitoba Department of Agriculture,

1943, 1988) with mostly mottled clayey texture. The MS4 and MS7 outlets have small holding dams and retention ponds located immediately upstream of them for stormwater control purposes; the pond behind MS7 has the tendency to overflow during snowmelt and extreme rainstorm events. The HWY240 site, which is located at the edge of the escarpment, is characterized by a deeply incised stream channel atop intensely fractured shale bedrock. Surficial deposits in the vicinity of the escarpment are gravelly sand to clays (ranging in thickness from a few cm up to 2 m) and overlying glacial till (often containing considerable stones) and fractured shale bedrock (Manitoba Department of Agriculture, 1988). The Miami site marks the outlet of the whole STCW and sits within flat, lowland terrain (Figure 2-1) below the escarpment. Surficial materials below the escarpment are mainly medium- to coarse-grained glaciolacustrine deposits, which progressively become finer-grained moving downstream. The major differences in streamflow generation mechanisms across the nested sites, which have been observed through more than 15 years of active field research in the STCW, are thought to be a consequence of the soil and geological differences that exist above, atop and below the escarpment.

The “MS” sites behave like typical prairie systems, in that they experience Hortonian overland flow in the form of sheet flow over frozen ground in early spring (e.g., Fang et al., 2007), shallow subsurface flow in late spring, Hortonian overland flow in response to short-lived, convective summer storms (e.g., Shook and Pomeroy, 2012), and saturation-excess overland flow in extremely wet periods. Water movements in the vicinity of the Pembina escarpment (i.e., HWY240 and Miami) occur mostly vertically (i.e., surface water-groundwater exchanges) rather than laterally (i.e., hillslope-to-stream transfers) (Hutchinson, 1977; Betcher et al., 1995). Bedrock fractures also maintain a permanent hydraulic link between the incised stream channel and the groundwater table, thus making HWY240 the only outlet where perennial water is observed. Streamflow at the Miami site is mainly fed by Hortonian overland flow and deep groundwater flow from the Miami aquifer (Betcher et al., 1995). Agricultural activities take place throughout the STCW, with corn, wheat, and canola being the major crops planted.

2.2.2 Hydrometric data collection

The STCW outlet, as well as each sub-catchment outlet, was equipped with different types of weir (either v-notch or rectangular) in combination with a Campbell Scientific snow and water depth sensor SR50A (1 cm accuracy) for stage measurements, subsequently converted to discharge via the weir equations. Discharge data was acquired at a minimum frequency of 15 minutes at all the sites and then averaged to daily time steps and normalized by watershed drainage area. Daily rainfall amounts were determined by Texas Electronic Tipping Bucket rain gages (TE525-L, 0.02 cm precision) connected to Campbell Scientific data loggers at all the sites.

2.2.3 Flow Duration Curves

Flow duration curves (FDCs) from normalized daily streamflow from each outlet location were constructed following the Weibull plotting formula (Sugiyama et al., 2003) (Eq. 2-1). FDCs were constructed separately for late spring, summer, and fall of 2014 and 2015, as well as the whole open-water period of each year (May-October). In this manner, shifts in streamflow dynamics in response to various storage release mechanisms could be identified as the year progresses. The late spring season was chosen to start from May 1st when snowmelt-dominated conditions were assumed to have switched totally to rain-dominated ones. Summer and fall seasons started from June 20th and September 23rd, respectively. Precipitation duration curves (PDCs) were superimposed on the FDCs for easier assessment of streamflow generation processes in light of precipitation input dynamics:

$$p = \frac{r}{(N+1)} * 100 \qquad \text{(Eq. 2-1)}$$

where p is the percentage of time that a given flow or precipitation value is equaled or exceeded, N is the total number of data points within the period considered, and r is the rank assigned to each flow or precipitation value within the period considered. Frequency classes (0-33)%, (33-66)%, and (66-99)% corresponding to the leftmost, middle and rightmost segments of the FDCs (Yokoo and Sivapalan, 2011) were isolated for the purpose of assessing the characteristics of streamflow in reaction to different rates of total storage release. Streamflow characteristics were assessed by estimating the slopes of different segments of the FDC, which serve as surrogate measures of flow variability in time (Sawicz et al., 2011). For instance, for the middle segment, the slope is calculated using the 33rd and 66th flow percentiles (Eq. 2-2) (Yadav et al., 2007; Zhang et al., 2008): high slope values indicating variable flow regimes and small values indicating damped responses (Sawicz et al., 2011).

$$Slope\ FDC = \frac{\ln(Q33\%) - \ln(Q66\%)}{(0.66 - 0.33)} \qquad \text{(Eq. 2-2)}$$

where Q33% and Q66% are the streamflow values at the 33rd and 66th percentiles respectively. For the other FDC segments or frequency classes, the respective flow percentiles are substituted in Eq. 2-2 for the estimation of the slope.

2.2.4 Baseflow duration curves and baseflow index

A method for low-pass filtering of hydrographs (baseflow separation method) developed by Eckhardt (2005) was used to separate total streamflow into baseflow and fastflow components. Prior to the calibration, the range of initial parameters for baseflow separation, namely site-dependent alpha

values and maximum BFI coefficients, was set to 0 to 0.6 and 0 to 0.8, respectively. The initial range of alpha values was determined based on literature values (Lim et al., 2010; Zhang et al., 2013; Zomlot et al., 2015; Bosch et al., 2017). The summer and fall season portions of the hydrographs were used as references for selecting initial maximum BFI for the model, as it was assumed that streamflow at that time is predominantly coming from baseflow. The baseflow was then divided by the total streamflow to obtain the BFI. In addition to the total flow duration curve described in the previous section (hereafter referred to as tFDC), FDCs were also established for the separated components of fastflow (fFDC) and baseflow (bFDC): the three FDCs notably aimed at assessing the watershed and sub-catchments' total storage, dynamic storage, and passive storage release dynamics. BFI values, as well as fFDCs and bFDCs, were established separately for the years 2014 and 2015. To further elucidate the effects of passive storage release on streamflow generation processes, the baseflow distribution within each of the frequency classes, i.e., (66-99)%, (33-66)%, and (0-33)%), was assessed via boxplots (outlier values were below or above 1.5 times the interquartile range). The distribution of the BFI within the (66-99)% and (33-66)% frequency classes (i.e., the classes representing the rightmost and middle segments of the FDC, respectively) was also evaluated via boxplots.

2.2.5 Event-based initial abstractions and runoff ratios

In order to evaluate the effects of dynamic storage release mechanisms on streamflow generation processes over short-term (event) scales, we used an automated tool (HydRun) by Tang and Carey (2017) to delineate major rainfall-runoff events that occurred during the study period (2014-2015). Minor rainfall-runoff events that were omitted by the automated tool were delineated manually. In all, 43 and 35 events were delineated during the 2014 and 2015 open-water periods, respectively across all outlet. These events occurred across the late spring, summer and fall seasons (Table 2-1). For each delineated

event, the total event rainfall (TR), event peak flow (PF), initial abstraction (Ia), ratio of Ia to TR, and runoff ratio (RR) were determined. The distribution of RRs, PFs, TR, Ia, and ratio of Ia to TR across the eight sites over the two years were assessed using boxplots.

Table 2-1. Number of events delineated across the catchments during the 2014 and 2015 study years. Instrumental failure occurred at MS9 in 2015, hence no flow measurements were made at that site.

	MS1		MS2		MS3		MS4		MS7		MS9		HWY240		Miami		TOTAL	
	2014	2015	2014	2015	2014	2015	2014	2015	2014	2015	2014	2015	2014	2015	2014	2015	2014	2015
Spring	2	5	3	3	8	3	2	2	5	2	2		4	4	6	4	30	23
Summer	0	2	1	0	1	3	1	0	1	1	1		3	3	5	3	13	12
Fall	0	0	0	0	0	0	0	0	0	0	0		0	0	0	0	0	0
TOTAL	2	7	4	3	9	6	3	2	6	3	3		7	7	11	7	43	35

2.3 Results

2.3.1 Total storage release dynamics

The slopes of the middle (33-66)% segment of the annual FDC were generally steeper at the majority of the outlets in 2014, compared to those observed in 2015 (e.g., 2.16 and 1.52 respectively for the Miami outlet) (Table 2-2). Except for site MS2, the slopes of the (66-99)% exceedance frequency class of the annual FDC were higher in 2015 than in 2014 (Table 2-2). The normalized flows (in mm/day) recorded in the spring of 2015 at most of the sites were higher than those recorded during the same period in 2014 (Figure 2-3). Regarding the spatial variability of streamflow, the headwater sites (MS1 and MS2) appeared to be registering higher normalized flows than the other sites, regardless of the year (or season) considered (Figures 2-3a & 2-3b).

Table 2-2. Summary characteristics of the various flow duration and precipitation duration curves derived based on data for the 2014 and 2015 study years.

	MS1	MS2	MS3	MS4	MS7	MS9	HWY240	Miami	
Slope of FDC, whole season	0	0	1.31	0	0.18	9.7	2.64	2.16	2014
Slope, (99 - 66)% frequency segment	0.02	0.77	0.01	0.05	0	0.03	0.02	0.01	
Slope, (66 - 33)% frequency segment	0	0	0	0	0	0.01	0	0	
Slope, (33 - 1)% frequency segment	0	0	0	0	0	0	0	0	
Slope of FDC, spring	0	1.98	6.92	0	7.37	14.93	2.64	4.39	
Slope, (99 - 66)% frequency segment	0.02	0.77	0.01	0.01	0.01	0.03	0.02	0.01	
Slope, (66 - 33)% frequency segment	0	0	0	0	0	0.02	0	0	
Slope, (33 - 1)% frequency segment	0	0	0	0	0	0	0	0	
Slope of FDC, summer	0	0	0	0	0	0	1.13	0.5	
Slope, (99 - 66)% frequency segment	0	0	0	0.05	0	0.01	0	0	
Slope, (66 - 33)% frequency segment	0	0	0	0	0	0	0	0	
Slope, (33 - 1)% frequency segment	0	0	0	0	0	0	0	0	
Slope of FDC, fall	-	-	-	-	-	-	-	-	
Slope of FDC , whole season	0	0	0.86	0	0		2.52	1.52	2015
Slope, (99 - 66)% frequency segment	0.17	0.31	0.02	0.11	0.03		0.03	0.05	
Slope, (66 - 33)% frequency segment	0	0	0	0	0		0	0	
Slope, (33 - 1)% frequency segment	0	0	0	0	0		0	0	
Slope of FDC, spring	9.09	0	1.02	0	1.31		1.59	3.14	
Slope, (99 - 66)% frequency segment	0.13	0.31	0.02	0.11	0.03		0.03	0.05	
Slope, (66 - 33)% frequency segment	0.03	0	0	0	0		0	0	
Slope, (33 - 1)% frequency segment	0	0	0	0	0		0	0	
Slope of FDC, summer	0	0	0	0	0		0.66	0.42	
Slope, (99 - 66)% frequency segment	0.01	0	0	0	0		0	0	
Slope, (66 - 33)% frequency segment	0	0	0	0	0		0	0	
Slope, (33 - 1)% frequency segment	0	0	0		0		0	0	
Slope of FDC, fall	-	-	-	-	-		0.13	-	

The shape of the precipitation duration curves (PDCs), in terms of inflection points, appeared similar to the shape of the annual FDCs at sites HWY240 and Miami during both years of study (Figure 2-3g & 2-3h). A similar behavior was observed at site MS2 in 2014, as the PDC and the annual FDC were similar (Figure 2-3b). At sites MS4 and MS7, however, it was only during the spring of

2015 that the PDC and the FDC showed similar inflection points (Figure 2-3d & 2-3e). In 2015, the PDC was similar to the annual FDC at site MS1 (Figure 2-3a).

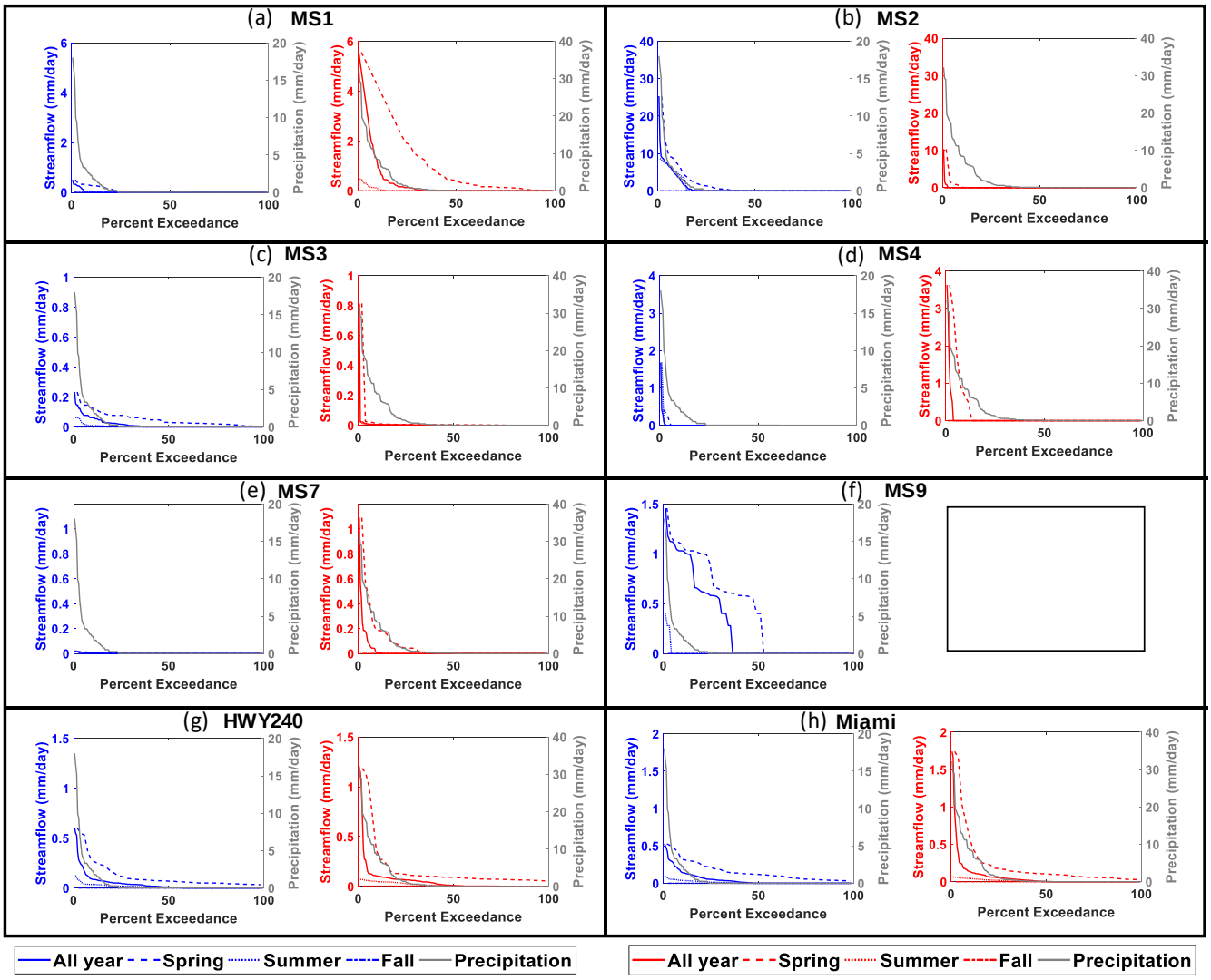

Figure 2-3. Normalized seasonal flow duration curves (FDC) and precipitation duration curves (PDC) for the 2014 (blue y-axis) and 2015 (red y-axis) study years. No flow data were available for site MS9 in 2015 due to instrument failure.

2.3.2 Passive storage release dynamics

An evaluation of the dynamics prevailing within the various frequency classes of the fFDC and bFDC (Figure 2-4) revealed a marked temporal variability – from one year to another – and notable spatial variability – among the sites (Figure 2-5).

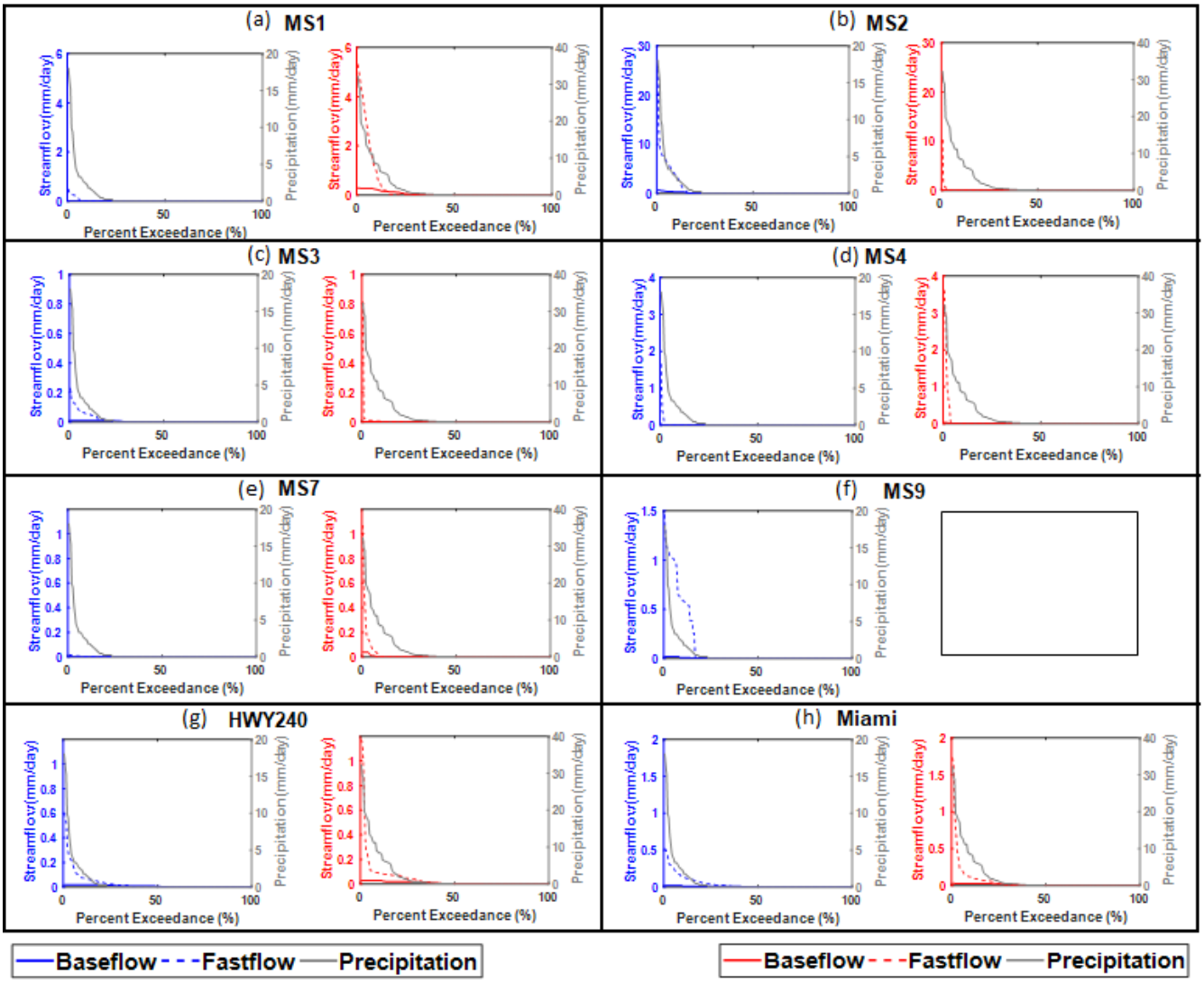

Figure 2-4. Normalized flow duration curves and precipitation duration curves (PDC) for the fastflow (fFDC) and baseflow (bFDC) components of streamflow. FDCs were constructed after hydrograph separation with the blue y-axis showing 2014 results and the red y-axis showing 2015 results. No flow data were available for site MS9 in 2015 due to instrument failure.

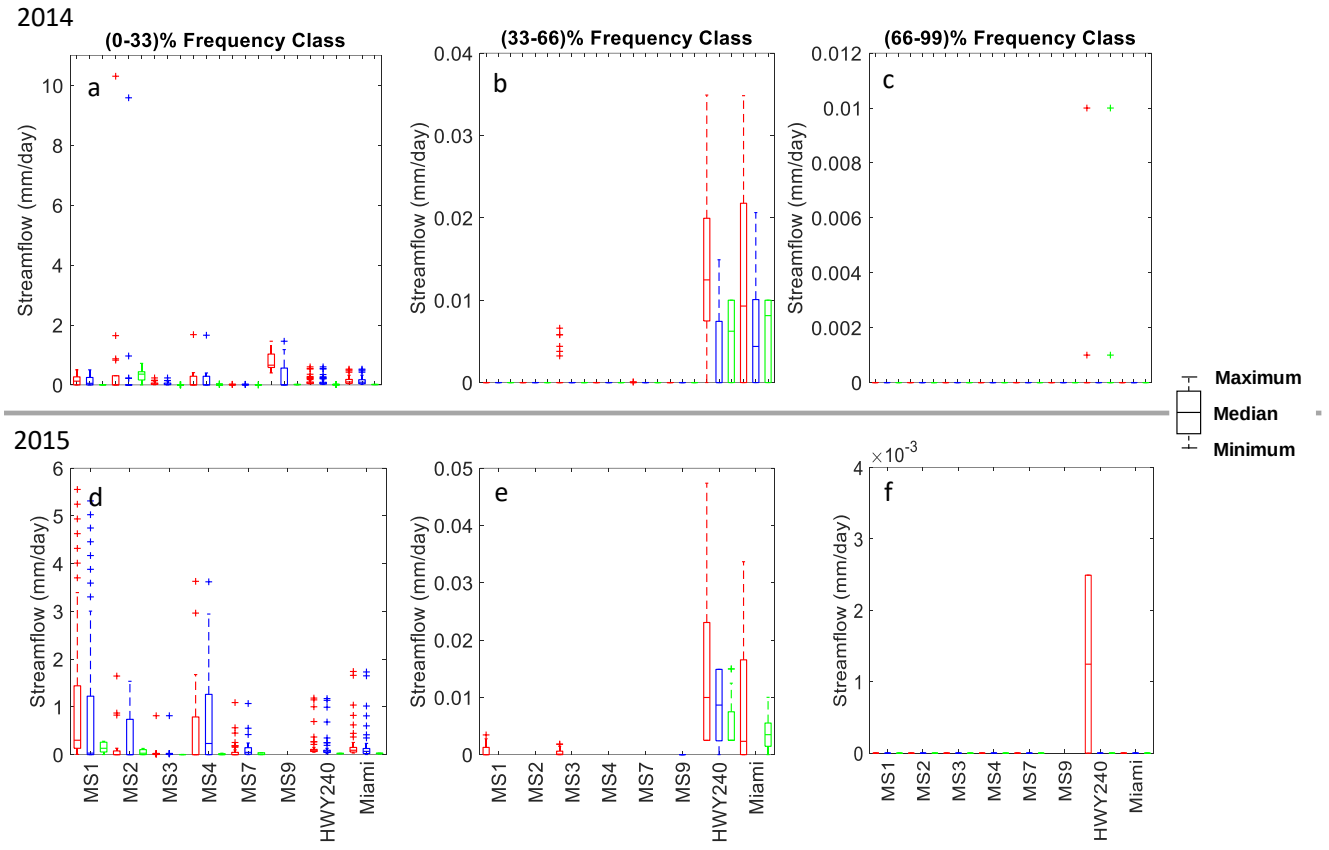

Figure 2-5. Range of total specific flow (red boxes), specific fastflow (blue boxes) and specific baseflow values (green boxes) for different frequency classes (i.e., upper, middle, and lower segments of the total or component-specific flow duration curves). The horizontal line shows the median value, while the bottom and top of each box show the 25th and 75th percentile, respectively, of the data distribution. Whiskers extending beyond above and below each box indicate the lowest and highest values. Small plus signs beyond whiskers are statistical outliers.

Evidence of passive storage release through baseflow was pronounced within the intermediate frequency class (i.e., (33-66)%) of the bFDC, especially for the relatively bigger watersheds, i.e., those associated with the HWY240 and Miami outlets (Figures 2-5b & 2-5e). The recorded baseflows were almost zero at the "MS" sites in both years of study when the (33-66)% frequency class was considered

(Figure 2-5). Across all the sites, the variability in the baseflow index (BFI) was more pronounced in 2015 compared to 2014 (Figure 2-6). The median BFI values in both years of study for the (33-66)% class were higher at the HWY240 (0.18 and 1, respectively, for 2014 and 2015) and Miami (0.05 and 0.04, respectively, for 2014 and 2015) sites, compared with the "MS" sites (less than 0.01) (Figure 2-6). In general, the median BFI value across all the sites was less than 0.2, the one exception being the HWY240 site for the 2015 sampling year (median BFI = 1) within the (33-66)% frequency class (Figure 2-6). The maximum BFI values occurred in 2015 at most of the sites (Figure 2-6).

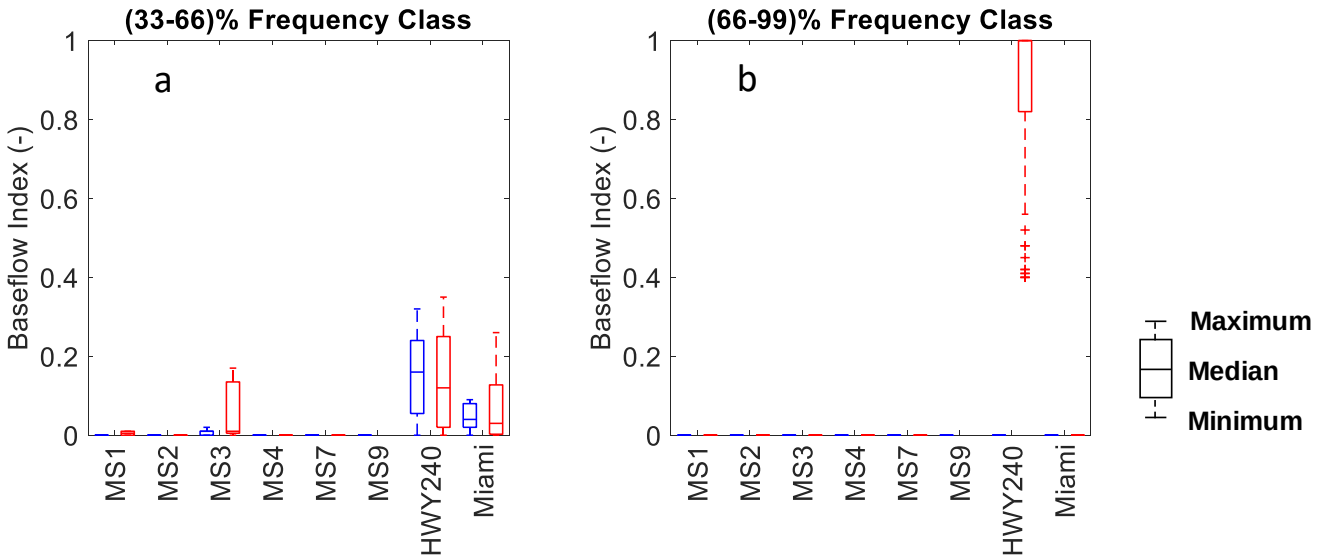

Figure 2-6. Range of baseflow index (BFI) values for different frequency classes of flow (i.e., middle, and lower segments of the flow duration curves). The upper segment was assumed to be negligible and was thus omitted from the plots. Blue and red boxes indicate 2014 and 2015 results respectively. The horizontal line shows the median value, while the bottom and top of each box show the 25th and 75th percentile, respectively, of the data distribution. Whiskers extending beyond above and below each box indicate the lowest and highest values. Small plus signs beyond whiskers are statistical outliers.

2.3.3 Dynamic storage release at short timescales

The range of total rainfall amount associated with the 2014 events was highest at site MS7 and lowest at site MS1 (Figure 2-7a). In the 2015 monitoring year, the range of total event rainfall amounts was rather highest at site MS7 and lowest at site MS2 (Figure 2-7a). The widest range of event peak flows occurred at site MS2 in both 2014 and 2015 (Figure 2-7b). The narrowest range of event peak flows occurred at sites MS7 and MS4 for the 2014 and 2015 events, respectively (Figure 2-7b). In general, event peak flows appeared to be the smallest at the watersheds with larger drainage areas, i.e., those associated with the HWY240 and Miami outlets (Figure 2-7b). The highest range of Ia values associated with the 2014 events was observed at site HWY240 (0.30 mm $\leq$ Ia $\leq$ 94.00 mm), while the highest range of Ia values associated with the 2015 events was rather observed at site MS7 (8.40 mm $\leq$ Ia $\leq$ 94 mm) (Figure 2-7c). The minimum absolute Ia values in 2014 and 2015 occurred at sites HWY240 (Ia = 0.30 mm) and MS1(Ia = 0.10 mm), during the spring season, while the maximum absolute Ia values occurred at sites HWY240 (Ia = 94 mm) and MS7 (Ia = 94 mm), during the summer season (Figure 2-7c). With the exception of sites MS4 and MS7, initial abstraction (Ia) values during the events of 2014 were higher than those associated with the 2015 events (Figure 2-7c). The maximum median Ia values occurred at sites HWY240 and MS7 during the 2014 and 2015 events, respectively (Figure 2-7c). The median value of the ratio of Ia to total event precipitation (TR), i.e., Ia/P, was highest at site MS3 in 2014 and 2015 (Figure 2-7d).

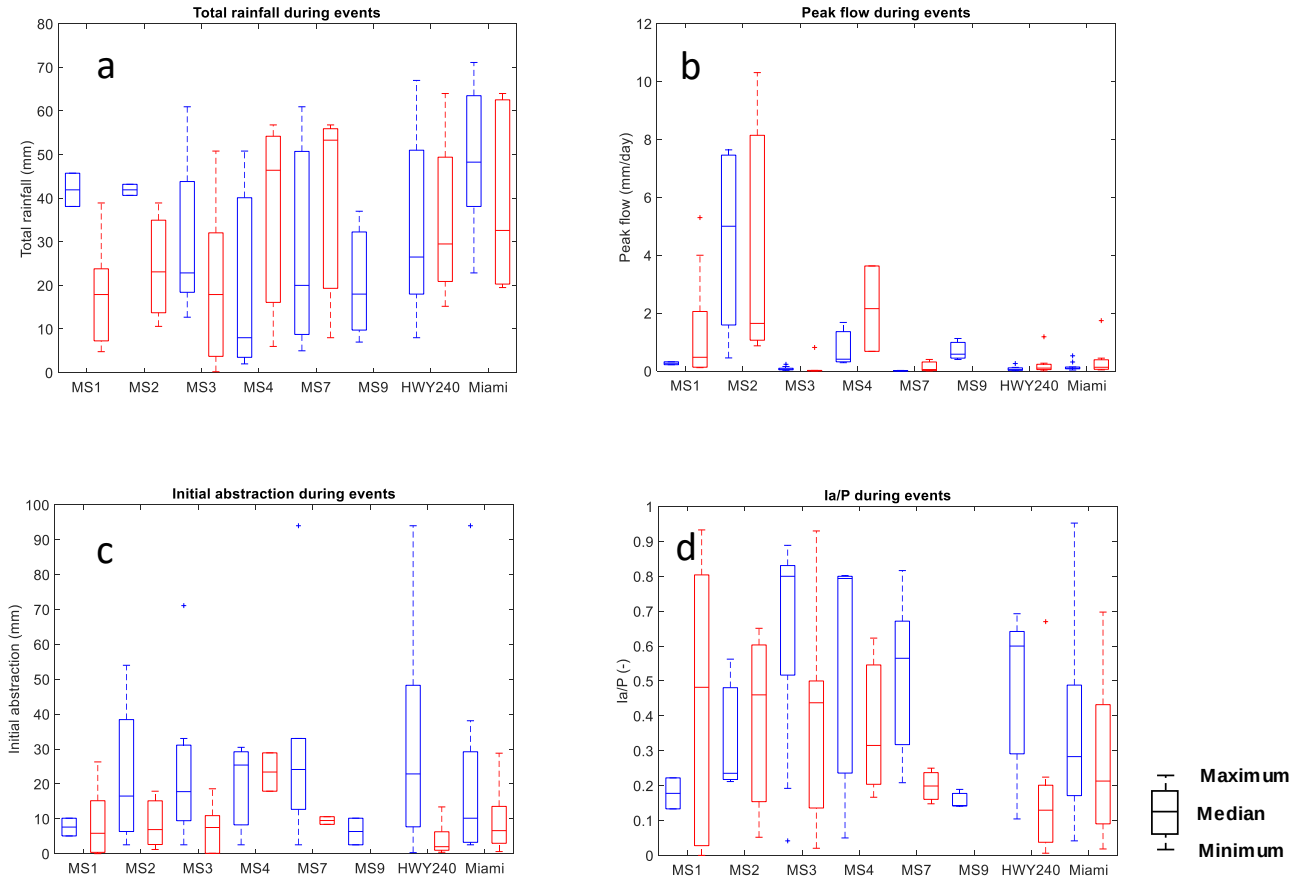

Figure 2-7. Boxplots of total event rainfall (TR), event peak flow (PF), initial abstraction (Ia), and ratio of Ia to TR (Ia/P) for all events delineated within the catchments. Blue boxes show 2014 results and red boxes show 2015 results. The horizontal line shows the median value, while the bottom and top of each box show the 25th and 75th percentile, respectively, of the data distribution. Whiskers extending beyond above and below each box indicate the lowest and highest values. Small plus signs beyond whiskers are statistical outliers.

As for event runoff ratios (RR), they were more variable from one event to another in 2014, compared to 2015, the one exception being at site MS4 (Figure 2-8). For the vast majority of sites across both years, RRs were extremely low, i.e., below 0.1, especially during the summer season. There was, also, no scaling of RR values with watershed size: Figure 2-8 clearly shows that most of the RRs observed

at the terminal Miami outlet were extremely low (Figure 2-8h), while upstream sites could be associated with RRs in excess of 0.5 (e.g., Figure 2-8a, 2-8d, 2-8f and 2-8g). The maximum range of RR values across 2014 events occurred at site HWY240 ($0.02 \leq RR \leq 1.33$), while the range of RR values observed across 2015 events was largest for site MS4 ($0.00 \leq RR \leq 0.65$) (Figure 2-8d and 2-8g). The maximum absolute RR in 2014 and 2015 occurred at sites HWY240 and MS4 respectively (Figure 2-8d and 2-8g). The range of median RR across the sites was between 0 and 0.25, with the highest median value (0.25) occurring at site HWY240 in 2014 (Figure 2-8g).

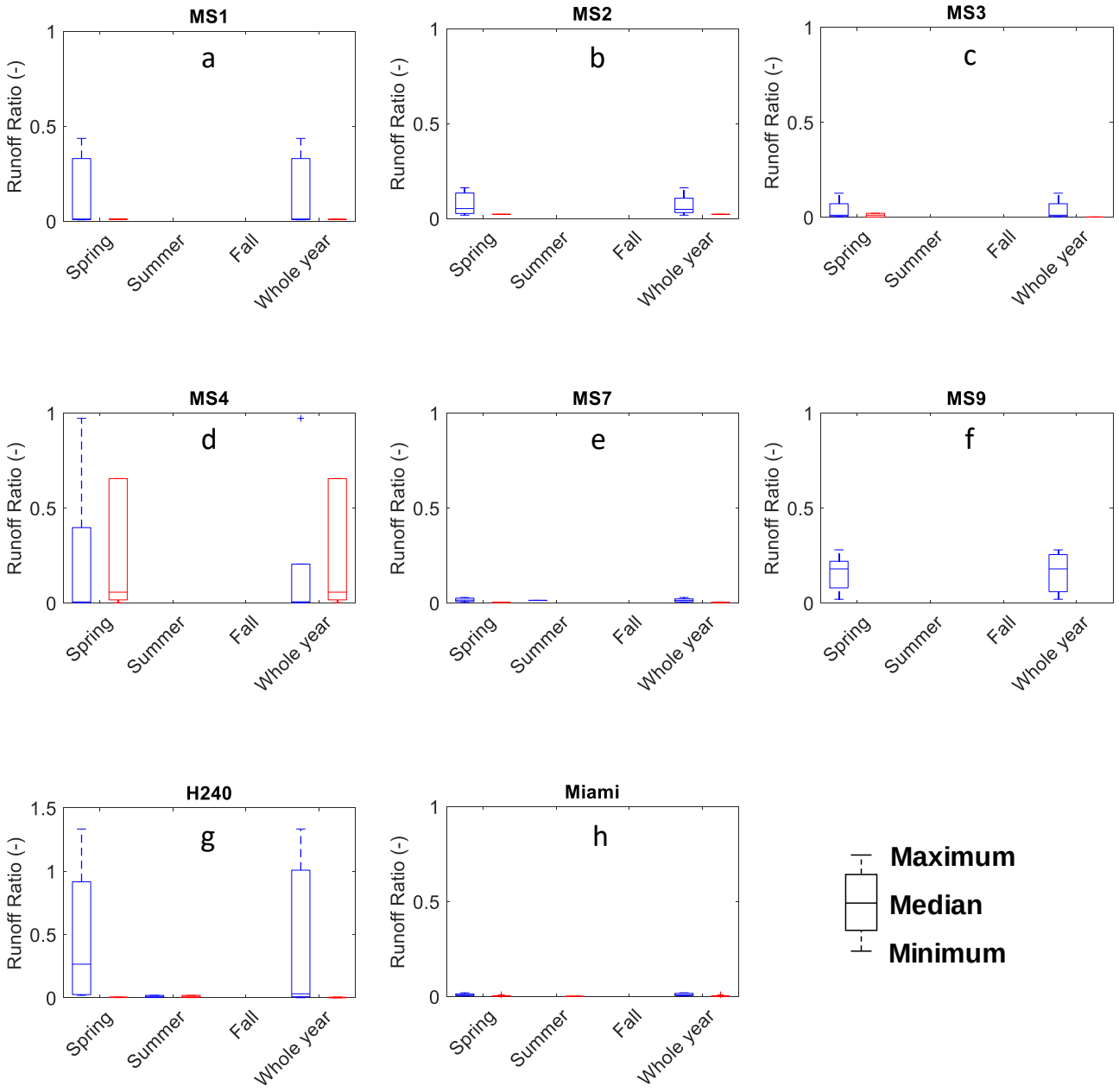

Figure 2-8. Range of runoff ratios (RR) for all events delineated within each season across the eight nested catchments. Blue and red boxes indicate 2014 and 2015 results respectively. The horizontal line shows the median value, while the bottom and top of each box show the 25th and 75th percentile, respectively, of the data distribution. Whiskers extending beyond above and below each box indicate the lowest and highest values. Small plus signs beyond whiskers are statistical outliers.

2.4 Discussion

2.4.1 Streamflow generation in the context of total storage release

The steeper slopes observed for the rightmost segment (i.e., (66-99)% frequency class) of the annual FDC in 2015 (Figure 2-3, Table 2-2), compared to 2014, suggest a stronger temporal stability of streamflow in the latter year. In other words, there was more variability in streamflow dynamics in 2015 compared to 2014, according to previous interpretations of FDC segment slopes reported in the literature (e.g., Ye et al., 2012; Cheng et al., 2012; Yokoo and Sivapalan, 2011). This observed difference could be attributable to a higher potential for the watersheds to hold water in storage and release them slowly during the 2014 year, compared to 2015. This hypothesis, if verified in the STCW, would be consistent with the findings of Chouaib et al. (2018): in that study, watersheds having higher slopes of the FDC were classified as having low retention capacities with associated higher variability in flow regimes. However, the weather conditions prevailing in each year in the STCW do not appear to support that hypothesis: indeed, while total annual rainfall was only slightly higher in 2014 compared to 2015 (i.e., 257.5 mm in 2014, versus 243.7 mm in 2015), mean daily air temperatures were much higher in 2015. The aridity index, which is a measure of drought conditions in a watershed, was also much higher in 2015 than in 2014 (1.49 in 2015 against 1.19 in 2014). The evaluation of rainfall totals and aridity index values implies that 2014 was a wetter year than 2015. While drier years are typically assumed to be associated with larger total storage deficits and hence high retention potentials (e.g., Melo et al., 2016), the higher slopes of the computed FDCs rather imply low retention capacities in the drier year (i.e., 2015) considered in the present study. There was, therefore, a major discrepancy in the storage-related inferences made in the present study, depending on whether climate data only were used or whether literature-driven FDC interpretations were relied upon. When it comes to the question of how much

"delay" exists between precipitation input and streamflow initiation, the similar shapes of the annual FDCs and the PDCs (in terms of their inflexion points) for the HWY240 and Miami sites suggest that across larger watershed scales, there is a tight coupling between input precipitation and streamflow initiation – which may be evidence of a good efficiency of the landscape to transmit runoff to streams (e.g., Nikas et al., 2007). For sites MS4 and MS7, it was only during the spring season of 2015 that the FDCs and PDCs had similar inflection points (Figure 2-3d & 2-3e), which could also indicate tight coupling between input precipitation and streamflow initiation. For cases where the PDC and FDC did not appear to mimic each other, however, especially across the 'MS' sites lying within a hummocky landscape, precipitation was likely held in detention storage, awaiting conditions that would lead it to spill over and then contribute to streamflow at a later time, thus leading to a decoupling – in terms of timing – between input precipitation and streamflow initiation.

2.4.2 Spatial controls on fastflow-baseflow partitioning

During the 2014 year, the portion of total flow that came from fastflow at site MS2 for the (0-33)% frequency class (Figure 2-5a) may be a result of the important forest cover in the catchment upstream of that site, compared to others; indeed, the MS2 catchment ranks as the second most forested site amongst the six "MS" sites (Table 2-3). It is thought that forested watersheds deliver more saturation-excess overland flow as well as more shallow subsurface flow, relatively speaking, than non-forested ones (e.g., Lana-Renault et al., 2011; Lana-Renault et al., 2012; Barthold and Woods, 2015). While all the catchments considered in the present study are predominantly agricultural, some have a greater forest cover in their riparian areas. As long as the soil is not frozen, those forested riparian areas can act as major hydrological modifiers in two ways. On one hand, those riparian areas can "intercept" some of the surface runoff originating from adjacent fields, promote infiltration and lead to slower, shallow lateral

subsurface flow towards the stream. On the other hand, those forested riparian areas can, rather, be saturated and promote saturation-excess overland flow towards the stream. Relying on frequency classes of fastflow and baseflow alone (i.e., Figures 2-5 and 2-6) is, however, not sufficient to assess the predominance – or co-existence – of saturation-excess overland flow and subsurface flow at MS2. It should also be noted that in 2015, fastflow contributions at that same MS2 site were markedly lower than in 2014, albeit the total flow was also comparatively less (Figure 2-5d). As the spectrum shifts to the (33-66)% frequency class, we observed more contribution from baseflow at sites HWY240 and Miami, which also have a large proportion of their riparian areas that are forested (Figure 2-5b, Table 2-3): that forest cover may have promoted vertical percolation leading to deep subsurface flow. It should, however, be noted that in addition to the forested cover upstream of the HWY240 and Miami sites, potentially promoting higher subsurface flows, those sites may also be vertically connected to passive stores of water, notably through fractures in the shale bedrock associated with the escarpment. The BFI values estimated in the present study (Figure 2-6) point to relatively higher contributions of baseflow from delayed sources in 2015, compared to 2014; such results are plausible in the drier 2015 year since baseflow is known to be the main, if not sole, contributor to streamflow under dry conditions (e.g., Eckhardt, 2008; Beck et al., 2013). For example, at the HWY240 site, BFI values were as high as 1 in 2015 (Figure 2-6a), hinting at streamflows that were fed by passive water stores in a proportion of 100%. Conversely, median BFI values for the "MS" sites were generally below 0.2 in both years of study, indicating that a relatively higher proportion of the streamflow at those outlets may be coming from recent precipitation or dynamic storage. In a study of 22 predominantly humid catchments in Indiana, Gunn et al. (2012) found that BFI values ranged from 0.40 to 0.88 with an average of 0.60, suggesting that about 60% of long-term streamflow in those catchments is fed by groundwater and shallow subsurface flow. In the present study, BFI results point to less than a 20% contribution of subsurface flow to streamflow in the "MS" sites, with this percentage increasing towards the bigger watersheds (i.e.,

HWY240 and Miami). The anthropogenic controls behind sites MS4 and MS7 may suggest a higher contribution to baseflow (and hence a higher BFI) at those sites. However, this does not appear to be the case in the current study. Vertical percolation of water, as opposed to lateral transfer (akin to the study of Janzen and Westbrook, 2011), appears to be dominant at those two sites. The water that is contributed from behind the dam does not appear to contribute to flow (at least in the short term) immediately downstream.

2.4.3 Event-based controls on dynamic storage release

Large event peakflow values are usually observed either in association with widespread Hortonian overland flow, or in the case of simultaneous saturation-excess overland flow and lateral shallow subsurface flow. The last two mechanisms are typically active under forest cover, as indicated by Barthold and Woods (2015): in a synthesis study of 42 forested catchments, they found that 19 catchments were dominated by subsurface flow paths (shallow and deep) while 5 catchments were rather dominated by saturation-excess overland flow. In the present study, the highest values of event peak flows (PF) during the 2014 and 2015 study years were observed at site MS2 and may, therefore, have been a consequence of the relatively greater riparian forest cover upstream of this site, compared with the other "MS" sites (Table 2-3). The holding dams at sites MS4 and MS7, which are designed to attenuate peak flows by holding back water until they are full and then spill over, also make it plausible that the release of event rainfall into streams was gradual at those sites, thus resulting in some of the lowest PFs (0.01 mm/day $\leq$ PF $\leq$ 1.67 mm/day) recorded at those sites (Figure 2-7b). This assertion is consistent with research that focuses on the capacity of beaver dams to attenuate flow (e.g., Puttock et al., 2016).

Table 2-3. Watershed and sub-catchment physiographic characteristics for the STCW.

Name	Area (km^2)	Total flowpath length (km)	Total stream length (km)	Treed riparian area (m^2)	Proportion of all forest	Proportion of grassland	Mean elevation (m)	Elevation range (m)	Mean slope (º)	Slope range (º)	Proportion of coarse grained soils	Proportion of till blanket
MS1	0.28	17365.32	0.62	329	0.02	0.01	485.93	12	0.96	2.13	0.00	0.00
MS2	0.19	11378.3	0.23	0	0.15	0.10	486.83	16	1.30	2.72	0.00	0.00
MS3	0.48	73348.61	2.41	17915	0.07	0.03	481.83	28	1.08	4.39	0.00	1.00
MS4	0.31	23626.49	0.97	33162	0.23	0.09	482.67	31	1.59	4.97	0.00	0.00
MS7	1.27	140464.51	4.94	101562	0.13	0.14	473.23	52	1.41	4.97	0.00	1.00
MS9	1.88	181625.58	7.15	118648	0.1	0.12	464.71	59	1.26	4.97	0.00	1.00
HWY240	34.65	3325774.85	92.97	5600880	0.18	0.14	455.13	121	1.79	16.16	0.14	0.87
Miami	74.41	6917609.47	301.03	12130700	0.18	0.13	429.04	190	1.92	20.99	0.38	0.58
Min	***0.19***	***11378.3***	***0.23***	***0***	***0.02***	***0.01***	***429.04***	***12***	***0.96***	***2.13***	***0.00***	***0.00***
Max	***74.41***	***6917609.47***	***301.03***	***12130700***	***0.23***	***0.14***	***486.83***	***190***	***1.92***	***20.99***	***0.38***	***1.00***
Mean	***14.18***	***1336399.14***	***51.29***	***2250399.5***	***0.13***	***0.10***	***469.92***	***63.63***	***1.41***	***7.66***	***0.07***	***0.56***
CV	***1.91***	***1.89***	***2.06***	***1.97***	***0.51***	***0.5***	***0.04***	***0.97***	***0.24***	***0.91***	***2.08***	***0.86***

The relatively high median RRs occurring at site HWY240 in 2014 hint at a tight coupling between input precipitation and streamflow initiation, and it is likely due to the fractured nature of the bedrock at that site which enables infiltrated water to quickly move through the watershed. Those high median RR values must, however, be reconciled with the very high BFI values associated with that site: one potential explanation for high runoff ratios and high BFI values is piston flow, i.e., a mechanism enabling "old" water from passive stores to be quickly pushed into the stream to contribute to event streamflow. Here the phrase "old water" is used to refer to water that was stored in the watershed or a sub-catchment prior to the event under consideration, as opposed to "new water" that is precipitation introduced by the event under consideration. The fact that some of the RR values obtained for the HWY240 were higher than 1 (Figure 2-8g) is also consistent with a piston flow mechanism hypothesis, since it would imply that the volume of stormflow feeding the stream was made of both "old" and "new" water and was therefore larger than the amount of precipitation associated with the current event, thus leading to a numerator that is much larger than the denominator in the RR formula. The findings of Zhang et al. (2014) point to catchment properties such as slope, geology, and land use as stronger controlling factors of RR than climatic conditions; the results of the present study appear to support that assertion. In 2015, the observed wide range of RRs at site MS4 may have resulted from water being held in detention and only pushed into the stream when there was added water onto the reservoir from recent events.

It appears that in 2014, at site MS2, in response to rainfall events, relatively low storage deficits needed to be compensated for before the initiation of streamflow: this is aligned with the fact that 2014 was a wetter year, as well as the fact that prolonged saturation conditions were likely in the riparian areas of the MS2 sub-catchment given the forest cover and the absence of fractured bedrock that would have enhanced vertical percolation and dewatering of the vadose zone. For other sub-catchments such as the

one associated with the HWY240 outlet, however, the evaluation of different metrics could lead to contradictory interpretations, thus underlining the necessity of confronting the analysis of both long-term and short-term hydrographs. For HWY240 in the spring of 2014, small Ia values were observed (they were the smallest across all sites), which, on their own, would have pointed to a "flashy" condition at that site where introduced precipitation quickly satisfied small storage deficits and contributed to streamflow. This was not the interpretation made earlier on the basis of median RR and BFI values at this site, as the hypothesis of piston flow of old water toward the stream seemed more likely. It is therefore possible that at HWY240 during the summer, since most of the streamflow may have been coming from storage release of "old" water, newly introduced precipitation may have gone to satisfy the storage deficit without contributing much to flow over the short-term, thus making it difficult to use Ia values for process inferences (Figure 2-7c). In 2015, however, Ia values at site MS7 were useful to assess the weak coupling between precipitation input and streamflow initiation: high median Ia values could be observed (Figure 2-7c) and plausibly linked to the fact that the dam located upstream of the MS7 outlet holds up introduced precipitation and slowly releases it to the stream. It should, however, be noted that snowmelt-driven events were not considered in the present study, due to the large uncertainties associated with the estimation of daily melt rates across the whole STCW. The comparison made here between the results of long-term and short-term hydrograph analyses may have led to different interpretations or conclusions if all types of events had been considered across both study years.

2.5 Conclusion

This work assessed watershed storage and release dynamics in the context of streamflow generation. Total storage release was, indirectly, evaluated via total flow duration curves. Baseflow index analysis was used to assess passive storage-release dynamics, while dynamic storage-release evaluations were made via the examination of fastflow duration curves, as well as the computation of event-specific initial abstraction values and runoff ratios. In relation to total storage release assessments, evaluations of the middle segments of the flow duration curves (FDCs) suggested that flow was more variable in the dry year (2015) compared to the wet year (2014). The analysis of the FDCs, however, led to a counter-intuitive conclusion of lower storage retention potential during dry conditions, thus raising the question of whether literature-based interpretations based on slopes of a FDC are universally applicable across sites and across segments of the FDC. In assessing passive storage and release dynamics, the analysis of baseflow duration curves and the computation of baseflow index (BFI) values revealed that there was more baseflow in 2015 than in 2014, which is consistent with 2015 being a drier year. Baseflow contributions to streamflow at the "MS" sites are nearly non-existent while contributions however increased towards the relatively bigger watersheds draining to HWY240 and Miami. Site MS2, which was the most forested amongst the "MS" sites, had the highest peak flow values amongst the "MS" sites. There were also relatively high Ia values at site MS7, mainly due to a retention dam holding back water and later releasing it slowly into the stream. In terms of runoff ratios (RR), several hypotheses were considered depending on the site. For instance, HWY240 had relatively high RR values, which is plausible only if the fractured nature of the bedrock at that site promotes piston flow processes thanks to which passive stores of "old" water are pushed to the stream during precipitation events. At MS4, however, the high RRs observed may, rather, be a result of a retention dam getting full such that any added precipitation quickly flows over the dam into the stream. The multi-scale analysis of stream

hydrographs used in this study was, therefore, useful to derive hypotheses about dominant storage-release dynamics across nested Prairie watersheds. This multi temporal-scale analysis based on hydrometric data only could, however, lead to counter-intuitive results, and it was also insufficient for providing detailed assessments of storage-release dynamics, either through the quantification of "new" versus "old" water contributions to the outlets, or through the estimation of water ages at the outlet or transit times of water through the upstream watersheds. Such assessments can, however, be made through the use of isotopic data, which is the focus of the next chapters of this thesis. Results from this hydrometric analysis can, nonetheless, have implications for watershed management in the context of drainage design and flood control, as well as leaching of fertilizers and nutrients from terrestrial to aquatic environments.

2.6 Acknowledgments

We acknowledge the support of the first author through a University of Manitoba Graduate Fellowship**.** We also acknowledge the financial support made available by the Natural Sciences and Engineering Research Council of Canada (NSERC) through a Discovery Grant awarded to Dr. Genevieve Ali. The authors thank Larry Braul and Erin Zoski of AAFC who contributed greatly in site-setup and data collection efforts.

2.7 References

Ahilan, S., O'Sullivan, J. J., Bruen, M., Brauders, N., & Healy, D. (2013). Bankfull discharge and recurrence intervals in Irish rivers. *Proceedings of the Institution of Civil Engineers-Water Management, 166*(7), 381-393. doi:10.1680/wama.11.00078.

Baltas, E. A., Dervos, N. A., & Mimikou, M. A. (2007). Technical Note: Determination of the SCS initial abstraction ratio in an experimental watershed in Greece. *Hydrology and Earth System Sciences, 11*(6), 1825-1829. doi:10.5194/hess-11-1825-2007.

Barthold, F. K., & Woods, R. A. (2015). Stormflow generation: A meta-analysis of field evidence from small, forested catchments. *Water Resources Research, 51*(5), 3730-3753. doi:10.1002/2014wr016221.

Basso, S., Schirmer, M., & Botter, G. (2016). A physically based analytical model of flood frequency curves. *Geophysical Research Letters, 43*(17), 9070-9076. doi:10.1002/2016gl069915.

Beck, H.E., van Dijk A. I. J. M., Miralles, D. G., de Jeu, R. A. M., Bruiinzeel, L. A., McVicar, T. R. & Schellekens J. (2013). Global patterns in base flow index and recession based on streamflow observations from 3394 catchments. *Water Resources Research*, *49*(12), 7843-7863.

Betcher, R., Grove G., & Pupp C. (1995). Groundwater in Manitoba: hydrogeology, quality concerns, management; *National Hydrology Research Institute Contribution No. CS-93017,* Environmental Sciences Division, NHRI, Environment Canada, 53 pp.

Birkel, C., Soulsby, C., & Tetzlaff, D. (2011). Modelling catchment-scale water storage dynamics: reconciling dynamic storage with tracer-inferred passive storage. *Hydrological Processes, 25*(25), 3924-3936. doi:10.1002/hyp.8201.

Biswas, A., Chau, H. W., Bedard-Haughn, A. K., & Si, B. C. (2012). Factors controlling soil water storage in the hummocky landscape of the Prairie Pothole Region of North America. *Canadian Journal of Soil Science, 92*(4), 649-663. doi:10.4141/cjss2011-045.

Black, P. E. (1997). Watershed functions. *Journal of the American Water Resources Association, 33*(1), 1-11. doi:10.1111/j.1752-1688.1997.tb04077.

Blaney, H. F., Criddle, W.D. (1962). Determining consumptive use and irrigation water requirements. U.S. Department of Agriculture Research Service Technical Bulletin 1275.

Bloomfield, J. P., Allen, D. J., & Griffiths, K. J. (2009). Examining geological controls on baseflow index (BFI) using regression analysis: An illustration from the Thames Basin, UK. *Journal of Hydrology, 373*(1-2), 164-176. doi:10.1016/j.jhydrol.2009.04.025.

Bosch, D. D., Arnold, G. J., Allen, P. G., Lim, J. K., & Park, Y. S. (2017). Temporal variations in baseflow for the Little River experimental watershed in South Georgia, USA. *Journal of Hydrology: Regional Studies*, 10 (2017) 110–121, http://dx.doi.org/10.1016/j.ejrh.2017.02.002.

Brauman, K. A., Daily, G. C., Duarte, T. K., & Mooney, H. A. (2007). The nature and value of ecosystem services: An overview highlighting hydrologic services, *Annals of Reviews on Environmental Resources*, 32, 67–98.

Buttle, J. M. (2016). Dynamic storage: a potential metric of inter-basin differences in storage properties. *Hydrological Processes, 30*(24), 4644-4653. doi:10.1002/hyp.10931.

Buttle, J. M. (2018). Mediating stream baseflow response to climate change: The role of basin storage, *Hydrological Processes, 32*(2018), 363-378.

Campolo, M., Soldati, A., & Andreussi, P. (1999). Forecasting river flow rate during low-pow periods using neural networks. *Water Resources Research, 35*(11), 3547-3552. doi:10.1029/1999wr900205.

Cancelliere, A., & Salas, J. D. (2004). Drought length properties for periodic-stochastic hydrologic data. *Water Resources Research, 40*(2). doi:10.1029/2002wr001750.

Carey, S. K., & DeBeer, C. M. (2008). Rainfall-runoff hydrograph characteristics in a discontinuous permafrost watershed and their relation to ground thaw. Proceedings of the Ninth *International Conference on Permafrost*, Fairbanks.

Cheng, L., Yaeger, M., Viglione, A., Coopersmith, E., Ye, S., & Sivapalan, M. (2012). Exploring the physical controls of regional patterns of flow duration curves - Part 1: Insights from statistical analyses. *Hydrology and Earth System Sciences, 16*(11), 4435-4446. doi:10.5194/hess-16-4435-2012.

Chouaib, W., Caldwell, P. V., & Alila, Y. (2018). Regional variation of flow duration curves in the eastern United States: Process-based analyses of the interaction between climate and landscape properties. *Journal of Hydrology, 559*, 327-346. doi:10.1016/j.jhydrol.2018.01.037.

Chow, V. T. (1964). Handbook of Hydrology. McGraw-Hill Book Company, New York, New York. 529pp.

Coopersmith, E., Yaeger, M. A., Ye, S., Cheng, L., & Sivapalan, M. (2012). Exploring the physical controls of regional patterns of flow duration curves - Part 3: A catchment classification system based on regime curve indicators. *Hydrology and Earth System Sciences, 16*(11), 4467-4482. doi:10.5194/hess-16-4467-2012.

Cyr, J. F., Landry, M., & Gagnon, Y. (2011). Methodology for the large-scale assessment of small hydroelectric potential: Application to the Province of New Brunswick (Canada). *Renewable Energy, 36*(11), 2940-2950. doi:10.1016/j.renene.2011.04.003.

Day, C. A. (2009). Modelling impacts of climate change on snowmelt runoff generation and streamflow across western US mountain basins: a review of techniques and applications for water resource management. *Progress in Physical Geography-Earth and Environment, 33*(5), 614-633. doi:10.1177/0309133309343131.

Dingman, S. L. (2002). Physical Hydrology. Volume 1. Princeton Hall, NJ. 646pp.

Eckhardt, K. (2005). How to construct recursive digital filters for baseflow separation. *Hydrological Processes, 19*(2), 507-515. doi:10.1002/hyp.5675.

Eckhardt, K. (2008). Comparison of baseflow indices, which were calculated with seven different baseflow separation methods. *Journal of Hydrology*, (352) 168–173.

Fang X., Minke, A., Pomeroy, J., Brown, T., Westbrook, C., Guo, X., & Guangul S. (2007). A review of Canadian Prairie hydrology: Principles, modelling and response to land use and drainage change (Vol. 2). Saskatoon, Saskatchewan: Centre for Hydrology.

Freer, J., McDonnell, J. J., Beven, K. J., Peters, N. E., Burns, D. A., Hooper, R. P., Kendall, C. (2002). The role of bedrock topography on subsurface storm flow. *Water Resources Research, 38*(12). doi:10.1029/2001wr000872.

Geris, J., Tetzlaff, D., & Soulsby, C. (2015). Resistance and resilience to droughts: hydropedological controls on catchment storage and run-off response. *Hydrological Processes, 29*(21), 4579-4593. doi:10.1002/hyp.10480.

Griffiths, G. A., & Clausen, B. (1997). Streamflow recession in basins with multiple water storages. *Journal of Hydrology, 190*(1-2), 60-74. doi:10.1016/s0022-1694(96)03060-0.

Gunn, R., Martin, A., Engel, B., & Ahiablame, L. (2012). Development of two indices for determining hydrologic implications of land use changes in urban areas. *Urban Water Journal, 9*(4), 239-248. doi:10.1080/1573062x.2012.660957.

Hall, F.R. (1968). Base-flow recessions—a review. *Water Resources Research* 4 (5), 973–983.

Heidbuechel, I., Troch, P. A., Lyon, S. W., & Weiler, M. (2012). The master transit time distribution of variable flow systems. *Water Resources Research, 48*. doi:10.1029/2011wr011293

Hewlett, J. D. & Hibbert, A. R. (1967). Factors affecting the response of small watersheds to precipitation in humid areas, in: Proceedings of the *International Symposium on Forest Hydrology*, Pergamon, New York, p. 275-290.

Huang, H.J., Cheng, S.J., Wen J. & J. Lee J. (2008). Effect of growing watershed imperviousness on hydrograph parameters and peak discharge. *Hydrological. Processes 22 (13), 2075–2085*.

Hutchinson, R.D. (1977). Groundwater resources of Cavalier and Pembina counties, North Dakota. U.S Geological Survey, Bulletin 62 – Part III, 75pp.

Janzen, K., & Westbrook, C.J., (2011) Hyporheic Flows Along a Channeled Peatland: Influence of Beaver Dams , Canadian Water Resources Journal, 36:4, 331-347, DOI: 10.4296/cwrj3604846

Jencso, K. G., & McGlynn, B. L. (2011). Hierarchical controls on runoff generation: Topographically driven hydrologic connectivity, geology, and vegetation. *Water Resources Research, 47*. doi:10.1029/2011wr010666.

Kirchner, J. W. (2009). Catchments as simple dynamical systems: Catchment characterization, rainfall-runoff modeling, and doing hydrology backward. *Water Resources Research, 45*. doi:10.1029/2008wr006912.

Kneis, D., Buerger, G., & Bronstert, A. (2012). Evaluation of medium-range runoff forecasts for a 50 km(2) watershed. *Journal of Hydrology, 414*, 341-353. doi:10.1016/j.jhydrol.2011.11.005.

Kronholm, S. C., & Capel, P. D. (2016). Estimation of time-variable fast flow path chemical concentrations for application in tracer-based hydrograph separation analyses. *Water Resources Research, 52*(9), 6881-6896. doi:10.1002/2016wr018797.

Lana-Renault, N., Latron, J., Karssenberg, D., Serrano, P., Reguees, D., & Bierkens, M. F. P. (2012). Seasonal differences in runoff between forested and non-forested catchments: a case study in the Spanish Pyrenees. *Revisiting Experimental Catchment Studies in Forest Hydrology, 353*, 58-73.

Lana-Renault, N., Latron, J., Karssenberg, D., Serrano-Muela, P., Reguees, D., & Bierkens, M. F. P. (2011). Differences in stream flow in relation to changes in land cover: A comparative study in two sub-Mediterranean mountain catchments. *Journal of Hydrology, 411*(3-4), 366-378. doi:10.1016/j.jhydrol.2011.10.020.

Li, D. (2014). Assessing the impact of interannual variability of precipitation and potential evaporation on evapotranspiration. *Advances in Water Resources, 70(2014)* 1-11. http://dx.doi.org/10.1016/j.advwatres.2014.04.012.

Li, X., Shao, M. a., Jia, X., Wei, X., & He, L. (2015). Depth persistence of the spatial pattern of soil-water storage along a small transect in the Loess Plateau of China. *Journal of Hydrology, 529*, 685-695. doi:10.1016/j.jhydrol.2015.08.039.

Lim, K.J., Park, Y.S., Kim, J., Shin, Y.-C., Kim, N.W., Kim, S.J., Jeon, J.-H., Engel, B.A. (2010). Development of genetic algorithm-based optimization module in WHAT system for hydrograph analysis and model application. Computer Geoscience. 36 (2010), 936–944, http://dx.doi.org/10.1016/j.cageo.2010.01.004.

Manitoba Department of Agriculture (1943). Reconnaissance soil survey of South-central Manitoba. Report number D4. Government of Manitoba, Canada.

Manitoba Department of Agriculture (1988). Soils of the Rural Municipalities of Grey, Dufferin, Roland, Thompson and parts of Stanley. Report number D60. Government of Manitoba, Canada.

Matile, G.L.D. & Keller, G.R. (2004). Surficial geology of the Brandon map sheet (NTS 62G), Manitoba Geological Survey, Surficial Geology Compilation Map Series, SG-62G, scale 1: 250,000.

McNamara, J. P., Tetzlaff, D., Bishop, K., Soulsby, C., Seyfried, M., Peters, N. E., & Hooper, R. (2011). Storage as a Metric of Catchment Comparison. *Hydrological Processes, 25*(21), 3364-3371. doi:10.1002/hyp.8113.

Melo, D.C.D., Scanlon, B.R., Zhang, Z., Wendland, E., & Yin L. (2016). Reservoir storage and hydrologic responses to droughts in the Paraná River basin, south-eastern Brazil. *Hydrology and Earth System Sciences, 20*, 4673-4688.

Mohamoud, Y. M. (2008). Prediction of daily flow duration curves and streamflow for ungauged catchments using regional flow duration curves. *Hydrological Sciences Journal-Journal Des Sciences Hydrologiques, 53*(4), 706-724. doi:10.1623/hysj.53.4.706.

Mueller, M. F., Dralle, D. N., & Thompson, S. E. (2014). Analytical model for flow duration curves in seasonally dry climates. *Water Resources Research, 50*(7), 5510-5531. doi:10.1002/2014wr015301.

Muller-Wohlfeil, D. I., Jorgensen, J. O., Bjorklund, C., & Forsman, A. (2002). Model-based regional estimation of groundwater nitrogen loads from diffuse sources. *Agricultural Effects on Ground and Surface Waters: Research at the Edge of Science and Society*(273), 201-205.

Mueller, M. F., Dralle, D. N., & Thompson S. E. (2014). Analytical model for flow duration curves in seasonally dry climates, *Water Resources Research*, *50*(7), 5510-5531.

Narayanan, K., & Jaehak J. (2011). An Approach for Estimating Stream Health Using Flow Duration Curves and Indices of Hydrologic Alteration. *Conference proceeding on AgriLife research and Extension,* Texas, P. 22.

Nikas, K., Antonakos, A., Lambrakis, N. & Kallergis, G. (2007). The use of 'antecedent precipitation index' and 'delay factor' to estimate runoff from rainfall; a case study from eight drainage basins-Achaia, Peloponessos, Greece. *Geological Society of Greece*. Proceedings of the 11th international congress, Athens, May 2007.

Nosetto, M. D., Jobbagy, E. G., Brizuela, A. B., & Jackson, R. B. (2012). The hydrologic consequences of land cover change in central Argentina. *Agriculture Ecosystems & Environment, 154*, 2-11. doi:10.1016/j.agee.2011.01.008.

Puttock, A., Graham, H.A., Cunliffe, A.M., Elliot, M. & Brazier, R.E. (2017). Eurasian beaver activity increases water storage, attenuates flow and mitigates diffuse pollution from intensively-managed grasslands. *Science of the Total Environment* 576 (2017) 430–443.

Sawicz, K., Wagener, T., Sivapalan, M., Troch, P. A., & Carrillo, G. (2011). Catchment classification: empirical analysis of hydrologic similarity based on catchment function in the eastern USA. *Hydrology and Earth System Sciences, 15*(9), 2895-2911. doi:10.5194/hess-15-2895-2011.

Searcy, J. K. (1959). Flow-Duration Curves, US Geological Survey Water Supply Paper 1542-A, 33 pp.

Shook, K., & Pomeroy, J. (2012). Changes in the hydrological character of rainfall on the Canadian prairies. *Hydrological Processes, 26*(12), 1752-1766. doi:10.1002/hyp.9383.

Smakhtin, V. U. (2001). Low flow hydrology: a review. *Journal of Hydrology*, *240*(3-4), 147-186. doi:10.1016/s0022-1694(00)00340-1.

Sugiyama, H., Vudhivanich, V., Whitaker, A. C., & Lorsirirat, K. (2003). Stochastic flow duration curves for evaluation of flow regimes in rivers. *Journal of the American Water Resources Association, 39*(1), 47-58. doi:10.1111/j.1752-1688.2003.tb01560.

Szeftel, P., Moore, R.D. & M. Weiler (2010). Influence of distributed flow losses and gains on the estimation of transient storage parameters from stream tracer experiments, *Journal of Hydrology, 396(2011),* 277-291.

Tang, W., & Carey, S. K. (2017). HydRun: A MATLAB toolbox for rainfall-runoff analysis. *Hydrological Processes, 31*(15), 2670-2682. doi:10.1002/hyp.11185.

Tiessen, K. H. D., Elliott, J. A., Yarotski, J., Lobb, D. A., Flaten, D. N., & Glozier, N. E. (2010). Conventional and Conservation Tillage: Influence on Seasonal Runoff, Sediment, and Nutrient Losses in the Canadian Prairies. *Journal of Environmental Quality, 39*(3), 964-980. doi:10.2134/jeq2009.0219.

Verma, R. K., Murthy, S., Verma, S., & Mishra, S. K. (2017). Design flow duration curves for environmental flows estimation in Damodar River Basin, India. *Applied Water Science, 7*(3), 1283-1293. doi:10.1007/s13201-016-0486-0.

Vogel, R. M., & Fennessey, N. M. (1994). Flow-duration curves: new interpretation and confidence-intervals. *Journal of Water Resources Planning and Management-Asce, 120*(4), 485-504. doi:10.1061/(asce)0733-9496(1994)120:4(485).

Vogel, R. M., & Fennessey, N. M. (1995). Flow duration curves: a review of applications in water-resources planning. *Water Resources Bulletin, 31*(6), 1029-1039.

Ward, R. C., & Robinson M. (1990). Principles of Hydrology, 3rd Edn., McGraw-Hill, Berkshire, England, 428pp.

Yadav, M., Wagener, T., Gupta, H. (2012). Regionalization of constraints on expected watershed response behavior for improved predictions in ungauged basins. *Advances in Water Resources, 30*(8), 1756-1774.

Yaeger, M., Coopersmith, E., Ye, S., Cheng, L., Viglione, A., & Sivapalan, M. (2012). Exploring the physical controls of regional patterns of flow duration curves - Part 4: A synthesis of empirical analysis, process modeling and catchment classification. *Hydrology and Earth System Sciences, 16*(11), 4483-4498. doi:10.5194/hess-16-4483-2012.

Ye, S., Yaeger, M., Coopersmith, E., Cheng, L., & Sivapalan, M. (2012). Exploring the physical controls of regional patterns of flow duration curves - Part 2: Role of seasonality, the regime curve, and associated process controls. *Hydrology and Earth System Sciences, 16*(11), 4447-4465. doi:10.5194/hess-16-4447-2012.

Yokoo, Y., & Sivapalan, M. (2011). Towards reconstruction of the flow duration curve: development of a conceptual framework with a physical basis. *Hydrology and Earth System Sciences, 15*(9), 2805-2819. doi:10.5194/hess-15-2805-2011.

Yuan, Y., Mitchell, J. K., Hirschi, M. C., & Cooke, R. A. C. (2001). Modified SCS curve number method for predicting subsurface drainage flow. *Transactions of the Asae, 44*(6), 1673-1682.

Zhang, Y., Vaze, J., Chiew, F. H. S., Teng, J., & Li, M. (2014). Predicting hydrological signatures in ungauged catchments using spatial interpolation, index model, and rainfall-runoff modelling. *Journal of Hydrology, 517*, 936-948. doi:10.1016/j.jhydrol.2014.06.032.

Zhang, Y., Ahiablame, L., Engel, B., Liu, J. (2013). Regression modeling of baseflow and baseflow index for Michigan USA. Water 5 (2013Z), 1797–1815,http://dx.doi.org/10.3390/w5041797.

Zomlot, Z., Verbeiren, B., Huysmans, M., Batelaan, O. (2015). Spatial distribution of groundwater recharge and base flow: assessment of controlling factors. Journal of Hydrology Regional Studies. 4 (2015), 349–368, http://dx.doi.org/10.1016/j.ejrh.2015.07.005.

Zhang, Z., Wagener, T., Reed, P., Bhushan, R. (2008). Reducing uncertainty in predictions in ungauged basins by combining hydrologic indices, regionalization and multiobjective optimization . *Water Resources Research, 44(12),* W00B04.

Zhao, F., Xu, Z., & Zhang, L. (2012). Changes in streamflow regime following vegetation changes from paired catchments. *Hydrological Processes, 26*(10), 1561-1573. doi:10.1002/hyp.8266.

CHAPTER 3: EVALUATING THE EFFECTS OF TRACER CHOICE AND END-MEMBER DEFINITIONS ON HYDROGRAPH SEPARATION RESULTS ACROSS NESTED SEASONALLY COLD WATERSHEDS

Abstract

Isotope-based hydrograph separation (IHS) is a widely used method in studies of runoff generation and streamflow partitioning. Challenges in choosing and characterizing appropriate tracers and end-members have, however, led to presumably highly uncertain IHS results. Here we tested the effects of end-member definitions and tracer choices on IHS results in nested Prairie watersheds of varying size and landscape characteristics. Specifically, the consideration of eight potential "new" water end-members, eight potential "old" water end-members, and two stable water isotope tracers led to 80 potential IHS results for each stream water sample. IHS-related uncertainty was evaluated using a Gaussian error propagation method. Results show that choosing an appropriate "new" water end-member is most challenging during the freshet: highly variable "old" water fractions associated with high uncertainties were attributed to changing conditions from melting snow only to rain-on-snow. In summer and fall, it was rather the choice of an appropriate "old" water end-member that was most problematic. IHS results obtained using $\delta^{18}O$ versus $\delta^{2}H$ as a tracer were significantly different except in the flattest and most wind-sheltered watersheds examined. Overall, $\delta^{2}H$-based IHS results were more uncertain than their $\delta^{18}O$-based counterparts. Recommendations are therefore made toward careful selection of a tracer and a sampling strategy aimed at characterizing the most appropriate end-members for IHS, especially when dealing with seasonally cold watersheds.

Keywords: hydrograph separation, oxygen-18, deuterium, Canadian Prairies, end-member definitions, uncertainty, sensitivity

3.1 Introduction

Environmental isotopes have been used as indicators of runoff generation at varying spatial and temporal scales (e.g., Uhlenbrook et al., 2002; St. Amour et al., 2005; Laudon et al., 2007; Munoz-Villers and McDonnell, 2012). Notably, the two stable isotopes of oxygen and hydrogen, whose ratios are expressed as $\delta^{18}O$ and $\delta^{2}H$, have been widely used for hydrograph separation (HS) to distinguish temporal sources of streamflow, namely "old" water (defined as water that existed in a watershed before the onset of a precipitation event) and "new" water (defined as water brought in by the precipitation event under consideration). Isotope-based HS (or IHS) is traditionally achieved by solving equations corresponding to a two-component mass balance, making it a straightforward tool to infer water sources. However, the simple IHS method is tied to a rather long list of assumptions that were first detailed by Sklash and Farvolden (1979) and then Buttle (1994; 2005) as follows:

1. The isotopic signatures of the "new" and "old" water sources are significantly different from one another.
2. "New" and "old" water must maintain constant isotopic signatures in space and time, or any variations they might be subject to must be quantifiable.
3. Soil water contributions from the vadose zone must either be negligible or share the isotopic signature of phreatic groundwater, since the latter is the water source often implied when using the phrase "old" water.
4. Surface (i.e., depression) storage contributes minimally to streamflow.

While the usefulness of IHS is undeniable, some of the assumptions behind it are easily violated unless strict methodological choices are made. One example of such violations is the selection of a representative "new" water end-member during snowmelt that satisfies assumptions #1 and #2. Dincer et al. (1970), Rodhe (1981) and Cooper et al. (1991) melted snow cores – analysed as depth integrated

samples – to characterize the "new" water end-member during the freshet. However, their approach did not address the issue of changing snow isotopic signatures due to depth stratification (Huth et al., 2004) or isotopic fractionation (Taylor et al., 2001, 2002; Feng et al., 2002) that occurs during the melting of the snow. The use of snow lysimeters during snowmelt and rain-on-snow events is believed to address that issue (Buttle et al., 1995). During post-freshet rainfall events, temporal variation of the "new" water end-member also exists due to the "amount" effect, and can potentially be accounted for using an incremental weighting approach for defining the isotopic composition of rain (McDonnell et al., 1991). The challenge of sampling and characterizing "composite" events that involve snow, rain-on-snow, snowmelt and then rain – due to rapidly changing air temperatures in seasonally cold watersheds – remains difficult. As a result, significant uncertainties can be introduced into IHS results due to the spatiotemporal variability of end-member signatures (Delsman et al., 2013).

Regarding assumption #3, early work by DeWalle et al. (1988) showed that soil water and groundwater can have distinct isotopic signals. Kennedy et al. (1986) also showed that soil water – and hence the vadose zone – can contribute significantly to streamflow during storms. Blume et al. (2008) showed that failure to distinguish between soil water and groundwater can lead to "old" water contributions to streamflow that exceed 100% or fall below 0%, thus making the two-component mass balance problem ill-defined, from a mathematical standpoint. To resolve that issue, the expansion of two-component IHS to three-component end-member mixing has been suggested (DeWalle et al., 1988; Ogunkoya and Jenkins, 1993), where two tracers (usually one stable isotope tracer and another environmental tracer) are used to characterize the possible water sources. This three-component method has the advantage of revealing geographic source components in addition to the time source, but it requires a second conservative or quasi-conservative tracer – such as chloride or silica in certain environments. When results of two-component IHS and three-component end-member mixing have been compared, some studies estimated similar "old" water fractions with the two approaches (e.g., in a

permafrost-dominated alpine catchment in Yukon in a study by Carey and Quinton (2005), and in a volcanic substrate-dominated tropical montane cloud forest in central-eastern Mexico in a study by Munoz-Villers and McDonnell (2012)), while others found a 10% difference in "old" water contributions between the two methods (e.g., in a study done in the Black Forest Mountains of Germany by Wenninger et al. (2004)). To get around assumption #3, Wels et al. (1991) and St. Amour et al. (2005) also performed two-component IHS in two steps, where the "old" water fraction was separated into soil water and groundwater in the second step. Wels et al. (1991) estimated a 90% subsurface water contribution to streamflow in the first step of the hydrograph separation process, 65% of which was determined to originate from groundwater in the second step. In the case of St. Amour et al. (2005), up to 54% of groundwater was determined to have formed the portion of the subsurface contribution to the streamflow.

Regarding tracer choice, the fact that $\delta^{18}O$ is used more often than $\delta^{2}H$ in IHS studies has traditionally led to the conclusion that using both provides redundant information about a given system. Some authors have, however, shown that IHS results can be tracer-dependent. Rice and Hornberger (1998) notably used $\delta^{2}H$ in combination with any one of $\delta^{18}O$, DOC, chloride and sodium in their study at a forested catchment in north-central Maryland: they found large differences (> 50%) in the computed fractions of "old" and "new" water. Lyon et al. (2009) also obtained diverging results when performing IHS using $\delta^{18}O$ versus $\delta^{2}H$ during a single runoff event in a forested catchment located in Arizona. Only a handful of IHS studies (e.g., Burns and McDonnell, 1998; Rice and Hornberger, 1998; Gibson et al., 2000; Lyon et al., 2009) have used a combination of $\delta^{18}O$ and $\delta^{2}H$ (rather than just one) in their work. The potential benefits of using both $\delta^{18}O$ and $\delta^{2}H$ data for IHS include a better characterization of event water when one tracer over- (or under-) estimates its contribution. Those potential benefits were recently reaffirmed by Klaus and McDonnell (2013), but the dual-tracer strategy has yet to be widely adopted by the hydrologic community.

Overall, many studies have relied on two-component IHS to quantify "new" and "old" water contributions to streamflow even when some of the aforementioned assumptions were possibly violated. It is worth noting that studies focusing on more than two end-members (i.e., end-member mixing analyses) have used various statistical tools to constrain end-member and tracer-related uncertainty (e.g., Hooper, 2003; James and Roulet, 2006; Barthold et al., 2011). When it comes to two-component IHS, however, the only methodology available was put forward by Genereux (1998): it is based on Gaussian error propagation to evaluate uncertainties associated with the spatiotemporal variability of end-members as well as laboratory errors. Out of the 22 papers focusing on two-component IHS published since Genereux (1998) that we reviewed, only 18% estimated and reported uncertainties. Even when the Genereux approach was applied, only average uncertainty values were reported – either in a sentence or two or in a summary table – making it impossible to evaluate how IHS results and associated errors change seasonally and spatially.

In light of the aforementioned issues associated with the use of two-component IHS, the overarching goal of the current paper was to evaluate the sensitivity of IHS results to not only tracer choice ($\delta^{18}O$ versus $\delta^{2}H$) but also assumption violation (in particular assumptions #1, #2 and #3). Rather than make subjective choices regarding the "best" tracer to use and assuming the temporal invariance of end-member isotopic signatures at the event and seasonal scales, we evaluated two tracers ($\delta^{18}O$ versus $\delta^{2}H$), eight potential definitions for the "new" water end-member (based on snow, snowmelt and rain data), and eight potential definitions for the "old" water end-member (based on shallow, intermediate and deep groundwater data). Each combination of one tracer, one "new" water end-member definition and one "old" water end-member definition constituted a IHS scenario. Each IHS scenario was applied to a range of streamflow samples from nested watersheds of varying size, land-use and physiographic characteristics. Three specific questions guided the analysis, namely:

1. How spatially and temporally variable are "old" water contributions to streamflow under different IHS scenarios?
2. What is the effect of tracer choice ($\delta^{18}O$ versus $\delta^{2}H$) and end-member choice on the computed "old" water contributions to streamflow?
3. Which IHS assumption violations lead to the largest uncertainties in computed "old" water contributions?

3.2 Materials and Methods

3.2.1 Study site

The focus was on 7 sub-watersheds (Table 3-1; Figure 3-1) ranging in size from 0.19 to 34.65 km^2 and nested within the 74.41 km^2 South Tobacco Creek Watershed (STCW) in the province of Manitoba, Canada (Figure 3-1). The study area is located in the Prairies ecozone, which means that it is characterized by semi-arid to sub-humid temperate conditions, i.e., cold lengthy winters and short cool summers (Gray and Landine, 1988; Fang et al., 2007; Van der Kamp et al., 2008; Tiessen et al., 2010; Pomeroy et al., 2013; Shook et al., 2013; Hayashi et al., 2016). The mean annual precipitation recorded in the STCW is 545.6 mm (Environment Canada, 2014), of which 25-30% falls as snow between the months of November and March. The mean daily air temperature is 3.5°C, with -11.5°C and 17.2°C being the means for the months of December and June, respectively (Environment Canada, 2014). The STCW is characterized by a shale bedrock overlain by moderately to strongly calcareous glacial till and clay-loam soils (Matile and Keller, 2004; Tiessen et al., 2010). It is also traversed by the NW-SE-trending Pembina escarpment, which originated approximately 50 to 84 million years ago because of the Laramide Orogeny. Glacial debris deposited as moraines during successive glaciations also form the escarpment,

which marks the boundary of Glacial Lake Agassiz (Bamburak and Christopher, 2004). Soils in the watershed are mainly classified as Dark Gray Chernozems (Mollisols), with mean slopes ranging from 1.7 to 3.4%. An elevation drop of approximately 200 m exists between the STCW headwaters and its outlet near the town of Miami (Figure 3-1).

The watershed is a mix of different landscapes, including: 1) undulating terrain above the escarpment, where six of the targeted sub-watershed outlets ("MS" sites) are located; 2) the escarpment, where the HWY240 sub-watershed outlet is located; and 3) flatter plains below the escarpment, where the Miami outlet is located. The sub-watersheds above the escarpment have drainage areas ranging from 0.19 to 1.88 km^2 and elevation ranges between 12 and 59 m (Table 3-1). The MS4 and MS7 outlets have small farm dams and retention ponds located immediately upstream of them, for stormflow control purposes, while the MS9 outlet is situated in a wind-sheltered area. The sub-watershed draining into HWY240 has an area of 34.65 km^2 and an elevation range of 121 m (Table 3-1).

3.2.2 Sample collection and laboratory analyses

Sampling took place during the 2014 open water period from spring to fall (i.e., April-October). Weekly samples (as well as higher-frequency samples during storm events) of snow, snowmelt, stream, rain, and samples of shallow, intermediate and deep groundwater, were collected in each of the seven sub-watersheds and in the lower portion of the STCW. Apart from snow and snowmelt samples that were spatially distributed across each sub-watershed and averaged into composite samples, other listed sample types were collected at a single site proximal to the sub-watershed or watershed outlet. Each outlet was equipped with rain collectors and different types of weirs – either v-notch or rectangular, in combination with a Campbell Scientific snow and water depth sensor SR50A (1 cm accuracy) – for discharge measurements.

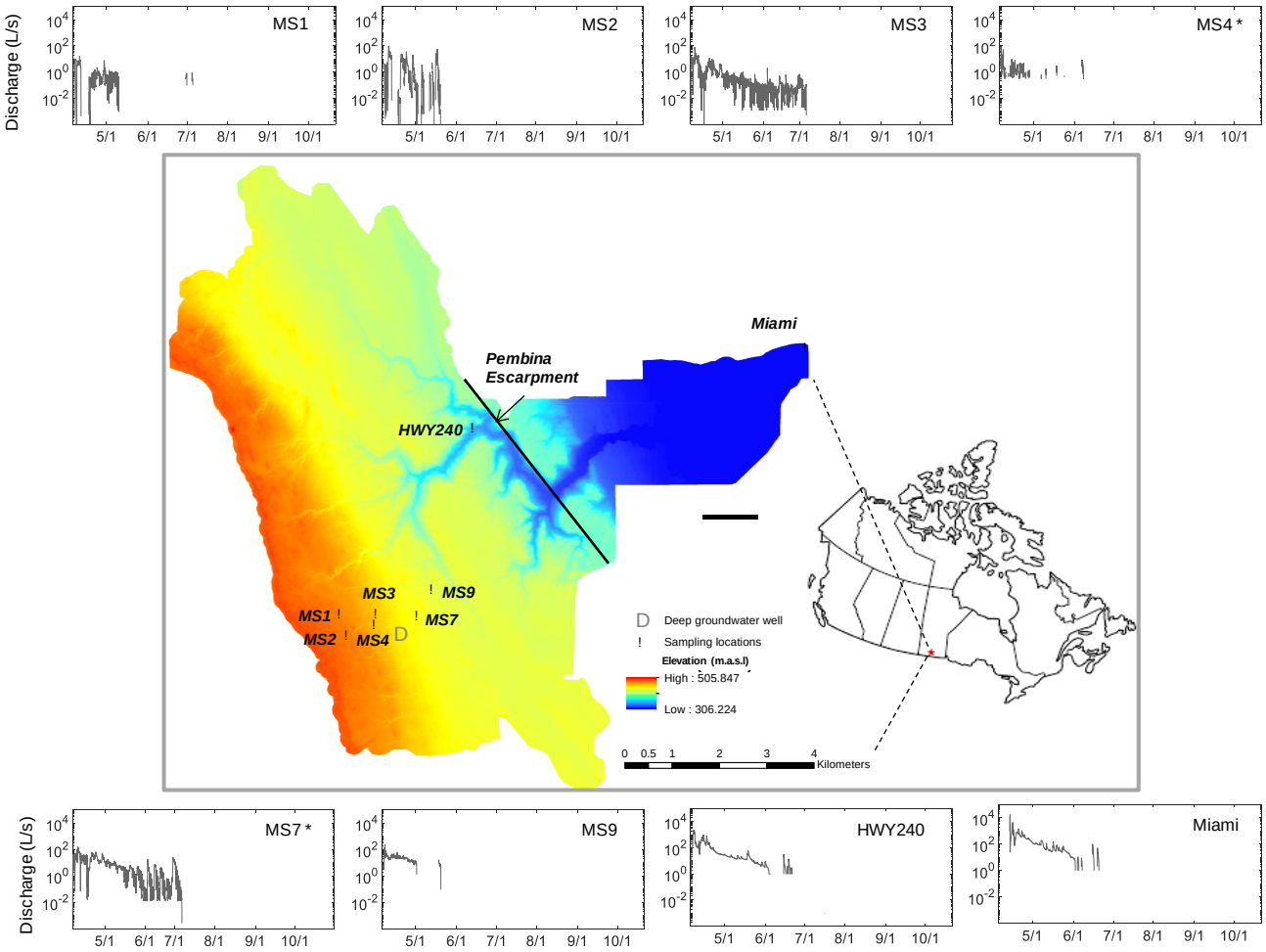

Figure 3-1. Location and digital elevation model (1 m horizontal resolution) of the South Tobacco Creek Watershed (STCW). Sub-watershed outlets (and stream water sampling locations) are indicated. m.a.s.l.: meters above sea level. Hydrographs (log scale) covering the sampling period at each of the sub-watershed outlets are also shown. Sites marked with (*) on the hydrographs have reservoirs immediately upstream of them. Blanks in the timeseries signal zero-flow periods.

Table 3-1. Characteristics of the eight (sub-) watersheds targeted in the current study. Miami is the outlet of the entire STCW. Min, Max, Mean and CV are the minimum, maximum, mean and coefficient of variation of each characteristic across the eight sites.

Name	Area (km^2)	Total flowpath length ($x10^6$km)	Total stream length (km)	Proportion of forest land (%)	Mean elevation (m)	Elevation range (m)	Mean slope (º)	Slope range (º)	Proportion of coarse grained soils (%)	Proportion of till blanket (%)
MS1	0.28	0.02	0.62	2	485.93	12	0.96	2.13	0	0
MS2	0.19	0.01	0.23	15	486.83	16	1.30	2.72	0	0
MS3	0.48	0.07	2.41	7	481.83	28	1.08	4.39	0	100
MS4	0.31	0.02	0.97	23	482.67	31	1.59	4.97	0	0
MS7	1.27	0.14	4.94	13	473.23	52	1.41	4.97	0	100
MS9	1.88	0.18	7.15	10	464.71	59	1.26	4.97	0	100
HWY240	34.65	3.33	92.97	18	455.13	121	1.79	16.16	14	87
Miami	74.41	6.92	301.03	18	429.04	190	1.92	20.99	38	58
Min	***0.19***	***0.01***	***0.23***	***2***	***429.04***	***12***	***0.96***	***2.13***	0	***0***
Max	***74.41***	***6.92***	***301.03***	***23***	***486.83***	***190***	***1.92***	***20.99***	***38***	***100***
Mean	***14.18***	***1.34***	***51.29***	***13***	***469.92***	***63.63***	***1.41***	***7.66***	***7***	***56***
CV	***1.91***	***1.89***	***2.06***	***51***	***0.04***	***0.97***	***0.24***	***0.91***	***208***	***86***

Canola oil was placed at the bottom of the rain collectors to prevent fractionation and evaporative losses of water samples between site visits. Rainfall amounts were determined by a Texas Electronic Tipping Bucket rain gages (TE525-L, 0.01 of an inch precision) connected to Campbell Scientific data loggers. Shallow and intermediate groundwater was sampled from piezometers screened at 0.6 m and 1.5 m, respectively, using a bailer (which was rinsed with deionised water in between sites). Deep groundwater was sampled with a peristaltic pump from an 8 m well. Automatic water samplers were used to collect stream samples during storm events while grab samples were also collected during weekly field visits. Sampling covered 39 different days and 47 hydrological events (across all sites) during the 2014 open water period, for a total of: 92 snow and snowmelt samples, 86 rain samples, 143 shallow and intermediate groundwater samples, 9 deep groundwater samples and 213 stream water samples. All samples were stored in 10 mL glass vials sealed with parafilm and refrigerated until analysis. They were analyzed for $\delta^{18}O$ and $\delta^{2}H$ using a Picarro^{TM} Liquid Water Isotope Analyzer (LWIA, model L2130-i) based on Cavity Ring-Down Spectroscopy (CRDS) technology. Delta (δ) values were recorded in permil (‰) deviations from the Vienna Standard Mean Ocean Water (VSMOW) (Craig, 1961) with a precision of 0.025‰ and 0.1‰ for $\delta^{18}O$ and $\delta^{2}H$, respectively.

3.2.3 Hydrograph separation and uncertainty analyses

Two-component IHS, based on the steady-state mass balance equations of water and concentration equilibrium (Pinder and Jones, 1969), was used to calculate the fractions of "old" water (noted as F) in streamflow (Eq. 3-1).

$$F = \frac{\delta_{stream} - \delta_{new}}{\delta_{old} - \delta_{new}} \qquad \text{(Eq. 3-1)}$$

where δ is the tracer concentration, the subscripts indicate the different water sources considered, and F is the computed fraction of "old" water in the stream.

Since the goal of this paper was to evaluate the effect of end-member definitions and tracer choice on IHS results, wide-ranging scenarios based on the combination of one (out of eight potential) "new" water end-member definition, one (out of eight potential) "old" water end-member definition, and one tracer (out of two potential tracers, i.e., $\delta^{18}O$ or $\delta^{2}H$) were evaluated (Tables 3-2 and 3-3). Recommendations made by Hooper and Shoemaker (1986) regarding possible definitions for end-members were followed and are graphically illustrated in appendices B-1 and B-2. For example, end-member definitions labelled as "most recent" (i.e., MR in the acronyms listed in Tables 3-2 and 3-3) rain, snow or groundwater were such that each stream sample was matched with the antecedent end-member sample that was the closest, in time, to stream sampling. As for the end-member definitions identified as being a seasonal average (i.e., SA in the acronyms listed in Tables 3-2 and 3-3), only the end-member samples collected during the same season as (but prior to) the stream sample were used. Each combination of a "new" water end-member definition, an "old" water end-member definition and a tracer forms a methodological scenario with an associated scenario number. A total of 80 methodological scenarios (i.e., 40 based on $\delta^{18}O$ and 40 based on $\delta^{2}H$) were possible to estimate F for each stream water sample collected; 17,040 IHS computations were therefore attempted across all sites (i.e., 213 stream water samples × 80 scenarios). However, 9,690 of the attempted IHS computations could not be completed due to: (1) the sampling of some potential end-members not being possible during certain periods (e.g., no snow, dry piezometer), or (2) some end-members not being applicable considering the hydrological conditions at the time of stream sample collection (e.g., it is not plausible to consider that spring snowmelt signatures still constitute a valid "new" water source in August).

Lastly, the uncertainty associated with each of the calculated "old" water fractions (i.e., F values) was estimated for three outlets: one atop the escarpment (MS1), one at the edge of the escarpment

(HWY240) and one below the escarpment (Miami) (see Appendix B-3). The goal was to assess the spatial and temporal variability of errors associated with the estimation of end-member concentrations – both conceptually in terms of end-member definition but also analytically in terms of laboratory measurements (Genereux, 1998; Uhlenbrook and Hoeg, 2003). The Gaussian error propagation technique based on the first-order Taylor series expansion was used (Eq. 3-2; Genereux, 1998):

$$W = \sqrt{\left(\frac{c_{new} - c_{stream}}{(c_{new} - c_{old})^2} Wc_{old}\right)^2 + \left(\frac{c_{stream} - c_{old}}{(c_{new} - c_{old})^2} Wc_{new}\right)^2 + \ldots\ldots\ldots + \left(\frac{-1}{(c_{new} - c_{old})} Wc_{stream}\right)^2} \quad \text{(Eq. 3-2)}$$

where W is the total uncertainty related to the computed fraction of "old" water. Wc_{old}, Wc_{new}, and Wc_{stream} are the uncertainty in the "old", "new", and stream water isotopic ratios, respectively. The uncertainty in each component is computed by multiplying the standard deviations of measurements by the *t* values of the student's *t* distribution at the 70% confidence level (Appendix B-3; Genereux, 1998). The aforementioned three sites were selected for uncertainty evaluation because MS1 is the beginning of the South Tobacco Creek channel, Miami is the outlet of the whole STCW, and the HWY240 sub-watershed discharges at the edge of the escarpment where unique hydrological characteristics prevail. An uncertainty cut-off of 4% was set after evaluation of the average uncertainties reported in past studies (e.g., Laudon et al., 2002; Uhlenbrook et al., 2002; St Amour et al., 2005; Pu et al., 2013). Compared to that cut-off, the uncertainty values computed in the current study were evaluated to ascertain if some methodological scenarios led to systematically high (i.e., ≥ 4%) or low (i.e., < 4%) error.

Table 3-2. List of "new" water and "old" water end-member definitions and associated acronyms used in the current study.

"New" water end-member Definitions	***"Old" water end-member Definitions***
Snow-MR: Most recent snowpack sample	**Sgw-MR**: Most recent shallow groundwater samples from 0.6 m piezometer
Melt-MR: Most recent meltwater sample	**Igw-MR**: Most recent intermediate groundwater sample from 1.5 m piezometer
Melt-SA: Seasonal average of meltwater samples	**ASgwIgw-MR**: Average of most recent 0.6 m shallow groundwater (Sgw) and 1.5 m deep groundwater (Igw) samples
Snow-SA: Seasonal average of snowpack samples	**Sgw-SA**: Seasonal average of Sgw samples
ASMR-MR: Average of most recent snow, melt and rain samples	**Igw-SA**: Seasonal average of Igw samples
AMR-MR: Average of most recent melt and rain samples	**SgwIgw-SA**: Seasonal average of Sgw and Igw samples
Rain-MR: Most recent rain samples	**Qbf**: Stream water sample at baseflow
Rain - SA: Seasonal average of rain samples	**Dgw:** Deep groundwater sample from 8 m well

Table 3-3. Combinations of tracer choice and end-member definitions used in this study. For acronyms, refer to Table 3-2.

Scenario # for $\delta^{18}O$	End-member definition		Scenario # for $\delta^{2}H$
	New water	Old water	
1	Snow-MR	Sgw-MR	41
2	Snow-MR	Igw-MR	42
3	Snow-MR	ASgwIgw-MR	43
4	Snow-MR	Qbf	44
5	Snow-MR	Dgw	45
6	Melt-MR	Sgw-MR	46
7	Melt-MR	Igw-MR	47
8	Melt-MR	ASgwIgw-MR	48
9	Melt-MR	Qbf	49
10	Melt-MR	Dgw	50
11	Melt-SA	Sgw-SA	51
12	Melt-SA	Igw-SA	52
13	Melt-SA	SgwIgw-SA	53
14	Melt-SA	Qbf	54
15	Melt-SA	Dgw	55
16	Snow-SA	Sgw-SA	56
17	Snow-SA	Igw-SA	57
18	Snow-SA	SgwIgw-SA	58
19	Snow-SA	Qbf	59
20	Snow-SA	Dgw	60
21	ASMR-MR	Sgw-MR	61
22	ASMR-MR	Igw-MR	62
23	ASMR-MR	ASgwIgw-MR	63
24	ASMR-MR	Qbf	64
25	ASMR-MR	Dgw	65
26	AMR-MR	Sgw-MR	66
27	AMR-MR	Igw-MR	67
28	AMR-MR	ASgwIgw-MR	68
29	AMR-MR	Qbf	69
30	AMR-MR	Dgw	70
31	Rain-MR	Sgw-MR	71
32	Rain-MR	Igw-MR	72
33	Rain-MR	ASgwIgw-MR	73
34	Rain-MR	Qbf	74
35	Rain-MR	Dgw	75
36	Rain-SA	Sgw-SA	76
37	Rain-SA	Igw-SA	77
38	Rain-SA	SgwIgw-SA	78
39	Rain-SA	Qbf	79
40	Rain-SA	Dgw	80

3.3 Results

3.3.1 Isotopic composition of water samples

All samples collected in 2014 plotted on or near both meteoric water lines (local and global MWLs, Figure 3-2). Snow and snowmelt samples were the most depleted in heavy isotopes, in contrast to groundwater samples which appeared relatively enriched. Precipitation samples were distributed across the whole extent of the MWLs, which is consistent with many previous studies (e.g., McGuire and McDonnell, 2006). In Figure 3-2, samples that plot below the point (-17.5‰,-130‰) towards the depleted end of the MWLs were from the freshet or early spring season, i.e., from the start of the snowmelt until rain-on-snow conditions began. Precipitation samples that plotted above the point (-17.5‰,-130‰) were from three different seasons: (1) late spring (which lasted from the beginning of rain-on-snow conditions until June 20th), (2) summer (which was considered to end on September 21st), and (3) fall (which ended in October when freezing temperatures set in). Precipitation that fell after the late spring season appeared to scatter slightly above and below the MWLs, suggesting it was originating from different vapour sources. Stream samples collected later in the year also appeared to fall slightly below the MWLs, which is likely due to the stream's evaporative response to increasing temperatures.

3.3.2 Spatio-temporal variability of old water fractions

The computed F values for the different outlets showed a general increasing trend from April to October (Figure 3-3). On some occasions, however, IHS yielded mathematically possible but physically unrealistic F values – i.e., below zero or above 1.

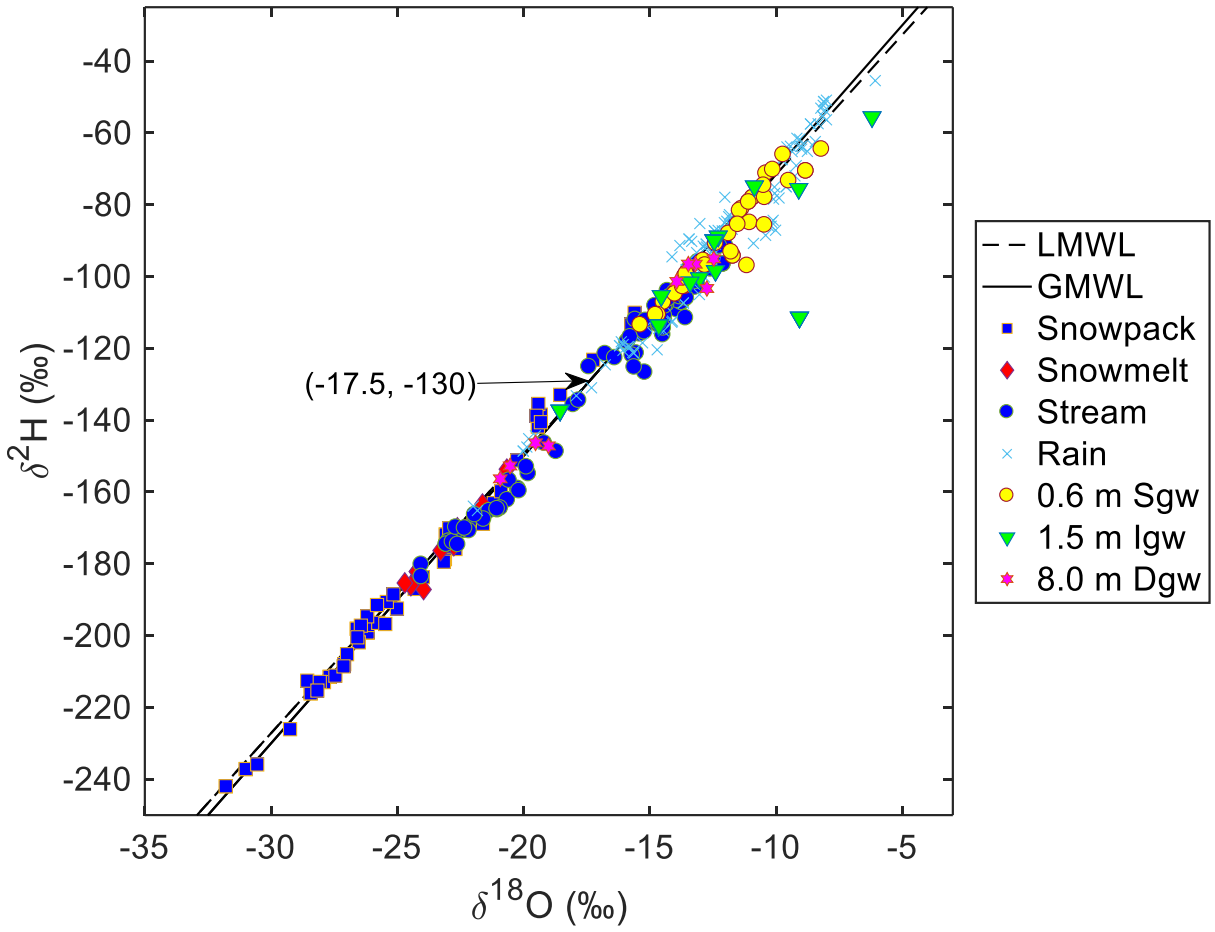

Figure 3-2. Isotopic composition ($\delta^{18}O$ and $\delta^{2}H$) of all water samples collected across the STCW in 2014, plotted relative to the local (LMWL) and global (GMWL) meteoric water lines. GMWL: $\delta^{2}H = 8 \bullet \delta^{18}O + 10$. LMWL: $\delta^{2}H = 7.78 \bullet \delta^{18}O + 6.22$. Sgw: shallow groundwater from 0.6 m deep piezometer; Igw: intermediate groundwater from 1.5 m deep piezometer; Dgw: deep groundwater water from 8 m well.

Negative F values were mostly obtained in early spring and tended to occur more frequently for the methodological scenarios associated with δ^2H-based data and "new" water end-members defined based on combined rain and snow data (Figures 3-3a to 3-3d and 3-3g). Later in the year (i.e., in summer and fall), physically unrealistic F values tended to be greater than 1 (Figures 3-3a to 3-3h) and were associated with both δ^{18}O and δ^2H data. Worthy of note was the dominance of F values above 1 at site MS7 – which has a small dam and a reservoir – between May 21st and July 4th (Figure 3-3e). The other site associated with such man-made features, i.e., MS4, had fewer F values in excess of 1 than MS7 around that period. F values at MS4 were generally higher than those at MS7 (Figure 3-3d and 3-3e). Despite draining similar areas (Table 3-1), MS4 had larger F values than MS3, especially during the freshet when most of the IHS results yielded physically unrealistic F values at MS3 (Figures 3-3c and 3-3d). HWY240, which is the site located at the edge of the escarpment, had uncharacteristically high F values during the freshet, notably on April 7th. However, 48 hours later (on April 9th), much lower F values were estimated at that site. A month later (May 9th), F values at the HWY240 outlet started to increase again and remained high until the end of the sampling period (Figure 3-3g).

3.3.3 Effect of tracer choice on computed old water fractions

F values computed using $\delta^{18}O$ data were generally higher than those computed using $\delta^{2}H$ data across most of the eight outlets during the early spring season (Figures 3-4a to 3-4d and 3-4g). It is, however, worth noting that F values that were within 10% of one another or less when using $\delta^{18}O$ versus $\delta^{2}H$ were more frequently found in early to late spring than in any of the other monitored seasons (Figures 3-4a to 3-4c, 3-4f and 3-4h). The largest discrepancies between F values estimated using $\delta^{18}O$ versus $\delta^{2}H$ data were during the summer season at all sites (Figures 3-4a and 3-4e to 3-4g). Conversely, the best agreement between F values computed using $\delta^{18}O$ versus $\delta^{2}H$ data was observed in the early and late spring seasons at sites MS9 (i.e., the wind-sheltered site) and Miami (i.e., the site associated with the largest proportion of low-lying, flat areas) (Figures 3-4f and 3-4g).

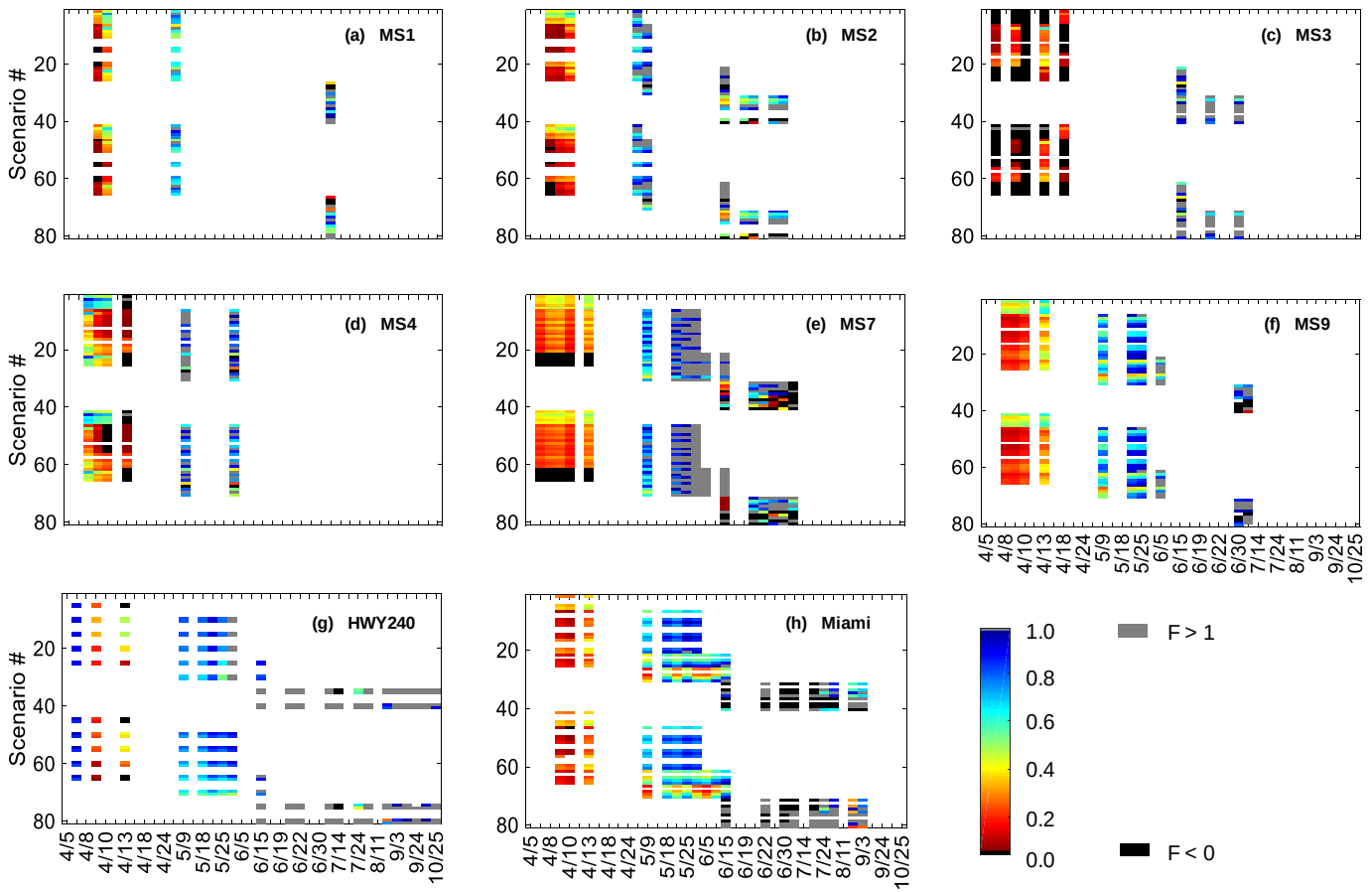

Figure 3-3. Temporal variation of scenario-specific old water fractions (i.e., F values) at each of the eight outlets in 2014. White cells that run across a whole column (from top to bottom of plot) indicate that no water was available in the stream and/or piezometers and wells so scenario-specific F values could not be computed. White cells that do not run across a whole column flag scenarios that were not hydrologically plausible and hence could not be applied to perform IHS. Black cells: the computed F values were negative. Gray cells: the computed F values were above 1.

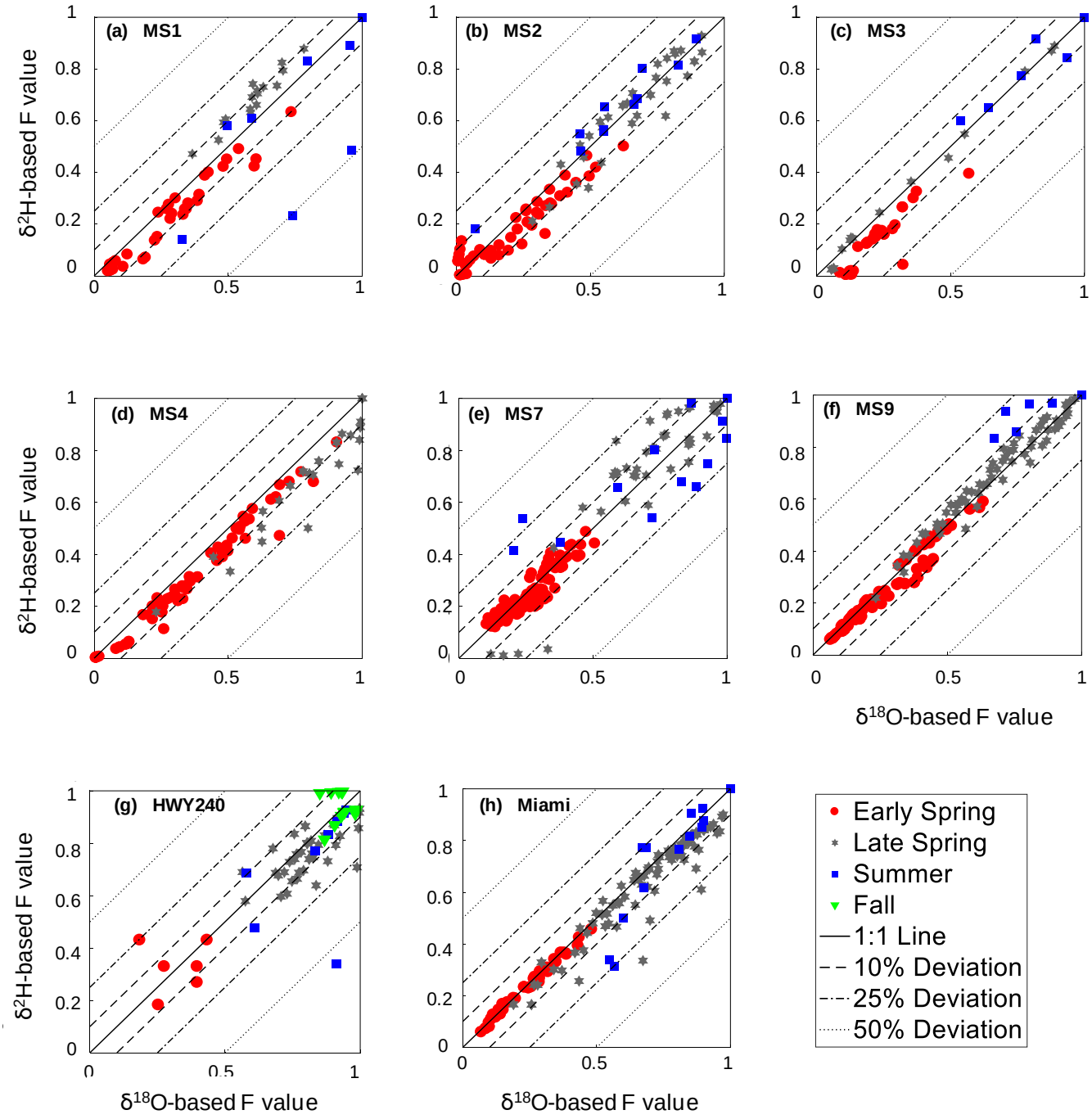

Figure 3-4. Comparison of F values computed using $\delta^{18}O$ versus $\delta^{2}H$ data at the different outlets. The lack of agreement between the results provided by the two tracers can be assessed visually using band widths of 10%, 25% and 50% deviations from the 1:1 line.

3.3.4 Effect of end-member definitions on estimated old water fractions

Figure 3-5 shows that the computed F values were strongly sensitive to the data used to characterize the "new" water end-member. For instance, scenarios relying on the Rain-MR end-member definition for "new" water generated some of the largest F values (mean and median F values in excess of 0.5, see Figure 3-5). The "new" water end-member definitions associated with snow and melt samples (i.e., Snow-MR, Melt-MR, Melt-SA and Snow-SA) led to very small temporal variability in F values, as indicated by the small height of the boxes and relatively short whiskers on Figures 3-5c to 3-5f and 3-5h. Conversely, scenarios that relied on rain data (i.e., ASMR-MR, AMR-MR, Rain-MR and Rain-SA) to characterize the "new water" end-member generated F values with the greatest data spread (Figures 3-5c to 3-5f and 3-5h) for all sites except MS1, MS2 and HWY240 (Figures 3-5a, 3-5b and 3-5g). The F values at HWY240 were all greater than 0.5, irrespective of the tracer or end-member choice. In general, the ability of the two tracers to generate similar ranges of F values across the eight sites decreased as rain data was introduced – either alone or in combination with other data (e.g., ASMR-MR, AMR-MR, Rain-MR and Rain-SA) – to characterize the "new" water end-member (Figure 3-5).

Figure 3-6 shows that the computed F values were not very sensitive to the data used to characterize the "old" water end-member. For each "old" water end-member definition, the ranges of F values obtained using $\delta^{18}O$ versus $\delta^{2}H$ tracer data were generally similar. Sites HWY240 and Miami (Figures 3-6g and 3-6h) had the highest F values when deep groundwater or streamflow at baseflow were used as "old" water end-members.

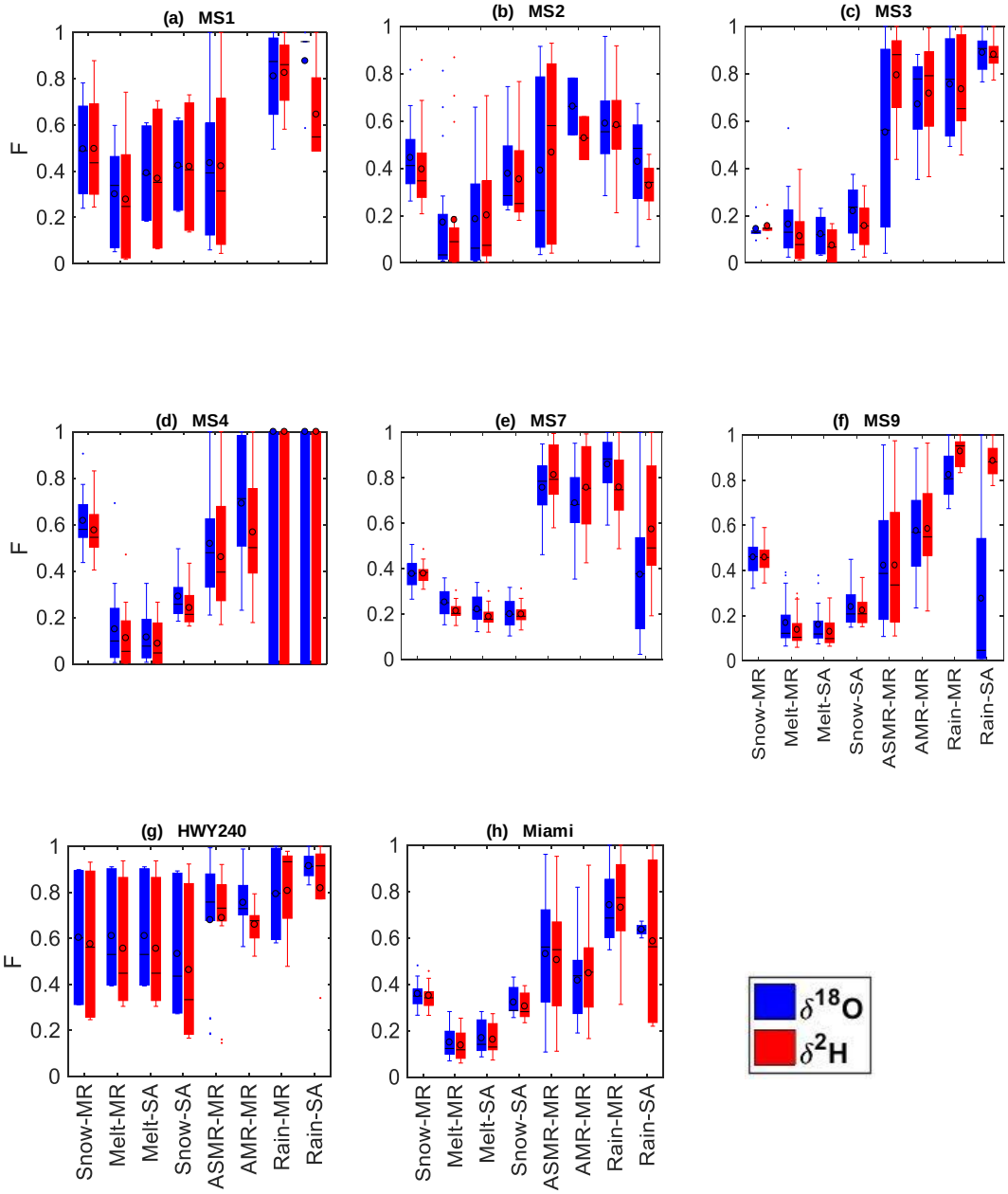

Figure 3-5. Variability of computed F values as a function of the "new" water end-member definition. The horizontal black line and the black-rimmed circle in each box show the median and mean of F values, respectively, when each "new" water end-member definition is used. Whiskers extending above and below each box indicate the lowest and highest F values computed for each "new" water end-member definition. Small dots beyond whiskers are statistical outliers. For acronym definitions, refer to Table 3-2.

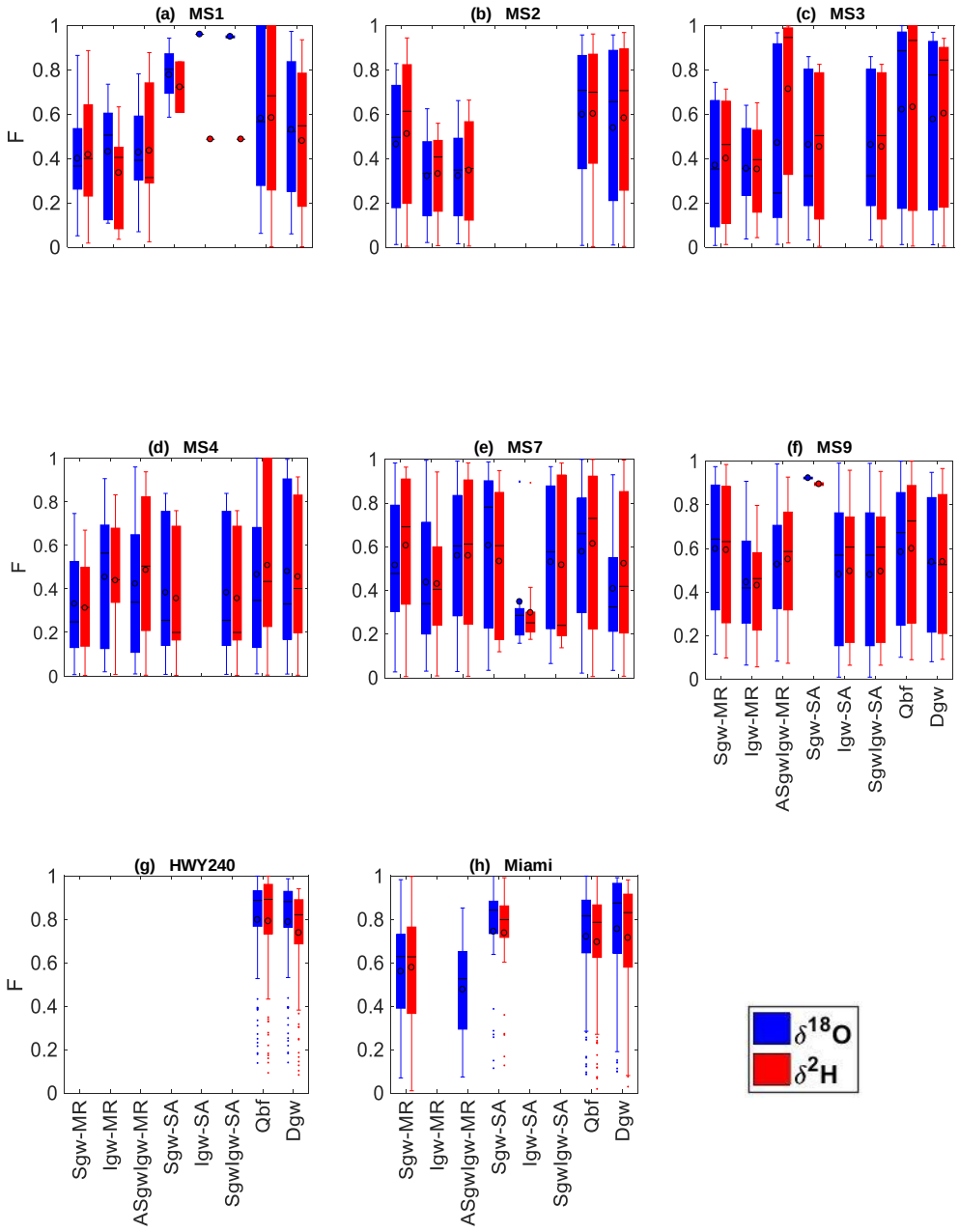

Figure 3-6. Variability of computed F values as a function of the "old" water end-member definition. The horizontal black line and the black-rimmed circle in each box show the median and mean of F values, respectively, when each "old" water end-member definition is used. Whiskers extending above and below each box indicate the lowest and highest F values computed for each "old" water end-member definition. Small dots beyond whiskers are statistical outliers. For acronym definitions, refer to Table 3-2.

3.3.5 Uncertainties associated with computed old water fractions

Across all methodological scenarios and all sampling dates, the average uncertainty associated with $\delta^{18}O$-based IHS results was 7.2%, 5.1% and 8.4% for sites MS1, HWY240 and Miami, respectively (Table 3-4). $\delta^{2}H$-based IHS results were, however, associated with higher and more temporally variable uncertainty values, regardless of whether we looked at all uncertainties (Table 3-4) or low uncertainties only (i.e., values below the 4% cut-off; Figure 3-7a). When the focus was on low uncertainties only (i.e., below 4%, Figure 3-7), similar average (low) uncertainty values were observed for $\delta^{18}O$-based and $\delta^{2}H$-based scenarios up to the end of the spring season at the HWY240 outlet, located at the edge of the escarpment (Figure 3-7b). For summer sampling dates, however, $\delta^{18}O$-based scenarios yielded significantly lower uncertainty values than $\delta^{2}H$-based scenarios at site HWY240 (Figure 3-7b). At the Miami site (Figure 3-7c), the average (low) uncertainties associated with both tracers were similar until late summer. Contrary to sites MS1 and HWY240, however, $\delta^{18}O$-based scenarios applied at the Miami site for August 2014 yielded higher and more temporally variable uncertainty values than $\delta^{2}H$-based scenarios.

Table 3-4. Summary statistics for the uncertainty values computed across all the $\delta^{18}O$-based and $\delta^{2}H$-based methodological scenarios applied at sites MS1, HWY240 and Miami.

	MS1		**HWY240**		**Miami**	
	$\delta^{18}O$	$\delta^{2}H$	$\delta^{18}O$	$\delta^{2}H$	$\delta^{18}O$	$\delta^{2}H$
Minimum uncertainty (%)	0.6	2.8	0.6	1.9	0.3	1.6
Maximum uncertainty (%)	19.9	50.1	53.8	33	244.1	463.8
Median uncertainty (%)	6.3	8.2	4.1	4.7	3.6	3.5
Mean uncertainty (%)	7.2	11.0	5.1	6.5	8.4	7.1
Standard deviation of uncertainty (%)	3.8	9.3	5.3	5.8	25.1	29.6
Number of IHS results	62	54	137	113	338	347

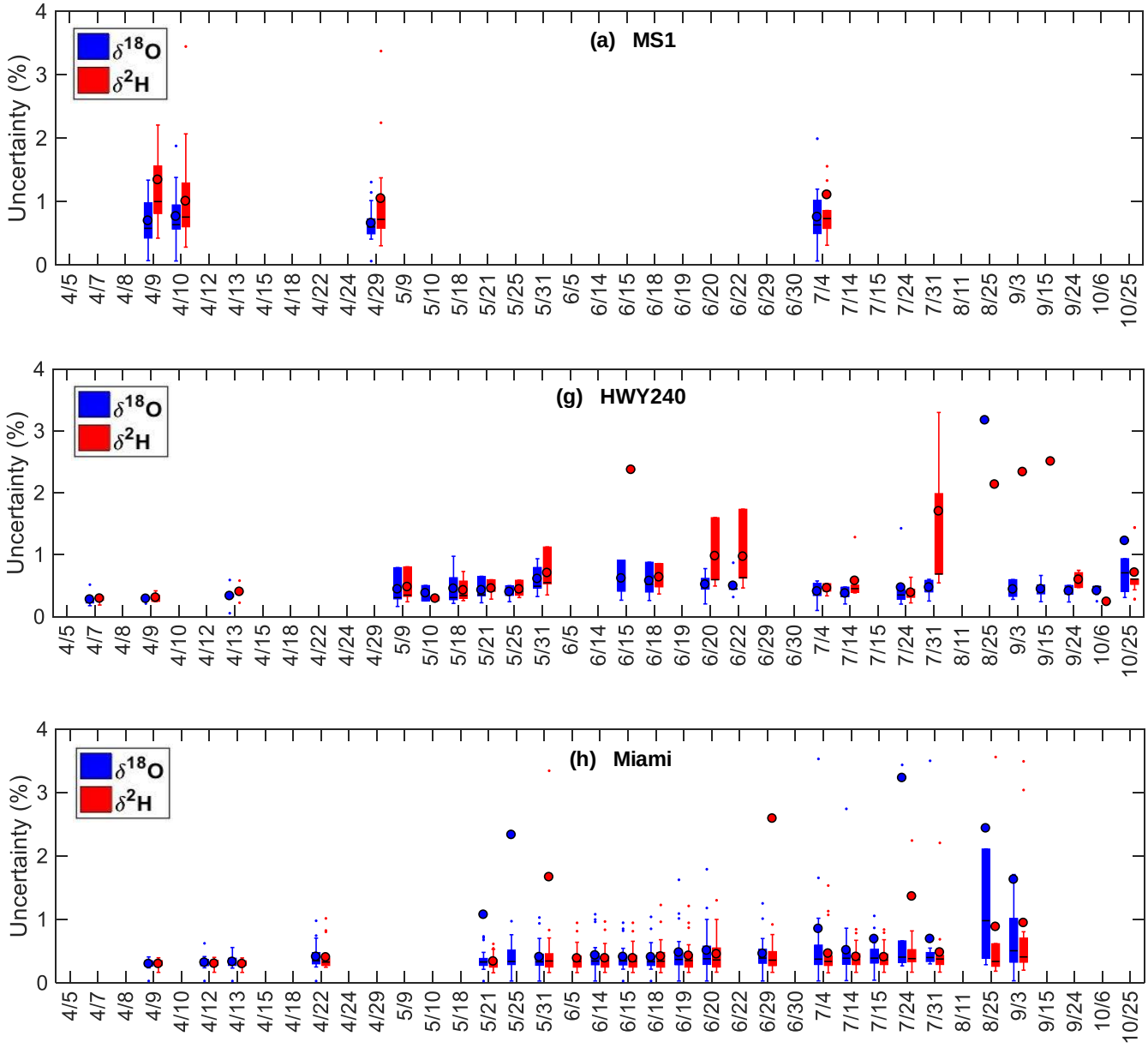

Figure 3-7. Boxplots showing the variability of F-related uncertainties across all scenarios considered for each sampling date at sites MS1, HWY240 and Miami. The y-axis limits were set to vary from 0 to 4% for better readability. The horizontal black line and the black-rimmed circle in each box show the median and mean uncertainty value, respectively. Whiskers extending above and below each box indicate the lowest and highest uncertainty value. Small dots beyond whiskers are statistical outliers.

Over the sampling period, high uncertainty values (above 4%, i.e., outlier uncertainties) were observed using both $\delta^{18}O$ and $\delta^{2}H$ data at the three sites considered (Table 3-4; Figure 3-8). Indeed, the maximum uncertainties estimated across all sites, scenarios and seasons varied between 19.9% and 463.8% (Table 3-4). Median uncertainties were also above the 4% cut-off for both MS1 and HWY240, regardless of tracer choice (Table 3-4). At MS1, outlier uncertainties were more frequent with $\delta^{2}H$-based scenarios (Figure 3-8). Outlier uncertainties, however, appeared to be evenly distributed between $\delta^{18}O$-based scenarios and $\delta^{2}H$-based scenarios at sites HWY240 and Miami (Figure 3-8). Some specific end-member definitions appeared to be frequently associated with outlier uncertainty values. At MS1, for example, it was notably the case for scenarios that relied on $\delta^{2}H$ data, the most recent melt sample for the "new" water end-member definition, and the most recent shallow groundwater sample for the "old" water end-member definition (e.g., scenario #46; Figure 3-8). Along the same lines, at the HWY240 site, outlier uncertainty values were observed on two occasions for scenario #34, which relied on $\delta^{18}O$ data, the most recent rain sample for the "new" water end-member definition, and stream water samples at baseflow for the "old" water end-member definition (Figure 3-8). At the Miami site, several sampling dates between late spring and late summer were associated with outlier uncertainties for $\delta^{18}O$-based scenarios and their $\delta^{2}H$-based counterparts (e.g., scenarios #30 and 70; scenarios #33 and 73; see Figure 3-8). Scenarios #30 and 70 both rely on the average of the most recent melt and rain samples for the "new" water end-member definition, and the most recent intermediate groundwater sample for the "old" water end-member definition. As for scenarios #33 and 73, they rely on the most recent rain samples and the average of the most recent shallow and intermediate groundwater samples for the "new" and "old" water end-member definitions, respectively (Figure 3-8).

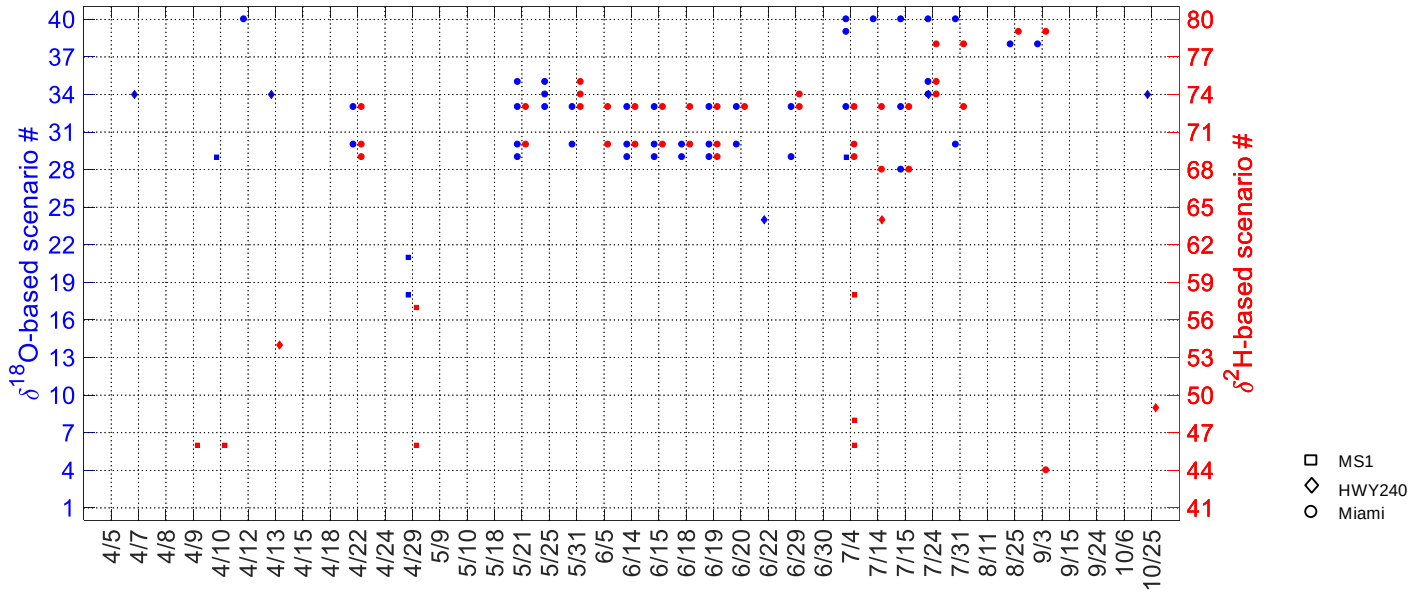

Figure 3-8. Scenarios leading to F-related uncertainty values above the 4% cut-off (i.e., outlier uncertainties) for each sampling date. Blue symbols flag δ^{18}O-based methodological scenarios while red symbols show δ^{2}H-based methodological scenarios with uncertainty values in excess of 4%.

3.4 Discussion

3.4.1 Interpretation of F values in light of dominant runoff processes

Overall, the F values obtained in this study are consistent with the seasonality in dominant runoff processes observed in Prairie regions. For instance, in early spring, infiltration-excess (Hortonian) overland flow is known to occur on frozen ground and transport "new" water to streams (Fang et al., 2007). This is in agreement with the low F values observed in Figure 3-3 for the month of April. The best agreement between δ^{18}O and δ^{2}H-based F values was also observed in early spring (Figure 3-4) as a result of cooler temperatures, leading to minimal isotope fractionation. With warmer temperatures in late spring, however, ground thawing allows water to infiltrate and percolate deeper, causing streams to

be fed by not only shallow subsurface flow, which can occur at the interface between organic and mineral soil horizons as a mix of "old" and "new" water, but also deeper groundwater – made of "old" water. That shift in dominant flow processes was reflected in the higher F values estimated for the month of May (Figure 3-3). The agreement between $\delta^{18}O$ and $\delta^{2}H$-based F values was weaker in late spring (Figure 3-4), likely due to higher fractionation losses driven by higher temperatures. Typically, the Prairies are strongly affected by evapotranspiration in summer and early fall (Fang et al., 2007). This results in streams that run dry unless they are fed by deep groundwater: such dynamics can also be seen on Figure 3-3. Significant summer surface runoff can be seen in response to high-intensity convective rain events when the infiltration capacity of the soil is exceeded (Shook and Pomeroy, 2012). Saturation-excess overland flow can also occur, albeit exceptionally, in summer. Significant rainfall events notably occurred in June and July 2014 and were associated with multiple runoff generation pathways, namely infiltration-excess and saturation-excess overland flow, and subsurface flow from various spatial sources. That multiplicity of water sources was likely not well captured by our two-component IHS analyses, and it likely explains why many of the estimated F values were above 1 during that time (Figure 3-3).

3.4.2 Spatial variability and physical realism of old water fractions

The general increase in F values observed across all eight outlets from the freshet to the fall season is consistent with other findings reported in the literature (Metcalfe and Buttle, 2001; Liu et al., 2008). However, the F values estimated in the current study for the freshet period were generally lower than those reported in studies done in Canada (e.g., Gibson et al., 1993 in the Manners Creek Watershed also within the Liard and Mackenzie river basin near Fort Simpson, Northwest Territories; St Amour et al., 2005 in five watersheds within the Liard and Mackenzie river basin, Northwest Territories) and elsewhere (e.g., Rodhe, 1998; Laudon et al., 2002). Our generally lower F values during the freshet are

likely attributable to sheet flow of "new" water over frozen ground, which is a dominant runoff generation mechanism in early spring in Prairie environments (Gray and Landine, 1988; Fang et al., 2007). The physically unrealistic negative F values observed in late spring may be a result of indistinct isotopic differences between “new” and “old” water sources, due to melt water directly feeding streamflow (via in-channel melting of snow) as well as the piezometers (via downward percolation in recently thawed soils). Later in the year (i.e., summer and fall), physically unrealistic F values rather tended to be greater than 1 (Figure 3-3), which may signal the presence of two “old” water end-members (i.e., shallow and deeper groundwater) as alluded to by Kennedy et al. (1986), DeWalle et al. (1988), McDonnell et al. (1991) and Blume et al. (2008). F values in excess of 1 were notably observed at the MS7 site where exceptionally large rainfall events in June and July 2014 (Figure 3-1e) likely led to contributions from surface storage – through the overspillage of the reservoir behind the dam – as well as shallow and intermediate groundwater contributions through saturated soils.

F values are generally known to decrease with watershed size (Shanley et al., 2002), due to increased “new” water inputs from upstream channel flow. This was generally verified across the STCW, except for sites MS4 and MS7 – which have retention ponds immediately upstream of them –, and site HWY240 – which sits at the edge of the escarpment. Retention ponds are known to significantly alter the hydrology of a basin by decreasing runoff to downstream outlets (Kim et al., 2007): “new” water coming from the upstream channel is impounded by the retention dam and flows slowly under it. Water can take long flowpaths below and around the dam before emerging at the outlet downstream, by which time it is referred to as “old” water. This may explain why F values at MS4 were generally higher than F values at MS2 (Figures 3-3b and 3-3d) and MS3 (Figures 3-3c and 3-3d). Lower F values at the Miami outlet were also observed, compared to upstream sites MS7 and MS9 (Figures 3-3e, 3-3f and 3-3h), thus raising the question of how landscape characteristics below the escarpment promote the transmission of “new” water to the outlet. The HWY240 site (Figure 3-3g) acted differently from the others with relatively high

$\delta^{18}O$-based and $\delta^{2}H$-based F values in early spring. Those values significantly decreased within 48 hours before increasing again, indicating that the water that was previously in the channel had been "flushed". This early-spring "flushing" behavior was not observed at any of the other seven outlets. The HWY240 outlet sits right on the edge of the Pembina escarpment with an underlying rock and soil system that is relatively coarser (and more permeable due to the till deposits and fractured bedrock) than the other outlets (Table 3-1). Therefore, at this site, precipitation is thought to quickly infiltrate into deep groundwater and then flow laterally into the stream.

3.4.3 Inter- and intra-seasonal comparison of $\delta^{18}O$-based and $\delta^{2}H$-based old water fractions

The best convergence of F values estimated using $\delta^{18}O$ versus $\delta^{2}H$ data occurred in the early spring season (Figure 3-4) when the "new" water end-member was mostly documented using snow and snowmelt samples. This can be explained by the characteristics of the STCW. Indeed, variation in the isotopic composition of snow is thought to happen because of vapour exchange with soil water, vegetation, or atmospheric moisture (Kendall and McDonnel, 1998). The latter is the most plausible in the STCW as most of the ground is frozen and devoid of flowing soil water pre-melt, and vegetation is dormant at that time. Relatively low temperatures during spring led to minimal atmospheric moisture and hence a subdued vapour exchange with the snow and less isotopic fractionation of snow. In some watersheds, high winds increase ablation rates, snow crystallization and water vapor exchange: this can lead to increases in the $\delta^{18}O$ and $\delta^{2}H$ values of snowpacks in uplands (Cooper et al., 1993; Nikolayev and Mikhalev, 1995), while relatively negative $\delta^{18}O$ and $\delta^{2}H$ values are preserved in snowpacks in lower-lying and wind-sheltered areas. While this effect is opposite to the expected orographic decrease in heavy isotope content with increasing elevation (Friedman and Smith, 1970), there was evidence of it at the wind-sheltered MS9 site and the flatter Miami site, where there was little temporal change in the isotopic

signature of the snowpack. This may also have contributed to the convergence of $\delta^{18}O$-based and $\delta^{2}H$-based F values, which plotted very close to the 1:1 line in Figures 3-4f and 3-4h for the spring season. $\delta^{18}O$ and $\delta^{2}H$-based F values strongly fluctuated as the spring season progressed into mixed snowmelt- and rain-driven conditions, i.e., late spring, summer and fall seasons, likely due to the highly variable nature of the "new" water isotopic composition as different air masses create precipitation of varying isotopic compositions. This was also coupled with multiple "old" water end-members likely contributing to streamflow later in the summer and fall seasons (Kendall and McDonnell, 1998). The aforementioned discussions confirm the strong dependence of IHS results on the use of $\delta^{18}O$ versus $\delta^{2}H$ data, especially when characterizing the "new" water component. While it might be appropriate to use any of the two tracers in flat and wind-sheltered environments during the early spring period, $\delta^{2}H$ data could be problematic to use without any appropriate correction in later seasons, due to its relatively higher fractionation potential and variability. Ingraham and Taylor (1989) only used $\delta^{2}H$ data for IHS – even though $\delta^{18}O$ data were also available – because they gave consistent isotopic concentrations for soil and groundwater, thus allowing the accurate characterization of the "old" water end-member. Moore (1989), however, used both tracers for IHS in a watershed in Quebec, Canada and found that during the freshet, $\delta^{2}H$ data led to "old" water fraction estimates ranging between 0.5 and 0.65, an overestimation when compared to the values of 0.43 to 0.55 obtained when using $\delta^{18}O$ data.

3.4.4 Sensitivity of IHS results to end-member definitions

Scenarios based on the Rain-MR "new" water end-member definition yielded the highest and most variable average F values across all eight outlets in summer and fall (Figure 3-5). This high variability in F values is consistent with the high isotopic variability observed in rain in summer and fall. Conversely, scenarios based on Snow-MR, Snow-SA, Melt-MR and Melt-SA generally yielded the

smallest and least variable average F values in spring (Figure 3-5c to 3-5f; 3-5h). Those findings are partly consistent with Shanley et al. (2002) who found average "old" water fractions of over 50% in summer and less than 30% in spring in a watershed in Vermont, USA. Using snow data rather than melt data to characterize the "new" water end-member in spring also led to higher average F values (Figure 3-5): as snow is exposed to the elements for a long period, it may have undergone more fractionation as compared to meltwater. The choice of Rain-MR for "new" water characterization appears to be inappropriate in summer and fall. Combining this choice with the "old" water end-member further compounds the problem due to possible contrasting patterns in "old" water isotopic signatures usually observed due to multiple flow processes (e.g., shallow and deep lateral subsurface flow) prevailing at the same time. Ideally, the choice of an "old" water end-member should account for that multiplicity of processes. During most of the sampling period, no shallow or intermediate groundwater was present in the piezometers near the HWY240 outlet and hence, scenarios that did not rely on these data had to be used to characterize the "old" water end-member (Figure 3-6g). In the current study, characterizing the "old" water end-member appropriately in the summer and fall seasons was as problematic as characterizing the "new" water end-member in spring.

3.4.5 Evaluation of IHS uncertainties as a function of tracer choice, watershed characteristics and seasonal dynamics

For all sampling dates, uncertainty values associated with $\delta^{18}O$-based IHS scenarios at MS1 were lower and less variable than those associated with $\delta^{2}H$-based scenarios (Figure 3-7a). Similar dynamics were seen at the HWY240 site (Figure 3-7b) but only after the end of the spring season. The higher uncertainty in $\delta^{2}H$-based IHS results might be attributable to the relative ease with which ^{2}H fractionates in contrast to ^{18}O. The similarities between $\delta^{18}O$ and $\delta^{2}H$-based uncertainties during the early part of the

spring season at HWY240 (Figure 3-7b) could be due to the time-invariant isotopic composition of the "old" water end-member during the freshet as well as a "new" water end-member that has not been subjected to much fractionation. Baseflow and deep groundwater samples were used to characterize the "old" water end-member isotopic compositions at HWY240 due to the lack of samples in the piezometers over the whole sampling period (Figure 3-6g; Table 3-4). This is consistent with the findings of Darling et al. (2003) in the British Isles where baseflow and groundwater isotopic signatures were assessed from samples collected from the River Thames at Wallingford: there was little variation in the isotopic composition of the river and groundwater samples for much of the year except in late summer and early fall. Low uncertainties and good inter-tracer agreement was also present at Miami in spring and summer (Figure 3-7c). However, no plausible mechanism was found to explain why δ^2H-based uncertainties were generally lower than δ^{18}O-based uncertainties at Miami (Table 3-4). δ^2H-based outlier uncertainties at MS1 were associated with scenarios based on the most recent melt and the most recent shallow groundwater data. This may be explained by the fact that in spring, meltwater feeds both the shallow piezometers and the stream, thus leading the "new" and "old" water signatures to not be distinct enough. We observed δ^{18}O-based outlier uncertainties at HWY240 (Figure 3-8b) for the most recent rain "new" water end-member and the baseflow "old" water end-member for a couple of sampling dates. The outlier uncertainties at the Miami site were mostly associated with end-member definitions based on averaged melt and rain samples, as well as deep groundwater samples. These results suggest that deep groundwater may not be a significant contributor to streamflow during the freshet and that shallower groundwater sources may be more significant. Other outlier uncertainties observed at the Miami site were associated with the use of the most recent rain samples and the use of the shallow and intermediate groundwater averages for the "new" and "old" water end-members, respectively, during the summer and fall seasons. This is similar to the observation involving outlier uncertainties at MS1 during the spring period where the "new" and "old" water end-members were likely indistinct. Most of the computed uncertainties for

MS1, HWY240 and Miami were generally smaller than those reported in other studies (e.g., Laudon et al., 2002; Uhlenbrook et al., 2002; St Amour et al., 2005). Our results imply that much of the error in our hydrograph separations originated from the definition of end-members, the spatial and temporal variability of end-member isotopic composition (see Uhlenbrook and Hoeg, 2003 for details) and other assumption violations.

3.5 Conclusions

The overarching goal of the current paper was to evaluate the sensitivity of IHS results to the nature of the "new" and "old" water end-members as well as the chosen tracer. Different methodological scenarios were created by combining eight potential "new" water end-members, eight potential "old" water end-members and two potential tracers. Several thousands of hydrograph separations and uncertainty assessments were attempted on 213 streamwater samples collected across eight nested watersheds of varying sizes and physiographic characteristics in a semi-arid Prairie landscape during the 2014 open water period. Results showed that highly uncertain and, sometimes, physically unrealistic F values (> 1) could be associated with both tracers and observed in the summer and fall. The adequate definition of end-members was also problematic in all seasons when either rain-on-snow conditions dominated or multiple runoff generation mechanisms co-existed during wet periods.

This study therefore raises questions that could form the basis of future case studies. Indeed, while several dozens of scenarios were tested here without making any *a priori* assumptions about dominant water sources, it is unreasonable to ask all IHS studies to adopt that approach given the shear amount of time and data it requires. We can, however, formulate recommendations regarding the methodological choices to make, and use the current study to illustrate the consequences associated with different choices when performing IHS (Figure 3-9), especially in seasonally cold watersheds. In view of the many physically unrealistic F values obtained here, future studies focusing on spring hydrological

dynamics in cold regions could choose one single definition for the “old” water end-member but resort to multiple potential definitions for the “new” water end-member and assess the sensitivity of obtained results to the “new” water-related assumptions. Alternatively, when focusing on summer and fall season dynamics, the sensitivity of obtained results to “old” water-related assumptions could be examined. In addition, for IHS to be applicable in wetland-dominated landscapes or human-dominated landscapes where distributed, man-made water reservoirs (e.g., retention ponds) are present, methodologies will be needed to evaluate whether the assumption of negligible contributions from surface detention or depression storage to streamflow is valid. This could be done qualitatively by defining “old” water as water that is older than the average reservoir residence time, or quantitatively by sampling water upstream and downstream of reservoirs. A dual water and isotopic mass balance would then be used to estimate the isotopic damping ratio dictated by reservoir residence time, and correct the “old” and “new” water end-member signatures accordingly. Gaining grounds on these issues would not only provide more confidence in IHS studies but also ensure that IHS can be used as an effective tool for streamflow partitioning in a wider range of environments, including human-modified landscapes.

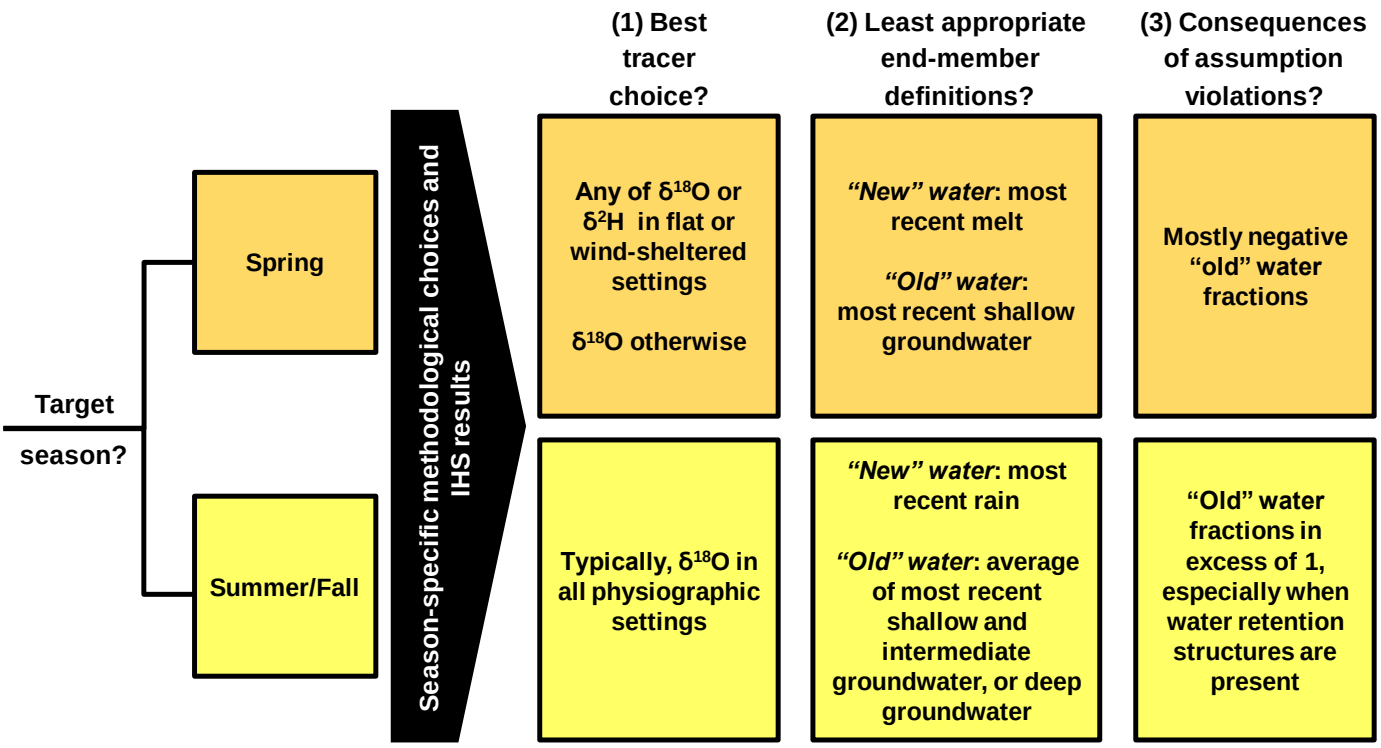

Figure 3-9. Summary of methodological choices and related result consequences based on the current IHS study.

3.6 Acknowledgments

We acknowledge the support of the first author through a University of Manitoba Graduate Fellowship**.** We also acknowledge the financial support made available by the Natural Sciences and Engineering Research Council of Canada (NSERC) through a Discovery Grant awarded to Dr. Genevieve Ali. The authors thank Nicole Pogorzelec, Aminul Haque, Adrienne Schmall, Janelle Laing, Marcos Lemes, Don Cruikshank, Kelvin Hildebrandt and Erin Zoski who contributed greatly in site-setup, data collection and laboratory analysis efforts. Special thanks go to Dr. Christopher Spence for his valuable insights and suggestions. We also thank the associate editor, Dr. David Rupp, as well as four anonymous reviewers for their comments and useful suggestions, all of which helped greatly in improving this manuscript.

3.7 References

Anderson D., & Cerkowniak, D. (2010). Soil formation in the Canadian Prairie Region. *Prairie soils and crops journal*, volume 3-2010, 57-64.

Bamburak, J. D., & Christopher, J. E. (2004). Mesozoic stratigraphy of the Manitoba Escarpment; WCSB/TGIII, Fieldtrip Guidebook, September 7-10, 2004, 87pp.

Barthold, F. K., Tyralla, C., Schneider, K., Vache, K.B., Frede, H., & Breuer, L. (2011). How many tracers do we need for end member mixing analysis (EMMA)? A sensitivity analysis, Water Resources Research, 47, W08519, doi:10.1029/2011WR010604.

Blume, T., Zehe, E., & Bronstert, A. (2008). Investigation of runoff generation in a pristine, poorly gauged catchment in the Chilean Andes II: Qualitative and quantitative use of tracers at three spatial scales. *Hydrological Processes, 22*(18), 3676-3688. doi:10.1002/hyp.6970.

Boucher, J. L., & Carey, S. K. (2010). Exploring runoff processes using chemical, isotopic and hydrometric data in a discontinuous permafrost catchment. *Hydrology Research, 41*(6), 508-519. doi:10.2166/nh.2010.146.

Burns, D. A., & McDonnell, J. J. (1998). Effects of a beaver pond on runoff processes: comparison of two headwater catchments. *Journal of Hydrology, 205*(3-4), 248-264. doi:10.1016/s0022-1694(98)00081.

Buttle, J. M. (2005). Isotope Hydrograph Separation of Runoff Sources, in *Encyclopedia of Hydrological Sciences*, edited by: Anderson, M.G., p. 10, 116, John Wiley & Sons, Ltd, Chichester, Great Britain, 2005.

Buttle, J. M. (1994). Isotope hydrograph separations and rapid delivery of pre-event water from drainage basins. *Progress in Physical Geography, 18*(1), 16-41. doi:10.1177/030913339401800102.

Buttle, J. M., Vonk, A. M., & Taylor, C. H. (1995). Applicability of isotopic hydrograph separation in a suburban basin during snowmelt. *Hydrological Processes, 9*(2), 197-211. doi:10.1002/hyp.3360090206.

Carey, S. K., & Quinton, W. L. (2005). Evaluating runoff generation during summer using hydrometric, stable isotope and hydrochemical methods in a discontinuous permafrost alpine catchment. *Hydrological Processes, 19*(1), 95-114. doi:10.1002/hyp.5764.

Cooper, L. W., Olsen, C. R., Solomon, D. K., Larsen, I. L., Cook, R. B., & Grebmeier, J. M. (1991). Stable isotopes of oxygen and natural and fallout radionuclides used for tracing runoff during snowmelt in an arctic watershed. *Water Resources Research, 27*(9), 2171-2179. doi:10.1029/91wr01243.

Cooper, L. W., Solis, C., Kane, D. L., & Hinzman, L. D. (1993). Application of o-18 tracer techniques to arctic hydrological processes. *Arctic and Alpine Research, 25*(3), 247-255. doi:10.2307/1551821.

Craig, H. (1961). Standard for reporting concentrations of deuterium and oxygen-18 in natural waters. *Science, 133*(346), 1833-&. doi:10.1126/science.133.3467.1833.

Darling, W. G., Bath, A. H., & Talbot, J. C. (2003). The O & H stable isotopic composition of fresh waters in the British Isles. 2. Surface waters and groundwater. *Hydrology and Earth System Sciences, 7*(2), 183-195.

Delsman, J.R., Oude Essink, G. H. P., Beven, K. J., Stuyfzand, P. J. (2013). Uncertainty estimation of end-member mixing using generalized likelihood uncertainty estimation (GLUE), applied in a lowland catchment. Water Resources Research 49, 4792-4806.

Dewalle, D. R., Swistock, B. R., & Sharpe, W. E. (1988). 3-component tracer model for stormflow on a small appalachian forested catchment. *Journal of Hydrology, 104*(1-4), 301-310. doi:10.1016/0022-1694(88)90171-0.

Dincer, T., Payne, B. R., Florkowski, T., Martinec, J., & Tongiorgi, E. (1970). Snowmelt runoff from measurements of tritium and oxygen-18. *Water Resources Research, 6*(1), 110-123. doi:10.1029/WR006i001p00110.

Environment Canada (2014). *Canadian climate normals 1981-2012 station data*. Retrieved from http://climate.weather.gc.ca/climate_normals/results_1981_2010_e.html?searchType=stnProv&lstProvince=MB&txtCentralLatMin=0&txtCentralLatSec=0&txtCentralLongMin=0&txtCentralLongSec=0&stnID=3582&dispBack=0.

Fang, X., Minke, A., Pomeroy, J., Brown, T., Westbrook, C., Guo, X., & Guangul, S. (2007). A review of Canadian Prairie hydrology: Principles, modelling and response to land use and drainage change (Vol. 2).Saskatoon, Saskatchewan: Centre for Hydrology.

Feng, X. H., Taylor, S., Renshaw, C. E., & Kirchner, J. W. (2002). Isotopic evolution of snowmelt - 1. A physically based one-dimensional model. *Water Resources Research, 38*(10), 8. doi:10.1029/2001wr000814.

Friedman, I., & Smith, G. I. (1970). Deuterium content of snow cores from Sierra Nevada area. *Science, 169*(3944), 467-&. doi:10.1126/science.169.3944.467.

Genereux, D. (1998). Quantifying uncertainty in tracer-based hydrograph separations. *Water Resources Research, 34*(4), 915-919. doi:10.1029/98wr00010.

Genereux, D. P., & Hooper R. P. (1998). Oxygen and hydrogen isotopes in rainfall-runoff studies, in *Isotope Tracers in Catchment Hydrology*, edited by C. Kendall and J.J McDonnell, Elsevier, Science and Technology Rights, New York.

Gibson, J. J., Edwards, T. W. D., & Prowse, T. D. (1993). Runoff generation in a high boreal wetland in Northern Canada. *Nordic Hydrology, 24*(2-3), 213-224.

Gibson, J. J., Price, J. S., Aravena, R., Fitzgerald, D. F., & Maloney, D. (2000). Runoff generation in a hypermaritime bog-forest upland. *Hydrological Processes, 14*(15), 2711-2730. doi:10.1002/1099-1085(20001030)14.

Gray, D.M., & Landine, P.G. (1988). An energy-budget snowmelt model for the Canadian Prairies. *Canadian Journal of Earth Sciences*, 25, 1292–1303, doi:10.1139/e88-124.

Hayashi, M., Quinton, W. L., Pietroniro, A., & Gibson, J. J. (2004). Hydrologic functions of wetlands in a discontinuous permafrost basin indicated by isotopic and chemical signatures. *Journal of Hydrology, 296*(1-4), 81-97. doi:10.1016/j.jhydrol.2004.03.020.

Hayashi, M., Van der Kamp, G. & Rosenberry, D.O. (2016). Hydrology of Prairie Wetlands: Understanding the Integrated Surface-Water and Groundwater Processes, *Wetlands* (2016) 36: doi: 10.1007/s13157-016-0797-9.

Hooper, P. R. (2003). Diagnostic tools for mixing models of stream water chemistry, *Water Resources Research*, *39*(3), 1055, doi:10.1029/2002WR001528.

Hooper, P.R & Shoemaker C. A. (1986). A comparison of chemical and isotopic hydrograph separation, *Water Resources Research, 22(*10), 1444-1454.

Huth, A. K., Leydecker, A., Sickman, J. O., & Bales, R. C. (2004). A two-component hydrograph separation for three high-elevation catchments in the Sierra Nevada, California. *Hydrological Processes, 18*(9), 1721-1733. doi:10.1002/hyp.1414.

Ingraham, N. L., & Taylor, B. E. (1989). The effect of snowmelt on the hydrogen isotope ratios of creek discharge in surprise valley, California. *Journal of Hydrology, 106*(3-4), 233-244. doi:10.1016/0022-1694(89)90074-7.

James, A. L., & Roulet, N. T. (2006). Investigating the applicability of end-member mixing analysis (EMMA) across scale: A study of eight small, nested catchments in a temperate forested watershed, Water Resources Research, *42*, W08434, doi:10.1029/2005WR004419.

Kendall, C., & McDonnell, J. J. (1998). Isotope Tracers in Catchment Hydrology. Elsevier: Amsterdam, The Netherlands.

Kennedy, V. C., Kendall, C., Zellweger, G. W., Wyerman, T. A., & Avanzino, R. J. (1986). Determination of the components of stormflow using water chemistry and environmental isotopes, Mattole river basin, California. *Journal of Hydrology, 84*(1-2), 107-140. doi:10.1016/0022-1694(86)90047-8.

Klaus, J., & McDonnell, J. J. (2013). Hydrograph separation using stable isotopes: Review and evaluation. *Journal of Hydrology, 505*, 47-64. doi:10.1016/j.jhydrol.2013.09.006.

Laudon, H., Hemond, H. F., Krouse, R., & Bishop, K. H. (2002). Oxygen 18 fractionation during snowmelt: Implications for spring flood hydrograph separation. *Water Resources Research, 38*(11), 10. doi:10.1029/2002wr001510.

Laudon, H., Sjoblom, V., Buffam, I., Seibert, J., & Morth, M. (2007). The role of catchment scale and landscape characteristics for runoff generation of boreal streams. *Journal of Hydrology, 344*(3-4), 198-209. doi:10.1016/j.jhydrol.2007.07.010.

Liu, K., Elliott, J. A., Lobb, D. A., Flaten, D. N., & Yarotski, J. (2013). Critical Factors Affecting Field-Scale Losses of Nitrogen and Phosphorus in Spring Snowmelt Runoff in the Canadian Prairies. *Journal of Environmental Quality, 42*(2), 484-496. doi:10.2134/jeq2012.0385.

Liu, Y. H., Fan, N. J., An, S. Q., Bai, X. H., Liu, F. D., Xu, Z., Liu, S. R. (2008). Characteristics of water isotopes and hydrograph separation during the wet season in the Heishui River, China. *Journal of Hydrology, 353*(3-4), 314-321. doi:10.1016/j.jhydrol.2008.02.017.

Lyon, S. W., Desilets, S. L. E., & Troch, P. A. (2009). A tale of two isotopes: differences in hydrograph separation for a runoff event when using delta D versus delta O-18. *Hydrological Processes, 23*(14), 2095-2101. doi:10.1002/hyp.7326.

Matile, G. L. D., & Keller, G. R. (2004). Surficial geology of the Brandon map sheet (NTS 62G), Manitoba Geological Survey, Surficial Geology Compilation Map Series, SG-62G, scale 1: 250,000.

McDonnell, J. J., Stewart, M. K., & Owens, I. F. (1991). Effect of catchment-scale subsurface mixing on stream isotopic response. *Water Resources Research, 27*(12), 3065-3073. doi:10.1029/91wr02025.

McGuire, K. J., & McDonnell, J. J. (2006). A review and evaluation of catchment transit time modeling. *Journal of Hydrology, 330*(3-4), 543-563. doi:10.1016/j.jhydrol.2006.04.020.

Metcalfe, R. A., & Buttle, J. M. (2001). Soil partitioning and surface store controls on spring runoff from a boreal forest peatland basin in north-central Manitoba, Canada. *Hydrological Processes, 15*(12), 2305-2324. doi:10.1002/hyp.262.

Moore, R. D. (1989). Tracing runoff sources with deuterium and o-18 during spring melt in a headwater catchment, Southern Laurentians, Quebec. *Journal of Hydrology*, *112*(1-2), 135-148. doi:10.1016/0022-1694(89)90185-6.

Munoz-Villers, L. E., & McDonnell, J. J. (2012). Runoff generation in a steep, tropical montane cloud forest catchment on permeable volcanic substrateRunoff generation in a steep, tropical montane cloud forest catchment on permeable volcanic substrate. *Water Resources Research, 48*, 17. doi:10.1029/2011wr011316.

Nikolayev, V. I., & Mikhalev, D. V. (1995). An oxygen-isotope paleothermometer from ice in Siberian permafrost. *Quaternary Research, 43*(1), 14-21. doi:10.1006/qres.1995.1002.

Ogunkoya, O. O., & Jenkins, A. (1993). Analysis of storm hydrograph and flow pathways using a 3-component hydrograph separation model. *Journal of Hydrology, 142*(1-4), 71-88. doi:10.1016/0022-1694(93)90005.

Pinder, G. F., & Jones, J. F. (1969). Determination of ground-water component of peak discharge from chemistry of total runoff. *Water Resources Research, 5*(2), 438-450. doi:10.1029/WR005i002p00438.

Pomeroy, J., Shook, K., Fang, X., & Brown, T. (2013). Predicting spatial patterns of inter-annual runoff variability in the Canadian Prairies. In G. Bloschl, M. Sivapalan, T. Wagener, A. Viglione, and H. Savenije (Eds.), *Runoff Prediction in Ungauged Basins: Synthesis across Processes, Places and Scales*. Cambridge: Cambridge University Press. doi:10.1017/CBO9781139235761.014.

Pu, T., He, Y., Zhu, G., Zhang, N., Du, J., & Wang, C. (2013). Characteristics of water stable isotopes and hydrograph separation in Baishui catchment during the wet seasons in Mt. Yulong region, south western China, *Hydrological Processes*, *27*(17), 3641-3648, doi: 10.1002/hyp.9479.

Rice, K. C., & Hornberger, G. M. (1998). Comparison of hydrochemical tracers to estimate source contributions to peak flow in a small, forested, headwater catchment. *Water Resources Research, 34*(7), 1755-1766. doi:10.1029/98wr00917.

Rodhe, A. (1998). Snowmelt dominated systems. In *Isotope Tracers in Catchment Hydrology*, Kendall C, McDonnell JJ (eds). Elsevier.

Rodhe, A. (1981). Spring flood meltwater or groundwater. *Nordic Hydrology*, *12*(1), 21-30.

Shanley, J. B., Kendall, C., Smith, T. E., Wolock, D. M., & McDonnell, J. J. (2002). Controls on old and new water contributions to stream flow at some nested catchments in Vermont, USA. *Hydrological Processes, 16*(3), 589-609. doi:10.1002/hyp.312.

Shook, K., & Pomeroy, J. (2012). Changes in the hydrological character of rainfall on the Canadian prairies. *Hydrological Processes* **26** (12): 1752–1766. doi: 10.1002/hyp.9383.

Shook, K., Pomeroy, W. J., Spence, C., & Boychuk, L. (2013). Storage dynamics simulations in prairie wetland hydrology models: evaluation and parameterization. *Hydrological processes*, doi: 10.1002/hyp.9867.

Sklash, M. G., & Farvolden, R. N. (1979). Role of groundwater in storm runoff. *Journal of Hydrology, 43*(1-4), 45-65. doi:10.1016/0022-1694(79)90164-1.

St Amour, N. A., Gibson, J. J., Edwards, T. W. D., Prowse, T. D., & Pietroniro, A. (2005). Isotopic time-series partitioning of streamflow components in wetland-dominated catchments, lower Liard River basin, Northwest Territories, Canada. *Hydrological Processes, 19*(17), 3357-3381. doi:10.1002/hyp.5975.

Taylor, S., Feng, X. H., Renshaw, C. E., & Kirchner, J. W. (2002). Isotopic evolution of snowmelt - 2. Verification and parameterization of a one-dimensional model using laboratory experiments. *Water Resources Research, 38*(10), 8. doi:10.1029/2001wr000815.

Tiessen, K. H. D., Elliott, J. A., Yarotski, J., Lobb, D. A., Flaten, D. N., & Glozier, N. E. (2010). Conventional and Conservation Tillage: Influence on Seasonal Runoff, Sediment, and Nutrient Losses in the Canadian Prairies. *Journal of Environmental Quality, 39*(3), 964-980. doi:10.2134/jeq2009.0219.

Uhlenbrook, S., Frey, M., Leibundgut, C., & Maloszewski, P. (2002). Hydrograph separations in a mesoscale mountainous basin at event and seasonal timescales. *Water Resources Research, 38*(6), 14. doi:10.1029/2001wr000938.

Uhlenbrook, S., & Hoeg, S. (2003). Quantifying uncertainties in tracer-based hydrograph separations: a case study for two-, three- and five-component hydrograph separations in a mountainous catchment. *Hydrological Processes, 17*(2), 431-453. doi:10.1002/hyp.1134.

Van der Kamp, G., Keir D., & Evans, M.S. (2008). Long-Term Water Level Changes in Closed-Basin Lakes of the Canadian Prairies, *Canadian Water Resources Journal*, Vol. 33(1): 23-38 (2008).

Wels, C., Cornett, R. J., & Lazerte, B. D. (1991). Hydrograph separation - a comparison of geochemical and isotopic tracers. *Journal of Hydrology, 122*(1-4), 253-274. doi:10.1016/0022-1694(91)90181.

Wenninger, J., Uhlenbrook, S., Tilch, N., & Leibundgut, C. (2004). Experimental evidence of fast groundwater responses in a hillslope/floodplain area in the Black Forest Mountains, Germany. *Hydrological Processes, 18*(17), 3305-3322. doi:10.1002/hyp.5686.

CHAPTER 4: STREAMWATER AGES IN NESTED, SEASONALLY COLD CANADIAN WATERSHEDS

Abstract

The mean transit time (MTT) is an important descriptor of water storage and release dynamics in watersheds. While MTT studies are numerous for many regions around the world, they are rare for prairie watersheds where seasonally cold or dry conditions require adequate methodological choices toward MTT estimation, especially regarding the handling of sparse data records and tracer selection. To examine the impact of such choices, we used timeseries of $\delta^{18}O$ and $\delta^{2}H$ from two contrasted years (2014 and 2015) and relied on two metrics and two modeling methods to infer MTTs in prairie watersheds. Our focus was on nested outlets with different drainage areas, geologies, and known runoff generation mechanisms. The damping ratio and young water fraction (i.e., the fraction of streamflow with transit times lesser than three months) metrics, as well as the sine-wave modeling and time-based convolution modeling methods, were applied to year-specific data. Results show that young water fractions and modeled MTT values were, respectively, larger and smaller in 2014, which was a wet year, compared to 2015. In 2014, most outlets had young water fractions larger than 0.5 and MTT values lesser than 6 months. The damping ratio, young water fraction and sine-wave modeling methods led to convergent conclusions about watershed water storage and release dynamics for some of the monitored sites. Contrasting results were, however, obtained when the same method was applied using $\delta^{2}H$ instead of $\delta^{18}O$, due to differing evaporation fractionation, or when the time-based convolution modeling method was used. Some methods also failed to provide any robust results during the dry year (i.e., 2015), highlighting the difficulty in inferring MTTs when data are sparse due to intermittent streamflow. This study therefore allowed the formulation of empirical recommendations for MTT estimation in prairie environments as a function of data availability and antecedent wetness conditions.

Keywords: mean transit time (MTT), metrics, modeling methods, prairie watersheds, oxygen-18, deuterium.

4.1 Introduction

The concepts of water age, residence time and transit time have been central to hydrology for several decades (Stewart et al., 2010). Since water stored within a watershed comes from different precipitation events and ultimately contributes to runoff and streamflow generation (after losses through evapotranspiration), the historic signal of precipitation inputs is embedded into streamwater mixtures. Differences exist between the concepts of water age, residence time and transit time. Typically, the residence time or age of water at any point along a flowpath in a catchment is defined as the time that has passed since a water molecule entered the catchment (Maloszewski and Zuber, 1982; Bethke and Johnson, 2008). The transit time is rather defined as the time water spends travelling from an input point (e.g., surface of the watershed after a precipitation event) to an output point (e.g., stream at the watershed outlet) via flowpaths in a watershed (McDonnell et al., 2010). Regardless of whether the goal is to quantify water age, residence time or transit time, the underlying rationale is typically to describe how catchments function by retaining and releasing water from storage. Those storage-release dynamics are especially fundamental to our understanding of streamflow generation processes (Wolock et al., 1997; Kendall and McDonnell, 1998; McGuire and McDonnell, 2006) and our characterization of controls on weathering rates (Pacheco and Van der Weijden, 2012; Frisbee et al., 2013), characteristic timescales of ecological processes (Brunke and Gonser, 1997; Hancock et al., 2005), and catchment response to climate change (Singleton and Moran, 2010; Manning et al., 2012; Rademacher et al., 2012).

There has been considerable interest in catchment transit time estimation since the advent of stable isotopes of oxygen and hydrogen as tracers a few decades ago (Dincer, et al., 1970;

Stewart et al., 2010). There is, however, significant variability in the methods and data used to infer mean transit times (MTTs). Time-based convolution integral modeling – which is among one of the most commonly used methods of transit time estimation (McGuire and McDonnell, 2006) – relies on the selection of a stationary transit time distribution (TTD) meant to reflect the storage, flow pathway heterogeneity and sources of water in a catchment. Typically, time-based convolution modeling employs, as a minimum, weekly tracer data spanning at least one year to infer and compare input and output isotopic fluxes for the catchment under consideration. The majority of MTT studies that have relied on the time-based convolution method have used only $\delta^{18}O$ data, but some have also used $\delta^{2}H$ data (e.g., Maloszewski, et al., 1983) or chloride data (e.g., Kirchner, et al., 2000). A few other studies attempted to use both $\delta^{18}O$ and $\delta^{2}H$ data (e.g., Stockinger et al., 2014; Timbe et al., 2014) but in the end decided to rely solely on $\delta^{18}O$ when the results obtained using either tracer were deemed similar. Although the great majority of MTT studies via time-based convolution modeling have used more than one year of data, some have used less: examples include Soulsby et al., (2014) who focused on the Scottish Highlands; Ma and Tamanaka (2013) in the context of a tracer-aided tank experiment; Lyon et al. (2010) in the determination of snowmelt MTT in a boreal catchment in Northern Sweden; Lyon et al., (2008) in an event-based MTT study at the Santa Catalina Mountains in Tucson, Arizona; and Stewart and McDonnell (1991) in the determination of soil water residence times at the Maimai Catchment in New Zealand. Convolution modeling can also be carried out in the frequency domain; however, it is often difficult to extract the TTDs – the kernel from which the MTT is obtained – from the resulting power spectra. Thus, only a few (e.g., Kirchner et al., 2000) have applied the spectral method to model catchment TTDs. A third and comparatively simpler MTT estimation method, i.e., the sine-wave modeling method, is also commonly used as it has the advantage of being

applicable with coarser and irregularly spaced data (McGuire and McDonnell, 2006), as long as seasonal cycles in isotopic timeseries can be captured.

Although they are widely used, the adequacy of currently available, stationary MTT estimation methods is the subject of ongoing debate. Kirchner (2016a, b) showed that common MTT estimation techniques (e.g., sine-wave, time-based convolution and spectral analysis methods) are liable to enormous aggregation errors and hence can lead to unreliable results. These errors stem mainly from catchment heterogeneity and the non-stationarity of the TTDs, driven by the rapidly changing water flowpaths and velocities in response to variable hydrologic forcing (Kirchner et al., 2001; Tetzlaff, et al., 2007; Hrachowitz et al., 2010; Heidbuchel et al., 2012; Birkel et al., 2012). Time-averaged TTDs may have been estimated in lieu of characterizing time-varying TTDs. To avoid dealing with those issues, Kirchner (2016a, b) proposed a metric, the young water fraction, defined as the fraction of streamflow with transit times of less than two or three months. This metric proved to be less susceptible to aggregation bias and able to infer dynamic water storage and release behavior (Benettin et al., 2017) in a variety of environments. Similar to the sine-wave method, the young water fraction metric has the advantage of being applicable with sparse and irregularly sampled isotopic data (Kirchner, 2016a, b), as opposed to the time-based convolution and spectral methods which require continuous, unbroken timeseries of input and output isotopic fluxes (McGuire and McDonnell, 2006; Hrachowitz et al., 2011). Prior to the young water fraction metric being proposed, another metric, called the damping ratio, was suggested as an inverse method for inferring catchment MTTs: it is computed by dividing the coefficient of variation of the isotopic timeseries in streamflow by the coefficient of variation of the isotopic timeseries of precipitation (e.g., McGuire et al., 2005; Tetzlaff et al., 2009; Soulsby et

al., 2015). Both the young water fraction and damping ratio metrics are simpler methods that can thus be applied on shorter timeseries data to estimate MTTs.

It is worth noting that a few exceptions aside, transit time studies have been conducted in temperate mid-latitudes. That has been notably the case in the majority of studies carried out in Europe and in the United States (e.g., Tetzlaff et al., 2009; Lyon et al., 2010; Heidbuchel et al., 2012), but there are also a few in Africa (e.g., Tekleab et al., 2014a) and New Zealand (e.g., McGlynn et al., 2003). Across those largely humid regions, catchments of varying sizes were examined (e.g., McDonnell et al., 1991; Soulsby et al., 2000; Uhlenbrook and Leibundgut, 2002; McGuire et al., 2005; McGuire and McDonnell, 2006; Tetzlaff et al., 2007; Soulsby and Tetzlaff, 2008). Most often than not, weekly input-output data (at the very least) were available for those sites, with very few gaps when, exceptionally, field sites could not be visited for one reason or another. Conversely, however, obtaining uninterrupted weekly input-output timeseries in seasonally cold and dry regions is quasi-impossible, not for lack of field visits but rather because of streams and rivers flowing intermittently or ephemerally. That is notably the case in the Canadian prairies, which are characterized by rolling to flat topography, large agricultural lands and non-negligible forested riparian areas, a sub-humid to semi-arid climate with alternating floods and droughts, and a lengthy winter season during which the ground is frozen. Achieving a better understanding of catchment transit times in a region like the Canadian prairies is especially important because of its uniquely uncommon hydrologic regime: it is not just impacted by man-made stormwater control structures such as drainage ditches but also farm dams, drained wetlands, and roads which altogether slow down or enhance surface and subsurface flow in ways that are not fully understood. One problem is that the reasons that make the characterization of transit times important in prairie regions are also the reasons that make it especially challenging. Worthy of

note are (i) the strong evaporative processes in the region, (ii) the presence of frozen ground which signals hydrologic inactivity as a consequence of the long severe winter, and (iii) alternating years of wetness and dryness. The aforementioned item (i) brings into question the choice of an adequate isotopic tracer to use for MTT estimation, since not all isotopes are equally affected by kinetic fractionation (Kendall and McDonnell, 1998; Cappa et al., 2003). As for the aforementioned items (ii) and (iii), they lead to timeseries of irregular length (i.e., from the start to the end of the open water season) and density (i.e., number of data points) from one year to the next and thus pose a challenge when assessing the most appropriate method for assessing MTTs. "StorAge Selection" functions (e.g., Benettin et al., 2015; Harman, 2015) have recently been introduced and could help address some of these challenges; however, they are not necessarily accessible to people who are not seasoned modelers, and they also require that an estimate of total catchment storage be available (Harman, 2015), which is often not available. While the aforementioned issues have prevented comprehensive transit time studies from taking place in the Canadian prairies, there is a strong rationale for applying some of the common MTT inference methods in that region to compare their relative efficiency in a challenging landscape type and thereby obtain first-order estimates of streamwater ages. In the current chapter, we address those issues "head-on" by focusing on a system of nested prairie watersheds for which isotopic data are available. Two of the metric-based methods and two of the modeling methods mentioned above were relied upon, namely the damping ratio method, the young water fraction method, sine-wave modeling, and time-based convolution modeling. Two main research objectives were pursued, namely:

1. Examine how the choice of one metric over the other influence MTT estimation; and
2. Assess how the choice of one modeling method over the other affect computed catchment MTTs.

The above research objectives were addressed using $\delta^{18}O$ and $\delta^{2}H$ as tracers. Timeseries of different length and density were also evaluated, as our focus was on two sampling years with contrasting characteristics, in terms of precipitation regime. Such an approach was chosen not only to help us assess the convergence or divergence of results obtained via the different MTT estimation methods, but also to qualitatively address the impact of tracer choice and sparse data record on the obtained results.

4.2 Methods

4.2.1 Study site

Our focus was on eight sites, i.e., seven sub-watersheds ranging in size from 0.19 km^2 to 34.65 km^2 and nested within the 74.41 km^2 South Tobacco Creek Watershed (STCW) in the province of Manitoba, Canada (Figure 4-1). The STCW is characterized by semi-arid to sub-humid temperate conditions typical of the Prairie ecozone, i.e., cold lengthy winters and short cool summers (Tiessen et al., 2010). The long-term averages (1996-2015) for total annual precipitation (including snowfall) and mean daily temperature in the region are 595.2 mm and 4.4°C, respectively (Environment Canada, 2015). Total annual precipitation was 529.5 mm in 2014 (including 91.5 mm of mean monthly rainfall), versus 607.5 mm in 2015 (with 84.4 mm of mean monthly rainfall) (Environment Canada, 2014, 2015). The mean daily air temperature was 2.9°C in 2014, and rather 5.8°C in 2015 (Environment Canada, 2014, 2015). In general, the net value of precipitation minus potential evapotranspiration (PET, as derived from the Blaney-Criddle method

(Blaney and Criddle, 1962) was higher in 2014 compared to 2015 (Figure 4-2), thus making the latter year relatively drier.

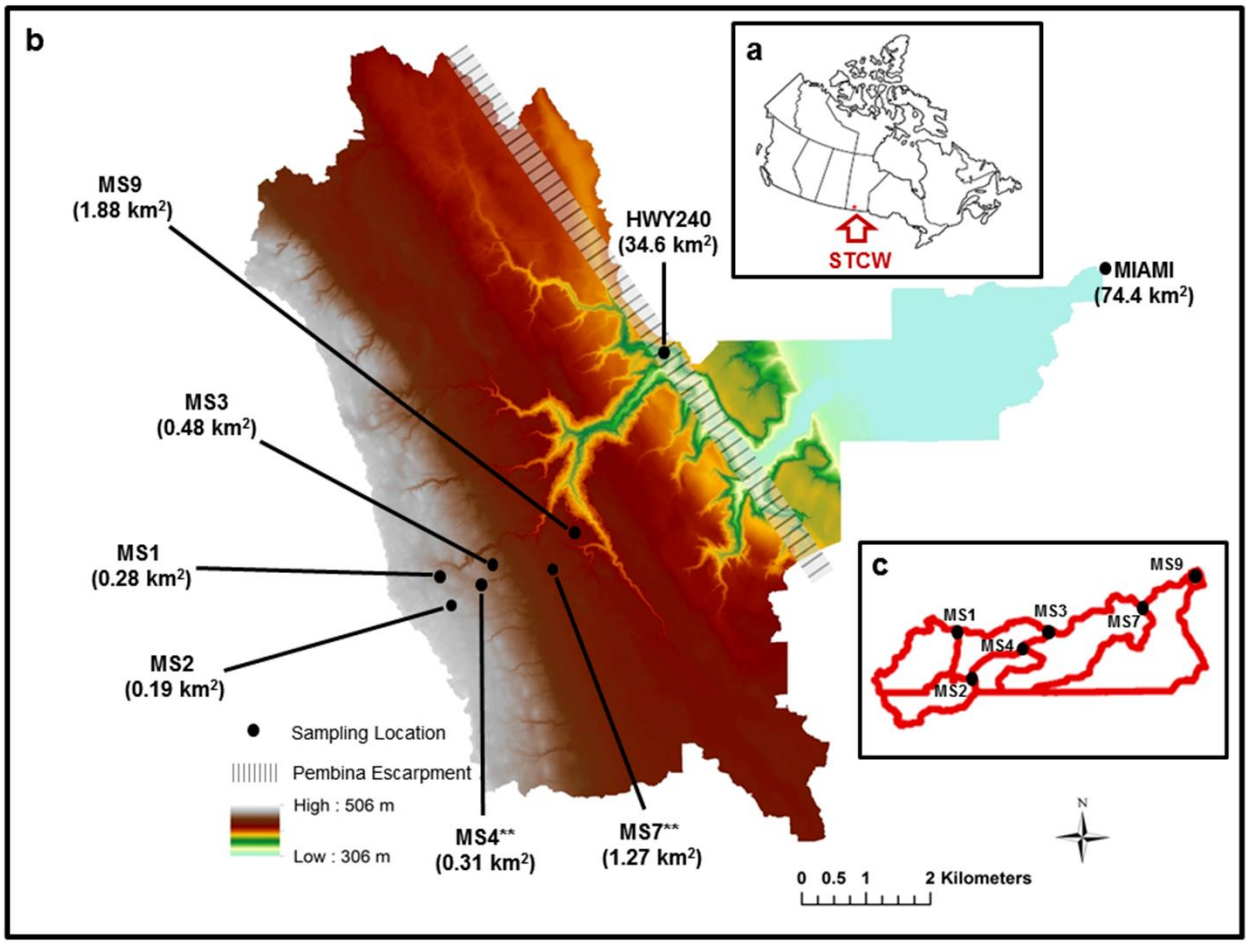

Figure 4-1. (a) Location of the South Tobacco Creek Watershed (STCW) in Canada. (b) Digital elevation model (horizontal resolution: 1 m) with sub-watershed outlets and drainage areas (in brackets) in the STCW. Elevation is in meters above sea level. '**' indicates MS outlets with holding dams. (c) Subwatershed boundaries for 'MS' sites.

The STCW is composed of a shale bedrock overlain by moderately to strongly calcareous glacial till and clay-loam soils (Matile and Keller, 2004; Tiessen et al., 2010). The NW-SE trending Pembina escarpment (Figure 4-1) traverses the watershed and originated approximately 50 to 84 million years ago because of the Laramide Orogeny (Matile and Keller, 2004; Tiessen et al., 2010): it causes an elevation drop of approximately 200 m between the STCW headwaters and its outlet near the town of Miami (Figure 4-1), and it is made of largely interconnected joints and fractures which provide seepage of groundwater as a main source of recharge to the nearby streams (Hutchinson, 1977). The surficial materials atop the escarpment are mainly glacial tills (ranging in thickness from a few centimeters up to 20 m) and comprise mixed deposits of shale, limestone and granite.

The outlets of the watershed and sub-watersheds chosen for the current study reflect the landscape diversity encountered in the region. The 'MS' sites are located above the escarpment (Figure 4-1), where low-relief to undulating (hereafter referred to as undulating) landscapes with slopes of up to 10% are present (Tiessen et al., 2010). Dominant soil types are from the Dezwood soil series (Orthic Dark Gray Chernozems) with primarily clay-loam texture and the Zaplin soil series (Gleyed Dark Gray Chernozem) (Manitoba Department of Agriculture, 1943; 1988). The MS4 and MS7 outlets have small holding dams and retention ponds located immediately upstream of them for stormwater control purposes; the pond behind MS7 has the tendency to overflow during snowmelt and extreme storm events. The HWY240 outlet is located at the edge of the escarpment: it is characterized by a deeply incised stream channel atop intensely fractured shale bedrock. Within the vicinity of the escarpment, soils are gravelly sand to clays (ranging in thickness up to 2 m) that overlay glacial till (often containing considerable stones) and fractured shale bedrock (Manitoba Department of Agriculture, 1988). As for the Miami site, it marks the

outlet of the whole STCW and sits within flat, lowland terrain (Figure 4-1) below the escarpment. Surficial materials below the escarpment are mainly medium- to coarse-grained glaciolacustrine deposits, which progressively become finer-grained moving downstream. The main soil and geological differences that exist above, atop and below the escarpment translate into major differences in runoff generation mechanisms, as has been observed through more than 15 years of active field research in the STCW. While most of the previously published papers focusing on the STCW targeted nutrient dynamics (e.g., Elliott et al., 1999; Tiessen et al., 2010, 2011; Li et al., 2011; Liu et al., 2013), they also relied on hydrometric data to compare and contrast the hydrologic regimes prevailing in the different physiographic units.

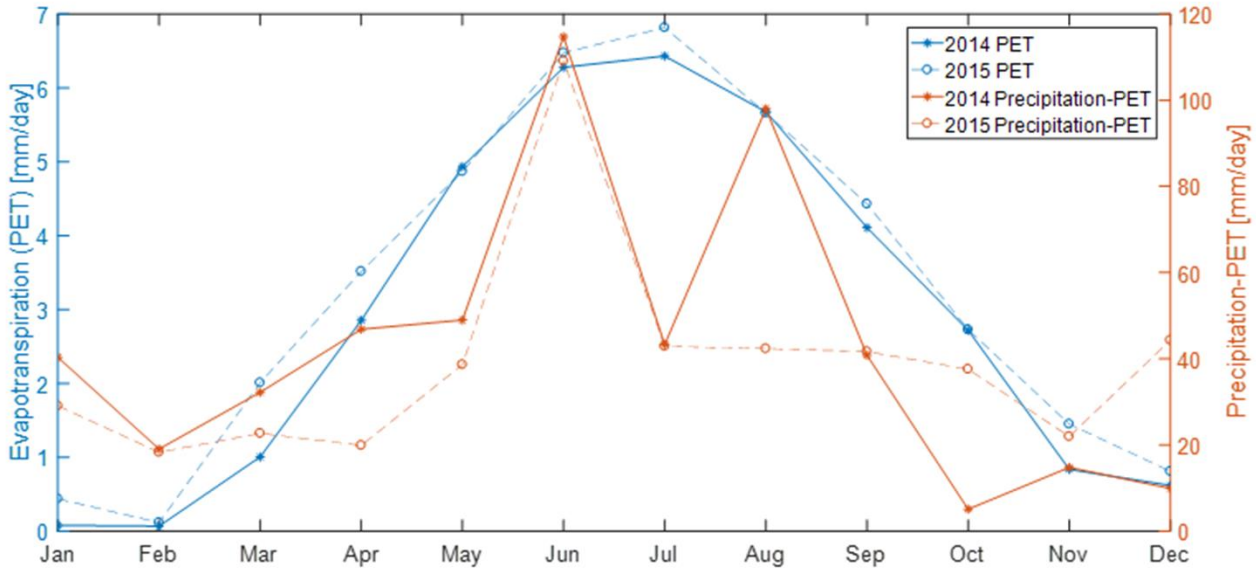

Figure 4-2. Comparison of 2014 and 2015 average monthly net atmospheric water input values for the 2014 and 2015 sampling years at the STCW.

Above the escarpment, the "MS" sites behave like typical prairie systems, in that they experience Hortonian overland flow in the form of sheet flow over frozen ground in early spring (e.g., Fang et al., 2007), shallow subsurface flow in late spring, Hortonian overland flow in response to short-lived, convective summer storms (e.g., Shook and Pomeroy, 2012), and saturation-excess overland flow in exceptionally wet conditions (Bansah and Ali, 2017). Water movements in the vicinity of the Pembina escarpment occur mostly vertically (i.e., surface water-groundwater exchanges) rather than laterally (i.e., hillslope-to-stream transfers) (Hutchinson, 1977; Betcher et al., 1995). Although steep terrain around the HWY240 outlet could theoretically promote quick overland flow, the thin soils and bedrock fractures allow the preferential downward movement of melt and rainwater, thus preventing shallow lateral flow from occurring. Bedrock fractures also maintain a permanent hydraulic link between the incised stream channel and the groundwater table, thus making HWY240 the only outlet where perennial, albeit at times stagnant or slow-moving, water is observed. A recent study using isotope-based hydrograph separation (Bansah and Ali, 2017) also confirmed the predominance of "old" streamwater at this site, as long as the "old water" end-member was portrayed by water collected from an 8 m-deep well (and not from piezometer with intake depths of 1.5 m or less). As for streamflow at the Miami site, it is mainly fed by Hortonian overland flow and deep groundwater flow from the Miami aquifer (Betcher et al., 1995). Agricultural activities take place throughout the STCW, with corn, wheat and canola being the major crops planted.

4.2.2 Sample collection and laboratory analyses

Water samples were collected during the 2014 and 2015 open water seasons at a frequency of at least once per week; higher-frequency sampling was also performed during storm events. Snow, snowmelt, rainwater and streamwater samples were collected in each of the seven sub-watersheds and in the lower portion of the STCW. Snow and snowmelt samples were collected using lysimeters and also manually during field visits. Rain catchers were used to collect rainwater; they were lined with canola oil to prevent fractionation and evaporative losses between site visits. As for streamwater, grab samples were collected manually during weekly field visits while automatic water samplers were used during storm events. Upon collection, all samples were stored in 10 mL glass vials sealed with parafilm and kept at 4°C until analysis. No more than 6 months after collection, all samples were tested for $\delta^{18}O$ and $\delta^{2}H$ using a Picarro^{TM} Liquid Water Isotope Analyzer (LWIA, model L2130-i) based on Cavity Ring-Down Spectroscopy (CRDS) technology. Delta (δ) values were recorded in permil (‰) deviations from the Vienna Standard Mean Ocean Water (VSMOW) (Craig, 1961) with a precision of 0.025 ‰ and 0.1 ‰ for $\delta^{18}O$ and $\delta^{2}H$, respectively. $\delta^{18}O$ and d-excess time series (Figure 4-3) were plotted to evaluate the temporal dynamics of precipitation and streamwater isotopes in the watersheds. In general, the $\delta^{18}O$ streamwater timeseries were slightly damped compared to $\delta^{18}O$ precipitation timeseries in both sampling years. Early spring $\delta^{18}O$ data showed the strongest evidence of depletion in heavy isotopes (Figure 4-3), as do snow and snowmelt samples in that region (Bansah and Ali, 2017), while summer and fall samples were the most enriched. Open-water evaporation effects were visible through d-excess data: streamflow d-excess values were slightly higher during periods of very low to no flow – albeit with quasi-stagnant water – in the channels, especially at the headwater

'MS' sites (Figure 4-3). d-excess values from the current study appeared consistent with those obtained from studies conducted in other Canadian watersheds (e.g., Froehlich et al., 2002; Jasechko et al., 2017).

4.2.3 Metrics of water age or MTT

The aforementioned data were used to compute two metrics. Firstly, the damping ratio method (Eq. 4-1) was applied as it takes advantage of the damping of precipitation isotopic signals in streamflow. It is an inverse transit time metric (e.g., Tetzlaff et al., 2009; Soulsby et al., 2015) which can be used to characterize, in a somewhat qualitative manner, the general trend and distribution of MTTs in watersheds. It is computed as:

$$\mathrm{DR} = \frac{\mathrm{CV\ of\ } \delta^{18}\mathrm{O\ (or\ } \delta^{2}\mathrm{H)\ in\ streamflow}}{\mathrm{CV\ of\ } \delta^{18}\mathrm{O\ (or\ } \delta^{2}\mathrm{H)\ in\ precipitation}} \qquad \text{(Eq. 4-1)}$$

where CV is the coefficient of variation. Eq. 4-1 was applied to individual years (2014 versus 2015) and tracer-specific data (δ^{18}O versus δ^{2}H isotopic timeseries) for comparison purposes. Secondly, the young water fraction was also computed following Kirchner (2016 a, b). We assumed the TTD, $g(\tau)$, of our watershed system to belong to a family of gamma distributions (Eq. 4-2) for which the MTT (τ) is equivalent to $\alpha\beta$ (Eq. 4-3):

$$g(\tau) = \frac{\tau^{\alpha-1}}{\beta^{\alpha}\Gamma(\alpha)} exp^{-\tau/\beta} \qquad \text{(Eq. 4-2)}$$

$$\tau = \alpha\beta \qquad \text{(Eq. 4-3)}$$

where α and β are the shape and scale factors of the gamma distributions, respectively.

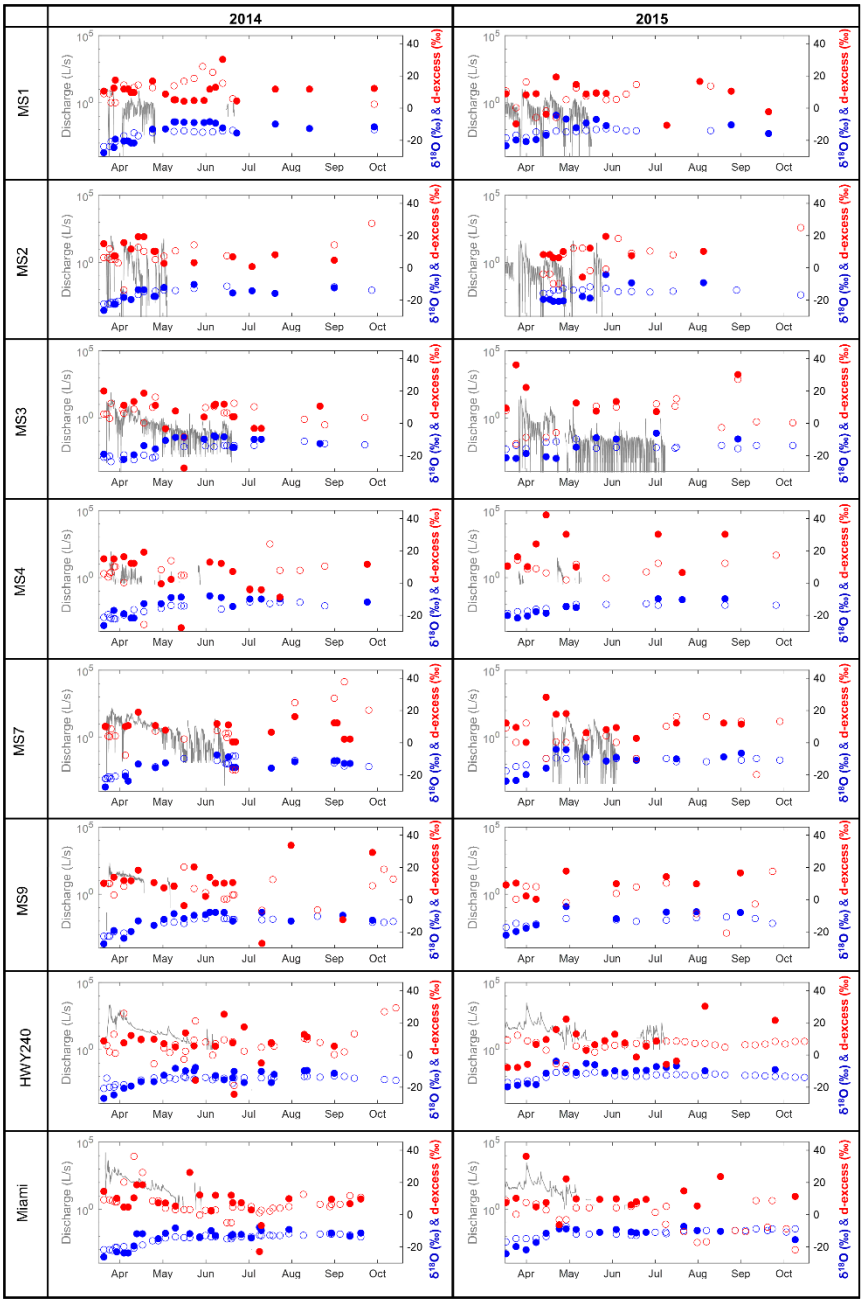

Figure 4-3. Timeseries of $\delta^{18}O$ and d-excess values in precipitation (filled symbols) and streamwater (open symbols) for the eight study outlets. Stream hydrographs are also shown and plotted on a log scale to enhance readability. There were periods of very low or no flow (as recorded by velocimeters) but stagnant water was present in the streams, thus allowing sample collection. Instrument failure occurred at MS9 in 2015; hence no discharge values were recorded.

Sinusoidal cycles were fitted to year-specific (2014 versus 2015) and tracer-specific ($\delta^{18}O$ versus $\delta^{2}H$) data to extract the amplitudes of precipitation and streamflow isotopic timeseries (Ap and As) for each of the eight outlets. The amplitudes are related to α and β via Eq. 4-4:

$$\frac{As}{Ap} = (1 + (2\pi f\beta)^2)^{-\alpha/2} \quad \text{(Eq. 4-4)}$$

where f is the frequency of the cycle (f = 1 year^{-1} for a seasonal cycle). Since the process of accurately determining α and β is generally not straightforward, we followed the recommendation of Kirchner (2016a) and assumed a "young" water age threshold (τ_{yw}) of three months for our study region. We then proceeded to apply Eq. 4-5 to estimate the fraction of young water (F_{yw}) arriving at each of the eight outlets as:

$$F_{yw} = \frac{As}{Ap} \quad \text{(Eq. 4-5)}$$

It should be noted that while we assumed an annual sinusoidal cycle (i.e., f = 1 year^{-1}) for our data, our timeseries only covered the open-water period which is shorter than a full calendar year, and hence the A_s/A_p ratios may have been underestimated in our study. The uncertainty associated with F_{yw} estimates was quantified by feeding the 95% confidence bounds for the fitted A_s and A_p values into Eq. 4-5.

4.2.4 MTT modeling methods

Two modeling methods were also applied for comparison purposes. Firstly, sine-wave fitting of the seasonal $\delta^{18}O$ and $\delta^{2}H$ variation in precipitation and streamflow (e.g., Maloszewski et al., 1983; DeWalle et al., 1997; McGuire et al., 2002; Rodgers et al., 2005; Tetzlaff et al., 2007) was performed to estimate watershed-specific MTTs (Soulsby et al., 2000; Rodgers et al., 2005).

The fitting was assumed to follow an exponential distribution. The input precipitation and output streamwater $\delta^{18}O$ and $\delta^{2}H$ timeseries can be modeled as:

$$\delta = Co + A[\cos(ct - \varphi)] \quad \text{(Eq. 4-6)}$$

where δ is the predicted $\delta^{18}O$ (or $\delta^{2}H$) composition, Co is the observed weighted mean annual $\delta^{18}O$ (or $\delta^{2}H$) composition, A is the amplitude of predicted $\delta^{18}O$ (or $\delta^{2}H$) composition, c = 0.017214 rad d^{-1} is the angular frequency constant, t is the time (in days) since the start of sampling, and φ is the phase lag (in radians) of predicted $\delta^{18}O$ (or $\delta^{2}H$) compositions. Eq. 4-6 can be evaluated via periodic regression (Bliss, 1970) as:

$$\delta = Co + a\cos(ct) + bsin(ct) \quad \text{(Eq. 4-7)}$$

The regression coefficients a and b are used to estimate the amplitudes of the input and output signals (Eq. 4-8) and the phase lag (Eq. 4-9):

$$A = \sqrt{a^2 + b^2} \quad \text{(Eq. 4-8)}$$

$$\varphi = tan^{-1}\left|\frac{b}{a}\right| \quad \text{(Eq. 4-9)}$$

Following from the determination of A in Eq. 4-8, the MTT, noted as τ and expressed in days, can be estimated by:

$$\tau = \frac{1}{c}\sqrt{\left(\frac{As}{Ap}\right)^{-2} - 1} \quad \text{(Eq. 4-10)}$$

where As and Ap are amplitudes of the $\delta^{18}O$ (or $\delta^{2}H$) isotopic signal in streamwater and precipitation respectively, and c is defined in Eq. 4-6. Similar to what was done for F_{yw} estimates, the 95% confidence bounds for the fitted A_s and A_p values were fed into Eq. 4-10 to quantify the uncertainty surrounding MTT estimates.

Secondly, convolution integral modeling was performed in the time domain using year-specific (2014 versus 2015) and tracer-specific ($\delta^{18}O$ versus $\delta^{2}H$) data aggregated at the weekly timescale. For all sites, timeseries had fewer data points in 2015 due to the prevailing drier conditions, compared to 2014. The two-parameter gamma distribution model was selected as a stationary TTD (noted as $g(t-\tau)$) and convolved with the amount-weighted $\delta^{18}O$ (or $\delta^{2}H$) isotopic timeseries of precipitation ($\delta_{in}(\tau)$) to predict the $\delta^{18}O$ (or $\delta^{2}H$) isotopic timeseries in streamflow ($\delta_{out}(t)$) (McGuire and McDonnell, 2006; Hrachowitz et al., 2010) via Eq. 4-11:

$$\delta_{out}(t) = \int_{-\infty}^{t} \delta_{in}(\tau)\, g(t-\tau) d\tau \qquad \text{(Eq. 4-11)}$$

Weekly precipitation totals from the Weather Survey of Canada were used to compute amount-weighted $\delta^{18}O$ (or $\delta^{2}H$) isotopic timeseries of precipitation. Precipitation totals for all the "MS" outlets were recorded by a weather station located above the Pembina escarpment within the STCW, while those for HWY240 and Miami were taken from weather stations located in the vicinity of each gauging station. For each site, a 30-year warm-up period was used to spin the model before the search for behavioral model parameters was conducted via 50,000 Monte Carlo (MC) simulations in MATLAB (R2016b). A generalized likelihood uncertainty error ([GLUE]; Beven and Freer, 2001) analysis was performed by setting a minimum Nash-Sutcliffe Efficiency ([NSE]; Nash and Sutcliffe, 1970) threshold of 0.3 for behavioral parameter sets. The MTT was estimated by multiplying the α and β parameters associated with the MC simulation that yielded the highest NSE. The parameters (α and β) associated with the highest NSE for each site were also fed into the gamma function equation (Eq. 4-2) to compare the shape of the TTD across the studied (sub-)watersheds. The uncertainty surrounding MTT estimates was quantified by multiplying α and β for each of the behavioral parameter sets and taking the range.

4.2.5 Comparison across sites

Since the four MTT estimation methods used in this paper do not measure the same quantities, our goal was not to compare their outputs in absolute terms but rather relatively, i.e., examine whether they led to a similar ranking of our sites from slowest to fastest water storage and release dynamics. Hence, based on the results of each estimation method, the study watersheds were assigned ranks from 1 through 8, with 1 being the watershed with the highest MTT or metric value and 8 being the watershed with the lowest. The only exception to that rule was the damping ratio method: as the damping ratio is an inverse transit time metric, the watershed with the highest damping ratio was deemed to have the youngest water (or fastest storage-release dynamics) and vice versa. Quantitatively, a Spearman's rank correlation analysis was performed to assess the relation (or lack thereof) between the site rankings inferred from the different metrics and MTT modeled values. Qualitatively, the propensity of a given site to be given the same ranks, regardless of the method relied upon, was evaluated. For the sake of brevity, results below focus on sites with ranks 1 and 8 only. Cumulative transit time distributions (CTTDs), up to one year, were constructed for each site based on the TBC modeling results. The proportions of input precipitation that arrive at the watershed outlets in three months or less were extracted from those CTTDs and compared to the sine-wave-derived metric, the young water fraction. Another Spearman's rank correlation analysis was done, this time to assess the degree of predictability of metrics and MTT modeled values from watershed characteristics such as drainage area, mean slope, proportion of treed riparian area, etc. (see Table 4-1). All Spearman's rank correlation coefficients, noted as rho (i.e., ρ), were evaluated at the 95 % significance level.

Table 4-1. Summary statistics of the watershed characteristics associated with the eight outlets monitored for the current study. CV: coefficient of variation (unitless). m.a.s.l: meters above sea level.

	Minimum	Maximum	Mean	Median	CV
Area (km^2)	0.19	74.40	14.18	0.88	1.91
Perimeter (km)	2.84	74.94	20.11	6.94	1.36
Total flowpath length (10^3 km)	11.38	6917.61	1336.40	106.91	1.89
Total stream length (km)	0.23	301.03	51.29	3.67	2.06
Treed riparian area (m^2)	0.00	12.13	2.25	0.06	0.00
Proportion of treed riparian area (-)	0.00	0.16	0.08	0.07	0.84
Mean elevation (m.a.s.l)	429.04	486.83	469.92	477.53	0.04
Elevation range (m)	12.00	190.00	63.63	41.50	0.97
Mean slope (^{o})	0.96	1.92	1.41	1.35	0.24
Slope range (^{o})	2.13	20.99	7.66	4.97	0.91
Proportion of grassland (-)	0.01	0.14	0.10	0.11	0.50
Proportion of coniferous plants (-)	0.00	0.00	0.00	0.00	2.01
Proportion of deciduous plants (-)	0.02	0.23	0.13	0.14	0.51
Proportion of crops (-)	0.59	0.91	0.71	0.67	0.17
Proportion of forest land (-)	0.02	0.23	0.13	0.14	0.51
Proportion of wetlands (-)	0.00	0.01	0.00	0.00	1.58
Proportion of coarse-grained soils (-)	0.00	0.38	0.07	0.00	2.08
Proportion of fine-grained soils (-)	0.00	0.00	0.00	0.00	0.00
Proportion of organic soils (-)	0.00	0.00	0.00	0.00	0.00
Proportion of till blanket (-)	0.00	1.00	0.56	0.72	0.86

4.3 Results

4.3.1 Metrics of water age or MTT

There was a marked difference in results generated by the damping ratio method using the 2014 versus 2015 data: irrespective of the tracer used, water arriving at the monitored outlets in 2014 appeared younger (i.e., high damping ratio values) compared to 2015 (Figure 4-4). The only exception was the HWY240 outlet for which results from both years were similar. This observation, which suggests nonstationarity in the hydrologic regime prevailing in 2014 and 2015 at all sites except HWY240, was

consistent with results obtained via the young water fraction method (Figure 4-5). When using $\delta^{18}O$ data, the young water fraction method showed that with the exception of the HWY240 and MS1 sites, the water arriving at the outlets was younger in 2014 compared to 2015. When using $\delta^{2}H$ data, results were only slightly different: water at the MS1 outlet in 2015 was younger than that in 2014, while at the Miami outlet, the young water fractions were comparable between the two years (Figure 4-5). In general, the fraction of young water arriving at the outlets based on the 2014 $\delta^{18}O$ data was higher than 0.5, except for MS1 and HWY240 (Figure 4-5).

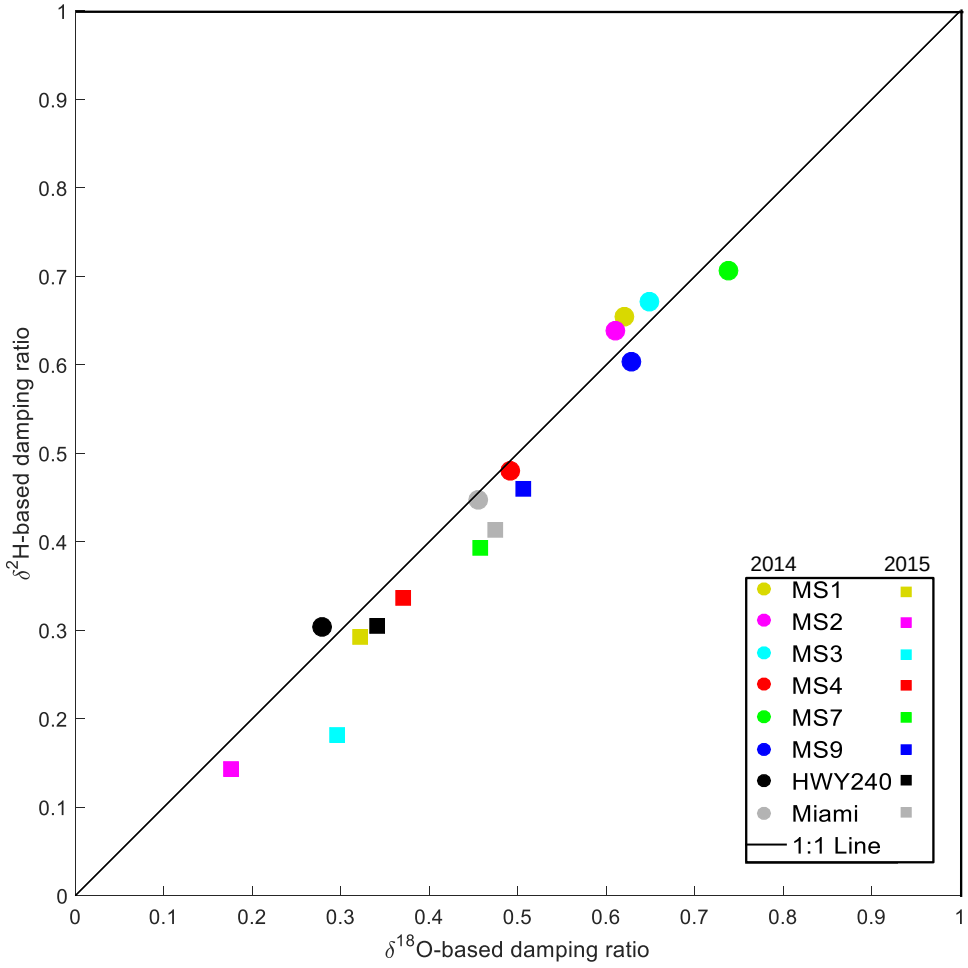

Figure 4-4. Damping ratio values based on 2014 and 2015 data for the eight outlets targeted in this study. Results based on $\delta^{18}O$ versus $\delta^{2}H$ data are compared relative to the 1:1 line (solid black diagonal line).

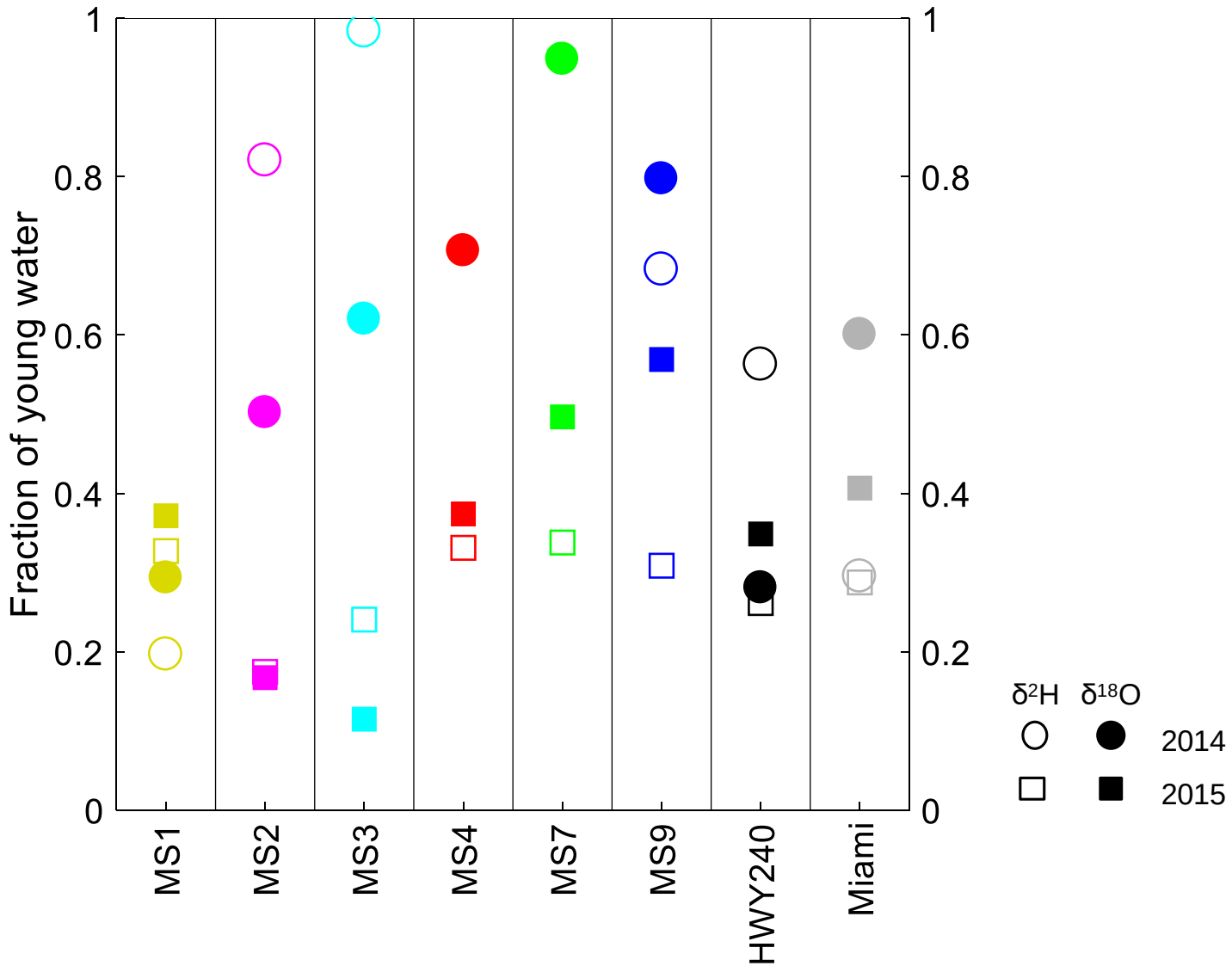

Figure 4-5. Estimated young water fractions after sine-wave modeling, based on 2014 (circles) and 2015 (squares) data for the eight outlets targeted in the current study. The use of δ^2H data in 2014 resulted in a higher amplitude in streamflow (A_s) compared to precipitation (A_p) at sites MS4 and MS7 and hence, there were no δ^2H-based results for those two sites.

4.3.2 MTT modeling

The average coefficients of determination (R^2mean) resulting from the sine-wave modeling of the 2014 precipitation and streamwater $\delta^{18}O$ and δ^2H data were similar: 0.50 and 0.56 for $\delta^{18}O$ and δ^2H in precipitation, respectively, and 0.83 and 0.81 for the same tracers in streamwater (see appendices C-1, C-2, and C-3). In 2015, R^2mean for the sine-wave modeling of $\delta^{18}O$ and δ^2H data were 0.71 and 0.69 for the precipitation data, and 0.61 and 0.64 for the streamwater data (appendices C-2 and C-4). In general, the goodness-of-fit estimates for the 2014 streamwater data were better than those for the 2015 streamwater data. When it comes to the precipitation data, however, the goodness-of-fit estimates were better in 2015. Results from the sine-wave modeling showed that, with the exception of the MS1 and HWY240 outlets, MTTs estimated based on 2014 data were shorter than those estimated based on 2015 data, irrespective of tracer choice (Tables 4-2 and 4-3). In general, sine-wave modeling results for either 2014 or 2015 data suggested that MTTs were less than one year for all of the eight watersheds (Tables 4-2 and 4-3). The uncertainty surrounding those estimates was, however, not negligible.

Table 4-2. Computed MTTs (in days) using the SW and TBC modeling methods and young water fractions at the outlets during the 2014 sampling year. 'n/a': results are not available either due to $A_s > A_p$ (SW method) or due to non-behavioral model parameters (TBC method). Associated uncertainties are also shown in rectangular brackets.

	SW				*TBC*				F_{yw}			
Site	**$\delta^{18}O$ data**	**[min, max]**	**$\delta^{2}H$ data**	**[min, max]**	**$\delta^{18}O$ data**	**[min, max]**	**$\delta^{2}H$ data**	**[min, max]**	**$\delta^{18}O$ data**	**[min, max]**	**$\delta^{2}H$ data**	**[min, max]**
MS1	189	[179, 219]	289	[240, 654]	550	[109, 1432]	482	[43, 1194]	0.29	[0.26, 0.31]	0.20	[0.09, 0.24]
MS2	100	[69, 117]	40	[52, 114]	1156	[1, 2794]	507	[1, 20110]	0.50	[0.44, 0.64]	0.82	[0.74, 1.08]
MS3	73	[52, 86]	10	[2, 49]	62	[22, 130]	47	[16, 110]	0.62	[0.56, 0.74]	0.98	[0.76, 1.67]
MS4	58	[36, 67]	n/a	[n/a]	115	[67, 981]	58	[5, 536]	0.71	[0.65, 0.85]	n/a	[n/a]
MS7	19	[18, 36]	n/a	[n/a]	509	[1, 1701]	158	[1, 2016]	0.95	[0.85, 1.20]	n/a	[n/a]
MS9	44	[43, 64]	62	[29, 77]	288	[1, 499]	157	[2, 2037]	0.80	[0.67, 1.1]	0.68	[0.60, 0.89]
HWY240	198	[144, 214]	85	[71, 114]	0.07	[0, 342]	n/a	[n/a]	0.28	[0.26, 0.37]	0.56	[0.40, 0.57]
Miami	77	[48, 93]	187	[164, 199]	95	[22, 921]	95	[36, 1273]	0.60	[0.53, 0.77]	0.30	[0.28, 0.33]

Table 4-3. Computed MTTs (in days) and young water fractions at the outlets during the 2015 sampling year. 'n/a': results are not available due to non-behavioral model parameters (TBC method). Associated uncertainties are also shown in rectangular brackets.

	SW				*TBC*				F_{yw}			
Site	**δ^{18}O data**	**[min, max]**	**δ^{2}H data**	**[min, max]**	**δ^{18}O data**	**[min, max]**	**δ^{2}H data**	**[min, max]**	**δ^{18}O data**	**[min, max]**	**δ^{2}H data**	**[min, max]**
MS1	145	[132, 173]	167	[161, 181]	n/a	[n/a]	n/a	[n/a]	0.37	[0.32, 0.40]	0.33	[0.30, 0.34]
MS2	342	[204, 663]	328	[263, 635]	n/a	[n/a]	n/a	[n/a]	0.17	[0.16, 0.27]	0.17	[0.09, 0.22]
MS3	503	[234, 404]	234	[202, 340]	n/a	[n/a]	n/a	[n/a]	0.11	[0.10, 0.24]	0.24	[0.17, 0.28]
MS4	144	[136, 161]	165	[164, 168]	n/a	[n/a]	n/a	[n/a]	0.37	[0.33, 0.39]	0.33	[0.32, 0.34]
MS7	101	[87, 140]	162	[149, 196]	n/a	[n/a]	n/a	[n/a]	0.50	[0.38, 0.55]	0.34	[0.28, 0.36]
MS9	84	[66, 92]	179	[156, 274]	n/a	[n/a]	n/a	[n/a]	0.57	[0.53, 0.66]	0.31	[0.20, 0.35]
HWY240	156	[125, 173]	214	[210, 225]	n/a	[n/a]	n/a	[n/a]	0.35	[0.31, 0.42]	0.26	0.24, 0.27]
Miami	130	[126, 141]	193	[175, 201]	n/a	[n/a]	n/a	[n/a]	0.41	[0.38, 0.42]	0.29	[0.27, 0.31]

While behavioral results were obtained for all sites through the time-based convolution modeling of the 2014 $\delta^{18}O$ data, such was not the case for site HWY240 when the 2014 $\delta^{2}H$ data were used (Table 4-2; Figures 4-6a, b; appendices C-5 and C-6). For that year, a minimum NSE of 0.49 for the $\delta^{18}O$-based modeling was obtained at site MS4, while a maximum of 0.99 was obtained for HWY240. When $\delta^{2}H$ data were used, rather, the minimum and maximum NSE values of 0.13 (non-behavioral) and 0.85 were recorded at sites HWY240 and MS9, respectively (Table 4-2 and Table 4-4). The variations in the α and β parameter values across the sites (Appendix C-7) are reflected in the shapes of the TTDs (Figures 4-6a, 4-6b): sites with higher α values were associated with higher probabilities of shorter transit times (e.g., MS3), while sites with higher β values were more likely to have longer transit times (e.g., MS2). For each outlet, a CTTD was plotted based on the 2014 $\delta^{18}O$ and $\delta^{2}H$ data: Figures 6c and 6d notably show that at least 50 % of the precipitation input travelled to all outlets in one year or less. Over 40 % of precipitation input travelled to seven outlets (i.e., all but MS1) in three months or less (Figure 4-6c). According to the estimated CTTD, all of the input water would pass through the catchment outlet at HWY240 within one or two time steps or almost immediately (Figure 4-6c). In general, estimated proportions of precipitation input arriving at the outlets within a specified time period were higher when 2014 $\delta^{2}H$ data were used, as opposed to 2014 $\delta^{18}O$ data (Figures 4-6c, 4-6d). With the use of $\delta^{18}O$ data, the proportion of precipitation input arriving at outlets MS2 (in comparison to MS1) and MS7 (in comparison to MS9) appeared to be higher during the first six months but the trend changed thereafter, with higher proportions of water arriving at outlets MS1 and MS9 (Figure 4-6c). This phenomenon also appeared to be present for the MS1/MS2 and MS7/MS9 pairs of sites when $\delta^{2}H$ data were used (Figure 4-6b). Non-negligible uncertainty was associated with time-based

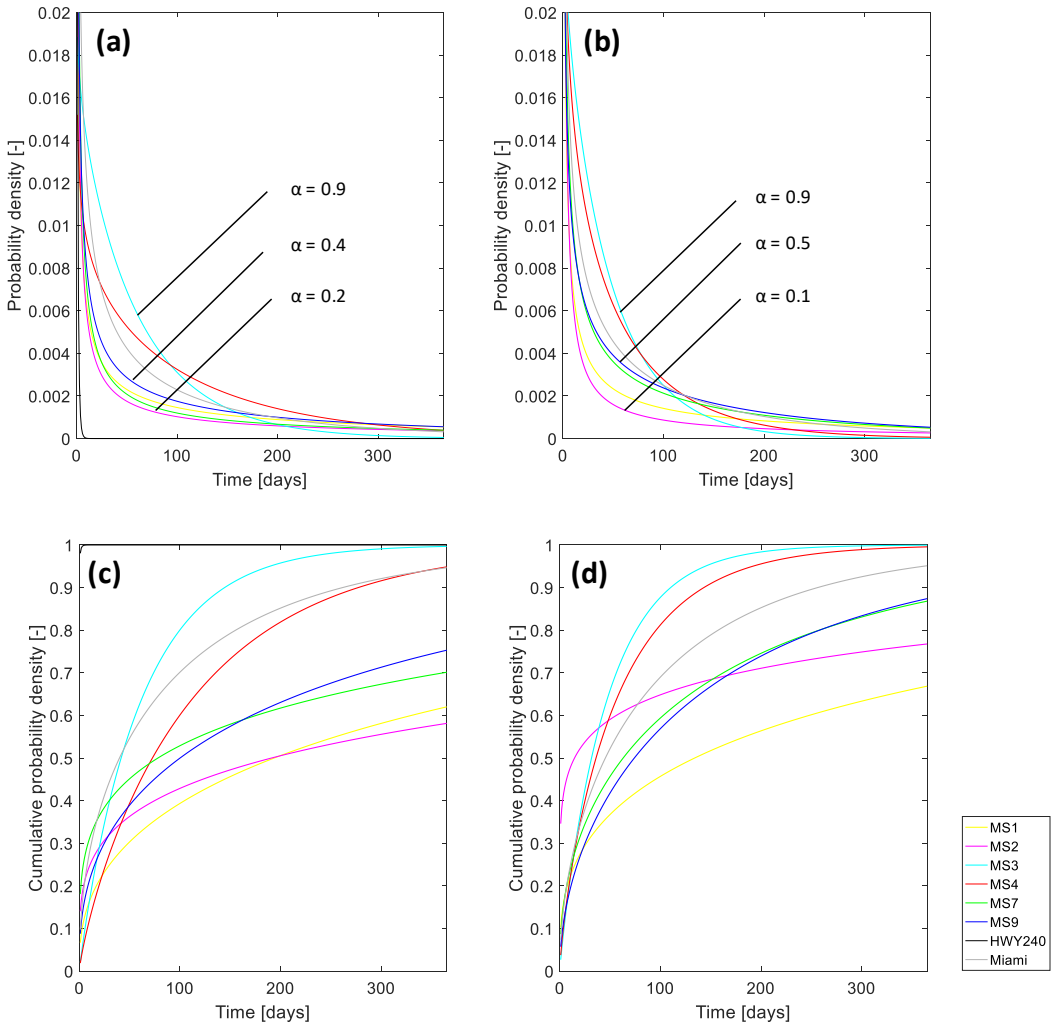

Figure 4-6. Transit time distributions (TTDs, panels a and b) and cumulative transit time distributions (CTTDs, panels c and d) estimated via time-based convolution modeling based on 2014 $\delta^{18}O$ data (panels a and c) and 2014 $\delta^{2}H$ data (panels b and d). CTTDs (and TTDs) are plotted as (cumulative) probability density functions. Please note that the TTD and CTTD for the HWY240 outlet coincide with the axes in panels (a) and (c) due to the relatively short MTT (in the order of hours). The TTD and CTTD for that site are absent from panel (b) and (d) due to the lack of behavioral model parameters for that site when using 2014 $\delta^{2}H$ data. The range of α values for panel (a) is 0.04 – 0.93, while that for panel (b) is 0.14 – 0.92.

convolution modelling results in 2014 (Table 4-2). As for the use of 2015 data for time-based convolution modeling, it did not lead to any behavioral model parameters (Table 4-3).

Table 4-4. Alpha and beta parameters associated with the MC simulation with the highest NSE value after TBC modeling based on 2014 data. 'n/a': results are not available due to non-behavioral model parameters.

		MS1	MS2	MS3	MS4	MS7	MS9	HWY240	Miami
Alpha	$\delta^{18}O$ data	0.39	0.24	0.93	0.82	0.23	0.39	0.04	0.46
	$\delta^{2}H$ data	0.32	0.13	0.92	0.77	0.43	0.52	0.84	0.52
Beta	$\delta^{18}O$ data	1409	4748	66	140	2163	745	2	207
	$\delta^{2}H$ data	1477	3701	50	73	363	300	123	182
NSE	$\delta^{18}O$ data	0.69	0.79	0.51	0.49	0.72	0.93	0.99	0.71
	$\delta^{2}H$ data	0.79	0.71	0.60	0.69	0.73	0.85	n/a	0.66

4.3.3 Comparison across sites

Since the year 2014 was the only one for which all four MTT estimation methods could be successfully applied across the majority of sites and with both tracers, site rankings were only established for that year. Sites HWY240 and MS7 had the longest and shortest MTT (and oldest and youngest water), respectively, according to three out of the four methods applied to $\delta^{18}O$ data; those three methods (damping ratio, young water fraction and sine-wave modeling) happen to be the ones known for their ability to model coarse and irregularly spaced isotopic data (Figure 4-7a). These results are in agreement with the 2014 $\delta^{2}H$-based damping ratio method but not with the 2014 $\delta^{2}H$-based sine-wave method: the longest MTT was then detected at MS1 rather than HWY240 (Figure 4-7b). The 2014 $\delta^{18}O$-based time-based convolution modeling results show that the shortest MTT (of about three hours) was recorded at the HWY240 outlet, while the longest (of

about three years) was at the MS2 outlet (Table 4-2, Figures 4-7a, b). Outlet MS3 recorded the highest proportion of young water and shortest MTT when using the young water fraction, sine-wave, and time-based convolution modeling methods with δ^2H data (Figure 4-7b).

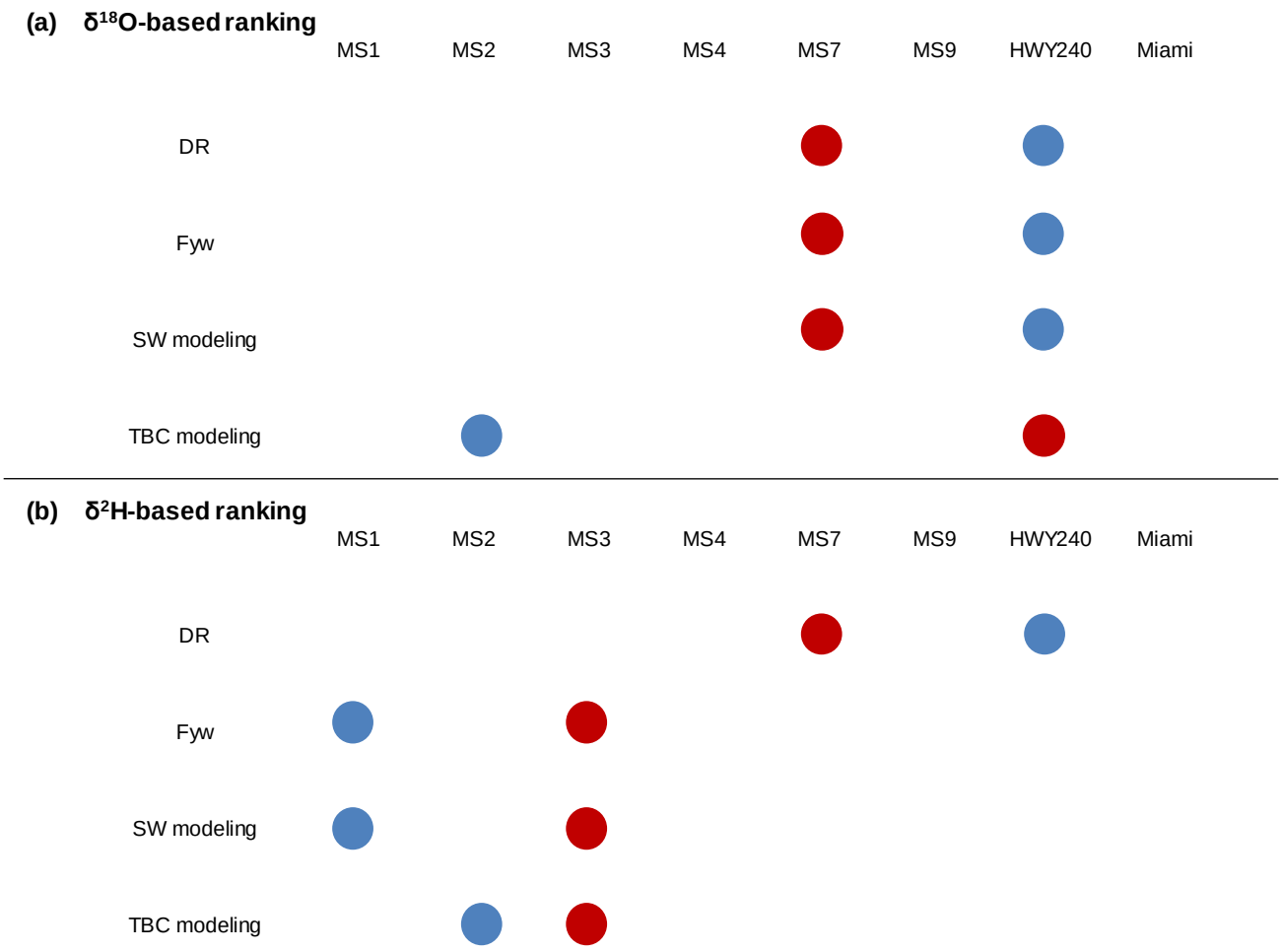

Figure 4-7. Watershed and sub-watershed outlets associated with the slowest (blue circles) and the fastest (red circles) water storage and release dynamics based on the results of two MTT metrics (damping ratio and young water fraction) and two MTT modeling methods (sine-wave and time-based convolution). Rankings are shown for: (a) $\delta^{18}O$ data, (b) δ^2H data acquired during the 2014 sampling year.

That observation at MS3 is confirmed in Figure 4-6a where at shorter transit times, high proportions of input precipitation arrive at the site. The proportion of precipitation input arriving at each of the outlets in three months or less was extracted from the CTTDs and compared with the young water fraction: there was no statistically significant correlation between time-based convolution derived young water fraction and young water fraction resulting from sine-wave fitting (Figures 4-8 and 4-9). There was, however, a statistically significant correlation between $\delta^{18}O$-based and $\delta^{2}H$-based time-based convolution MTT modeling results ($\rho = 0.96$; Figure 4-9). Statistically significant negative correlations were found between the $\delta^{18}O$ and $\delta^{2}H$-based sine-wave modeling results and the young water fraction metric ($\rho = -1.00$; Figure 4-9). $\delta^{18}O$-based time-based convolution MTT modeling results were also negatively correlated with the time-based convolution-derived young water fraction ($\rho = -0.81$; p-value = 0.02). Regarding the predictability of MTT estimates from physiographic data, there was no statistically significant correlation between $\delta^{18}O$ and $\delta^{2}H$-based time-based convolution or sine-wave modeling results and any of the watershed characteristics listed in Table 4-1. There was also no statistically significant correlation between watershed drainage area and $\delta^{18}O$- or $\delta^{2}H$-based damping ratio values, nor between watershed drainage area and $\delta^{18}O$- and $\delta^{2}H$-based young water fractions. There were, however, statistically significant correlations between the elevation range and the amount of treed riparian areas present in each watershed and $\delta^{18}O$- and $\delta^{2}H$-based DR values ($\rho \geq 0.74$).

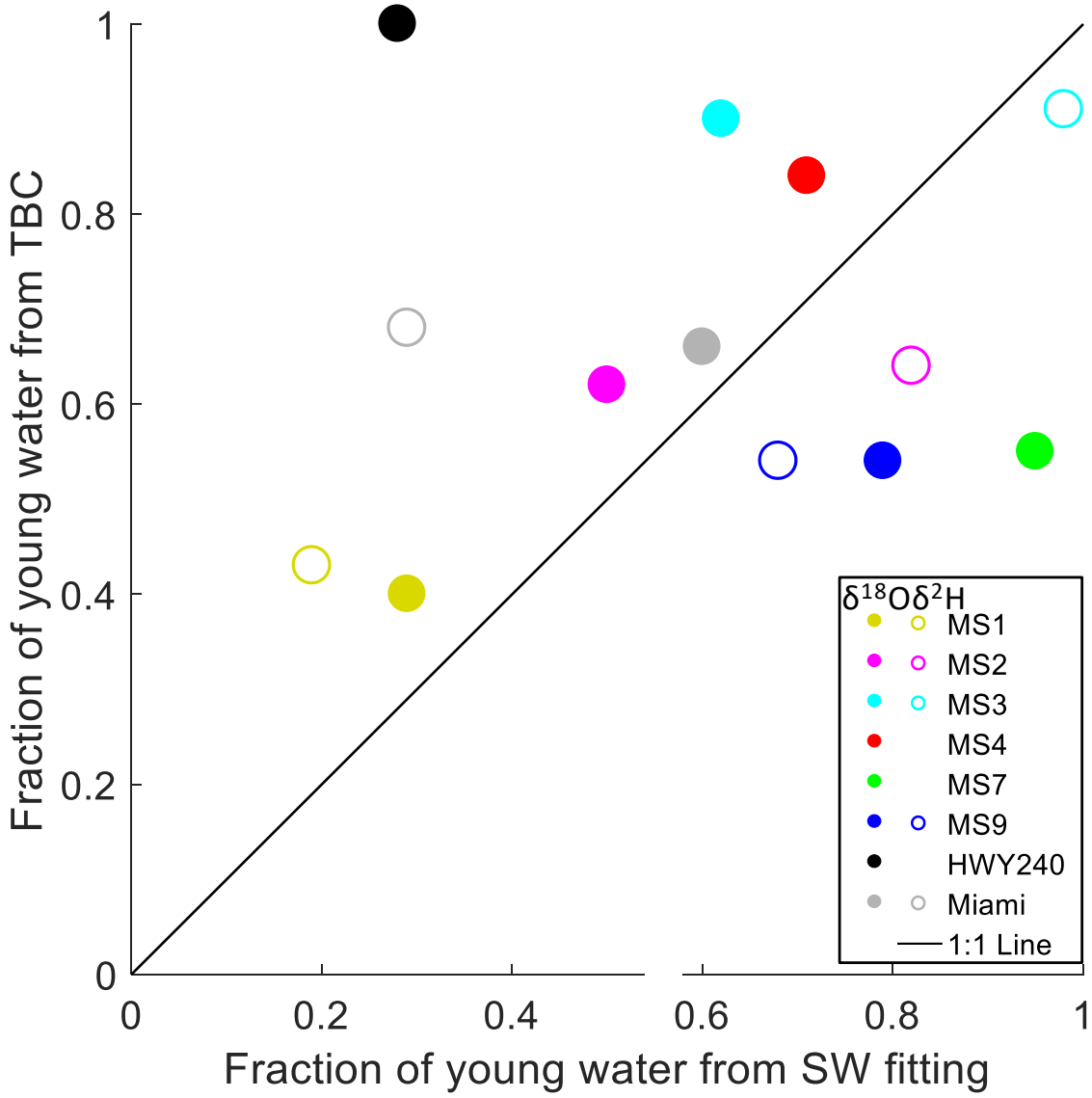

Figure 4-8. Comparison of sine-wave-derived young water fractions and time-based convolution -derived young water fractions based on 2014 $\delta^{18}O$ and $\delta^{2}H$ data for the eight studied outlets. $\delta^{2}H$-related results are not shown for sites MS4 and MS7 as young water fractions could not be computed (i.e., $A_s > A_p$). There were no behavioral model parameters generated via the TBC modeling of site HWY240 using the 2014 $\delta^{2}H$ data.

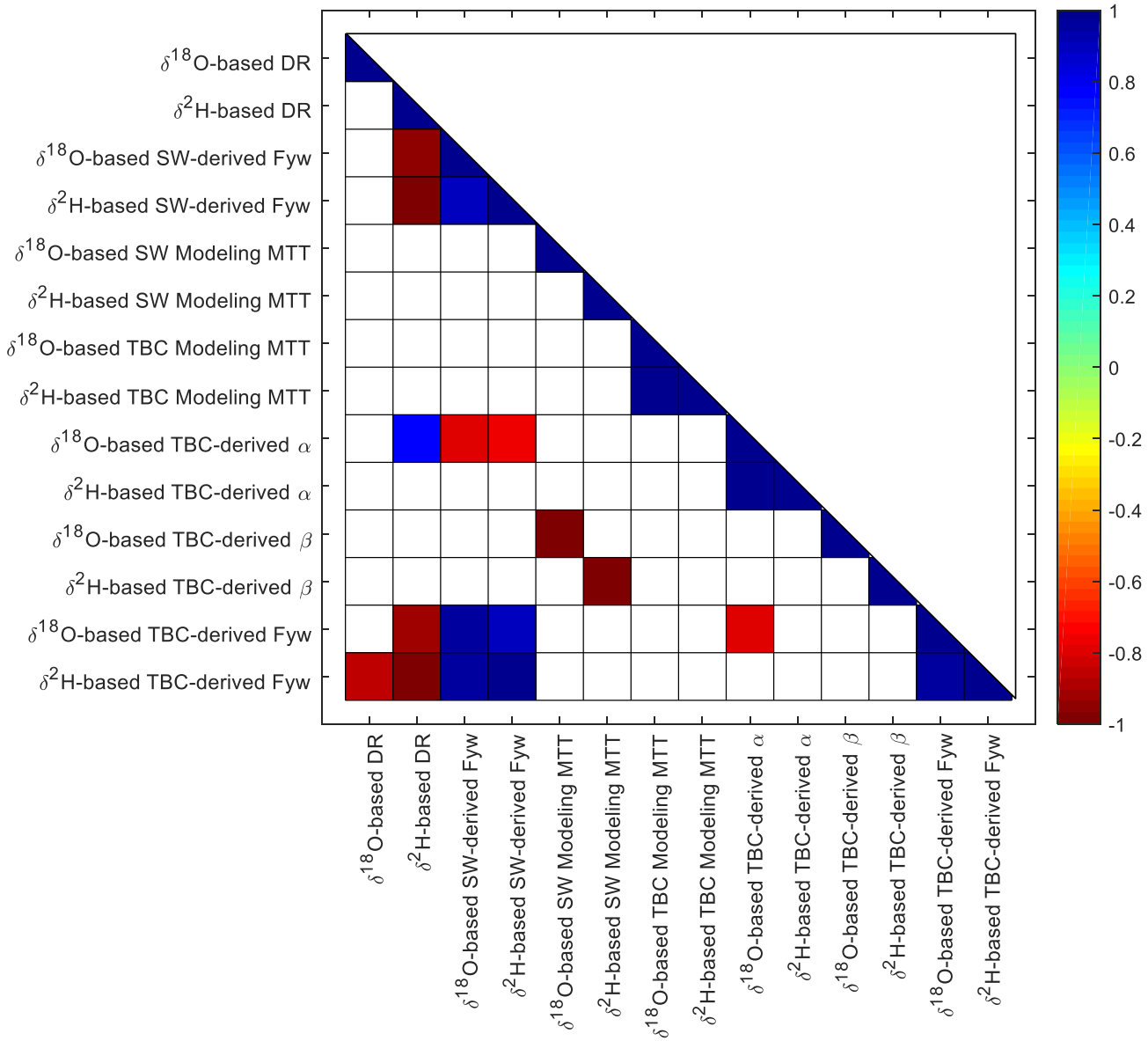

Figure 4-9. Correlation matrix showing the relation (or lack thereof) between MTT metrics, MTT modeled values and other model parameters. Blank cells signal Spearman's rank correlation coefficients that were not statistically significant at the 95% level.

4.4 Discussion

4.4.1 Physical realism of MTT estimates in light of dominant flow processes

Previous research in our study catchment mostly relied on hydrometric and water quality data as well as hydrogeological information and led to different hydrologic conceptualizations of dominant flow processes in the main physiographic units (refer to section 2.1). Here one goal was to confront those previously established conceptualizations to the MTT and water-age related estimates resulting from the present work. The generally larger fractions of "young" water and relatively shorter MTTs at most of the outlets in 2014 compared to 2015 (see Figures 4-4, 4-5; Tables 4-2, 4-3) are consistent with the climatic and hydrologic conditions experienced during the wet 2014 year and the relatively drier 2015 year. Even though Hortonian overland flow was present at the majority of the sites during the early spring periods of both years, two extreme and persistent rainstorm events in June and July of 2014 mobilized significant amounts of "young" water to the outlets via saturation excess overland flow (Bansah and Ali, 2017). When the damping ratio, young water fraction and sine-wave methods were applied, MTTs estimated from 2014 data were shorter than those estimated from 2015 data, irrespective of tracer used, for all but two outlets (see Tables 4-2, 4-3 and Figures 4-4, 4-5). The two exceptions to that rule were MS1, which marks the beginning of the channel in the STCW headwaters, and HWY240, for which similar MTT estimates were obtained for both 2014 and 2015. Comparisons between 2014 and 2015 couldn't be made with the time-based convolution method because of the non-behavioral parameters obtained for the relatively drier year. According to the damping ratio, young water fraction and sine-wave methods, the largest fraction of "young" water and the shortest MTT were recorded at site MS7 based on the 2014 data. The frequently observed overtopping of the retention dam at

MS7 - due to snowmelt and subsequent storm events in June and July 2014 - make the fraction of "young" water and MTT results for this site plausible. The time-based convolution modeling results were rather contrary to those obtained via the other three methods: they suggested that the MS7 site had one of the longest MTTs amongst all the eight outlets in 2014, while the shortest MTT was assigned to the HWY240 outlet (Table 4-2). The invariance of the results obtained using the damping ratio, young water fraction and sine-wave methods for site HWY240 in 2014 versus 2015 (Tables 4-2 and 4-3; Figures 4-4 and 4-5) supports the hydrologic conceptualization previously established for this site (refer to section 2.1) and according to which this outlet is perennially fed by the same source of water, likely passive stores of deep, "old" groundwater (Pearce, Stewart and Sklash, 1986). This hydrologic conceptualization was also confirmed through isotope-based hydrograph separations, which identified consistently high proportions of "old" water at HWY240 throughout 2014 (Bansah and Ali, 2017).

4.4.2 Landscape controls on MTT estimates

Statistically significant positive correlations were found between $\delta^{18}O$- and $\delta^{2}H$-based damping ratio values and both elevation range and treed riparian area watershed characteristics. Those correlations make sense from a physical standpoint. In spring, meltwater is quickly transported to outlets via Hortonian overland flow (aided by the elevation changes) into the "MS" outlets, while water from newly thawed ground in forested riparian areas is routed to streams via shallow subsurface flow. During intense storm events later in the year, plant water uptake in the treed riparian zones plays a role in the storage and release of young water via saturation excess overland flow to the streams, while elevation changes help drive water quickly into the streams,

especially in the “MS” undulating watersheds. It is believed that at the “MS” sites, plough pan development resulting from agricultural activities decrease the likelihood of deep water infiltration (Tekleab et al., 2014b), especially during the growing season. This hypothesis was corroborated by the CTTDs (Figures 4-6c, 4-6d) which show that at least 40 % of input precipitation reached the ‘MS’ outlets within 3 months. Vegetation cover has been shown to exhibit significant positive correlation with the young water fraction metric (e.g., Song et al., 2016 in a study at a permafrost dominated catchment within the Qinghai-Tibet Plateau); however, no such correlation was found across the STCW. Results from the current study didn’t reveal any significant correlation between any MTT estimates and watershed area, which is aligned with some findings reported in the literature (e.g., McGlynn et al., 2003; McGuire et al., 2005; Rodgers et al., 2005). The lack of significant correlations between MTT estimates and watershed characteristics related to land use, surficial geology, flowpath length or slope indirectly points to the fact that bedrock geology is one of the major controls on MTT in the study area.

4.4.3 Agreement (or lack thereof) between metrics and models of water age or MTT

Since the young water fraction was shown to be less liable to aggregation bias (see Kirchner, 2016a) even within heterogeneous systems fed by different proportions of water of dissimilar ages (see Stewart et al., 2017), it has gained some traction as a water age metric (e.g., Song et al., 2016). The apparent convergence in results between the young water fraction and damping ratio methods over the two years considered in this study (Figure 4-7) also suggests that the damping ratio method may indeed be useful for a quick approximation of MTTs (Soulsby and Tetzlaff, 2008). The 2014 $\delta^{18}O$-based MTT results from the sine-wave modeling method (Table

4-2) were in agreement with results from the young water fraction and damping ratio methods for the HWY240 and MS7 sites, in terms of MTT rankings (Figure 4-7a). The time-based convolution method, however, was divergent in that it assigned the shortest MTT to the HWY240 site (Figure 4-7a). Given that the time-based convolution is usually known to be the most adaptable at modeling datasets spanning many several seasonal cycles (McGuire and McDonnell, 2006), it may not be the most appropriate to estimate MTTs based on sparse data in the STCW. Indeed, sampling frequency, data length, and their associated implications for inter-catchment comparison of MTT results have been the subject of many discussions (e.g., McGuire and McDonnell, 2006; Hrachowitz et al., 2009a, 2010b; Hrachowitz et al., 2011). When only short data records are available, and/or when the MTT is suspected to be longer than the actual data record length, modeling errors stem from the non-recovery of all the tracer mass at the end of the calibration process. Gaps in input data record have been artificially filled or extended by various means, one of which is a sine-wave approximation technique (McGuire et al., 2002; Rodgers et al., 2005). In the current study, we made a backward extension of data records according to a "loop scenario" (*sensu* Hrachowitz et al., 2011) to generate long enough warm-up periods, this solely for time-based convolution modeling. This was done to avoid the consequences of potentially averaging out peak tracer concentrations over the sampling interval and to minimize modeling error (Hrachowitz et al., 2011), especially when low sampling frequencies were present – which was particularly the case for the headwater sites (i.e., MS1 and MS2). From an anecdotal standpoint, some of our sine-wave modeling results (see appendices C-1 to C-4) suggested that over our short open-water seasons of approximately six months, the captured isotopic cycles did not always follow or cover a full sine-wave cycle, an observation aligned with those made in other prairie watersheds by Jasechko et al., (2017). In addition, for HWY240 in 2014 and 2015, the peak

amplitude in the streamwater isotopic signal preceded the peak amplitude in the current-year precipitation isotopic signal (appendices C-1 and C-4, panel g), which may have led to uncertain or inaccurate MTT estimates for that site. One plausible explanation would be that the streamwater isotopic signal at that site reflects previous-year water inputs rather than current-year water inputs, a hypothesis aligned with the hydrologic conceptualization of groundwater discharge being dominant at this site. In our study, however, we did not have enough information to answer critical questions such as: (i) what is the minimum number of data points required to yield reasonable MTT estimates? or (ii) how may observational errors affect the computed MTT estimates? It is worth noting that while a NSE threshold criterion was used to categorize parameter sets as behavioral or non-behavioral and hence discard the lowest-performing parameter sets, a similar strategy was not applied to sine-wave modeling. However, apart from the 2015 streamwater fits for sites MS2 and MS3 (see appendix C-2, panels b and c) which had an R^2 of 0.2, all other sites had R^2 above 0.4, which means that very few sine-wave modeling results would have been discarded if an R^2 threshold criterion of 0.4 or less had been used to parse out "acceptable" results. Timbe et al. (2014) suggested that for catchments with MTTs that are known or suspected to be longer than nine weeks, hydrologists should at least employ two or more models for purposes of intercomparison, since results usually diverge in catchments with longer MTTs. Following their recommendations, we performed an intercomparison of four different methods, three of which gave convergent results for two key sites with unique water storage and release characteristics (i.e., MS7 and HWY240). The lack of significant correlation between time-based convolution-derived young water fraction values and sine-wave-derived young water fraction values (Figures 4-8 and 4-9), however, reinforces the idea that the time-based convolution method may not be appropriate when only sparse data records are available.

4.4.4 Influence of tracer choice on MTT estimates

It has always been thought that using $\delta^{18}O$ and $\delta^{2}H$ together to model a system provides redundant information. For instance, Stockinger et al. (2014) relied on both $\delta^{18}O$ and $\delta^{2}H$ to estimate MTTs in a humid temperate forested catchment in Germany; they ended up using only $\delta^{18}O$ in their analysis, even though several of their precipitation and streamwater isotopic signatures plotted off the meteoric water line – possibly as a result of isotopic fractionation effects (which are known to affect $\delta^{2}H$ data more). Timbe et al. (2014) also estimated MTTs in a San Francisco tropical mountain cloud forest catchment: only $\delta^{18}O$ was used, even though $\delta^{2}H$ was also measured. While collinear $\delta^{18}O$ and $\delta^{2}H$ behavior is typically assumed to exist, some studies have argued that modeling done using both tracers can help in inferring results acceptability in light of fractionation processes (e.g., McGuire and McDonnell, 2006). In the current study, the comparison of absolute MTT estimates between the $\delta^{18}O$- and $\delta^{2}H$-based applications of the time-based convolution and sine-wave methods in 2014 (see Table 4-2) showed that process interpretation can differ depending on tracer choice (Figures 4-7a, b). The only agreement in results between the two tracers was the ranking of the watersheds using the damping ratio method: both tracers assigned the longest and shortest MTT to sites HWY240 and MS7, respectively (Figure 4-7). Conversely, when it comes to the ranking of these two sites using the young water fraction, sine-wave and time-based convolution methods, there were some inconsistencies between the results obtained using $\delta^{18}O$ versus $\delta^{2}H$ (Figure 4-7). Timbe et al. (2014) made the assumption that MTT estimations would be similar with the use of any of $\delta^{18}O$ or $\delta^{2}H$. This assumption was however not fully confirmed in the current study: $\delta^{18}O$-based MTT results were strongly correlated with $\delta^{2}H$-based MTT results (when a correlation analysis by ranks was performed), but the

absolute MTT results obtained using each tracer were quite different (Table 4-2; Figure 4-9). The differences in results generated by the two tracers are likely attributable to the strong evaporative processes (see d-excess values in Figure 4-3) in the study area, resulting in preferential fractionation of hydrogen isotopes in the water. In a hydrograph separation study conducted for the same watershed outlets as the current study, uncertainties associated with the δ^2H-based results were generally also higher – especially in the summer and fall seasons (Bansah and Ali, 2017), thus hinting that tracer choice is critical for any isotope-based investigation conducted in seasonally cold and dry watersheds. In the current study, the comparison of the uncertainties associated with the MTT and water age results suggests that more constrained estimates (i.e., narrower uncertainty ranges) can be obtained using $\delta^{18}O$ (Tables 4-2 and 4-3). It should, also, be noted that the assumption of a "one year" annual cycle fit for our data may have underestimated the amplitudes of both the input precipitation (A_p) and the output streamflow (A_s) as far as sine-wave methods are concerned, but A_s and A_p estimates were likely affected by fractionation effects – albeit not in equal proportions. Since the amplitudes are used in the form of ratios for both the SW and F_{yw} methods, the uncertainties provided in Tables 4-2 and 4-3 may be helpful in making a decision on tracer choices for that particular region.

4.5 Conclusion

Four MTT estimation methods were applied on precipitation and streamwater stable isotopic data ($\delta^{18}O$ and δ^2H) across eight nested outlets within a prairie watershed, the South Tobacco Creek Watershed (STCW). The watershed encompasses contrasting physiographic characteristics with six of the monitored outlets located in a undulating terrain, one along the edge

of a fractured escarpment, and one in flat land. MTTs were derived separately based on data collected in a wet year (2014) and a relatively drier year (2015) for comparison purposes, so as to assess the ability of the different estimation methods to handle various degrees of sparse isotopic timeseries reflective of non-perennial flow conditions. Generally, fractions of young water and MTTs above the escarpment were, respectively, higher and shorter than those estimated atop the escarpment and on flat land. When it comes to "wet year" versus "drier year" differences, young water fractions and MTT values were higher and shorter in 2014, compared to 2015. Results obtained from the MTT and water age metrics (i.e., damping ratio and young water fraction) provided similar MTT ranking information for two of the monitored sites. One of the MTT modeling methods, i.e., the sine-wave method, was in agreement with the metrics while the other, the time-based convolution method, was not. The time-based convolution method failed to result in any behavioral parameters when applied to the drier 2015 year, thus highlighting its inadequacy with very sparse timeseries data coupled with dry antecedent conditions. The application of each method with $\delta^{18}O$ versus $\delta^{2}H$ data also led to different absolute values of young water fraction, damping ratio and modeled MTT, even though tracer-specific MTT values estimated via the time-based convolution method were positively correlated with one another. In terms of landscape controls on MTTs, strong influences of treed riparian area and watershed elevation range on streamwater isotopic damping were detected, while watershed area and slope were found to be non-influential. A qualitative comparison of MTT estimates across different watershed units suggested that bedrock geology, rather than surficial geology, surface topography or land use, is a major control of MTTs. Regarding the relative adequacy of MTT metrics versus modeling methods for sparse data, the damping ratio, young water fraction and sine-wave methods were easiest to apply and produced results that were aligned with flow process conceptualizations in the STCW.

Additional research into MTT estimation methods is certainly warranted across the prairies, preferably in areas where anecdotal knowledge or prior conceptualizations of dominant flow processes exist, and data spanning contrasted years are available, in order to confirm or infer the results from the current study. More advanced MTT estimation methods, such as StorAge Selection functions, could also be tested. In the meantime, we recommend that for the prairies in general and the STCW in particular, the damping ratio, young water fraction and sine-wave methods be preferentially chosen for MTT estimation because they handled sparse isotopic timeseries the best and also provided physically realistic results in both wet and drier conditions. We also suggest that $\delta^{18}O$ and $\delta^{2}H$ be used concurrently to further investigate potential fractionation-related issues and link them to evaporation dynamics. Such recommendations will ensure that until more research results become available, first-order approximations of MTTs can still be obtained. These first-order approximations can help inform land management activities related to the preservation of treed riparian buffers, the temporary detention of water in farm ponds or the timing of fertilizer applications: while the first two activities are likely to affect watershed storage and release dynamics, the third one can lead to acute water quality issues if contaminants reach the flowpaths via which most of the watershed storage release occurs.

4.6 Acknowledgments

We acknowledge the support of the first author through a University of Manitoba Graduate Fellowship**.** We also acknowledge the financial support made available by the Natural Sciences and Engineering Research Council of Canada (NSERC) through a Discovery Grant awarded to Dr. Genevieve Ali. The authors thank Nicole Pogorzelec, Aminul Haque, Adrienne Schmall, Janelle

Laing, Marcos Lemes, Don Cruikshank, Kelvin Hildebrandt, Larry Braul, Henry Wilson and Erin Zoski who contributed greatly in site-setup, data collection and laboratory analysis efforts. We also thank Dr. David Lobb for his useful suggestions, as well as the guest editors and three anonymous reviewers for their very constructive comments that helped improve this manuscript.

4.7 References

Bansah, S., & Ali, G. (2017). Evaluating the effects of tracer choice and end-member definitions on hydrograph separation results across nested seasonally cold watersheds. Water Resources Research, 53, doi.org/10.1002/2016WR020252.

Benettin, P., Rinaldo, A., & Botter, G. (2015). Tracking residence times in hydrological systems: forward and backward formulations. *Hydrological Processes, 29*(25), 5203-5213. doi:10.1002/hyp.10513.

Betcher, R., Grove, G. & Pupp, C. (1995). Groundwater in Manitoba: hydrogeology, quality concerns, management; *National Hydrology Research Institute Contribution No. CS-93017*, Environmental Sciences Division, NHRI, Environment Canada, 53 pp.

Bethke, C. M., & Johnson, T. M. (2008). Groundwater age and groundwater age dating. *Annual Reviews of Earth and Planetary Sciences.* 36, 121-152. doi: 10.1146/annurev.earth.36.031207.124210.

Beven, K., & Freer, J. (2001). Equifinality, data assimilation, and uncertainty estimation in mechanistic modelling of complex environmental systems using the GLUE methodology. *Journal of Hydrology, 249*(1-4), 11-29. doi:10.1016/s0022-1694(01)00421-8.

Birkel, C., Soulsby, C., Tetzlaff, D., Dunn, S., & Spezia, L. (2012). High-frequency storm event isotope sampling reveals time-variant transit time distributions and influence of diurnal cycles. *Hydrological Processes, 26*(2), 308-316. doi:10.1002/hyp.8210.

Blaney, H. F., Criddle, W.D. (1962). Determining consumptive use and irrigation water requirements. U.S. Department of Agriculture Research Service Technical Bulletin 1275.

Bliss, E. M. (1970). Frequency multiplication using properties of an angle-modulated wave. *Electronics Letters, 6*(4), 102-&. doi:10.1049/el:19700068.

Brunke, M., & Gonser, T. (1997). The ecological significance of exchange processes between rivers and groundwater. *Freshwater Biology, 37*(1), 1-33. doi:10.1046/j.1365-2427.1997.00143.

Cappa, D. C., Hendricks, B. M., DePaolo, D. J., & Cohen, R. C. (2003). Isotope fractionation of water during evaporation. *Geophysical Research*, 108, D16 (4525), doi: 10.1029/2003JD003597.

Craig, H. (1961). Standard for reporting concentrations of deuterium and oxygen-18 in natural waters. *Science, 133*(346), 1833-&. doi:10.1126/science.133.3467.1833.

Dewalle, D. R., Edwards, P. J., Swistock, B. R., Aravena, R., & Drimmie, R. J. (1997). Seasonal isotope hydrology of three Appalachian forest catchments. *Hydrological Processes, 11*(15), 1895-1906. doi:10.1002/(sici)1099-1085(199712)11:15.

Dincer, T., Payne, B. R., Florkowski, T., Martinec, J., & Tongiorgi, E. (1970). Snowmelt runoff from measurements of tritium and oxygen-18. *Water Resources Research, 6*(1), 110-124. doi:10.1029/WR006i001p00110.

Elliott, J.A., & Efetha, A. A. (1999). Influence of tillage and cropping system on soil organic matter, structure and infiltration in a rolling landscape. *Canadian Journal of Soil Sciences*. 79:457–463.

Environment Canada. (2014). *Canadian climate normals 1981-2014 station data*. Retrieved from http://climate.weather.gc.ca/climate_normals/results_1981_2010_e.html?searchType=stnProv&lstProvince=MB&txtCentralLatMin=0&txtCentralLatSec=0&txtCentralLongMin=0&txtCentralLongSec=0&stnID=3582&dispBack=0

Environment Canada. (2015). *Canadian climate normals 1981-2015 station data*. Retrieved from http://climate.weather.gc.ca/climate_normals/results_1981_2010_e.html?searchType=stnProv&lstProvince=MB&txtCentralLatMin=0&txtCentralLatSec=0&txtCentralLongMin=0&txtCentralLongSec=0&stnID=3582&dispBack=0

Etcheverry, D., & Perrochet, P. (2000). Direct simulation of groundwater transit-time distributions using the reservoir theory. *Hydrogeology Journal, 8*(2), 200-208.

Fang, X., Minke, A., Pomeroy, J., Brown, T., Westbrook, C., Guo, X., & Guangul, S. (2007). A review of Canadian Prairie hydrology: Principles, modelling and response to land use and drainage change (Vol. 2). Saskatoon, Saskatchewan: Centre for Hydrology.

Frisbee, M. D., Wilson, J. L., Gomez-Velez, J. D., Phillips, F. M., & Campbell, A. R. (2013). Are we missing the tail (and the tale) of residence time distributions in watersheds? *Geophysical Research Letters, 40*(17), 4633-4637. doi:10.1002/grl.50895.

Froehlich, K., Gibson, J.J., & Aggarwal, P.K. (2002). Deuterium excess in precipitation and its climatological significance (IAEA-CSP--13/P). International Atomic Energy Agency (IAEA), 34(10), 34017966. 23pp.

Hancock, P. J., Boulton, A. J., & Humphreys, W. F. (2005). Aquifers and hyporheic zones: Towards an ecological understanding of groundwater. *Hydrogeology Journal, 13*(1), 98-111. doi:10.1007/s10040-004-0421-6.

Harman, C. J. (2015). Time-variable transit time distributions and transport: Theory and application to storage-dependent transport of chloride in a watershed. *Water Resources Research, 51*(1), 1-30. doi:10.1002/2014wr015707.

Heidbuechel, I., Troch, P. A., Lyon, S. W., & Weiler, M. (2012). The master transit time distribution of variable flow systems. *Water Resources Research, 48*. doi:10.1029/2011wr011293.

Hrachowitz, M., Bohte, R., Mul, M. L., Bogaard, T. A., Savenije, H. H. G., & Uhlenbrook, S. (2011). On the value of combined event runoff and tracer analysis to improve understanding of catchment functioning in a data-scarce semi-arid area. *Hydrology and Earth System Sciences, 15*(6), 2007-2024. doi:10.5194/hess-15-2007-2011.

Hrachowitz, M., Soulsby, C., Tetzlaff, D., Malcolm, I. A., & Schoups, G. (2010). Gamma distribution models for transit time estimation in catchments: Physical interpretation of parameters and implications for time-variant transit time assessment. *Water Resources Research, 46*. doi:10.1029/2010wr009148.

Hrachowitz, M., Soulsby, C., Tetzlaff, D., Dawson, J. J. C., Dunn, S. M., & Malcolm, I. A. (2009a). Using long term data sets to understand transit times in contrasting headwater catchments. *Journal of Hydrology* **367**: 237–248.DOI: 10.1016/j.jhydrol.2009.01.001.

Hrachowitz M, Soulsby C, Tetzlaff D, Malcolm I.A. 2011. Sensitivity of mean transit time estimates to model conditioning and data availability. Hydrological Processes, 25: 980-990. DOI: 10.1002/hyp.7922.

Hutchinson R. D. (1977). Groundwater resources of Cavalier and Pembina counties, North Dakota. U.S Geological Survey, Bulletin 62 – Part III, 75pp.

Jasechko, S., Wassenaar, L.I., & Mayer, B. (2017). Isotopic evidence for widespread cold-season-biased groundwater recharge and young streamflow across central Canada. *Hydrological Processes* 31: 2196-2209. doi: 10.1002/hyp.11175.

Jasechko, S., Kirchner, J. W., Welker, J. M., & McDonnell, J. J. (2016). Substantial proportion of global streamflow less than three months old. *Nature Geoscience, 9*(2), 126-134. doi:10.1038/ngeo2636.

Kendall, C., & McDonnell, J. J. (1998). *Isotope Tracers in Catchment Hydrology*. Elsevier: Amsterdam, The Netherlands.

Kirchner, J. W. (2016a). Aggregation in environmental systems - Part 1: Seasonal tracer cycles quantify young water fractions, but not mean transit times, in spatially heterogeneous catchments. *Hydrology and Earth System Sciences, 20*(1), 279-297. doi:10.5194/hess-20-279-2016.

Kirchner, J. W. (2016b). Aggregation in environmental systems - Part 2: Catchment mean transit times and young water fractions under hydrologic nonstationarity. *Hydrology and Earth System Sciences, 20*(1), 299-328. doi:10.5194/hess-20-299-2016.

Kirchner, J. W., Feng, X. H., & Neal, C. (2000). Fractal stream chemistry and its implications for contaminant transport in catchments. *Nature, 403*(6769), 524-527. doi:10.1038/35000537.

Kirchner, J. W., Feng, X. H., & Neal, C. (2001a). Catchment-scale advection and dispersion as a mechanism for fractal scaling in stream tracer concentrations. *Journal of Hydrology, 254*(1-4), 82-101. doi:10.1016/s0022-1694(01)00487-5.

Li, S., Elliott, J.A., Tiessen, K.H.D., Yarotski, J.B., Lobb, D.A., & Flaten, D.N. (2011). The effects of multiple beneficial management practices on hydrology and nutrient losses in a small watershed in the canadian prairies. *Journal of Environmental Quality, 40*(5), pp. 1627-1642. doi: 10.2134/jeq2011.0054.

Liu, K., Elliott, J. A., Lobb, D. A., Flaten, D. N., & Yarotski, J. (2013). Critical factors affecting field-scale losses of nitrogen and phosphorus in spring snowmelt runoff in the Canadian Prairies. *Journal of Environmental Quality*, 42(2), 484–496. https://doi.org/10.2134/jeq2012.0385.

Lyon, S. W., Desilets, S. L. E., & Troch, P. A. (2008). Characterizing the response of a catchment to an extreme rainfall event using hydrometric and isotopic data. *Water Resources Research, 44*(6). doi:10.1029/2007wr006259.

Lyon, S. W., Laudon, H., Seibert, J., Morth, M., Tetzlaff, D., & Bishop, K. H. (2010). Controls on snowmelt water mean transit times in northern boreal catchments. *Hydrological Processes*, 24, 1672–1684. doi: 10.1002/hyp.7577.

Ma, W., & Yamanaka, T. (2013). Temporal variability in mean transit time and transit time distributions assessed by a tracer-aided tank model of a meso-scale catchment. *Hydrological Research Letters* 7(4), 104–109. doi: 10.3178/hrl.7.104.

Maloszewski, P., Rauert, W., Stichler, W., & Herrmann, A. (1983). Application of flow models in an alpine catchment-area using tritium and deuterium data. *Journal of Hydrology, 66*(1-4), 319-330. doi:10.1016/0022-1694(83)90193-2.

Maloszewski, P., & Zuber, A. (1982). Determining the turnover time of groundwater systems with the aid of environmental tracers 1. models and their applicability. *Journal of Hydrology, 57*(3-4), 207-231.

Manitoba Department of Agriculture. (1943). Reconnaissance soil survey of South-central Manitoba. Report number D4. Government of Manitoba, Canada.

Manitoba Department of Agriculture. (1988). Soils of the Rural Municipalities of Grey, Dufferin, Roland, Thompson and parts of Stanley. Report number D60. Government of Manitoba, Canada.

Manning, A. H., Clark, J. F., Diaz, S. H., Rademacher, L. K., Earman, S., & Plummer, L. N. (2012). Evolution of groundwater age in a mountain watershed over a period of thirteen years. *Journal of Hydrology, 460*, 13-28. doi:10.1016/j.jhydrol.2012.06.030.

McDonnell, J., Rowe, L., & Stewart, M. (1999). A combined tracer-hydrometric approach to assess the effect of catchment scale on water flow path, source and age. *Integrated Methods in Catchment Hydrology: Tracer, Remote Sensing and New Hydrometric Techniques*(258), 265-273.

McDonnell, J. J., McGuire, K., Aggarwal, P., Beven, K. J., Biondi, D., Destouni, G., Wrede, S. (2010). How old is streamwater? Open questions in catchment transit time conceptualization, modelling and analysis. *Hydrological Processes, 24*(12), 1745-1754. doi:10.1002/hyp.7796.

McDonnell, J. J., Stewart, M. K., & Owens, I. F. (1991). Effect of catchment-scale subsurface mixing on stream isotopic response. *Water Resources Research, 27*(12), 3065-3073. doi:10.1029/91wr02025.

McGlynn, B., McDonnell, J., Stewart, M., & Seibert, J. (2003). On the relationships between catchment scale and streamwater mean residence time. *Hydrological Processes, 17*(1), 175-181. doi:10.1002/hyp.5085.

McGuire, K. J., DeWalle, D. R., & Gburek, W. J. (2002). Evaluation of mean residence time in subsurface waters using oxygen-18 fluctuations during drought conditions in the mid-Appalachians. *Journal of Hydrology, 261*(1-4), 132-149. doi:10.1016/s0022-1694(02)00006-9.

McGuire, K. J., & McDonnell, J. J. (2006). A review and evaluation of catchment transit time modeling. *Journal of Hydrology, 330*(3-4), 543-563. doi:10.1016/j.jhydrol.2006.04.020.

McGuire, K. J., McDonnell, J. J., Weiler, M., Kendall, C., McGlynn, B. L., Welker, J. M., & Seibert, J. (2005). The role of topography on catchment-scale water residence time. *Water Resources Research, 41*(5). doi:10.1029/2004wr003657.

Nash, J. E., & Sutcliffe, J. V. (1970). River flow forecasting through conceptual models I: A discussion of principles. *Journal of Hydrology*, 10, 282–290.

Pacheco, F. A. L., & Van der Weijden, C. H. (2012). Integrating topography, hydrology and rock structure in weathering rate models of spring watersheds. *Journal of Hydrology, 428*, 32-50. doi:10.1016/j.jhydrol.2012.01.019.

Pearce, A. J., Stewart, M. K., & Sklash, M. G. (1986). Storm runoff generation in humid headwater catchments 1. where does the water come from. *Water Resources Research, 22*(8), 1263-1272. doi:10.1029/WR022i008p01263.

Rademacher, L. K., Clark, J. F., Clow, D. W., & Hudson, G. B. (2005). Old groundwater influence on stream hydrochemistry and catchment response times in a small Sierra Nevada catchment: Sagehen Creek, California. *Water Resources Research, 41*(2). doi:10.1029/2003wr002805.

Rodgers, P., Soulsby, C., Waldron, S., & Tetzlaff, D. (2005). Using stable isotope tracers to assess hydrological flow paths, residence times and landscape influences in a nested mesoscale catchment. *Hydrology and Earth System Sciences, 9*(3), 139-155.

Shook, K., & Pomeroy, J. (2012). Changes in the hydrological character of rainfall on the Canadian prairies. *Hydrological Processes* 26 (12): 1752–1766 doi: 10.1002/hyp.9383.

Singleton, M. J., & Moran, J. E. (2010). Dissolved noble gas and isotopic tracers reveal vulnerability of groundwater in a small, high-elevation catchment to predicted climate changes. *Water Resources Research, 46*. doi:10.1029/2009wr008718.

Song, C., Wang, G., Liu, G., Mao, T., Sun, X., & Chen, X. (2016). Stable isotope variations of precipitation and streamflow reveal the young water fraction of a permafrost watershed. *Hydrological Processes*, 31: 935–947 doi: 10.1002/hyp.11077.

Soulsby, C., Birkel, C., Geris, J., Dick, J., Tunaley, C., & Tetzlaff, D. (2015). Stream water age distributions controlled by storage dynamics and nonlinear hydrologic connectivity: Modeling with high-resolution isotope data. *Water Resources Research, 51*(9), 7759-7776. doi:10.1002/2015wr017888.

Soulsby, C., Birkel, C., Geris, J., & Tetzlaff, D. (2015). Spatial aggregation of time-variant stream water ages in urbanizing catchments. *Hydrological Processes, 29*(13), 3038-3050. doi:10.1002/hyp.10500.

Soulsby, C., Birkel, C., & Tetzlaff, D. (2014). Assessing urbanization impacts on catchment transit times. *Geophysical Research Letters, 41*(2), 442-448. doi:10.1002/2013gl058716.

Soulsby, C., Malcolm, R., Helliwell, R., Ferrier, R. C., & Jenkins, A. (2000). Isotope hydrology of the Allt a' Mharcaidh catchment, Cairngorms, Scotland: implications for hydrological pathways and residence times. *Hydrological Processes, 14*(4), 747-762. doi:10.1002/(sici)1099-1085(200003)14:4.

Soulsby, C., & Tetzlaff, D. (2008). Towards simple approaches for mean residence time estimation in ungauged basins using tracers and soil distributions. *Journal of Hydrology, 363*(1-4), 60-74. doi:10.1016/j.jhydrol.2008.10.001.

Spence, C., Guan, X. J., Phillips, R., Hedstrom, N., Granger, R., & Reid, B. (2010). Storage dynamics and streamflow in a catchment with a variable contributing area. *Hydrological Processes, 24*(16), 2209-2221. doi:10.1002/hyp.7492.

Stewart, M. K., Morgenstern, U., & McDonnell, J. J. (2010). Truncation of stream residence time: how the use of stable isotopes has skewed our concept of streamwater age and origin. *Hydrological Processes, 24*(12), 1646-1659. doi:10.1002/hyp.7576.

Stewart, M. K., Morgenstern, U., Gusyev, M. A., & Maloszewski, P. (2017). Aggregation effects on tritium-based mean transit times and young water fractions in spatially heterogeneous catchments and groundwater systems. *Hydrology and Earth System Science*., 21, 4615–4627. doi.org/10.5194/hess-21-4615-2017.

Stewart, M. K., & McDonnell, J. J. (1991). Modeling base flow soil water residence times from deuterium concentrations. *Water Resources Research*, 27(10), 2681-2693.

Stockinger, M. P., Bogena, H. R., Lucke, A., Diekkruger, B., Weiler, M., & Vereecken, H. (2014). Seasonal soil moisture patterns: Controlling transit time distributions in a forested headwater catchment. *Water Resources Research, 50*(6), 5270-5289. doi:10.1002/2013wr014815.

Tekleab, S., Mohamed, Y., Uhlenbrook, S., & Wenninger, J. (2014a). Hydrologic responses to land cover change: the case of Jedeb mesoscale catchment, Abay/Upper Blue Nile basin, Ethiopia. *Hydrological Processes, 28*(20), 5149-5161. doi:10.1002/hyp.9998.

Tekleab, S., Wenninger, J., & Uhlenbrook, S. (2014b). Characterisation of stable isotopes to identify residence times and runoff components in two meso-scale catchments in the Abay/Upper Blue Nile basin, Ethiopia. *Hydrology and Earth System Sciences, 18*(6), 2415-2431. doi:10.5194/hess-18-2415-2014.

Tetzlaff, D., Malcolm, I. A., & Soulsby, C. (2007). Influence of forestry, environmental change and climatic variability on the hydrology, hydrochemistry and residence times of upland catchments. *Journal of Hydrology, 346*(3-4), 93-111. doi:10.1016/j.jhydrol.2007.08.016.

Tetzlaff, D., Seibert, J., McGuire, K. J., Laudon, H., Burn, D. A., Dunn, S. M., & Soulsby, C. (2009a). How does landscape structure influence catchment transit time across different geomorphic provinces? *Hydrological Processes, 23*(6), 945-953. doi:10.1002/hyp.7240.

Tetzlaff, D., Seibert, J., & Soulsby, C. (2009b). Inter-catchment comparison to assess the influence of topography and soils on catchment transit times in a geomorphic province; the Cairngorm mountains, Scotland. *Hydrological Processes, 23*(13), 1874-1886. doi:10.1002/hyp.7318.

Tetzlaff, D., & Soulsby, C. (2008). Sources of baseflow in larger catchments - Using tracers to develop a holistic understanding of runoff generation. *Journal of Hydrology, 359*(3-4), 287-302. doi:10.1016/j.jhydrol.2008.07.008.

Tiessen, K. H. D., Elliott, J. A., Yarotski, J., Lobb, D. A., Flaten, D. N., & Glozier, N. E. (2010). Conventional and Conservation Tillage: Influence on Seasonal Runoff, Sediment, and Nutrient Losses in the Canadian Prairies. *Journal of Environmental Quality, 39*(3), 964-980. doi:10.2134/jeq2009.0219.

Timbe, E., Windhorst, D., Crespo, P., Frede, H. G., Feyen, J., & Breuer, L. (2014). Understanding uncertainties when inferring mean transit times of water trough tracer-based lumped-parameter models in Andean tropical montane cloud forest catchments. *Hydrology and Earth System Sciences, 18*(4), 1503-1523. doi:10.5194/hess-18-1503-2014.

Uhlenbrook, S., & Leibundgut, C. (2002). Process-oriented catchment modelling and multiple-response validation. *Hydrological Processes, 16*(2), 423-440. doi:10.1002/hyp.330.

Wolock, D. M., Fan, J., & Lawrence, G. B. (1997). Effects of basin size on low-flow stream chemistry and subsurface contact time in the Neversink River Watershed, New York. *Hydrological Processes, 11*(9), 1273-1286.

Woo, M. K., & Steer, P. (1983). Slope hydrology as influenced by thawing of the active layer, resolute, NWT. *Canadian Journal of Earth Sciences, 20*(6), 978-986. doi:10.1139/e83-87

CHAPTER 5: SYNTHESIS AND CONCLUSIONS

5.1 Summary of major objectives and methods

The major goal of this Ph.D. study was to characterize the water storage and release dynamics of a prairie watershed. Specifically, the aim was to improve our understanding of how prairie watersheds store and release water from active and passive storage zones into streams. One motivation for this work related to the issue of leaching of fertilizer from soils and other mechanisms that lead to nutrient loading – and more broadly contaminant loading – to streams. The frequency and duration of contaminant export from terrestrial systems to aquatic systems is highly correlated with the persistence of pollutants in watersheds, which, in turn, depends on the spatial distribution of water storage zones within watersheds and their release dynamics (e.g., Hancock et al., 2005; Van Meter and Basu, 2017). This Ph.D. study was, therefore, critical in assessing the potential for short-term and long-term contaminant export in a prairie context, mainly through the assessment of active storage release – which mainly helps mobilizing surface and near-surface contaminants – versus passive storage release – which predominantly affects contaminants at depth (Park and Park, 2015). A combination of hydrometric and isotopic data was used, and the approach was to first put forward hypotheses regarding the water storage and release phenomenon through multi-scale hydrograph analysis (Chapter 2). This was then followed by a determination of the relative proportions of active storage water (i.e., "new" water) and passive storage water (i.e., "old" water) released to streams and their variability across seasons, this through isotope-based hydrograph separation (Chapter 3). Lastly, four methods of water age and transit time estimation were used to infer how old the released water (from both active and passive storage) was (Chapter 4). The focus was on a nested system of eight watersheds spanning three main physiographic units: (1) a hummocky terrain with numerous small-scale natural depressions and

larger-scale man-made ponds, (2) an intensely fractured bedrock zone located along an escarpment, and (3) a lowland area. The results of the study were examined in the context of these physiographic characteristics and across two years of contrasting hydroclimatic regimes; only one of the years was considered in this synthesis.

5.2 Synthesis of findings emanating from different methodological approaches

5.2.1 Comparing hydrograph analysis and hydrograph separation results

Chapter 2 focused on using solely hydrometric data to help formulate hypotheses about what the water storage and release dynamics were across the eight outlets. Of the various metrics considered in that chapter, the baseflow index (BFI) and the runoff ratio (RR) notably provided insight into the passive and active storage release dynamics at the various outlets, albeit from a qualitative standpoint since hydrometric data – in the form of streamflow – represent a mixture of waters released from different storage sources (e.g., Chang et al., 2014; Miller et al., 2016). In Chapter 3, the partitioning of water originating from passive and active storage stores was examined using $\delta^{18}O$ and $\delta^{2}H$ data, which carry information about the travel history and age of water and therefore provide more process-driven, storage-related information than hydrometric data. In Chapter 3, the proportions of streamwater originating from passive (pOld) and active (pNew) storage release were determined. Some of the metrics obtained in Chapters 2 and 3 could therefore be compared, to assess the agreement – or lack thereof – of the conclusions emanating from different methodological approaches. In that regard, site-specific scatter plots of BFI values against pOld values for the 2014 sampling year are shown in Figure 5-1. Figure 5-1 appears to

show a lack of agreement between BFI and pOld values at most of the "MS" sites, especially during the late spring and summer seasons (Figure 5-1 a-f). That lack of agreement was, also, not consistent across sites, meaning that some 'MS' sites showed slightly better agreement between their BFI and pOld values (i.e., they plotted close to the 1:1 line) than others. The best agreement between the two metrics at the "MS" sites was observed during the early spring season at MS3 (Figure 5-1 c). In general, the Pearson's correlation coefficients considering all the sites for the early spring, late spring, and summer seasons were 0.12, 0.35, 0.69, respectively, but none of those correlation coefficients were statistically significant (p-value > 0.1). During the early spring period of 2014, it is likely that passive water (or "old" water) that was held in storage from the previous season was released at the same time as snowmelt water (i.e., active storage or "new" water) and was transmitted to streams. The apparent underestimation of the BFI values in relation to the tracer-inferred pOld values in early spring and summer across most of the "MS" sites raises questions about not only the definition of passive storage adopted in this thesis, but also about the appropriateness of hydrograph-based versus isotope-based methods to quantify passive storage release. Indeed, earlier in this thesis passive storage was defined as the long-duration and persistent storage of water in the saturated zone and was mainly associated with baseflow. However, the equivalency between passive storage and old water might not always be straightforward. Indeed, old water that is stored in soil may qualify as either active or passive storage, depending on the depth at which it is located and the speed with which it can be mobilized to feed streamflow. Also, some runoff generation mechanisms such as return flow may cause "old" soil water to be exfiltrated at the surface and be part of the surface runoff contribution to streams, thus making it more akin to active storage release based on the definitions adopted earlier in this thesis. When it comes to making a choice between hydrograph-based methods and isotope-based methods for

passive storage release assessment, it has been argued that mass balance approaches are more objective than graphical approaches such as hydrograph analysis, because the former provide a direct relation to physical processes and flowpaths in a basin (e.g., Stewart et al., 2007; Zhang et al., 2013). In the present study, one interesting result was the fact that as the year 2014 moved into the summer and fall seasons, there appeared to be an improved agreement between BFI and pOld values, which might be attributed to a switch from snow-influenced conditions to fully rain-dominated conditions. In rain-dominated conditions, isotope-inferred old water proportions and hydrograph-inferred baseflow are more likely to be drawn from the same passive source, i.e., deep groundwater, as opposed to snow-influenced conditions when "passive" stores of water could still be in the vadose zone. From a spatial standpoint, the agreement between BFI and pOld values was also better for the HWY240 and Miami sites (Figure 5-1 g & h), which not only drain the two largest of the studied watersheds but are also subject to very different physiographic controls than the 'MS' sites. The apparent creation of the geohydrologic break between the "MS" sites and the others by the escarpment causes passive stores of water to originate from deep groundwater sources at sites HWY240 and Miami as there is less surface runoff at HWY240 and Miami.

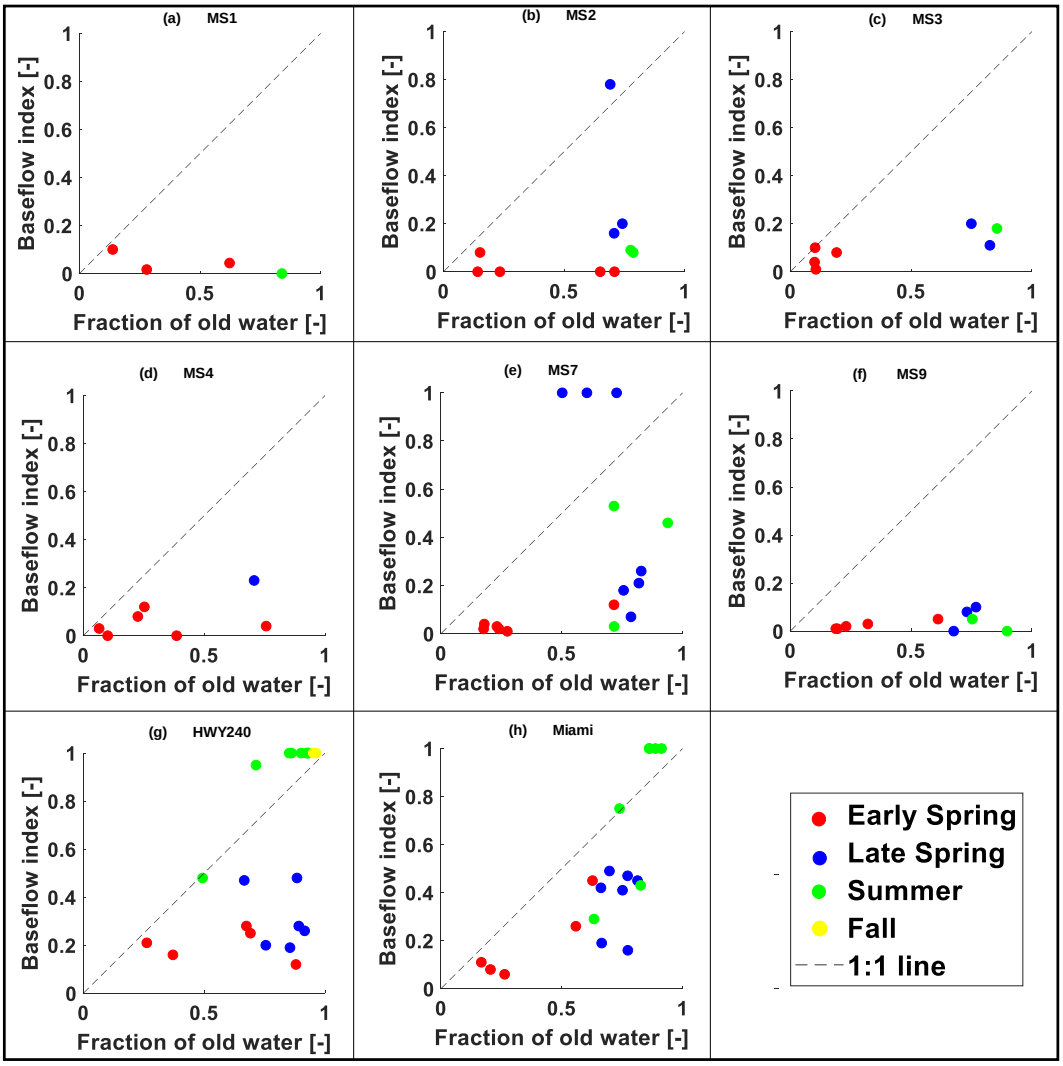

Figure 5-1. Scatter plots of the fraction of old water and the baseflow index with respect to the 1:1 line at the eight outlets based on the 2014 sampling. On each plot, a single circle represents results from a single day.

5.2.2 Hydrograph separation, water age and travel time estimation results

Chapter 4 dealt with the determination of transit times and streamwater ages at the eight outlets. Of the four major methods used – namely the damping ratio, fraction of young water, sine-wave modeling, and time-based convolution integral modeling – considered in that chapter, the fraction of young water (F_{yw}) is the metric that is the closest, conceptually, to the proportion of new water obtained from isotope-based hydrograph separation (pNew), since it represents the fraction of the total streamwater that is of age three months or less. F_{yw} values (determined in Chapter 4) and pNew (calculated as 1 minus pOld, from Chapter 3) were, therefore, compared to ascertain if they could lead to similar conclusions about active storage release mechanisms in the study watershed. Achieving this may help answer the question as to whether one metric may be used as a surrogate for the other. As shown in Chapters 3 and 4, for each site, pOld (and hence pNew) values were calculated for several days spanning all seasons in 2014, while the F_{yw} estimation method leads to a single value being calculated for 2014 and a single value being calculated for 2015. For synthesis purposes, Figure 5-2 shows boxplots of the distribution of pNew in the various outlets during the 2014 sampling year. F_{yw} values for the 2014 sampling year were superimposed on the seasonal distribution of pNew to see if median pNew values would match F_{yw} values. Figure 5-2 shows that F_{yw} values fall below the median pNew values during the early spring season at all the outlets except MS7 and MS9; the F_{yw} is rather above the median pNew value at MS7 and it coincides with the median pNew value at MS9 (Figure 5-2). Outlet MS7 is the only site where there was overtopping of the dam during snowmelt and extreme rainfall events (see Bansah and Ali, 2019), which would explain why the introduction of water from atop the dam makes the outlet have relatively higher F_{yw}. The match between the median pNew value and the

F_{yw} at site MS9 suggests that the two metrics could serve as surrogates for each other at that site, albeit only during the spring period. Figure 5-2 also reveals that F_{yw} greatly overestimated pNew at the majority of the sites from the late spring season onwards. In some cases, the F_{yw} is above the 75^{th} percentile or above the whiskers of the pNew distribution (e.g., Figures 5-2c, e, f, g, h). Taking into consideration the fact that the F_{yw} metric followed from results of the sine-wave modeling, there may have been carried-over uncertainties stemming from the assumed sine-wave approximation of the input and output isotopic variables (see Jasechko et al., 2017; Bansah and Ali, 2019). Meanwhile, the pNew estimation method rather relies on an assumption of a simple mixing hypothesis and may hence be more reliable in the context of evaluating active storage release dynamics.

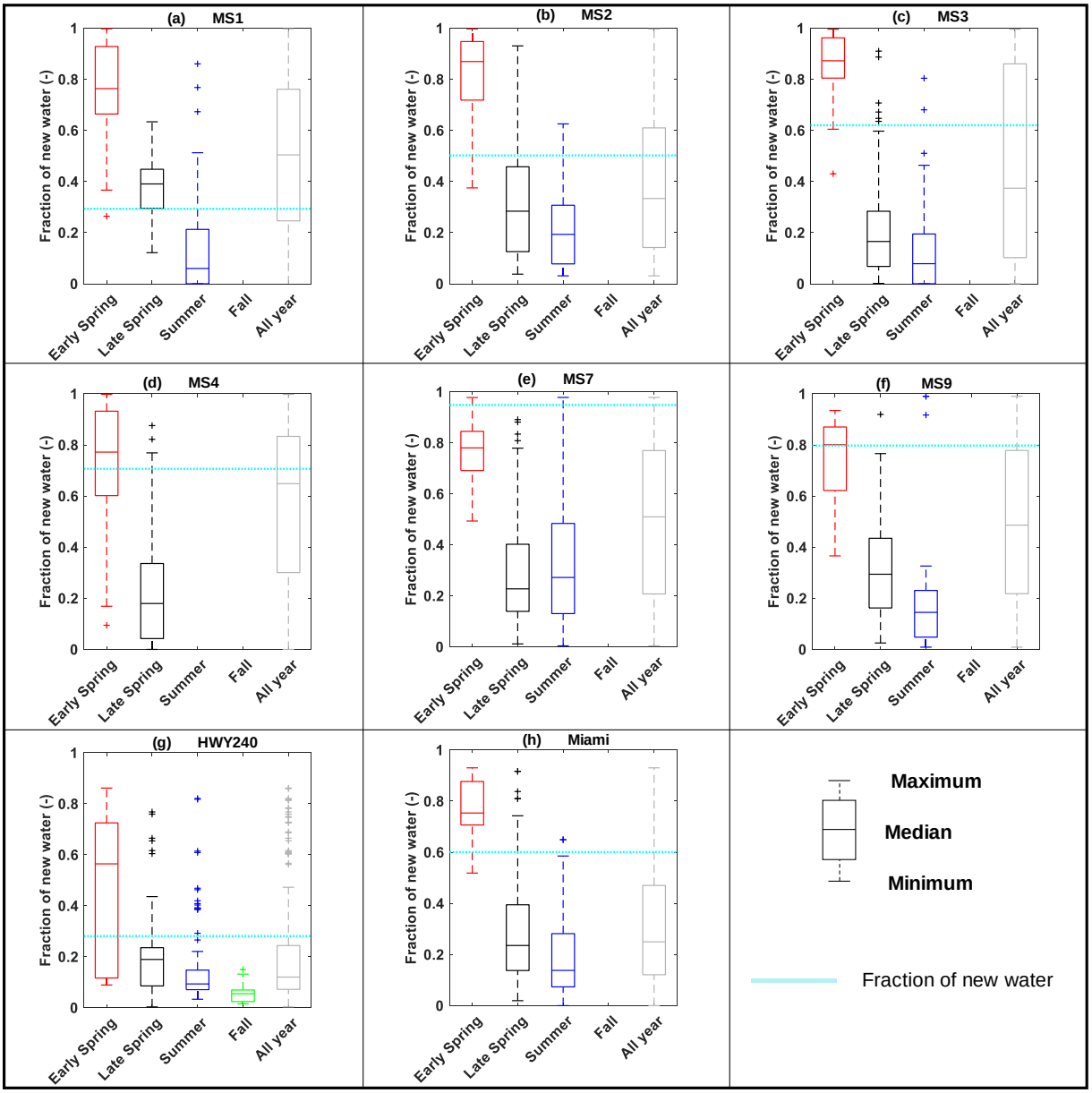

Figure 5-2. Boxplots showing the distribution of the fraction of new water within each of the four seasons in relation to the fraction of young water (horizontal cyan line) at the eight outlets. The horizontal line within each box shows the median value, while the bottom and top of each box show the 25th and 75th percentile, respectively, of the data distribution. Whiskers extending beyond above and below each box indicate the lowest and highest values. Small plus signs beyond whiskers are statistical outliers.

A qualitative comparison of mean transit time (MTT) estimates (via the time-based convolution integral method) across the different watershed physiographic units suggested that bedrock geology, rather than surficial geology, surface topography or land use, is a major control of MTTs. The damping ratio (DR) metric (from Figure 4-4), F_{yw} and sine-wave (SW) methods produced results that were aligned with flow process conceptualizations in the STCW, especially for the sites above the escarpment (Figure 5-3). The intensely fractured nature of the bedrock in the vicinity of HWY240 suggests that precipitation quickly infiltrates and percolates downward into deeper groundwater, rather than flowing laterally via shallow soils toward the outlet (Figure 5-3). This hypothesis is supported by the significant damping of precipitation isotopic signals in streamwater at HWY240 (Bansah and Ali, 2019; Figure 4-3; Appendices C-1 to C-4). Additional research into MTT estimation methods is certainly warranted across the prairies, preferably in areas where anecdotal knowledge of dominant flow processes and flow connectivity and data spanning contrasted years are available, in order to confirm or infirm the results from the current study.

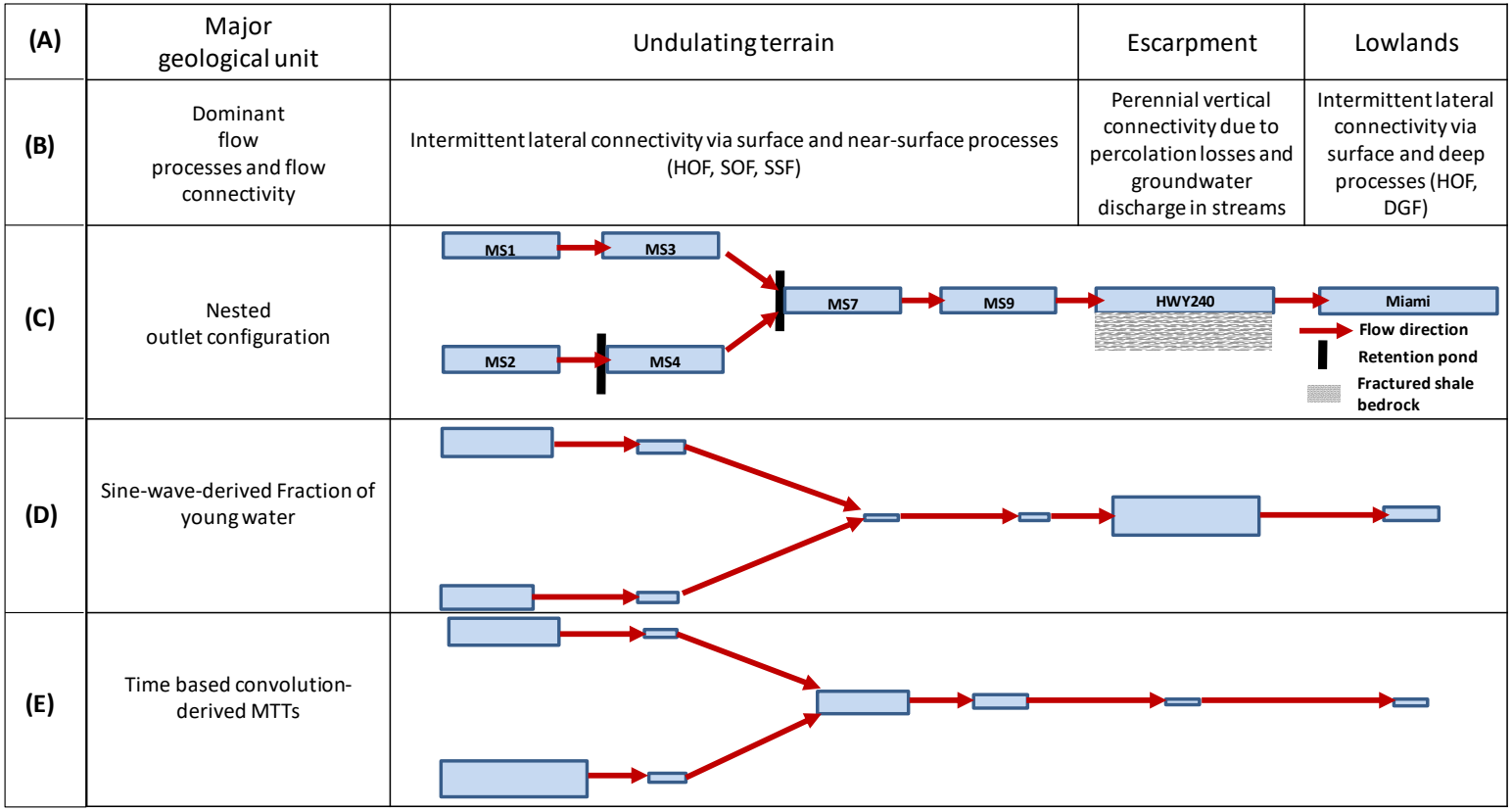

Figure 5-3. Schematic diagram allowing the comparison of different geologies and flow processes prevailing upslope of each monitored outlet (rows A, B and C), and the young water fractions and MTT values estimated for each outlet based on the TBC modeling methods (rows D and E). In rows D and E, the size of each blue box is proportional to the value of the F_{yw} metric or modeled MTT values for a given outlet. HOF: Hortonian overland flow. SOF: saturation-excess overland flow. SSF: shallow subsurface flow. DGF: deep groundwater flow.

5.2.3 Interpreting the lack of agreement between methodological approaches

A comparative analysis between the average baseflow index (BFI) values and the mean transit times (MTT) at the various outlets (Table 5-1) during the 2014 sampling year does not show any clear association between the two metrics. It would have been expected that high BFI values would translate into long MTTs as both metrics primarily measure passive storage release dynamics. In the same vein, high runoff ratios (RR) did not necessarily translate into short MTTs; it was only at the HWY240 outlet that the highest RR translated to the shortest MTT (Table 5-1). Relying on the sole results of RR (from Chapter 2) and MTT values (from Chapter 4) may have led to a conclusion of rapid active storage release to streamflow at HWY240. However, confronting these two metrics with few others (such as BFI from Chapter 2, pOld from Chapter 3, and DR and F_{yw} from Chapter 4) (Table 5-2) rather suggests a flow process that may be at odds with what may have originally been perceived, namely the piston flow of old water. The application of multiple metrics has, therefore, given weight to the hypothesis of a rapid release from passive stores of old water via the fractured bedrock at HWY240 through a piston flow mechanism, thus validating the conceptual dominant flow process (Figure 5-3) established for that site. The use of multiple approaches did not always lead to convergent conclusions, however. An example of a site where using multiple metrics led to conflicting results was MS1. Indeed, the RR, BFI (from Chapter 2), pOld (from Chapter 3), and DR (from Chapter 4) metrics (Table 5-2) suggested the presence of rapid active storage release at MS1. However, that proposed hypothesis is in conflict with the F_{yw} and MTT values (from Chapter 4) at MS1 (Table 5-2), which suggest a relatively low F_{yw} and a long MTT. Hence, no definitive interpretive conclusion could be reached on the dominant water release dynamics at MS1. As shown in these two examples from sites HWY240 and MS1, inasmuch as using multiple metrics can help confirm flow processes dominating at an outlet of a watershed, these same multiple approaches could lead to conflicting results – as was in the case for MS1.

Table 5-1. Average values of key watershed storage and release metrics (i.e., baseflow index, runoff ratio, fraction of old water, young water fraction, and mean transit time) across the eight outlets during the 2014 sampling year.

Site	BFI (-)	RR (-)	pOld (-)	F_{yw} (-)	MTT (days)
MS1	0.00	0.23	0.48	0.29	550
MS2	0.07	0.57	0.56	0.50	1156
MS3	0.15	0.23	0.42	0.62	62
MS4	0.00	0.26	0.41	0.71	115
MS7	0.12	0.23	0.57	0.95	509
MS9	0.00	0.16	0.53	0.80	288
HWY240	0.30	0.61	0.82	0.28	0.07
Miami	0.17	0.39	0.69	0.60	95

Table 5-2. Ranking of watersheds from the standpoint of passive storage release dynamics using the key metrics and methods considered in this study for the 2014 sampling year. 8 indicates fast release and/or short MTT while 1 indicates slow release and/or long MTT. Because the F_{yw} metric and SW method are interrelated, the latter was not considered in the counts assigned to the last column of the table.

	BFI	**RR**	**pOld**	**DR**	**F_{yw}**	**SW**	**TBC**	**Highest # of times of metric agreements**
MS1	8	2	6	6	2	2	2	3
MS2	5	7	4	5	3	3	1	1
MS3	3	3	7	7	5	5	7	2
MS4	7	5	8	3	6	6	5	1
MS7	4	4	3	8	8	8	3	2
MS9	6	1	5	4	7	7	4	1
HWY240	1	8	1	1	1	1	8	4
Miami	2	6	2	2	4	4	6	2

5.3 Study limitations and recommendations for future research

This PhD study, albeit novel and insightful in many ways, had some major limitations mainly relating to data acquisition. This was especially the case for the transit time modeling in Chapter 4. Due to the approximately six months of hydrologic inactivity in the streams, between October and March, liquid streamwater samples were unavailable during that period. There were also gaps in the isotopic timeseries – not due to lack of sampling but rather caused by streams running dry – which required approximating by a sine wave interpolation technique. Given the fact that the seasonal isotopic cycle

may not follow the typical sine wave model in the prairies (see Jasechko et al., 2017), the opportunity is there for future studies to be carried out in other prairie watersheds to help classify the various cycles that precipitation and streamflow isotopic signature may follow. Another limitation associated with data acquisition was related to precipitation data. A single weather station (the only active station available during the study period) was used to represent all the eight watersheds. This assumption of uniform meteorological conditions across all the watersheds is however at odds with past studies which relied on currently inactive weather stations; meteorological differences, mainly between the sites above and below the escarpment were found (Li et al., 2011). The use of data from a single weather station may have impacted the precipitation exceedance curves and the event rainfall-runoff analysis in Chapter 2, as well as the estimation of the input isotopic fluxes for the TBC modeling in Chapter 4. While not a limitation per se, Chapter 4 only focused on one type of transit time distribution (TTD) when several exist. Popular TTDs such as piston flow (McGlynn et al., 2003), advection-dispersion (Maloszewski and Zuber, 1982), two-parallel linear reservoir (Shaw et al., 2008) etc. were not compared in this study, but it might be useful to do so in the future as geological controls were shown to be critical and are very likely to cause spatial variability in the shape of the real TTD across the STCW. In the future, it may also be worthwhile to try the application of storage selection functions (Benettin et al., 2015; Harman, 2015) to the STCW, should catchment total storage estimates be available, to help better define the mean transit time. Lastly, one thesis objective that was originally identified but then became difficult to pursue was a spatial aggregation of metrics to look at scaling effects from small to larger watershed scales. Indeed, it was originally intended to use the eight outlets of the STCW as a model to establish such an upscaling concept. However, the escarpment at HWY240 exerted such a strong geological control on hydrological dynamics that it was impossible to distinguish its effect on storage release dynamics from that of watershed drainage area. It is suggested that a future study focus on examining scaling effects while still

implementing the metrics utilized in the current study but at a watershed that is a bit more uniform in terms of geologic controls.

5.4 References

Bansah, S. & Ali, G. (2019) Streamwater Ages in Nested, Seasonally Cold Canadian Watersheds. *Hydrological Processes*. 2019;1–17. https://doi.org/10.1002/hyp.13373.

Benettin, P., Rinaldo, A., & Botter, G. (2015). Tracking residence times in hydrological systems: forward and backward formulations. *Hydrological Processes, 29*(25), 5203-5213. doi:10.1002/hyp.10513.

Chang, H., Johnson, G., Hinkley, T., & Jung, I. (2014) Spatial analysis of annual runoff ratios and their variability across the contiguous U.S. Journal of Hydrology 511(387-402), http://dx.doi.org/10.1016/j.jhydrol.2014.01.066.

Hancock, P. J., Boulton, A. J., & Humphreys, W. F. (2005). Aquifers and hyporheic zones: Towards an ecological understanding of groundwater. *Hydrogeology Journal, 13*(1), 98-111. doi:10.1007/s10040-004-0421-6.

Harman, C. J. (2015). Time-variable transit time distributions and transport: Theory and application to storage-dependent transport of chloride in a watershed. *Water Resources Research, 51*(1), 1-30. doi:10.1002/2014wr015707.

Jasechko, S., Wassenaar, L.I., & Mayer, B. (2017). Isotopic evidence for widespread cold-season-biased groundwater recharge and young streamflow across central Canada. *Hydrological Processes* 31: 2196-2209. doi: 10.1002/hyp.11175.

Li, S., Elliott, J. A., Tiessen, K. H. D., Yarotski, J., Lobb, D. A., & Flaten, D. N. (2011). The Effects of Multiple Beneficial Management Practices on Hydrology and Nutrient Losses in a Small Watershed in the Canadian Prairies. *Journal of Environmental Quality, 40*(5), 1627-1642. doi:10.2134/jeq2011.0054.

Maloszewski, P., & Zuber, A. (1982). Determining the turnover time of groundwater systems with the aid of environmental tracers 1. models and their applicability. *Journal of Hydrology, 57*(3-4), 207-231.

McGlynn, B., McDonnell, J., Stewart, M., & Seibert, J. (2003). On the relationships between catchment scale and streamwater mean residence time. *Hydrological Processes, 17*(1), 175-181. doi:10.1002/hyp.5085.

Miller, P.M., Buto, S. G., Susong, D.D. & Rumsey, C. A. (2016). The importance of base flow in sustaining surface water flow in the Upper Colorado River Basin, *Water Resources Research, 52,* doi:10.1002/2015WR017963.

Park, M. & Park, M. (2015). Evaluation of Watershed Susceptibility to Contaminants of Emerging Concern. *Journal of American water works association*. http://dx.doi.org/10.5942/jawwa.2015.107.0015.

Shaw, S. B., Harpold, A. A., Taylor, J. C., & Walter M. T. (2008). Investigating a high-resolution stream chloride time series from the Biscuit Brook Catchment, Catskills, NY. *Journal of Hydrology*, 348(3-4), 245–256, doi:10.1016/j.jhydrol.2007.10.009.

Stewart, M., Cimino, J., & Ross, M. (2007). Calibration of baseflow separation methods with streamflow conductivity. *Ground Water*, 45, 17–27, doi:10.1111/j.1745-6584.2006.00263.

Van Meter, K. J., & Basu, N. B. (2017). Time lags in watershed-scale nutrient transport: an exploration of dominant controls. *Environmental Research Letters*, 12 (2017) 084017. https://doi.org/10.1088/1748-9326/aa7bf4.

Zhang, R., Li, Q., Chow, T. L., Li, S., & Danielescu, S. (2013). Baseflow separation in a small watershed in New Brunswick, Canada, using a recursive digital filter calibrated with the conductivity mass balance method, *Hydrological Processes,* 27, 259–2665, doi:10.1002/hyp.9417.

APPENDICES

Appendix A Supplemental Materials Related to Chapter 2

Appendix A-1. Flow duration and precipitation duration curves plotted on a log scale for better visualisation of high flows. Curves are shown for all seasons of the sampling year; blue is used for 2014 while red is used for 2015.

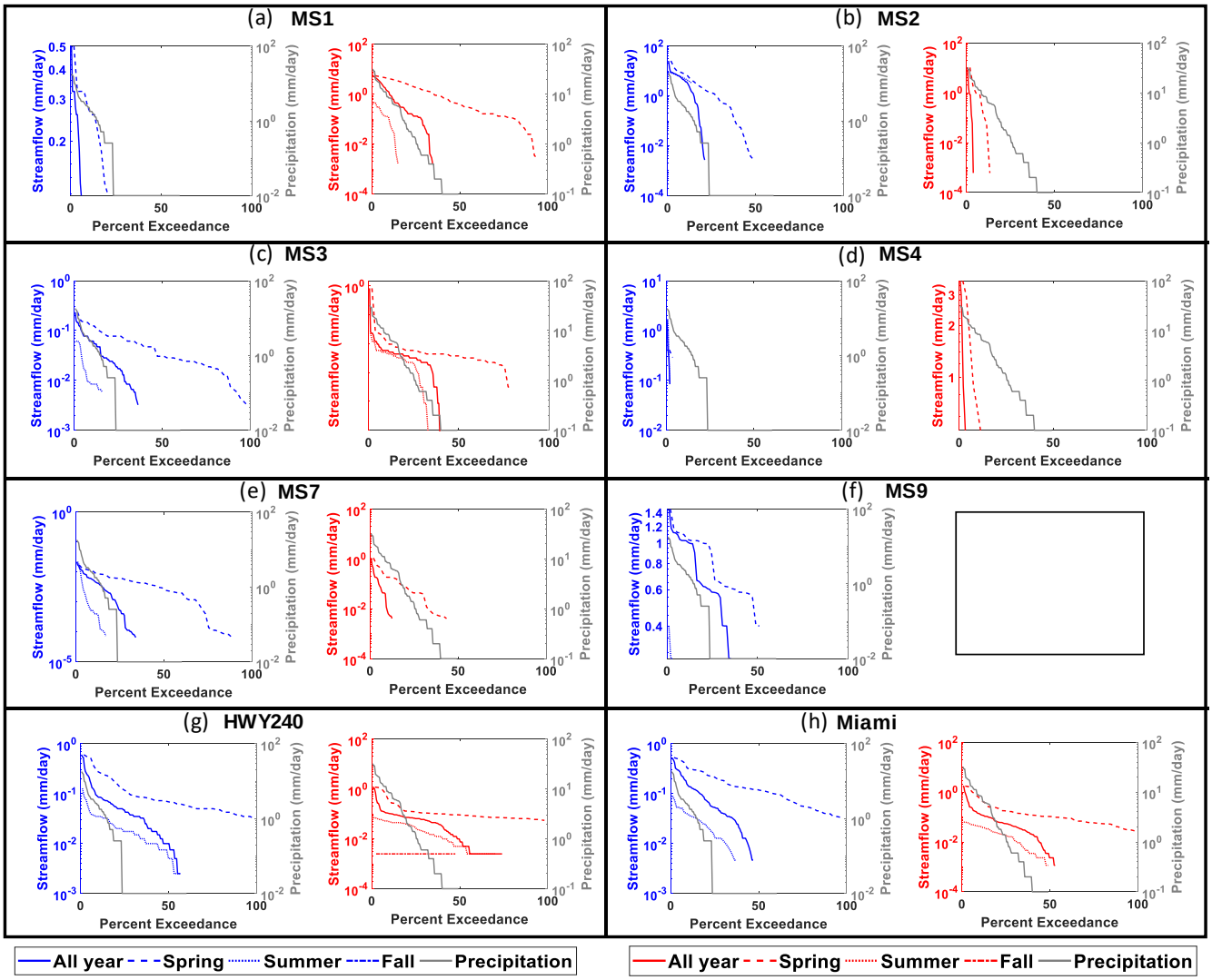

Appendix A-2. Flow duration curves (for the fastflow and baseflow portions of total flow) and precipitation duration curves plotted on a log scale for better visualisation of high flows. Blue font flag 2014 and red font flag 2015.

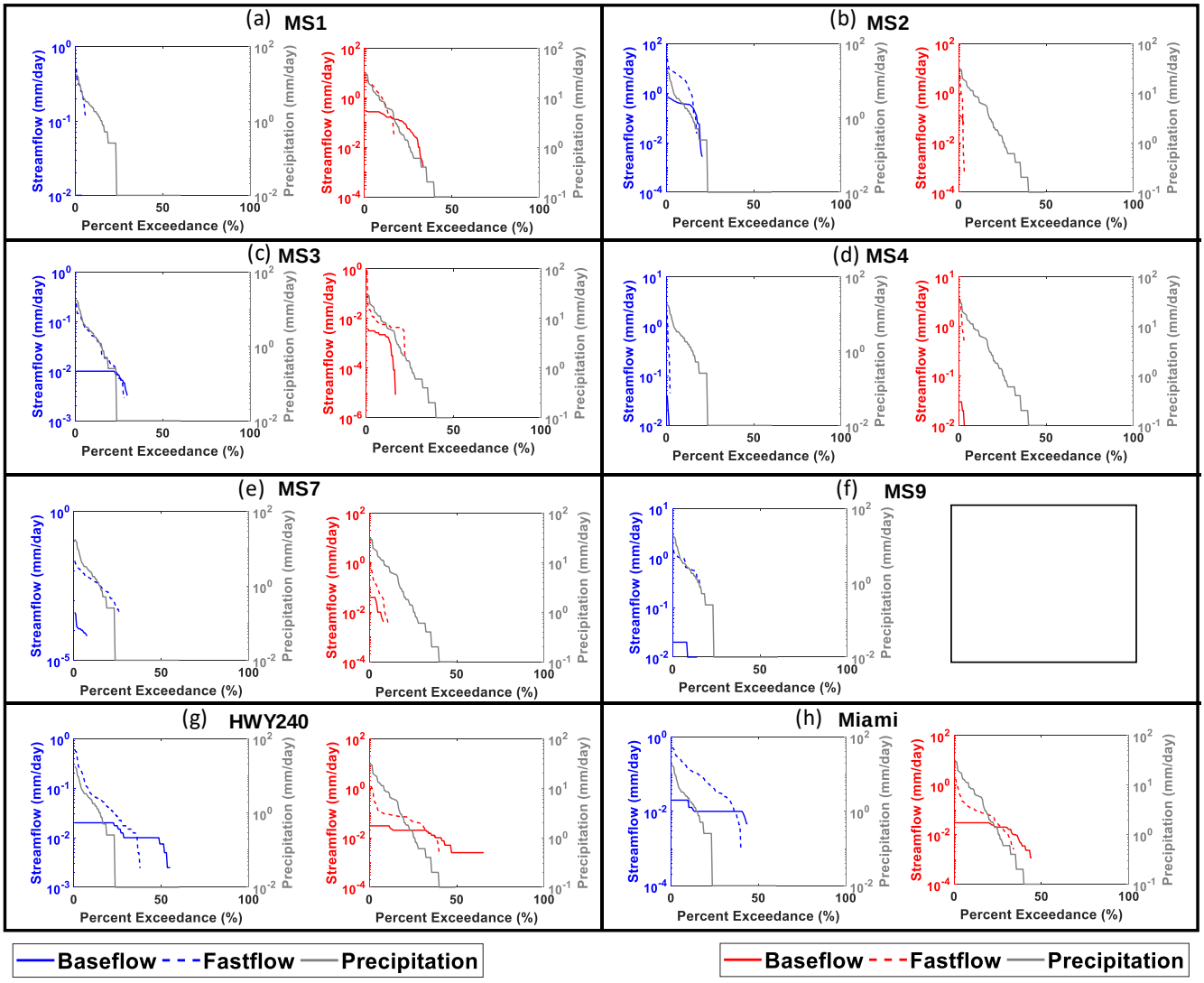

Appendix B Supplemental Materials Related to Chapter 3

Appendix B-3. Schematic illustration of the timing of stream water sampling and "new water" sampling for each potential "new" water end-member definition. Symbols illustrated in the same color flag samples that are "matched-up" to complete a given IHS scenario. For acronyms, refer to Table 3-2.

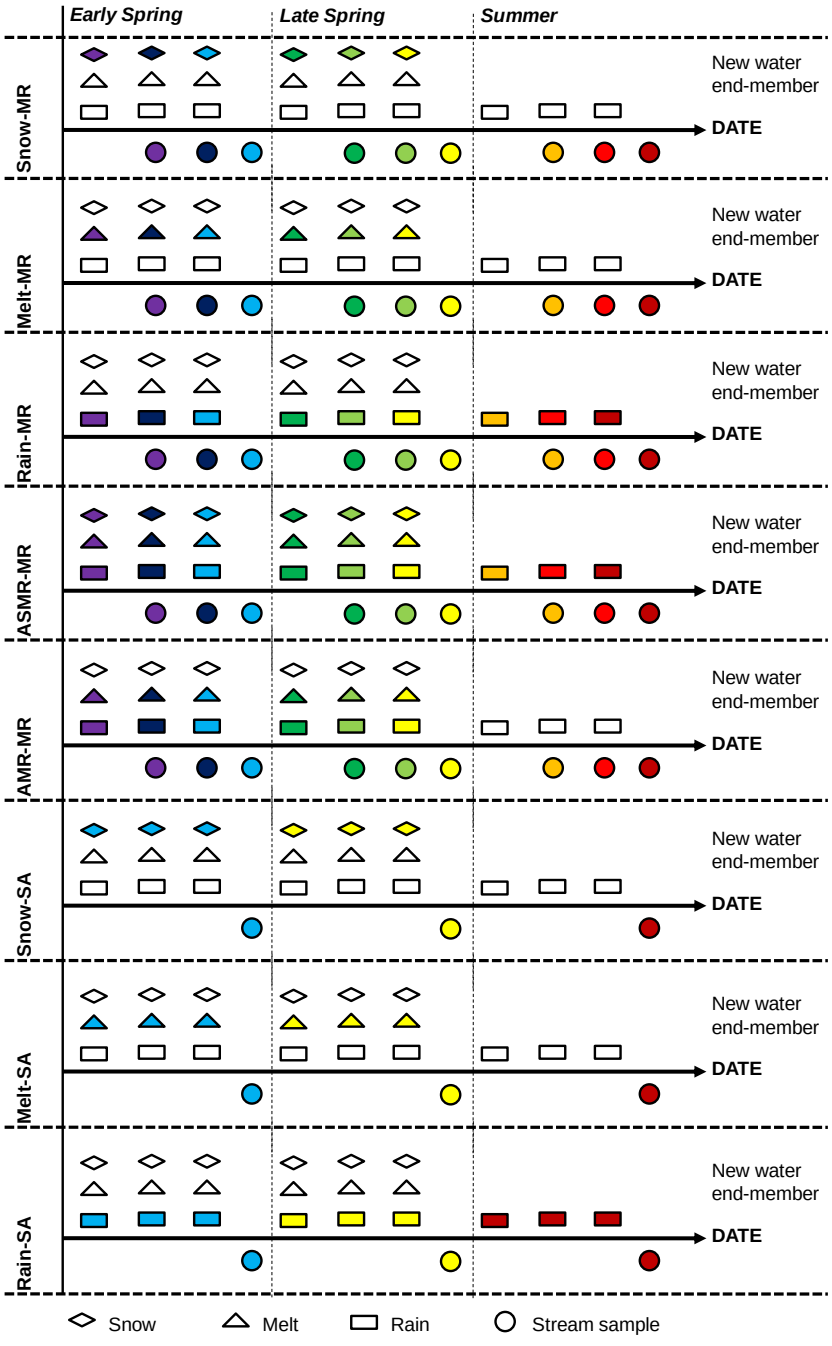

Appendix B-4. Schematic illustration of the timing of stream water sampling and "old water" sampling for each potential "old" water end-member definition. Symbols illustrated in the same color flag samples that are "matched-up" to complete a given IHS scenario. For acronyms, refer to Table 3-2.

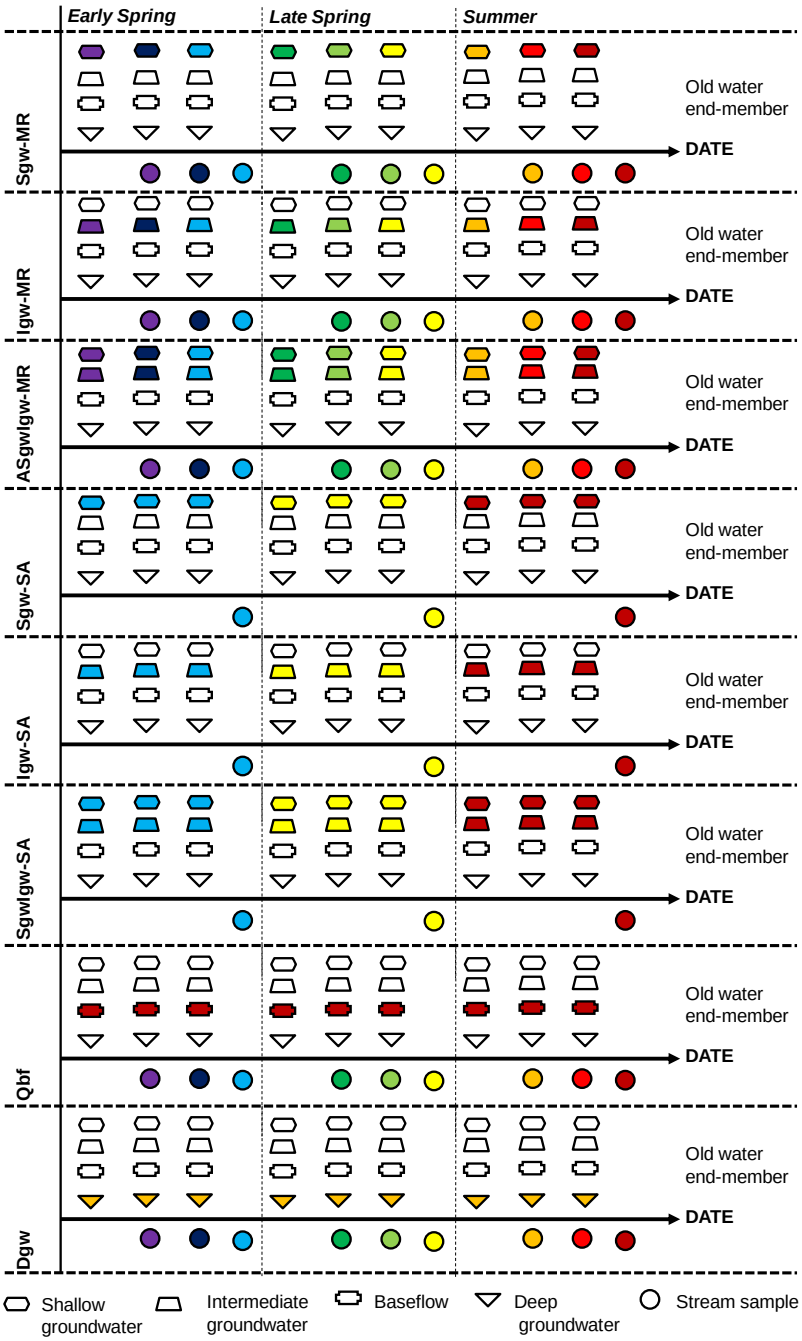

Appendix B-5. $\delta^{18}O$ and $\delta^{2}H$ data used for computing uncertainties associated with "old water" fractions at three key locations of the STCW during the 2014 sampling period.

	MS1						HWY240						Miami					
	Snow	Melt	Stream	Rain	Igw	Sgw	Snow	Melt	Stream	Rain	Igw	Sgw	Snow	Melt	Stream	Rain	Igw	Sgw
								$\delta^{18}O$(‰)										
n[a]	12	4	4	20	3	3	6	3	22	18	0	1	8	14	19	15	0	12
Mean[b]	-23.2	-21.9	-18.4	-13.3	-17.6	-13.5	-21.1	-18.9	-15.1	-12.6	n/a	n/a	-25.8	-21.8	-15.5	-14.5	n/a	-11.7
Standard[c] deviation	3.9	2.3	4.1	4.3	5.4	1.7	2.6	2.2	1.7	3.2	n/a	n/a	2.7	1.3	3.3	3.9	n/a	1.6
t/70% [d]	1.088	1.25	1.25	1.066	1.385	1.385	1.156	1.385	1.063	1.069	n/a	n/a	1.119	1.079	1.067	1.076	n/a	1.088
W/70% [e]	4.2	2.8	5.1	4.6	7.5	2.3	3.0	3.0	1.8	3.5	n/a	n/a	3.1	1.4	3.5	4.2	n/a	1.7
								$\delta^{2}H$ (‰)										
n[a]	12	4	4	20	3	3	6	3	22	18	0	1	8	14	19	15	0	12
Mean[b]	-175.4	-162.9	-138.5	-98.8	-140.9	-107.4	-158.1	-142.6	-115.9	-93.8	n/a	n/a	-194.1	-166.6	-119.6	-109.1	n/a	-87.6
Standard[c] deviation	31.3	18.4	34.0	34.2	29.5	12.4	24.9	17.3	14.6	25.7	n/a	n/a	22.9	11.3	24.7	31.5	n/a	11.7
t/70%[d]	1.088	1.25	1.25	1.066	1.385	1.385	1.156	1.385	1.063	1.069	n/a	n/a	1.119	1.079	1.067	1.076	n/a	1.088
W/70%[e]	34.1	23	42.5	36.5	40.9	17.2	28.8	24.0	15.5	27.5	n/a	n/a	25.6	12.2	26.3	33.9	n/a	12.7

[a] Number of sample points used in computing the mean.

[b] Mean tracer concentrations of $\delta^{18}O$ and $\delta^{2}H$, relative to VSMOW reference.

[c] Standard deviation of the samples used to define the mean

[d] Appropriate t statistic at the 70% confidence level

[e] Propagated uncertainties (i.e., the uncertainty in each concentration at the 70% confidence level) of the various water samples

Appendix C Supplemental Materials Related to Chapter 4

Appendix C-1. 2014 precipitation and streamwater $\delta^{18}O$ data fitted by a sine-wave model, with the coefficient of determination (R^2) illustrating the goodness-of-fit. Mean R^2 for all fits for the precipitation and streamwater data were 0.50 and 0.83, respectively.

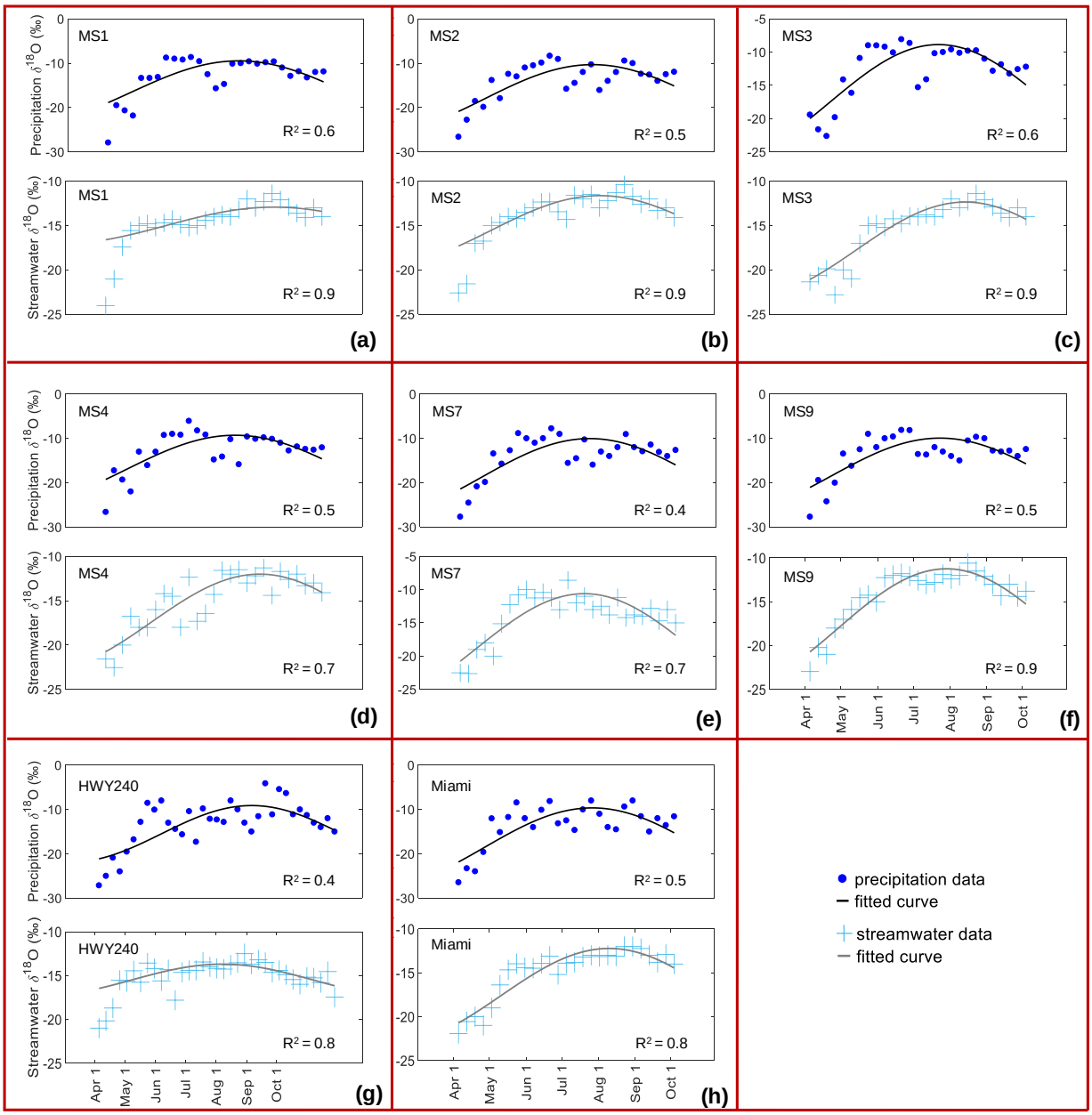

Appendix C-2. 2015 precipitation and streamwater $\delta^{18}O$ data fitted by a sine-wave model, with the coefficient of determination (R^2) illustrating the goodness-of-fit. Mean R^2 for all fits for the precipitation and streamwater data were 0.71 and 0.61, respectively.

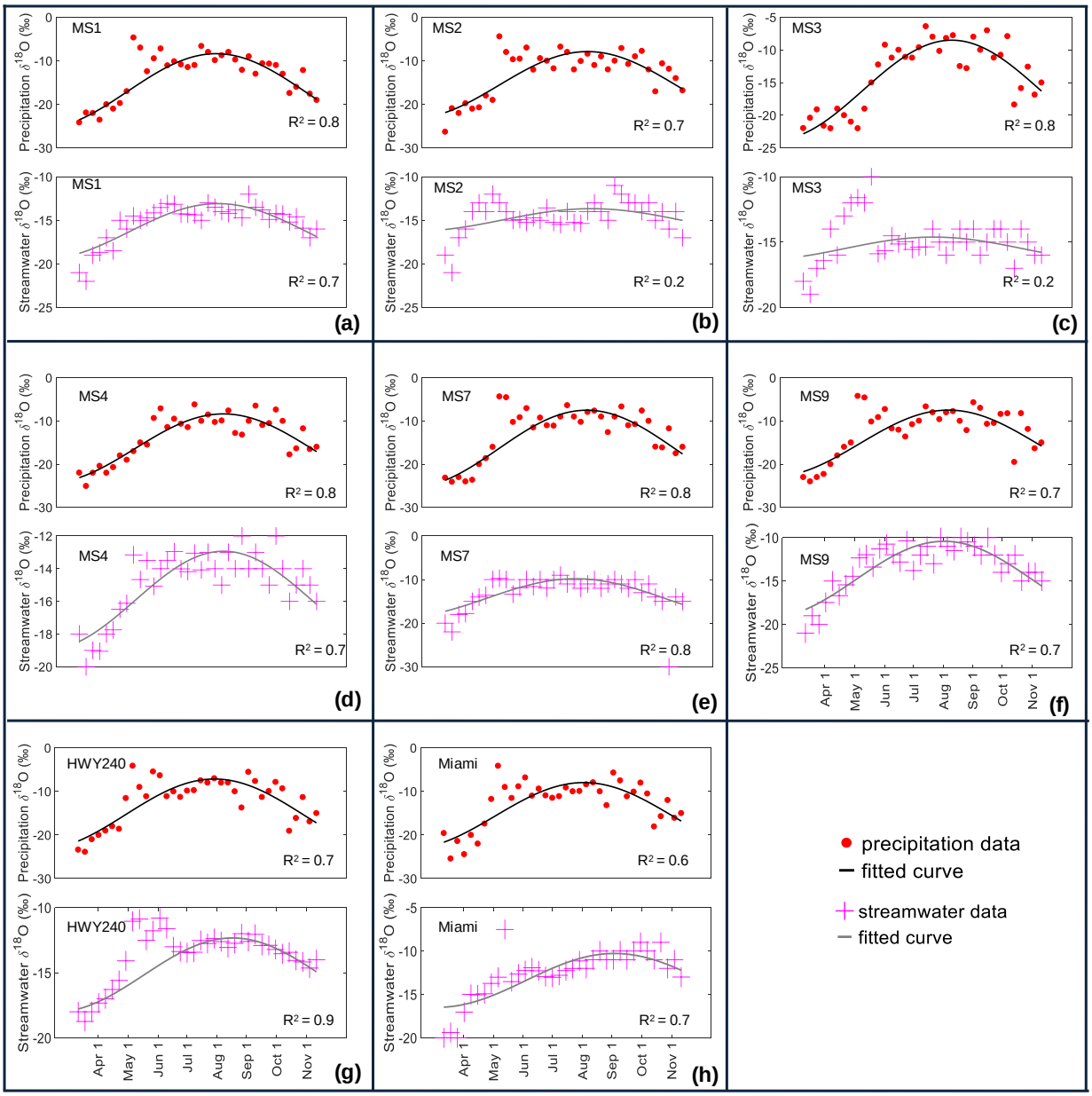

Appendix C-3. 2014 precipitation and streamwater δ^2H data fitted by a sine-wave model, with the coefficient of determination (R^2) illustrating the goodness-of-fit. There were no results for outlets MS4 and MS7 because the amplitude in streamwater (A_s) was greater than that in precipitation (A_p). Mean R^2 for all possible fits for the precipitation and streamwater data were 0.56 and 0.81, respectively.

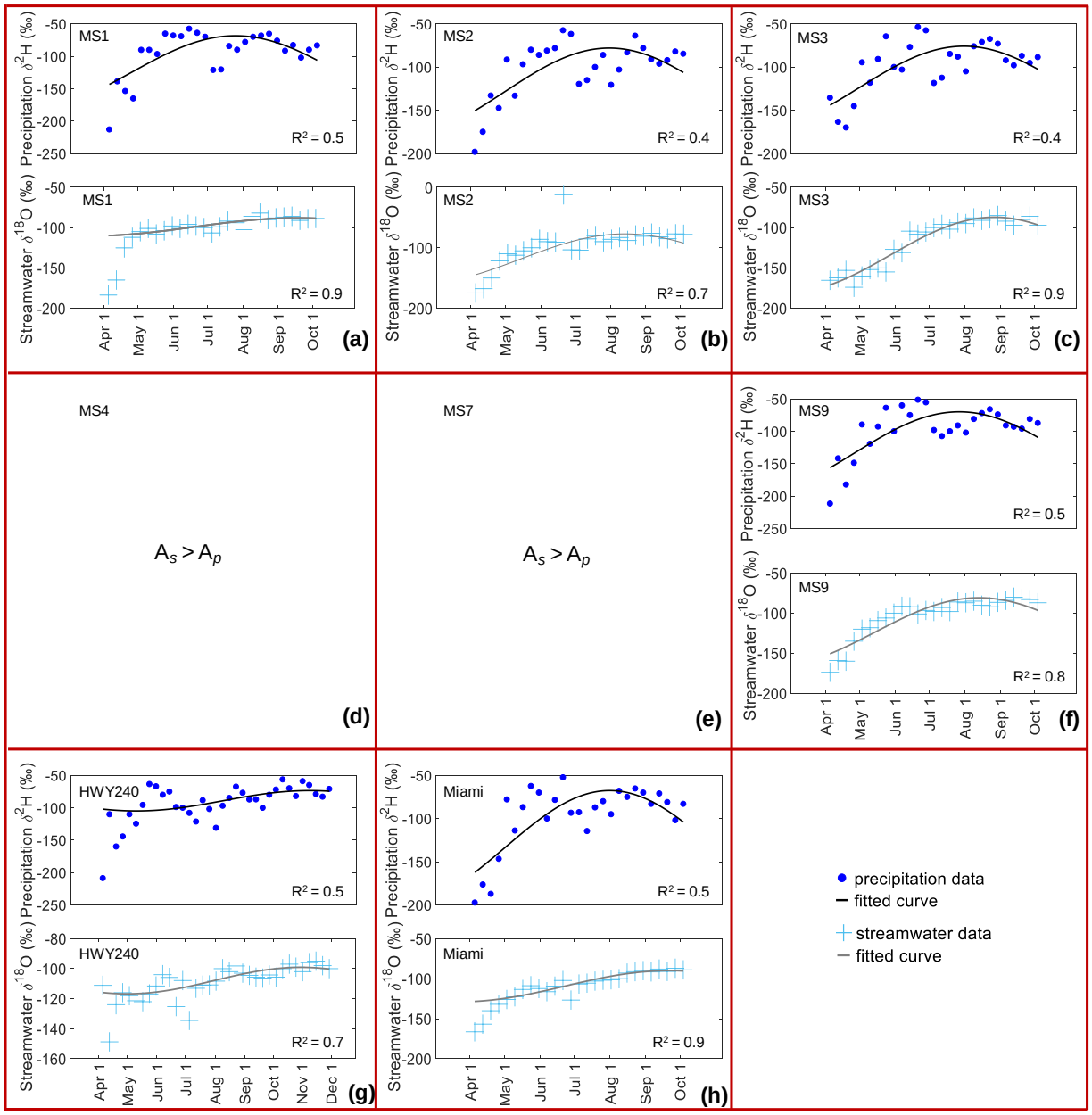

Appendix C-4. 2015 precipitation and streamwater δ^2H data fitted by a sine-wave model, with the coefficient of determination (R^2) illustrating the goodness-of-fit. Mean R^2 for all fits for the precipitation and streamwater data were 0.69 and 0.64, respectively.

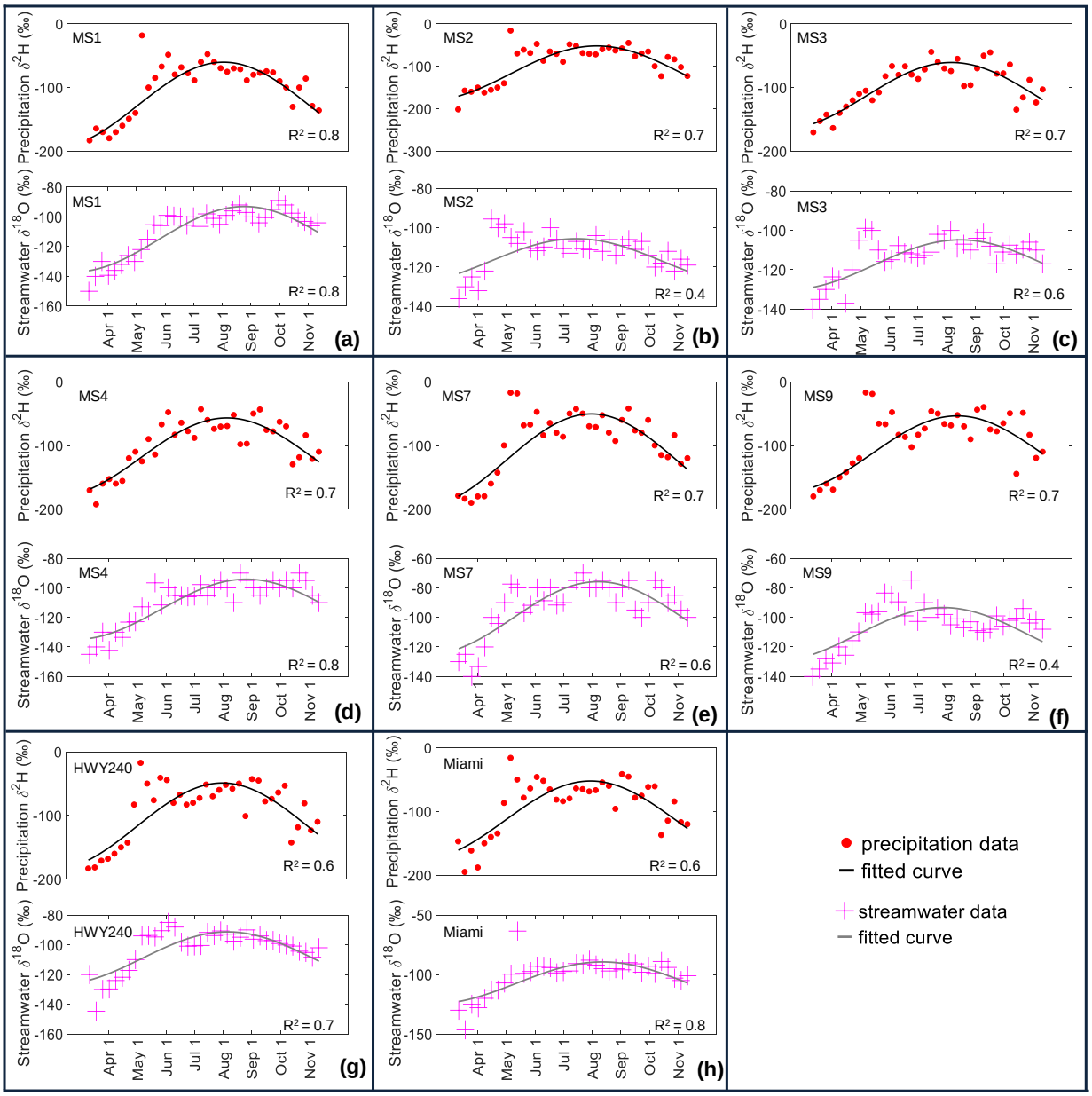

Appendix C-5. Fitted curves to the 2014 $\delta^{18}O$ timeseries in streamwater for the eight outlets according to the TBC method, based on the Monte Carlo (MC) simulation that resulted in the highest NSE. Gray envelopes represent all MC simulations with NSE above 0.3.

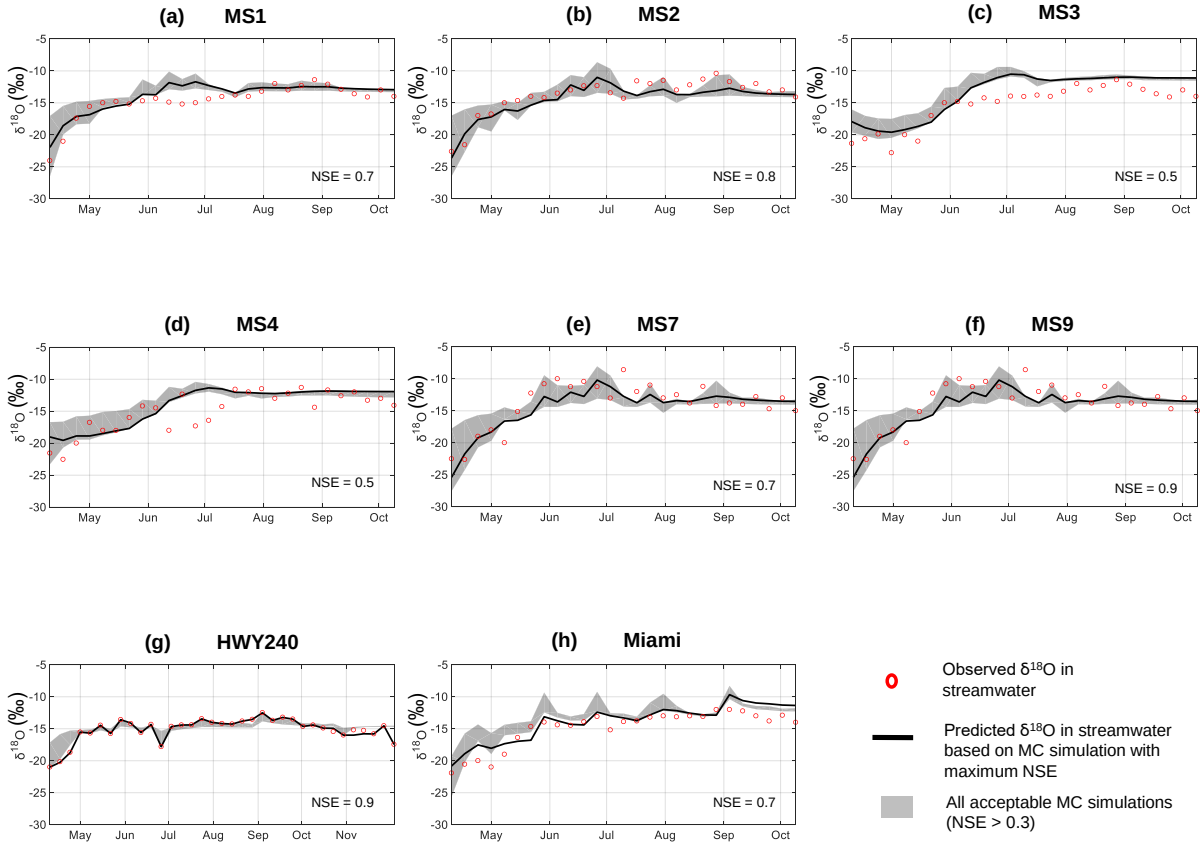

Appendix C-6. Fitted curves to the 2014 δ^2H timeseries in streamwater for the eight outlets according to the TBC method, based on the Monte Carlo (MC) simulation that resulted in the highest NSE. A blank panel is shown for the HWY240 outlet, i.e., panel (g), due to all the NSE values associated with the 50,000 MC simulations being less than 0.3.

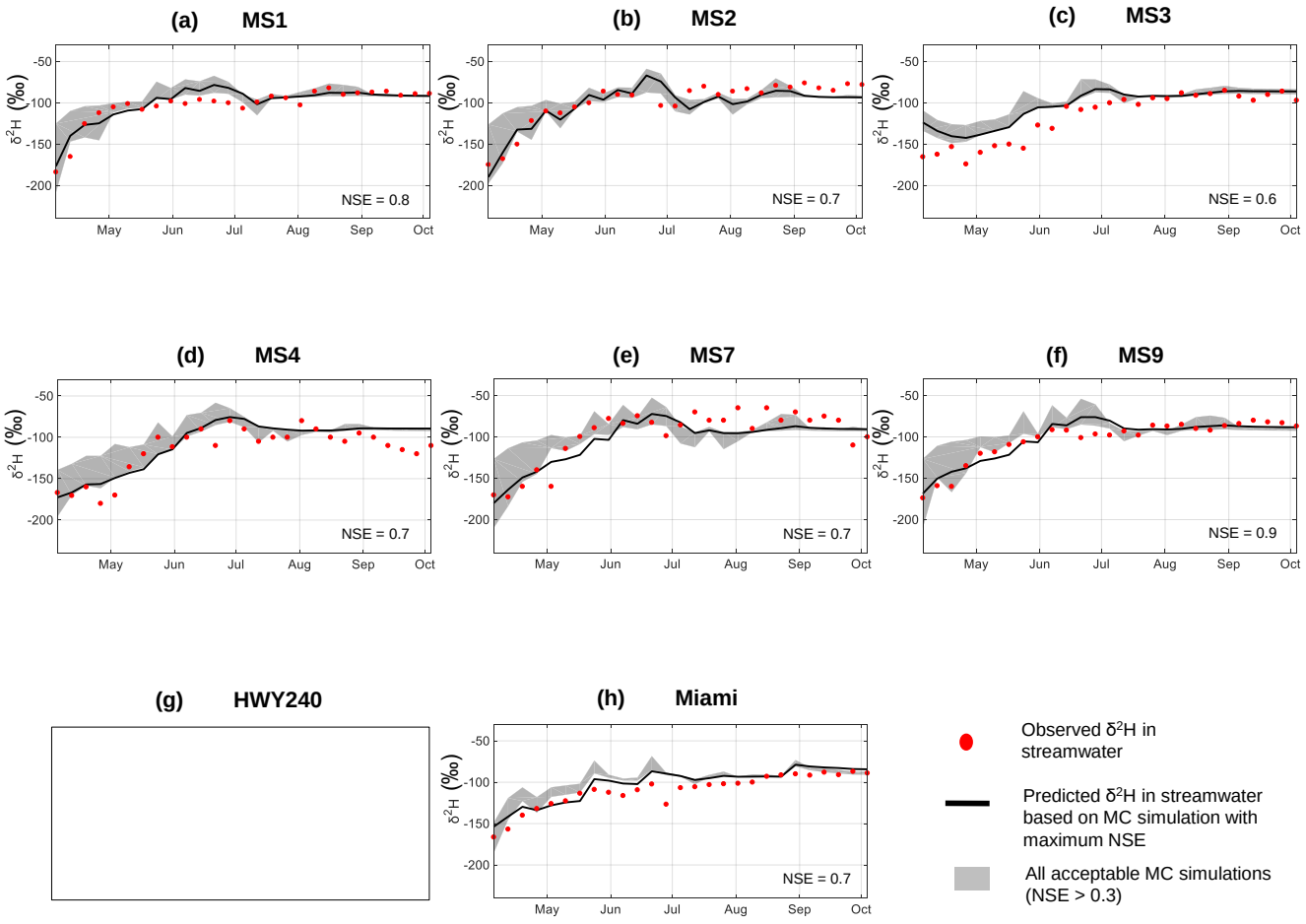

Appendix C-7. Summary statistics of the 2014 MTT proxy metrics and MTT modeling parameters across the eight outlets considered in this study. CV: coefficient of variation (unitless).

	Minimum	**Maximum**	**Mean**	**Median**	**CV**
$\delta^{18}O$-based DR (-)	0.18	0.51	0.37	0.36	0.30
$\delta^{2}H$-based DR (-)	0.14	0.46	0.31	0.32	0.35
$\delta^{18}O$-based SW-derived F_{yw} (-)	0.28	0.95	0.59	0.61	0.39
$\delta^{2}H$-based SW-derived F_{yw} (-)	0.19	1.39	0.76	0.75	0.55
$\delta^{18}O$-based SW modeling MTT (days)	19.00	198.00	94.75	75.00	0.69
$\delta^{2}H$-based SW modeling MTT (days)	10.00	289.00	112.17	73.50	0.94
$\delta^{18}O$-based TBC modeling MTT (days)	0.07	1156.00	346.88	201.50	1.11
$\delta^{2}H$-based TBC modeling MTT (days)	47.00	507.00	214.86	157.00	0.91
$\delta^{18}O$-based TBC-derived alpha (-)	0.04	0.93	0.44	0.39	0.69
$\delta^{2}H$-based TBC-derived alpha (-)	0.14	0.93	0.56	0.52	0.48
$\delta^{18}O$-based TBC-derived beta (-)	1.70	4748.00	1184.96	476.00	1.38
$\delta^{2}H$-based TBC-derived beta (-)	50.00	3701.00	783.88	241.00	1.62
$\delta^{18}O$-based TBC-derived F_{yw} (-)	0.40	1.00	0.69	0.64	0.30
$\delta^{2}H$-based TBC-derived F_{yw} (-)	0.43	0.91	0.65	0.64	0.26